UCSF
UC San Francisco Electronic Theses and Dissertations

Title
Mechanism of [pi]-bond oxidation by cytochrome P-450

Permalink
https://escholarship.org/uc/item/7ms7997t

Author
Komives, Elizabeth A.

Publication Date
1987

Peer reviewed|Thesis/dissertation

eScholarship.org Powered by the California Digital Library
University of California

THE MECHANISM OF π-BOND OXIDATION BY CYTOCHROME P-450 : ACETYLENES AS PROBES

by

ELIZABETH A. KOMIVES

DISSERTATION

Submitted in partial satisfaction of the requirements for the degree of

DOCTOR OF PHILOSOPHY

in

PHARMACEUTICAL CHEMISTRY

in the

GRADUATE DIVISION

of the

UNIVERSITY OF CALIFORNIA

San Francisco

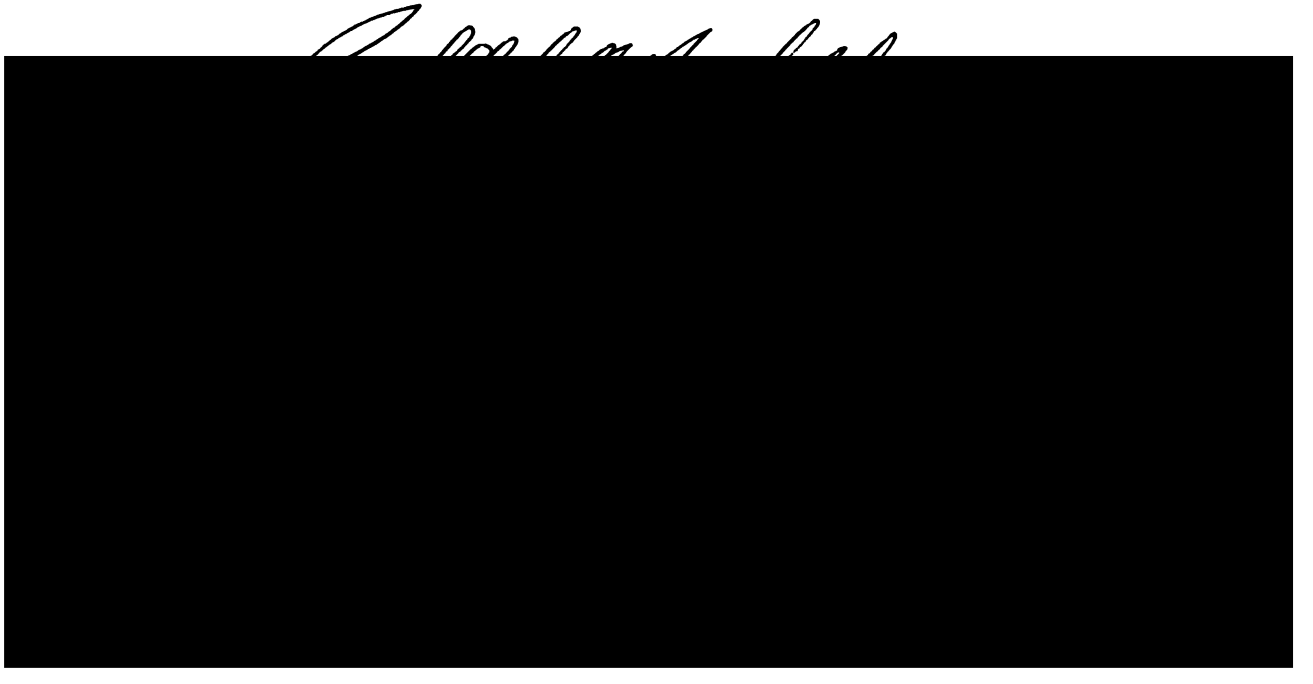

ELIZABETH A. KOMIVES

THE MECHANISM OF π-BOND OXIDATION BY CYTOCHROME P-450: ACETYLENES AS PROBES

ABSTRACT

The mechanism of π-bond oxidation by cytochrome P-450 has been examined using acetylenes as probes. Phenylacetylene and biphenylacetylene are oxidized by microsomal and purified P-450 to the corresponding arylacetic acids. During this transformation, the acetylenic hydrogen undergoes a 1,2 shift which causes a kinetic isotope effect of 1.8 on the overall enzymatic rate. The same products and kinetic isotope effects are observed when the arylacetylenes are oxidized by m-chloroperbenzoic acid. Suicide inactivation of P-450 by the arylacetylenes, which occurs simultaneously with metabolite formation, is insensitive to isotopic substitution so the partition ratio changes from 26 for phenylacetylene to 14 for [1-^{2}H]phenylacetylene.

Electronic effects on the oxidation of phenylacetylene by purified, reconstituted P-450 were probed using a series of substituted phenylacetylenes. The rates of formation of the corresponding aryl acetic acids show a linear free energy correlation with the substituent constants. The rho value of -2.2 indicates substantial electron density is siphoned from the π-bond at the transition state. Suicide inactivation of

cytochrome P-450 by the substituted acetylenes is insensitive to the electronic effects so the partition ratios change from 38 for (p-methylphenyl)acetylene to 4 for (p-nitrophenyl)acetylene. The insensitivity of enzyme inactivation to electronic effects strongly argues against radical cation intermediates in this process. Inactivation rates are also insensitive to steric effects, but decrease 3 fold if cytochrome b_5 is included in the reconstitution mixture. The differential effects of isotopic substitution and electronic effectors on metabolite formation and enzyme inactivation require the two pathways to diverge early in the catalytic process, well before oxygen transfer.

Reductive metabolism of α-diazoketones by model porphyrin systems as well as by P-450 have been used to probe the intermediacy of α-ketocarbenes in the oxidation of acetylenes. Diazoacetophenone forms a long wavelength absorbing adduct with both tetraphenylporphyrin models and with P-450. The adduct is also observed during oxidation of phenylacetylene by purified cytochrome P-450. The structure of the tetraphenylporphyrin complex is that in which the diazoacetophenone has lost N_2, the terminal carbon is bound to the porphyrin ring nitrogen, and the enolized ketone is ligated to the iron. ^{13}C-NMR studies suggest that the same structure is present in P-450cam as in the tetraphenylporphyrin complex. This indicates that the N-alkylporphyrin is formed directly in all cases, and that the α-ketocarbene, if formed, is not a detectable intermediate.

ACKNOWLEDGEMENTS

Words will never be able to express my gratitude to Professor Paul Ortiz de Montellano for his infinite patience, support and optimism. I only hope that my future scientific efforts will give testimony to the superb education I have received in his lab. He is truly a great educator as well as scientist who sets high standards by his example but then patiently waits for his students to discover their own goals and limitations. These have been the four best years of my life.

I would also like to thank the POM group for their friendship and support, especially the Club 1136 Eastern Block (Mark, Carlos and Jae) who stood by patiently during the total eclipses.

Part of the discussion and interpretation of the results pertaining to partitioning in enzymatic reactions is due to Professor Norbert Reich and Dr. Ron Raines.

The mass spectrometry instrumentation was provided by Professor A. L. Burlingame with the expert assistence of Pat Bethel. Help with the NMR was provided by Vladimir Basus.

Finally, I would like to thank the Department of Pharmaceutical Chemistry for bringing together a remarkable group of scientists who are truly interested in their students as well as in science.

LIST OF FIGURES

LIST OF SCHEMES

LIST OF TABLES

LIST OF ABBREVIATIONS AND COMMON NAMES

NADPH	Reduced nicotine adenine dinucleotide phosphate
FAD	Flavin adenine dinucleotide
FMN	Flavin mononucleotide
DETAPAC	Diethylenetriamine pentaacetic acid
PPIX	Protoporphyrin IX
TPP	Tetraphenylporphyrin
7-EC	7-Ethoxycoumarin
MCPBA	meta-Chloroperbenzoic acid
DAP	Diazoacetophenone
Me-DAP	1-Diazo-1-phenyl-2-propanone
EDA	Ethyldiazoacetate
Heme	Iron protoporphyrin IX regardless of the iron oxidation state and ligands
P-450	Cytophrome P-450
Reductase	Cytochrome P-450 reductase
b_5	Cytochrome b_5
LSIMS	Liquid secondary ion mass spectrometry
HPLC	High performance liquid chromatography
GC/MS	Gas chromatography interfaced to mass spectrometry
NMR	Nuclear magnetic resonance spectroscopy
SDS PAGE	Polyacrylamide gel electrophoresis in the presence of sodium dodecylsulfate
O.D.	Optical density

CHAPTER 1

INTRODUCTION

A. General Characteristics of Cytochrome P-450

Cytochrome P-450 is one of the most interesting enzymes because it easily performs reactions that are almost impossible to carry out in purely chemical systems (Ortiz de Montellano, ed. 1986). Practically all organisms have P-450 enzymes, including some prokaryotes such as Pseudomonas putida, which uses camphor as its sole carbon source and requires P-450cam to initiate its oxidative catabolism. Mammalian P-450's can be classified according to their substrate specificity, as either biosynthetic or xenobiotic; the latter class is the one that is considered here. The xenobiotic P-450's are mainly found in the hepatic endoplasmic reticulum, are membrane bound, have molecular weights of 50 - 55 kD, and show broad substrate specificities. These P-450's, which are responsible for the metabolism of xenobiotics, frequently can be induced by the xenobiotics that they metabolize. All P-450's have similar characteristics and reactivities, so the results from studies of the catalytic mechanism of one P-450 isozyme are, in broad terms, applicable to all other P-450 isozymes.

1. P-450 Structure

The camphor-bound form of P-450cam was recently crystallized and its crystal structure refined to 1.9 A (Poulos et al, 1985). Knowledge of the enzyme structure now allows earlier conjectures

about the structure and its relationship to function to have a basis in reality. The protein provides a thiolate ligand to the heme and the chemistry of the enzyme is largely that expected for a heme in which the iron is activated by a thiolate ligand. The principle roles of the rest of the protein are to protect the activated oxygen species, to provide a hydrophobic binding pocket for the substrate, and to enable the ordered delivery of electrons to the iron. The substrate-free P-450cam has also been crystallized and the substrate binding pocket appears to be filled with water, one of which appears to be the sixth ligand to the heme iron (Poulos et al, 1986). The substrate must squeeze out the water upon binding since these water molecules are not present in the substrate-bound form.

2. Catalytic Cycle

The reactions catalysed by P-450 can be classified into three broad classes: hydroxylations, heteroatom oxidations, and N-bond oxidations. The oxidative potency required to perform these diverse and sometimes chemically difficult transformations comes from a highly activated oxygen species that is generated by the prosthetic heme group. The reaction stoichiometry is:

$$NADPH + substrate + O_2 + H^+ = NADP^+ + H_2O + substrate\text{-}O$$

The oxidation of NADPH is accomplished by P-450 reductase, a flavoprotein containing one molecule each of FAD and FMN, which transfers the electrons from NADPH to P-450 one at a time. Cytochrome b_5 is also sometimes involved in electron transfer to

P-450.

The catalytic cycle of P-450 is shown in Figure 1.1 (Ortiz de Montellano, 1986). The native resting state of the enzyme in most instances is low spin Fe(III) with a water molecule presumably occupying the sixth ligand position. Substrate binding causes departure of the water molecule and concomitant spin state change to the high spin form. The associated change in reduction rate (from 4.8/sec to 17/sec in P-450 LM2) facilitates the first electron transfer from the reductase (Iyanagi et al, 1978). After reduction to the Fe(II) state, oxygen is rapidly bound. If oxygen is excluded, the heme is capable of performing reductive reactions and of binding CO to give the characteristic absorbance at 450 nm. The $Fe(II)O_2$ complex has three known fates: it can transfer an electron to b_5 and return to native P-450 (Pompon and Coon, 1984); it can dissociate to form O_2^- and the resting state of the enzyme (Debey and Balny, 1973; Auclair et al, 1978 and Kuthan et al, 1978); or it can be further reduced by the reductase or, in some cases, by b_5 (Noshiro et al, 1981; Werringloer and Kawano, 1980). The involvement of b_5 is complicated. Studies with P-450 LM2 show that reduced b_5 increases the autooxidation rate of the ferrous dioxygen complex and decreases the steady state concentration of this species even though the b_5 is not significantly oxidized in the precess (Bonfils et al, 1981; Noshiro et al, 1981). Pompon and Coon (1984) suggested that two different ferrous dioxygen complexes may exist, only one of which is capable of being further reduced by b_5. The existence of two distinct dioxygen

Figure 1.1

The Catalytic Cycle of Cytochrome P-450

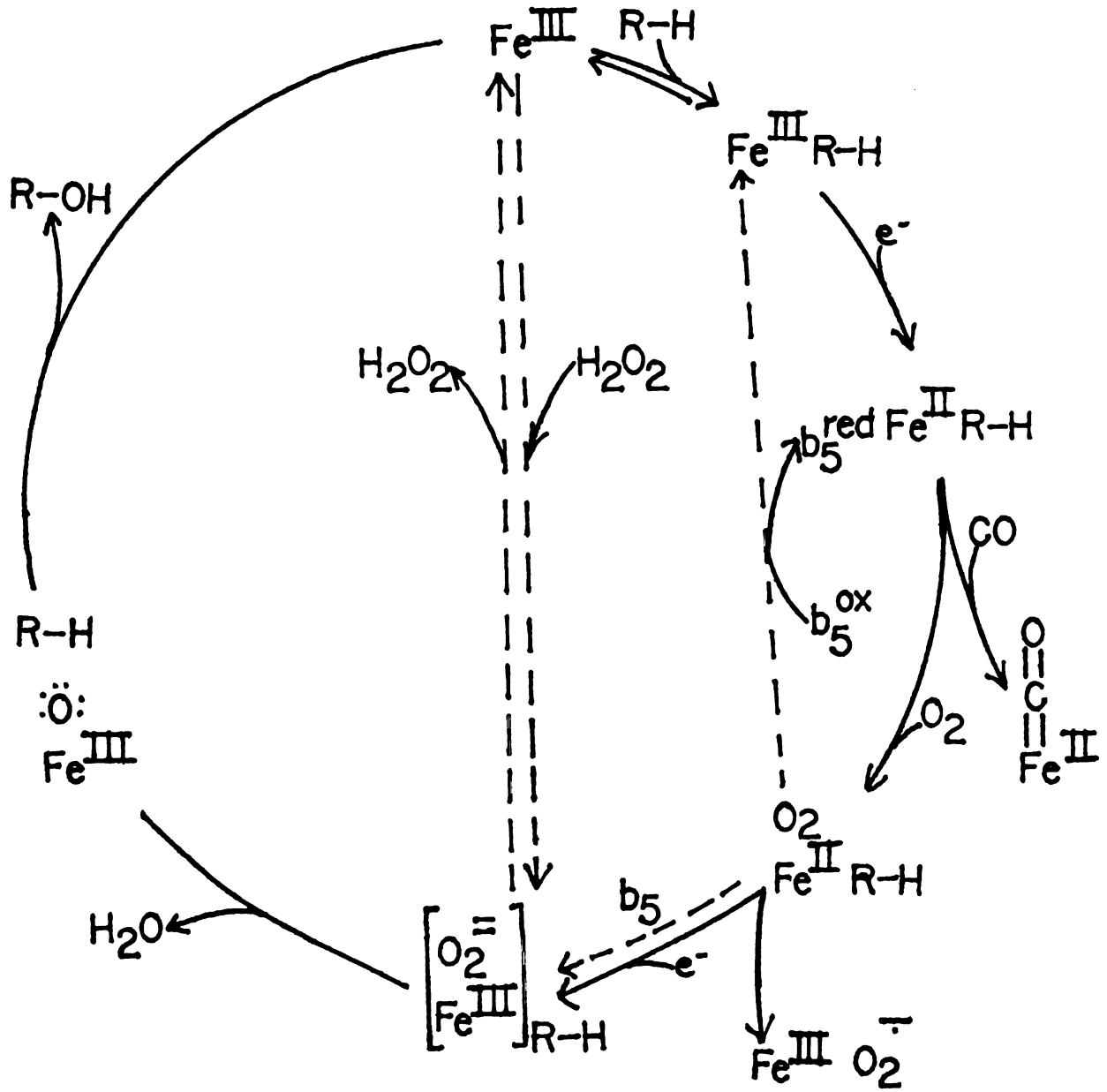

(modified from Ortiz de Montellano, 1986)

complexes provides a mechanism for rationalizing the two different consequences of acquiring a second electron, either cleavage of the O-O bond or H_2O_2 production. The second reduction step is rate limiting in P-450cam, and must be slow in other P-450 reactions because alterations in the rate of this step effect the overall rate of the catalytic reaction.

The $Fe(II)O_2^-$ thus formally produced, can lose H_2O_2, returning the enzyme to the resting state, or can undergo O-O bond scission to generate water and the activated oxygen species. Some evidence suggests further reduction of the activated iron oxo species by consumption of another equivalent of NADPH may occur if the substrate is difficult to oxidize. The activated oxygen then appears as a second molecule of H_2O (Staudt et al, 1974; Zhukov and Archakov, 1982; Gorsky et al, 1984). The nature of the activated species and the location of its electrons are not known, but it is thought to be electronically equivalent to compound I of the peroxidases and catalase. The reaction between the activated species and the bound substrate is generally quite rapid. Information about the activated species has been difficult to obtain because it decomposes rapidly, but studies of model porphyrin systems and the analogy to other heme proteins (e.g. the peroxidases) have provided some insights. The fates of the activated oxygen species and the mechanism by which it oxidizes substrates are matters of conjecture. Product analyses indicate that the activated oxygen of P-450 isozymes can perform one electron as well as two electron oxidations, but the nature of the reaction intermediates and the mechanism by which they are

formed remain unclear.

3. P-450 Models

The chemical behavior of P-450 mainly depends on the prosthetic heme group. It has therefore been possible to model many of the enzymatic reactions using metalloporphyrins in purely chemical systems. These model reactions provide a better understanding of certain aspects of P-450 catalysis that cannot be studied in the enzyme itself.

Iron porphyrins react with organic peroxides, periodate and iodosylbenzenes to directly generate active oxidizing species (Groves et al, 1981). Metalloporphyrins reduced by catalytic hydrogenation also react with molecular oxygen to give an active oxygen species (Tabushi and Yazaki, 1981). It is now generally accepted that these active oxidants have the same formal oxidation state and probably are quite similar to the P-450 activated iron oxo species (Groves and McMurry, 1986). Many studies of the reactivity of metalloporphyrin model systems indicate that all three of the basic reactions carried out by P-450 can be modeled by these chemical systems (Groves et al, 1979; Chang and Kuo, 1979; Lindsay-Smith and Sleath, 1982). Recently, catalysis-dependent heme alkylation has also been achieved in model systems (Mashiko et al, 1985; Mansuy et al, 1985).

B. Kinetic Isotope Effects

1.Partition Theory

The oxidation of substrates by P-450 often results in more than one product. Oxidation may occur at more than one site on the substrate molecule or may include the inactivated enzyme as

one of the products. In either case, it is useful to develop an intuitive understanding of partitioning in enzymatic reactions so that analyses of partitioning can be used accurately to define aspects of the catalytic mechanism. Transition state diagrams showing relative rate constants, and the method of steady state kinetics can be combined to analyze the partitioning event (Cleland, 1963 and R. Raines, unpublished). Perturbations of a rate constant, for example by isotopic substitution, can be analyzed by merely raising or lowering the height of the appropriate transition state in the diagram. This intuitive method has been useful in analyzing the data of others (see section 1.C) as well as data presented in this thesis (see Chapter 6). Figure 1.2 shows a typical diagram in which substrate A is transformed into intermediate I which partitions to 2 products P1 and P2 with rate constants k_1 and k_2 respectively. At steady state, dI/dt = 0, and the expressions for the velocities are as follows:

$V_1 = k_1 I = k_1 k_0 A/(k_1+k_2)$

$V_2 = k_2 I = k_2 k_0 A/(k_1+k_2)$

because $I = k_0 A/(k_1+k_2)$

Several scenarios develop depending on the ratio of k_1/k_2. For example, if the rate constants are equal, the velocities of production of the products P1 and P2 are equal. If $k_1 << k_2$ and if k_2 is slowed by isotopic substitution, for example, by a factor of 10, the equations become:

$I = k_0 A/(k_1+k_2/10)$ where k_2 is the rate constant before isotopic substitution.

Figure 1.2

The Transition State Diagram for a Partitioning Event

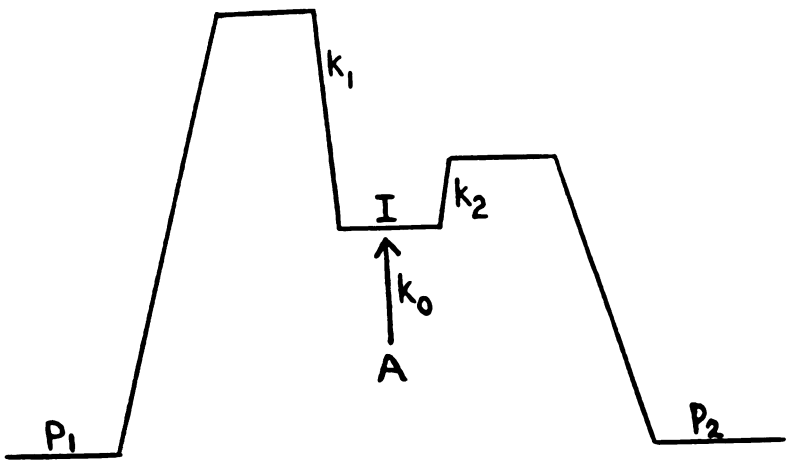

$V_1 = k_1 k_0 A/(k_1+k_2/10)$

$V_2 = (k_2/10)k_0 A/(k_1+k_2/10)$

In this case, the velocity of production of P1 has become greater while the velocity of production of P2 has become less. It should be noticed that the velocities depend directly on the concentration of the intermediate, I, which is assumed to be in the steady state. If, on the other hand, k_1 was decreased by isotopic substitution, no effect would be seen on V_2 because I is largely determined by k_2 since $k_1 << k_2$ and $I = k_0 A/k_2$.

The possibility that the intermediate, I, is not in the steady state needs to be considered. In this case, simple intuitive analyses can still be informative bearing in mind that I depends also on the back reaction k_{-0} and its relative magnitude relative to k_1 and k_2. Exact expressions for V_1 and V_2 are not readily derived, but it is still possible to intuitively understand a set of data based on this type of analysis.

2. Measurement of Isotope Effects on P-450 Reactions

Kinetic isotope effects have long been used to probe the mechanism of P-450 hydroxylation reactions. Kinetic isotope effects on the overall rates of P-450 reactions, like those on many other enzymatic reactions, are lower than expected for C-H bond scission reactions (Thompson and Holtzman, 1974; Bjorkhem and Hamberg, 1972 and others). Initially the low magnitude of the isotope effects was used to support a concerted oxygen insertion mechanism, but the phenomenon was later shown to merely reflect the fact that the isotopically sensitive step is one of several rate limiting steps, each of which contributes to the

overall rate of the enzymatic reaction. Indeed, studies with several different P-450 isozymes show that the kinetic isotope effect on the deethylation of 7-ethoxycoumarin (1) varies widely. This implies that the degree to which the isotopically sensitive step is rate limiting is different for different isozymes (Miwa et al, 1985). The intrinsic kinetic isotope effect, (i.e. that for the isolated isotopically sensitive step), however, was measured for each of the isozymes and shown to be invariant.

Several approaches have been taken to circumvent the problems of interpreting the kinetic isotope effects due to partially rate limiting steps. The simplest approach is to measure intramolecular kinetic isotope effects using specially designed substrates which have equivalent positioning of hydrogen and deuterium within the same molecule. Two examples of this are the kinetic isotope effect of 11 determined for the hydroxylation of [1,1-^{2}H]1,3-diphenylpropane (2) by Hjelmeland et al (1977) and the kinetic isotope effect of 11.5 for the hydroxylation of exo, exo, exo-2,3,5,6 tetradeuteronorbornane (3) measured by Groves et al, (1978). These two important experiments serve as strong evidence that P-450 hydroxylation occurs via a radical abstraction recombination reaction rather than, as originally suggested, a two electron insertion mechanism.

Care must be taken in these experiments to insure that the measurement truly reflects an enzymatic process and not a chemical decomposition step subsequent to the enzymatic step. For example, evidence is accumulating that the dealkylation of amines by P-450 probably involves initial radical cation

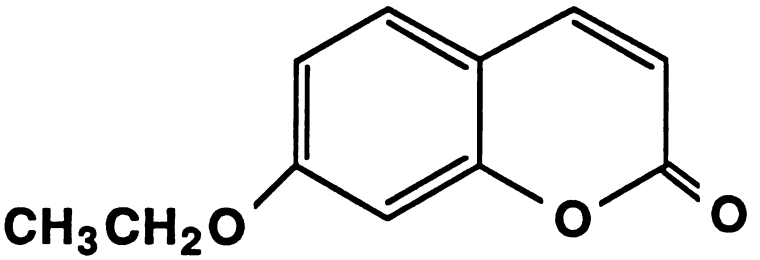

(1)

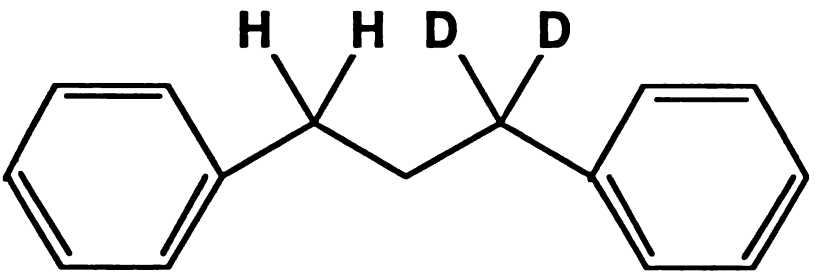

(2)

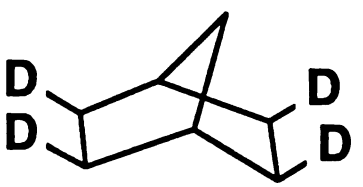

(3)

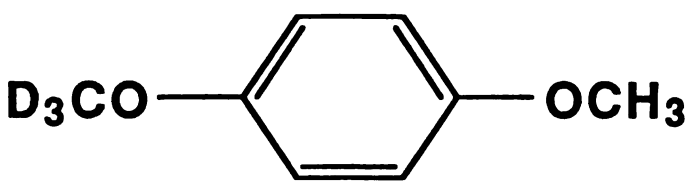

(4)

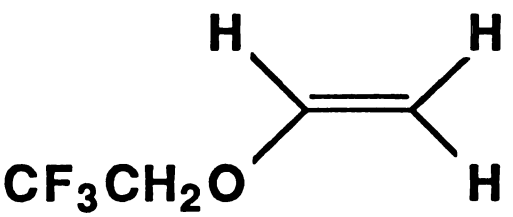

(5)

formation. It is not yet clear, however, whether the enzyme also catalyzes the loss of a hydrogen alpha to the cationic nitrogen or whether this is a non-enzymatic process. Likewise, the comparison of the intramolecular and intermolecular kinetic isotope effect on O-demethylation of p-trideuteromethoxyanisole (4) may give no information about the enzymatic reaction because this substrate is so highly oxidizable that it is likely that the initial enzymatic step is electron abstraction (Bjorkhem, 1977). The loss of one of the methyl group hydrogens may then occur in a subsequent chemical step that is not mediated by the enzyme. Observations such as this therefore do not provide good evidence that the substrate can change its binding orientation after the activated iron oxo has been generated but before oxygen transfer.

Miwa and Lu have taken a kinetic approach by calculating the intrinsic kinetic isotope effects from the experimentally measured deuterium and tritium effects using the kinetic scheme of Northrup (Northrup, 1975; Miwa et al, 1984). They also observed metabolic switching from O-deethylation to ring hydroxylation after deuteration of the ethoxy group in 7-ethoxycoumarin (Miwa et al, 1982). In this reaction, the turnover rate of the enzyme remained constant and the switching or partitioning toward ring hydroxylation unmasked the intrinsic kinetic isotope effect. The hypothesis that the unmasking of the isotope effect was due to switching was substantiated by the observation that the kinetic isotope effect remained unchanged over a range of temperatures and net catalytic rates (Lu and Miwa, 1982). The kinetics of the metabolic switching reaction

were interpreted as proof that the intermediate which switches is formed irreversibly (Harada et al, 1984). In fact, analysis of this reaction using partition theory shows that the intermediate need not be formed irreversibly; the same result would be obtained if the intermediate were not in the steady state. In any case, the observation of metabolic switching suggests that the enzyme can attempt an oxidation, sense its difficulty, and partition into another energetically accessible pathway. Trager's group has also recently corroborated this conclusion (Jones et al, 1986).

C. π-Bond Oxidation

1. Mechanism of P-450 Catalyzed Olefin Oxidations

A consensus is emerging that the mechanism of hydroxylation by P-450 involves hydrogen atom abstraction and radical recombination (Groves et al, 1978; Stearns and Ortiz de Montellano, 1985), and that N-dealkylation involves initial one electron oxidation (Augusto et al, 1982). The mechanism of π-bond oxidation, however, is still controversial. Many olefins are oxidized by P-450 to the corresponding epoxides with complete stereochemical retention suggesting a two electron concerted pathway similar to oxidation by peracids (Maynert et al, 1970; Watabe et al, 1971; Watabe and Akamatsu, 1974 and Ortiz de Montellano et al, 1983). Several lines of evidence argue against the concerted pathway, however. The report of secondary kinetic isotope effects on the oxidation of styrene suggests that the oxygen is added to the π-bond asymmetrically supporting the presence of an intermediate in which the oxygen is bonded to only

one of the carbons of the π-bond (Hanzlik and Shearer, 1978). Further evidence is the observation that metabolites other than the epoxides are often formed during the reaction, suggesting the existence of an intermediate prior to epoxide formation. Aldehydes and ketones have been found as trace metabolites of certain olefins and the hydrogen shift required for their formation appears to occur before the epoxide ring is closed (Mansuy, 1984 and Liebler and Guengerich, 1983) (Scheme 1.1). Chloroolefins show products from chlorine migration during oxidation which also do not appear to result from the epoxides (Miller and Guengerich, 1982 and Liebler and Guengerich, 1983). The alternative products could either be formed from parallel pathways that diverge early from the pathway leading to the epoxide or from a common intermediate that leads to both products. Some evidence that an intermediate actually precedes the epoxide has been provided by Groves' group who showed that oxidation of [1,1-^{2}H]propene by purified, reconstituted P-450 yields propene oxide in which a portion of the deuterium has been lost to the medium (Groves et al, 1986) (Scheme 1.2).

The most substantial evidence for an intermediate in the oxidation of olefins by P-450 is provided by the observation that terminal olefins suicidally inactivate the enzyme by forming heme adducts in which the activated oxygen has been transfered to the internal carbon of the π-bond (Ortiz de Montellano et al, 1981; 1982; 1984; Ortiz de Montellano, 1985; and Kunze et al, 1983). The epoxide has been unequivocally ruled out as the alkylating species. When the epoxides are added to the enzymatic reaction

Scheme 1.1

The Mechanism of Aldehyde Production from Olefins

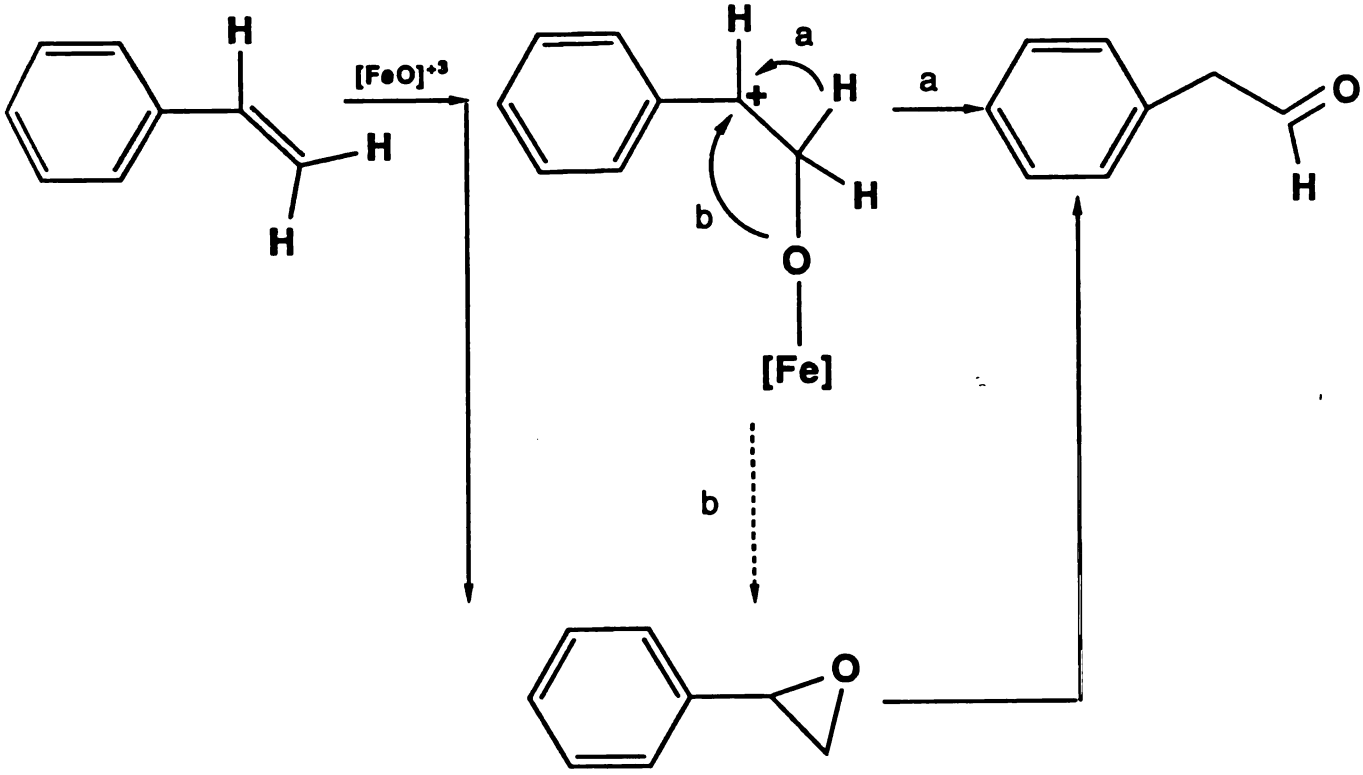

Scheme 1.2

Exchange of the Terminal Hydrogens of Propene During Oxidation by P-450

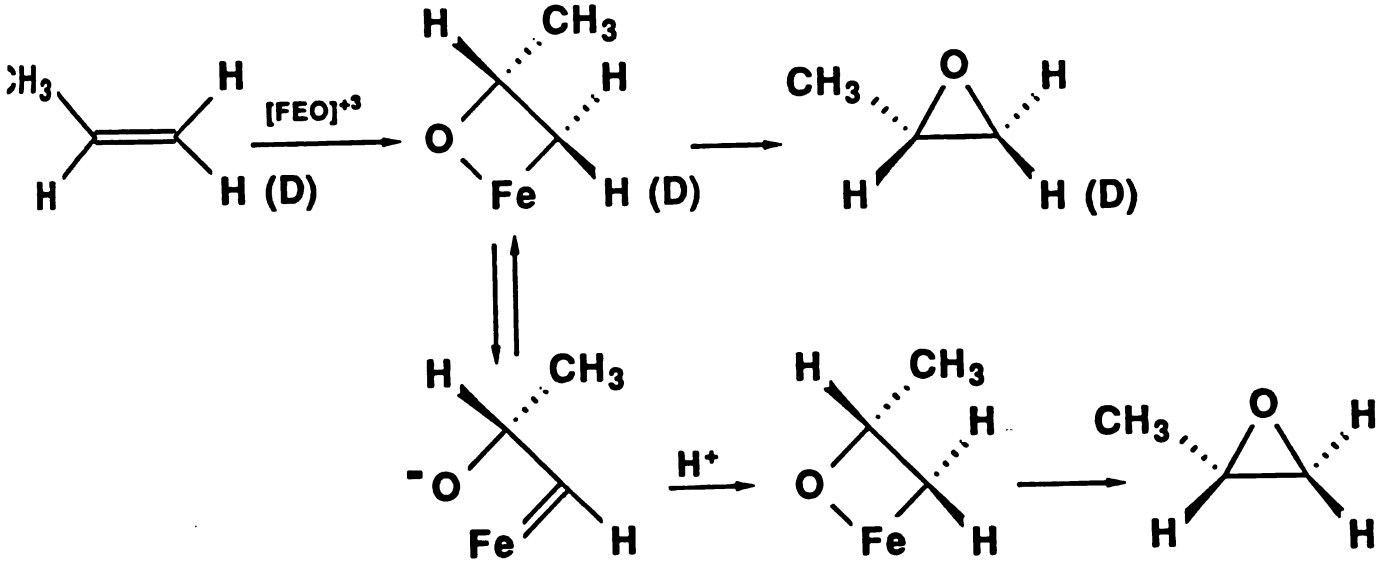

mixture, they do not alkylate the heme (Ortiz de Montellano and Mico, 1980). Stereochemical studies furthermore show the oxygen and nitrogen add to the same face of the double bond (Ortiz de Montellano et al, 1983), an orientation opposite to that expected from a nucleophilic attack of the porphyrin on the epoxide.

The fact that only terminal olefins alkylate the heme is an unexplained phenomenon. It is possible that an intermediate, or transition state leading to heme alkylation is sensitive to steric constraints (Ortiz de Montellano and Reich, 1986). On the other hand, the reaction appears not to be sensitive to electronic effects because destruction by fluroxene (5) involves alkylation of the terminal carbon of the π-bond, an orientation that is electronically highly disfavored (Ortiz de Montellano et al, 1982). In fact, the observation that fluroxene alkylates the heme at all suggests that the intermediate is probably not cationic, because a cation on the terminal rather than internal carbon of the fluroxene π-bond is particularly disfavored.

2. Model Studies of π-Bond Oxidation Reactions

Iron porphyrin models have been shown to carry out all of the reactions observed during π-bond oxidation by P-450. Recently, the process of suicidal inactivation by heme alkylation was also achieved in a model system (Mashiko et al, 1985; Mansuy et al, 1985). The model reactions provide support for two divergent mechanisms involving two different intermediates. These two mechanistic proposals have not been reconciled and both may actually occur in the models as well as in the enzyme.

Some model studies support the intermediacy of a σ-radical

cation that recombines with the oxygen (Scheme 1.3). Products of oxidation of transcyclooctene and norbornene by iron porphyrins are those expected from a radical intermediate (Traylor and Dolphin, 1986; and Traylor et al, 1986). While iron porphyrin oxidation of olefins results in retention of the olefin stereochemistry, manganese porphyrins give products in which stereochemistry is partially lost (Groves et al, 1980). This suggests either that a delicate balance may exist between alternative mechanisms or that radicals are produced but the degree of stereochemical retention depends on the rate of recombination of the oxygen with the radical. Support for transition state polarization is the observation of a substituent effect on the oxidation of styrenes by iron porphyrins (Lindsay-Smith and Sleath, 1982). This substituent effect was not observed on oxidation of styrenes by microsomal P-450, but the facts that many isozymes were present, and that the rate limiting step may not be substituent sensitive, compromise this result (Hanzlik and Shearer, 1978).

Evidence is also available for an intermediate π-complex or metallooxetane. The metallooxetane, first proposed by Sharpless et al, 1977, nicely explains the stereochemical retention observed in olefin oxidation (Scheme 1.4). Two groups have purportedly observed intermediates such as these by NMR and electronic absorption spectroscopy (Schroder and Constable, 1982; Groves and Watanabe, 1986), but their existence is not well established. The metallooxetane, or a simple π-complex may be the reversibly formed complex required to explain the observation

Scheme 1.3

A Postulated Mechanism for P-450 Oxidations Involving π-Bond Radical Cations

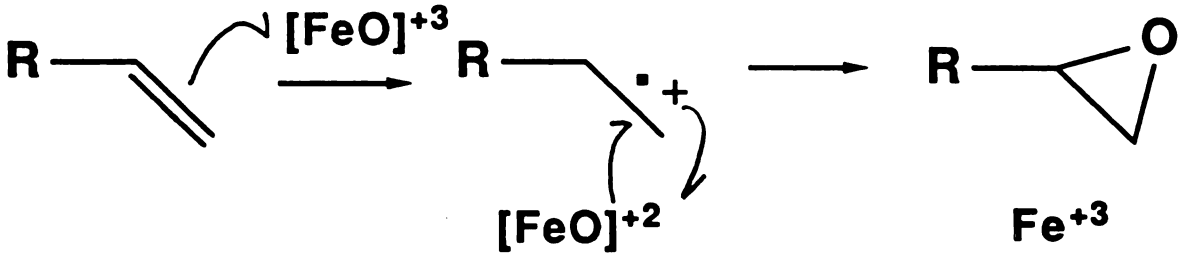

Scheme 1.4

The Sharpless Metallooxetane Mechanism

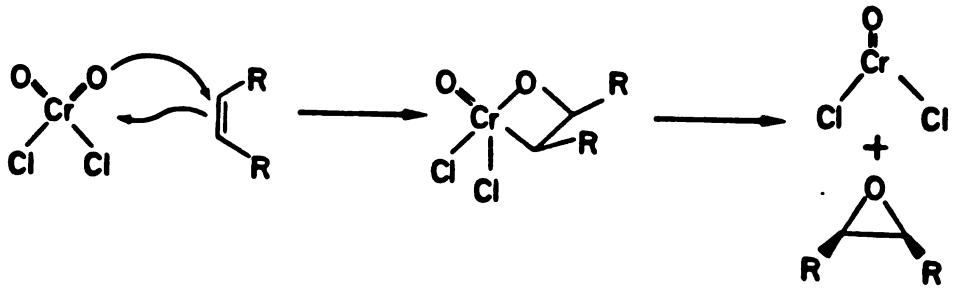

that the epoxidation of olefins by iron porphyrins is kinetically saturable (Collman et al, 1984; 1985). The observations of phenylacetaldehyde formation during oxidation of styrene (Scheme 1.1) and propene hydrogen exchange (Scheme 1.2) can be explained by either the metallooxetane mechanism or the radical cation mechanism, but the observation that the hydrogen cis to the phenyl ring is the one that shifts during phenylacetaldehyde formation suggests some rigidity in the system contributes to stereochemical retention (Collman et al, 1986). In the end, the data can be used to rationalize either mechanism, so both are possible. Both mechanisms may be involved, depending on the fine tuning of the porphyrin system, or a crossover point may exist in the reaction coordinates.

3. Acetylene Oxidation by P-450

Acetylenes may prove more useful as probes to sort out the details of the mechanism of π-bond oxidation by P-450. In this case, metabolite formation and enzyme inactivation are clearly separable processes because the oxygen in the metabolite ends up on the terminal carbon of the π-bond while the oxygen in the heme adduct ends up on the internal carbon (Scheme 1.5). The metabolic products of acetylene oxidation have been shown to be arylacetic acids in the case of arylacetylenes (El Masri et al, 1958; Wade et al, 1979; and Sullivan et al, 1979) and rearrangements in the case of ethinyl sterols (Ortiz de Montellano, 1985), (Scheme 1.6). Aliphatic acetylenes have also been shown to be oxidized to aliphatic acetic acids, although this is a minor metabolic pathway (C. Wheeler unpublished

Scheme 1.5

The Metabolic Pathways of Acetylene Oxidation by P-450

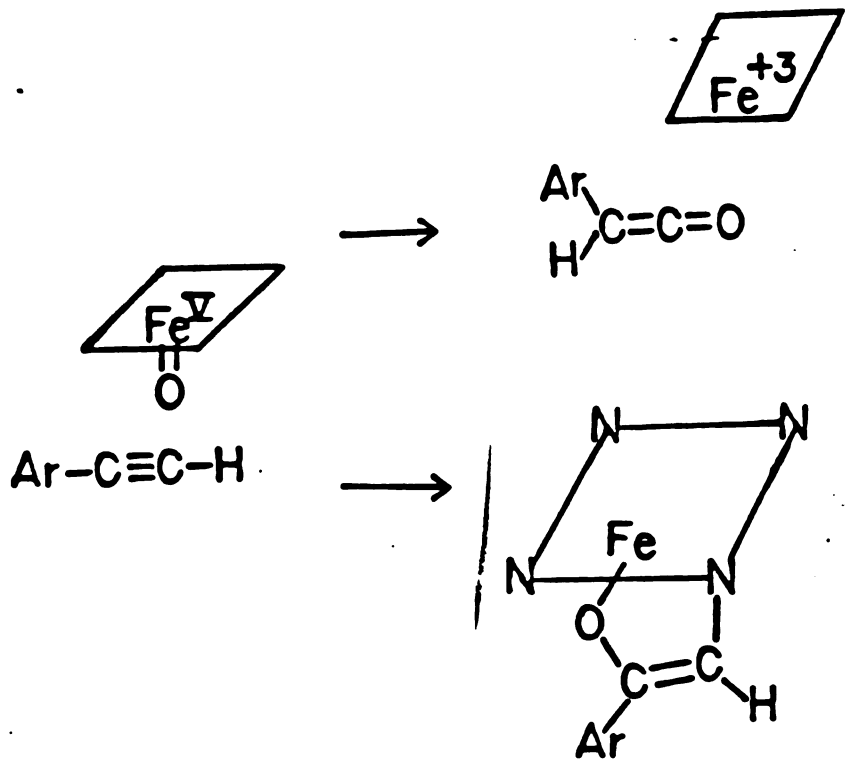

Scheme 1.6

Rearrangement of Ethinylestradiol During Oxidation by P-450

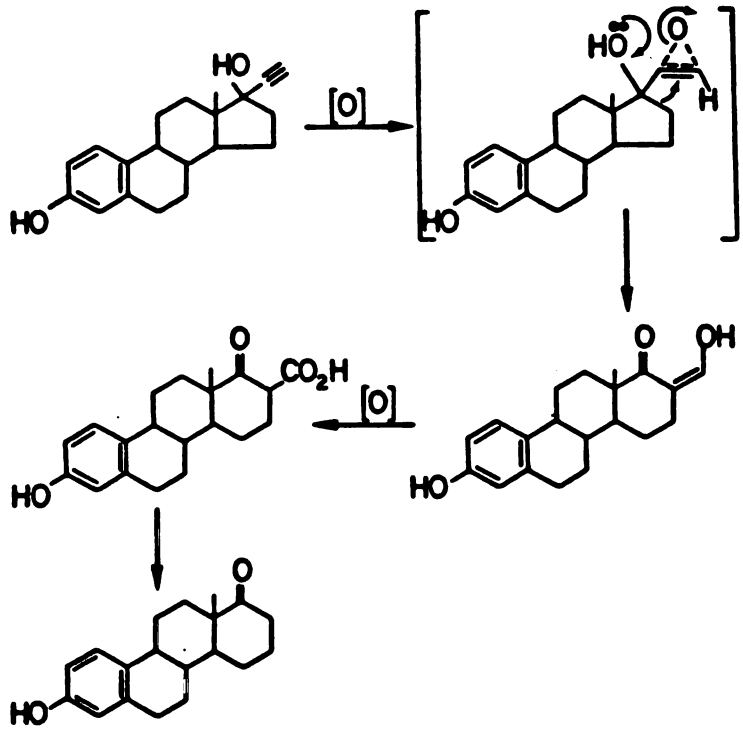

observations). The products are similar to those produced by the reaction of peracids with acetylenes, a process that has been claimed to pass through oxirene intermediates (McDonald and Schwab, 1964; Ciabattoni et al, 1970; and Concannon and Ciabattoni, 1973). The oxidation of acetylenes to arylacetic acids (Scheme 1.5) was shown to involve 1,2 hydrogen migration to give a ketene (not isolated) that is then trapped by water. The quantitative migration of the acetylenic hydrogen was demonstrated for both the metabolic and peracid oxidation reactions (Ortiz de Montellano and Kunze, 1980; 1981). This 1,2 shift was shown to be accompanied by a kinetic isotope effect in the case of biphenylacetylene and 4'-ethinyl-2-fluorobiphenyl, although the original interpretation of this result required some revision (McMahon et al, 1981). The proposal that the kinetic isotope effect reflected hydroxylation of the acetylenic C-H bond to give hydroxyacetylene had to be discarded because such an intermediate would not rearrange with retention of the acetylenic hydrogen. The required rearrangement is quantum mechanically forbidden and therefore unfavorable (Scheme 1.7). It is most likely, then, that oxidation of the acetylenic π-bond directly produces some member of the oxirene manifold (Scheme 1.8) that rearranges with migration of the hydrogen to the ketene (Stille and Whitehurst, 1964; Strausz et al, 1976; and Tanaka and Yoshimine, 1980).

Perusal of the oxirene manifold shows that besides the oxirene itself, the α-ketocarbenes would be viable intermediates in the oxidation of acetylenes by both chemical and enzymatic

Scheme 1.7

Mechanisms Postulated to Explain the Kinetic Isotope Effect on Acetylene Oxidation

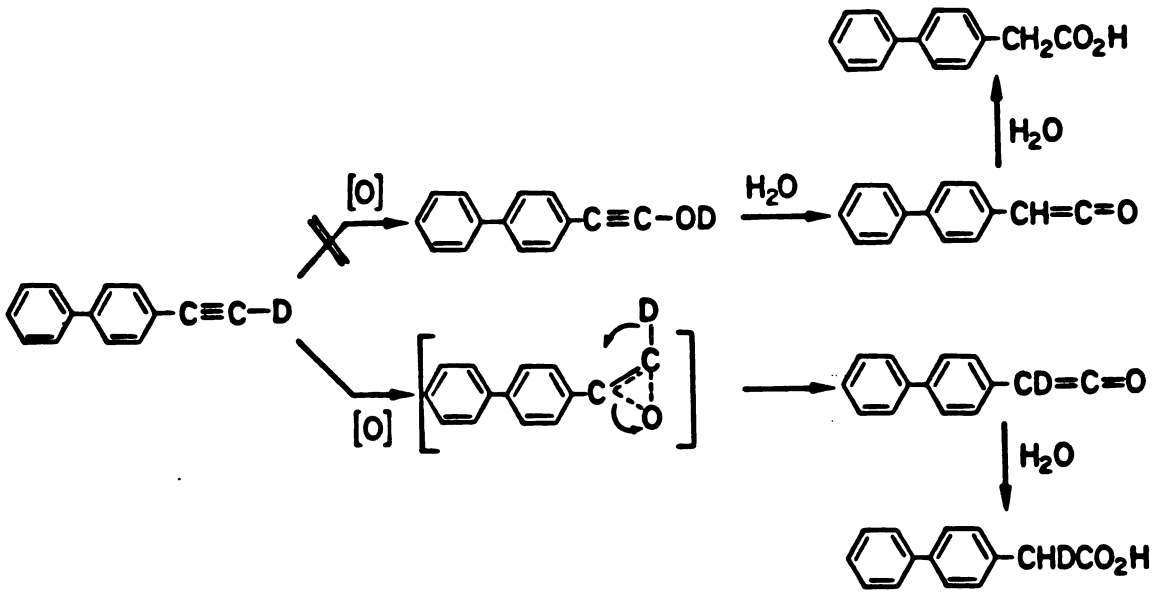

Scheme 1.8

The Oxirene Manifold

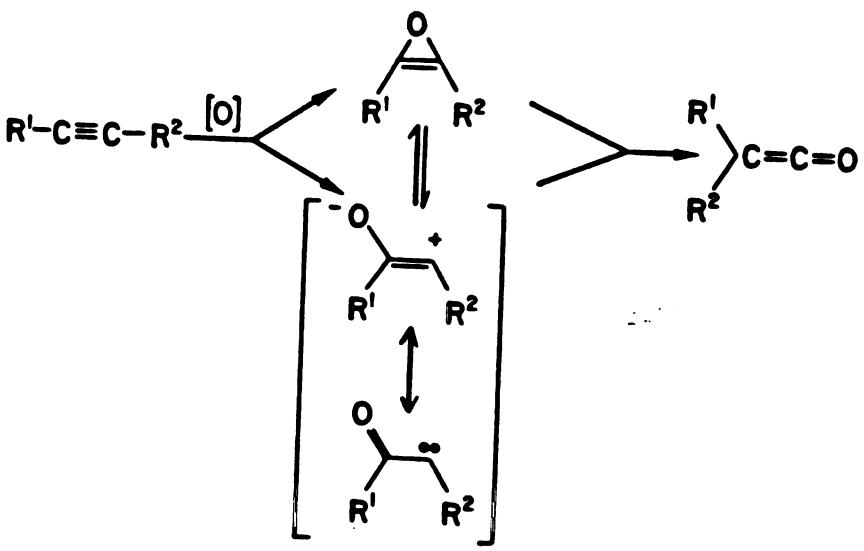

means. Carbenes are known to form in P-450 reductive reactions, and have been shown to yield N-alkylated porphyrins analogous to those formed from acetylenes (Lange and Mansuy, 1981; Latos-Grayzynski et al, 1981; and Ortiz de Montellano and Kunze, 1980b). Diazoketones thus react with zinc, nickel and cobalt porphyrins to yield the N-alkylated species, presumably via an α-ketocarbene (Callot et al, 1978; Callot and Schaffer, 1980; Johnson et al, 1975; and Johnson and Ward, 1976). The α-ketocarbenes thought to be generated from the α-diazoketones are also intermediates in the oxirene manifold and thus could be generated during the oxidation of acetylenes.

CHAPTER 2

MATERIALS AND METHODS

A. Materials

All chemicals and solvents were obtained from either Aldrich (Milwaukee, WI) or Sigma (St. Louis, MO) except where specifically indicated and were used without further purification. The reagents used in the protein purification are listed in Appendix II.

B. Instrumentation

1. Gas Chromatography

Gas chromatographic analyses were carried out using a Varian 2100 gas chromatograph equipped with flame ionization detectors and a 6 ft glass column packed with 3% OV-17 on gas chrom Q. The oven temperature was held at 110°C, and the flow rate was 30 ml/min of nitrogen carrier gas.

Capillary gas chromatographic analyses were carried out using a Hewlett Packard 5890 gas chromatograph equipped with flame ionization detectors and a Hewlett Packard 3390A recording integrator. The capillary gas chromatographic column was a 30 m DB5 column with 1 um film thickness (J & W Scientific). The splitless injection was at 35°C and the splitter was turned on after 0.5 minutes. The oven temperature was rapidly increased to 110°C after 1 minute and held for 30 minutes. Between each analysis, the column was cleared of remaining material by

increasing the oven temperature to 300°C over 10 minutes.

Most gas chromatographic analyses were carried out on ethereal extracts which had been methylated by treatment for 30 minutes with an excess of ethereal diazomethane immediately before analysis.

2. Gas Chromatography/Mass Spectrometry

Coupled gas chromatography/mass spectrometry (GC/MS) was carried out on a Kratos MS-25 Mass Spectrometer directly interfaced to a Varian model 3790 gas chromatograph equipped with a 30 m DB1 column of 1 um film thickness (J & W Scientific). The mass spectrometer was operated in the electron impact mode with 70 eV ionization energy. The samples were injected either in the splitless mode as described above for the capillary gas chromatographic analyses or directly onto the column using a J & W on-column injector. Whenever quantitation was desired, mass spectra were averaged over the entire chromatographic peak to avoid artifactual isotopic fractionation by the capillary gas chromatograph. Total ions detected were typically 50,000 - 200,000 in one chromatographic peak.

3. Mass Spectrometry

Electron impact mass spectrometric analyses of pure compounds were carried out on a Kratos MS-25 mass spectrometer using direct probe insertion of the sample.

Field desorption mass spectrometric analyses were carried out either on a Kratos MS-9 instrument or a Kratos MS-50 instrument. This mass spectrometric method worked best for N-alkylated PPIX adducts in the free base form. The porphyrins (1

- 2 ug) dissolved in methanol were loaded onto the emitter using a microliter syringe and the solvent was removed with a stream of nitrogen or air. The emitter current at which the porphyrins desorbed was 10 - 15 mA.

A method was recently developed for analyzing the N-alkylated PPIX derivatives as well as other porphyrins by LSIMS. These methods are based on the "pre-formed ion" hypothesis and therefore require preliminary electronic absorption spectral analysis of the porphyrin in dichloromethane solution in the presence of the liquid matrix (Musselman et al, 1986). LSIMS typically involves dissolution of the sample in a viscous liquid matrix that is bombarded with a focused beam of Cs ions which effect a soft ionization of both the compound and the matrix. The principles behind this ionization are not clear, but our experiments show that if the matrix causes protonation of the porphyrin, as determined by electronic absorbtion spectroscopy, then the cationic porphyrin will be observed in the mass spectrometer. For porphyrins, formation of the cation in the matrix appears to be required for observation of a strong molecular ion signal. The matrix of choice for most of the N-alkylated PPIX derivatives is sulfolane. Sulfolane is a non-polar matrix in which the porphyrins are relatively soluble, but it is still sufficiently acidic to protonate them. An example of this phenomenon is shown in Figure 2.1. In contrast, the mass spectra of the metal (either Zn or Fe) complexes of N-alkylated porphyrins can not be obtained under any conditions that were investigated if the porphyrin is PPIX, although the metal

Figure 2.1

Electronic Absorption Spectrum for Protonation of the Free Base of an N-Alkyl PPIX by Sulfolane

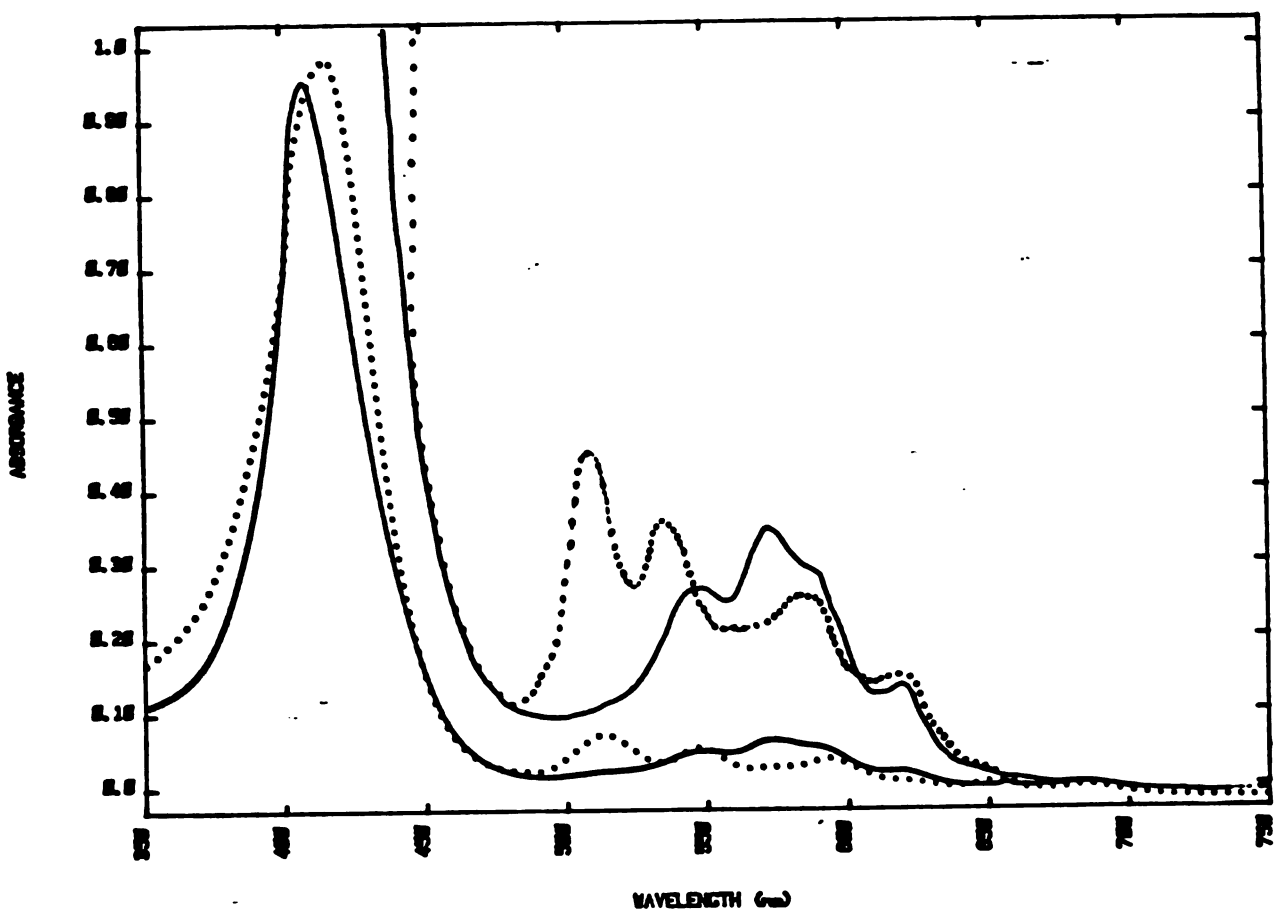

Approximately 10 ug of the PPIX-DAP adduct was dissolved in dichloromethane (-------). Sulfolane was added neat until the spectrum indicated complete formation of the cation had occurred (———). The amount of sulfolane required was 30 µl.

complexes of TPP can be analysed in sulfolane or tetraglyme. It is likely that the difference between these classes of compounds is due to the strength of the ionic bond between the positively charged porphyrin metal complex and the counter ion. If a softer counter ion could be substituted for chloride, it is likely that the PPIX metal complex derivatives would also be amenable to analysis by this method.

4. Electronic Absorption Spectroscopy

Electronic absorption spectroscopy was performed on two instruments. Spectra were normally obtained on a Hewlett Packard 8450A spectrophotometer equipped with a 7225B plotter in 0.5 or 1.0 ml clear-walled cuvettes, but spectra of turbid solutions such as microsomal suspensions were obtained on an Aminco DW-2a instrument in black-walled cuvettes.

5. Infrared Spectroscopy

Infrared spectra were obtained on a Nicolet FT/IR 5 DX spectrophotometer. Compounds were dissolved in chloroform and placed between two NaCl plates for analysis.

6. High Pressure Liquid Chromatography

High pressure liquid chromatography was performed on an Altex system consisting of two pumps, a solvent programmer and a mixer. The column was a Partisil PAC 5 from Alltech, and the detection system a Hewlett Packard 1040A diode array detector interfaced to an HP 85 computer. The zinc complexes of the N-alkylated porphyrins were chromatographed in 1 : 1 tetrahydrofuran: hexanes with a 1 hour 0 - 100% methanol gradient at a flow rate of 1 ml/min. The free-base porphyrins were

usually chromatographed in various mixtures of tetrahydrofuran and hexanes as they were considerably less polar than the zinc complexes.

7. Fluorescence Spectroscopy

Fluorescence spectra and measurements were obtained with a Perkin Elmer 650-10S fluorescence spectrophotometer equipped with a PE 150 Xenon power supply and an analog recorder. The analysis of 7-hydroxycoumarin was performed in 30 mM borate buffer pH = 9.2 in 3 ml quartz cuvettes with excitation at 368 nm and emmission at 458 nm.

8. Nuclear Magnetic Resonance Spectrometry

Nuclear magnetic resonance spectra were recorded with one of three instruments. Routine ^{1}H-NMR spectra of deuterochloroform solutions were obtained on a Varian FT-80 NMR Spectrometer. Chemical shifts were referenced to tetramethylsilane added to the sample. Samples were typically 1 mg in 0.5 ml of solvent and 10 transients were collected.

Porphyrin ^{1}H-NMR spectra were recorded on a GN 500 (General Electric) Spectrometer equipped with a Nicolet 1280 computer system. The zinc complexes of the N-alkylated PPIX derivatives as well as the TPP adducts were dissolved in 0.3 ml of 100% deuterochloroform. Samples of 50 to 100 ug were required. The spectral parameters are listed in Table 2.1.

TABLE 2.1

^{1}H AND ^{13}C-NMR PARAMETERS

Parameter	^{1}H-NMR Value	^{13}C-NMR Value
spectrometer frequency	500.065 MHz	60.99 MHz
sweep width	+/-5000 Hz	+/-50,000Hz
pulse width	10 usec	45 usec
delay time	3 sec	5 sec
number of transients	100-400	8000
block size	16K	16 K
reference line	7.25 ppm ($CHCl_3$)	77.5ppm ($CDCl_3$)
line broadening	0.5 ppm	0.5 ppm
decoupler power	40 Watts	None

^{13}C-NMR spectra were recorded on a custom built 5.6 Tesla NMR spectrometer equipped with a Nicolet 1180 computer system and a ^{13}C probe operating at a spectrometer frequency of 60.99 MHz. The porphyrin samples were dissolved in 2 ml of deuterochloroform in a 10 mm tube. The spectral parameters are listed in Table 2.1. The protein samples were dissolved in D_2O buffer (100 mM KPi, pD = 7.4.) and the same spectral parameters were employed. In this case, the chemical shifts were referenced to free substrate for which the chemical shift was assumed to be the same as it was in the deuterochloroform solution. The line broadening was 2 Hz to increase the signal to noise ratio.

C. Assays

1. Soret Loss

The reduced [Fe(II)] form of P-450 binds CO tightly and produces a Soret band at 450 nm in the electronic absorption spectrum (Omura and Sato, 1964). The difference between this absorbance and that of CO containing oxidized protein at the same wavelength gives an estimate of the concentration of native P-450. These assays were performed on an Aminco DW2A spectrophotometer using microsomes at a protein concentration of 1 mg/ml which corresponds to a P-450 concentration of 2 - 3 nmol/ml. To measure xenobiotic induced Soret loss, 10 ml of microsomes were diluted to a concentration of 1 mg/ml total protein and were incubated with the inactivator at 37°C. NADPH was added to start the reaction and an aliquot of the microsomal mixture was removed at various times and bubbled with CO. The aliquot was placed in a black-walled cuvette and was mixed with 1

- 2 mg of $Na_2S_2O_4$. A reference cuvette was prepared by bubbling an aliquot of the diluted microsomes with CO. The difference spectrum was recorded and the concentration of P-450 determined using the absorbance value: O.D.450-490/91,000 cm^{-1} M^{-1}. The Soret loss was also measured in a purified P-450 system in the same manner, except that in this case the protein concentration was .05 mg/ml and it was not necessary to use the Aminco spectrophotometer because the solution was not turbid.

2. Activity Loss

Many assays have been developed for measuring loss of P-450 activity, but the best activity assay for P-450b, phenobarbital-inducible form, is the loss of 7-ethoxycoumarin (7-EC) deethylase activity (Guengerich, 1978). 7-Hydroxycoumarin is fluorescent, so a very small amount of protein (about 1 ug of P450b) is required per assay.

The enzyme to be assayed (20 - 30 pmol of pure reconstituted P-450b) was added to a vial containing an assay mixture consisting
of 0.5 uM 7-EC and 5mM $MgCl_2$ in 1 ml of buffer C and 1mM NADPH. After 10 minutes, 0.1 ml of 2N HCl was added to stop the reaction, and 0.5 ml of the assay mixture was added to a centrifuge tube containing 2.5 ml of chloroform. The mixture was vortexed vigorously to extract the 7-hydroxycoumarin and centrifuged briefly. A portion of the chloroform layer (0.5 ml) was removed via pipette and added to another centrifuge tube containing 2.5 ml of 30 mM borate buffer (0.18 g boric acid/100 ml water, adjusted to pH 9.2 with 1 N NaOH). This mixture was

again vortexed vigorously and centrifuged. The fluorescence of the aqueous phase was determined on a Perkin Elmer fluorimeter with excitation at 368 nm and emmission at 458 nm. Typically, the activity was determined as a function of time by comparing the relative fluorescence obtained from aliquots of enzyme assayed at different time points to the fluorescence obtained at time 0 and the results reported as percent remaining activity. P-450b oxidizes 7-EC at a rate of 10.2 nmol/min/nmol P-450 under the conditions of the assay (J.S.Lee, unpublished). The extent of 7-EC deethylase activity was also occasionally used to measure competitive inhibition by other substrates or inhibitors. For these measurements, the competitive inhibitor was pre-incubated with enzyme in the absense of NADPH before the 7-EC activity was measured.

3. NADPH Consumption

P-450 uses two reducing equivalents from NADPH in the normal turnover of substrates and has been shown occasionally to use 4 equivalents in uncoupled turnover. The stoichiometry of NADPH and substrate turnover has been measured in some experiments to determine if uncoupling is occurring. The enzyme used in these studies was reconstituted as usual except that buffer C was chelexed because metals in the solution considerably increase the background NADPH consumption. NADPH consumption was monitored continuously at 340 nm immediately after addition of 0.2mM NADPH (O.D. = 2 at time 0). This was done for short times using the HP8450A absorption spectrophotometer. A simple method file was set up to monitor the absorbance at 340 nm every 3 seconds for 2

minutes and the data were plotted. Lines were calculated directly from the data by linear regression analysis. The method was: Meas to Abs 1 340 Yscale 0 to 1 Time 3,2,1 to 120. The line was fitted by calculating the avg dA/dT over the linear portion of the curve.

4. Determination of K_S of Phenylacetylene binding to P-450b

The reversible binding of substrates to cytochrome P-450 often results in a spin state change that can be observed by electronic absorption difference spectroscopy. If the substrate has no iron-coordinating groups, its binding will be of "Type 1" because it will cause a decrease in the low-spin form (O.D. 386nm) and an increase in the high spin form (O.D. 418 nm) (Schenkman et al, 1967). The concentration of substrate which saturates the enzyme can be determined using this assay by carefully adding small amounts of substrate in dimethylsulfoxide until the absorbance change reaches a maximum. This assay was performed with pure reconstituted P-450 on the HP 8450A spectrophotometer.

The binding constant for phenylacetylene to purified P-450b was assayed in 1 ml of reconstituted P-450b which was split into two cuvettes. Aliquots of 1 ul of a 182 mM phenylacetylene solution in dimethylsulfoxide (182 nmol /ul) were added to the sample cuvette while parallel additions of dimethylsulfoxide alone were made to the reference cuvette. The amount of phenylacetylene necessary to cause saturation was 1.6 mM, so the concentration of substrate which causes half saturation of binding (K_S) was 0.8 mM.

5. $^{18}O_2$ Incorporation

The incorporation of labeled oxygen was determined for biphenylacetylene. An incubation mixture containing hepatic microsomes (100 ml, 4 nmol/ml), biphenylacetylene (0.2 mmol), glucose-6-phosphate dehydrogenase (500 units), and $MgCl_2$ (40 mg) was placed in a sealed flask that was repeatedly evacuated to a pressure of 50 - 60 torr and brought back to atmospheric pressure with nitrogen gas (15 cycles). A solution of glucose-6-phosphate (0.8 mmol) and NADP (0.1 mmol)was bubbled with nitrogen gas to remove oxygen, and was added to the incubation via syringe. The complete mixture was evacuated and purged three more times, and $^{18}O_2$ was introduced by breaking the seal of an ampoule containing 3.66 mmol of 99.8% $^{18}O_2$ which was connected to the reaction vessel via vacuum tubing. Nitrogen gas was then introduced to bring the pressure within the reaction vessel back to atmospheric as assessed by a balloon attached to the apparatus. The reaction vessel was incubated at 37°C for 3 hours and was then quenched by adding 2N HCl to bring the pH to 4. The protein precipitated and the entire mixture was extracted with dichloromethane. The resulting emulsion was cleared by adding saturated NaCl and allowing the mixture to stand over night. The dichloromethane was removed by rotary evaporation and the residue was treated with excess diazomethane and analysed by GC/MS. A control incubation was carried out with unlabeled oxygen exactly as described for the labeled sample.

6. Biphenylacetylene Oxidation

Biphenylacetylene oxidation by meta-chloroperbenzoic acid

(MCPBA) or by microsomal P450 was assessed by an electronic absorbance assay. The product of biphenylacetylene oxidation is biphenylacetic acid or its methyl ester if the reaction is carried out in the presence of methanol. These compounds have the same absorbance spectrum with λ max = 254 nm and an extinction coefficient of 4.2×10^4. Biphenylacetylene itself has λ max = 273 nm and $e = 7.2 \times 10^4$. The absorbance band is broad so that a mixture of reactant and product shows only one band, but the absorbance at 273 nm went down linearly with time, and the absorbance at 254 nm increased at the same rate. Since the reactions were sometimes diluted, all data were normalized to the sum of the absorbance at 254 nm + absorbance at 273 nm for the time of the measurement divided by that for time 0. This normalization does not account for the difference in extinction coefficients, but the difference is insignificant if the reaction is studied when only a small amount of reactant is converted to product. The equations that convert the $O.D._{273}$ into the concentration of biphenylacetic acid methyl ester are presented below:

$$O.D._{273} = [\text{acetylene}]E_{273\text{acetylene}} + [\text{acid}]E_{273\text{acid}}$$

$$[\text{acetylene}]_o = [\text{acetylene}] + [\text{acid}]$$

$$O.D._{273} = ([\text{acetylene}]_o - [\text{acid}])E_{273\text{acetylene}} + [\text{acid}]E_{273\text{acid}}$$

$$= [\text{acid}](E_{273\text{acid}} - E_{273\text{acetylene}}) + E_{273\text{acetylene}}[\text{acetylene}]_o$$

$$[\text{acid}] = \frac{\text{O.D.}_{273} - E_{273\text{acetylene}}[\text{acetylene}]_o}{(E_{273\text{acid}} - E_{273\text{acetylene}})}$$

$$= \frac{\text{O.D.}_{273} - (\text{O.D.}_{273})_o}{-7 \times 10^4}$$

Where the extinction coefficients are as follows:

$E_{273\text{acetylene}} = 7.2 \times 10^4$

$E_{273\text{acid}} = 0.2 \times 10^4$

From the slopes of the lines obtained and the extinction coefficients, one can obtain the amount of biphenylacetylene in the reaction which has been converted to biphenylacetic acid. In the enzymatic reaction, the microsomes were acidified and extracted with dichloromethane and measurements were made on the extract so that protein absorbance did not interfere with the measurement.

7. Phenylacetylene Oxidation

The oxidation of phenylacetylene to phenylacetic acid was assessed by gas chromatography. Two variations of the assay were used; packed column gas chromatography was used to analyze the chemical and microsomal oxidation reactions, and capillary column gas chromatography was used to analyze the pure enzyme oxidations. The chemical and microsomal reactions were analyzed on a glass column packed with 3% OV 17 with benzoic acid added to the samples as an internal standard. For the enzymatic

reactions, 3.5 ml aliquots of microsomal protein were removed from 15 ml microsomal incubations containing 5mM phenylacetylene at various times after addition of 1mM NADPH and were added to a vial containing 3 ml of 2N HCl, 10 ml of ether, and 4 ul of a 1 mg/ml solution of benzoic acid. The mixture was immediately shaken and the ether layer separated and treated with 0.3 ml of diazomethane. The resultin ester samples were concentrated to 20ul and a lul aliquot was injected into the gas chromatograph. Analysis with the oven temperature held at 120°C gave retention times of 1.3 minutes for phenylacetylene, 2.4 minutes for the internal standard, and 4.2 minutes for methyl phenylacetate. Standard curves were constructed from samples of microsomes to which increasing amounts of phenylacetic acid had been added.

The modified assay used in the purified enzyme studies employed an HP 5890 capillary gas chromatograph. The internal standard in this instance was 4-phenyl-1-butyric acid because the pure enzyme extract contained a compound that coeluted with the methyl benzoate. Aliquots (1 ml) of reconstituted enzyme were removed from the reaction and added to vials containing 1 ml of 2N HCl, 5 ml of ether, and 3 ul of a 1 mg/ml solution of internal standard in methanol. The vials were shaken immediately and the ether separated and treated with 0.3 ml of ethereal diazomethane to methylate the carboxylic acids. The ether solutions were then concentrated to 20 ul and 1 ul aliquots were injected into the capillary gas chromatograph. The retention times were 9.7 min for methyl phenylacetate and 18.7 minutes for the internal standard when analyzed with the oven temperature at 110°C.

8. Oxidation of Substituted Acetylenes

The assays for oxidation of the substituted phenylacetylenes were patterned after the capillary gas chromatography assay described above for phenylacetylene. The chromatographic conditions for analysis of the products obtained from substituted acetylenes were the same as for phenylacetylene, except that the products from p-nitrophenylacetylene were analyzed at 180 °C. In this case, the internal standard came off before the methyl p-nitrophenylacetate. Table 2.2 gives the retention times for the methyl esters obtained from each of the substituted acetylenes.

TABLE 2.2

Retention Times for the Substituted Methyl Phenylacetates

Substituent	Retention Time (min)	[temperature]
p-CH_3	12.90	[110°C]
p-H	8.95	[110°C]
p-Cl	18.01	[110°C]
o-CH_3	12.65	[110°C]
p-NO_2	16.72	[180°C]

The retention time of the internal standard was 18.41 minutes except in the case of the p-NO_2 derivative, where it was 9.05 minutes.

Again, standard curves were generated for each ester product using standards obtained from Aldrich.

9. Heme Adduct Formation

The formation of heme adducts during the turnover of xenobiotics by P-450 can be assayed by in vivo or in vitro procedures. The choice between the two depends on the probable bioavailability of the xenobiotic. Heme adducts were formed in vivo by injecting approximately 20 phenobarbital pretreated rats with the substrate in dimethylsulfoxide solution. If the sample was a liquid, it was occasionally injected neat. After 3 to 4 hours, the rats were decapitated and their livers perfused with cold 1.15% KCl and homogenized in a Waring Blender. The homogenate was treated overnight with 2 - 4 liters of cold 5% H_2SO_4 in methanol. The extract was filtered to remove the precipitated protein, diluted 1 :1 with distilled water, and extracted twice with dichloromethane. The combined extracts were washed with water until they were no longer acidic, dried over anhydrous sodium sulfate, and concentrated by rotary evaporation in a 30^{o}C water bath. A solution of 20 mg zinc acetate in methanol was added and the residue was evaporated to dryness. The resulting porphyrins were chromatographed on 2000 uM silica gel G thin layer chromatography plates (Analtech) in 3 : 1 chloroform :acetone. The band containing the heme adduct was green and fluoresced red under ultraviolet light. Further purification was effected by a second thin layer chromatography step in 1:1 tetrahydrofuran:hexanes followed by HPLC on a Partisil PAC5 column with a 0-100% gradient of methanol into 1:1

tetrahydrofuran:hexanes. Yields depended on the substrate and ranged from 40 -800 ug.

The in vitro isolation procedure began with preparation of rat liver microsomes from 10 rats. The microsomes were diluted in 800 mls (3 - 5 nmol /ml) and the substrate (10 mM) was added. After preincubation for 5 minutes at 37°C, an NADPH regenerating system consisting of 1600 units of glucose-6-phosphate dehydrogenase, 270 mg $MgCl_2$, 1 g of glucose-6-phosphate, and 650 mg of NADP was added. After a period of 30 minutes to 1 hr, the entire microsomal mixture was poured into 3.5 liter of cold 5% H_2SO_4 in methanol and allowed to stand overnight at 4°C. The rest of the work-up was the same as for the in vivo isolation procedure.

10. Magnetic Susceptibility

Magnetic susceptibility was determined for the TPP-diazoacetophenone model complex in order to confirm the oxidation and spin states of the iron in the complex. The experiment, which followed that described by Evans (1959), was performed using a GN 500 NMR spectrometer. A solution of 5.1 mg of the TPP-DAP complex in 1 ml of deuterochloroform was prepared. Tetramethylsilane (2 ul) was added to the solution and about 1/10 as much was placed in a capillary (melting point) tube also containing deuterochloroform. The capillary tube was placed in the NMR tube containing the solution of TPP-DAP and the levels of the solutions were made equal. The NMR of the sample was determined at a sweep width of +/-200 Hz with the TMS peaks were in the middle of the spectrum. The small sweep width increased

the number of data points and thus the accuracy of the measurement. The paramagnetic character of the TPP-DAP complex causes the TMS methyl resonances to shift, and this chemical shift difference can be used to calculate the magnetic susceptibility by the following equation:

$$\mu_{eff} = [3kT\ X_{mol}/N\ u_B]^{1/2}$$

where the constants are defined as follows:

k = Boltzman's constant (1.38×10^{-16} ergs $^{o}K^{-1}$)

T = Temperature (293 ^{o}K)

N = Avogadro's number (6.02×10^{23})

μ_B = Bohr Magneton (9.27×10^{-21} erg gauss^{-1})

X_{mol} =[(3(f1-f2)/2 " f m) - 0.497×10^{-6}] x 788

where f1-f2 is the frequency difference of the TMS signals in the NMR experiment

f is the spectrometer frequency

m is the concentration of the compound in mg/ml

0.497×10^{-6} is the solvent correction

788 is the molar weight of the TPP-DAP complex

D. Proteins and Microsomes

1. Microsomes

Cytochrome P-450 can be obtained in an active form by isolating the microsomal fraction from rat livers. Male Sprague

Dawley rats were pre-treated with phenobarbital by daily intraperitoneal injection of a dose of 80 mg/kg in water for 4 or 5 days. On the day following the last injection, the rats were decapitated, their livers perfused with cold 1.15% KCl and homogenized in the same solution in a dounce homogenizer with a teflon pestle. The homogenate was centrifuged at 10,000g for 20 minutes to remove organelles and cellular debris. The microsomal fraction, isolated by centrifugation at 100,000g for 1 hour, was washed once with the KCl solution and centrifuged again for 1 hour. The final microsomal pellet was resuspended by homogenization in 100 mM Na/ K phosphate buffer containing DETAPAC. Just prior to use, the microsomes were diluted to 2 - 3 nmol/ml P-450 with the same buffer solution.

2. Purified P-450b

The purified cytochrome P-450 was obtained from rat liver microsomes prepared from 30 rats. The details of the purification procedure (Waxman and Walsh, 1982) are presented in Appendix II. In a typical preparation, 5 - 7 g of microsomal protein was obtained. The preparation of pure P-450 can be performed at room temperature as long as the stabilizing non-ionic detergent Emulgen 911 is present. The P-450 was solubilized with sodium cholate and the portion precipitating in 10 - 16% polyethyleneglycol was collected. This hemoprotein fraction contained P-450b, the major phenobarbital inducible P-450, as well as cytochrome b_5. The polyethyleneglycol precipitate was loaded onto a column of DE 52 and the phosphate concentration was increased slightly. This caused the P450 to form a band

about midway down the column and the b_5 to band at the top. These bands were each extruded and the portion of the gel containing the P-450 was loaded directly onto a second column of DE 52. The further purification of b_5 is described in Appendix II. A typical chromatogram from the second P-450 DE52 column is shown in figure 2.2. The yield after this column was usually 30 - 50 mg of protein. The fractions were separated at the point indicated by the arrow and the principal peak (which contained P-450b) was chromatographed on Biogel HTP to remove P-450e. P-450e can be isolated from the tail fractions (Chromatogram in Figure 2.2) obtained from the DE52 column. Finally, the emulgen was removed from the pure P-450b by chromatography on HTP by exchanging the emulgen for cholate which can be removed by extensive dialysis. The final yield of protein was 300 - 500 nmol or 20 - 30 mg of protein with a specific content of 12 - 15 nmol P-450 per mg protein and no detectable P-420. The protein was pure as assessed by SDS PAGE performed with the Bio-Rad electrophoresis kit by the method of Laemmli, 1970. A typical gel is shown in Figure 2.3. P-450 reductase was purified by the method of Shephard et al (1983) and is described in detail in Appendix II. Briefly, microsomes were prepared from 30 rats as described above. The proteins were solubilized in buffer containing phenylmethanesulfonyl fluoride, a protease inhibitor, by Na cholate extraction as described for P-450. The solubilized mixture was cleared of RNA and some proteins by protamine sulphate precipitation, and the entire mixture was loaded on the affinity resin 2',5'-ADP Sepharose. After several washes, pure

Figure 2.2

Purification of P-450b by DE 52 Chromatography

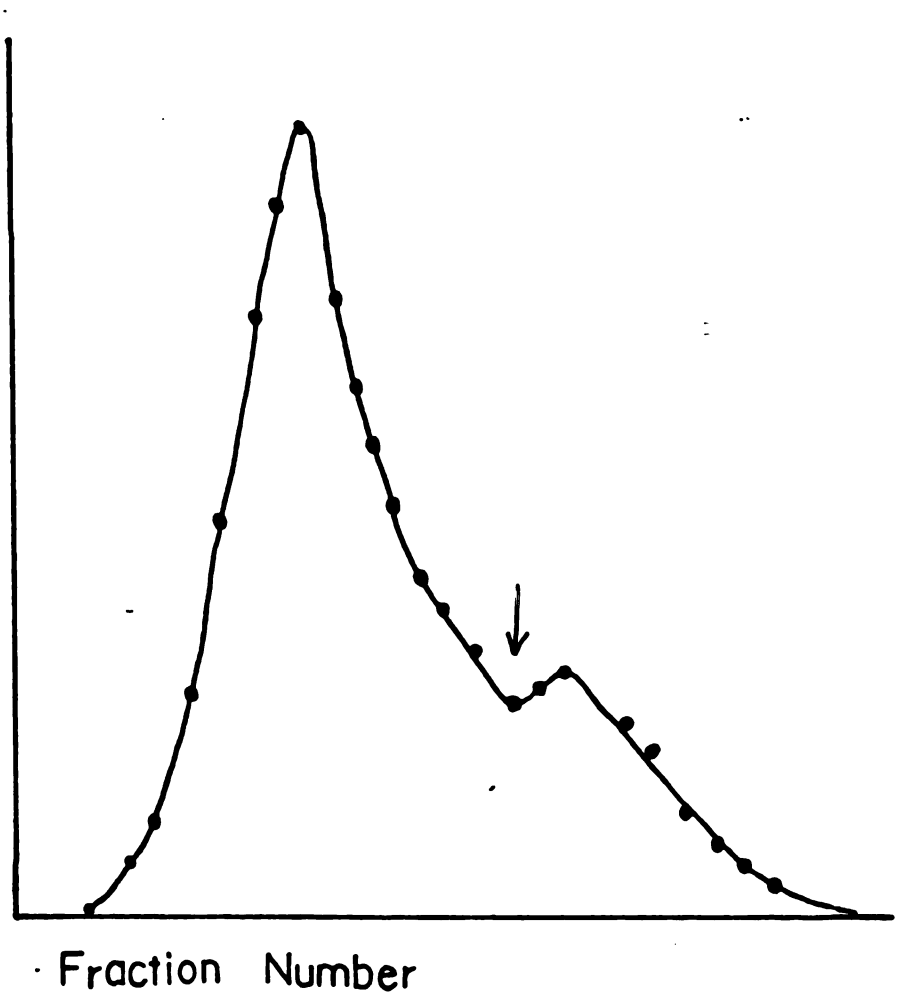

The amount of P-450 in each fraction was determined by monitoring the absorbance of the Soret (420 nm). The large peak is P-450b and the trailing peak P-450e.

Figure 2.3

A Typical SDS Polyacrylamide Gel of Purified P-450b, P-450 Reductase and Cytochrome b_5

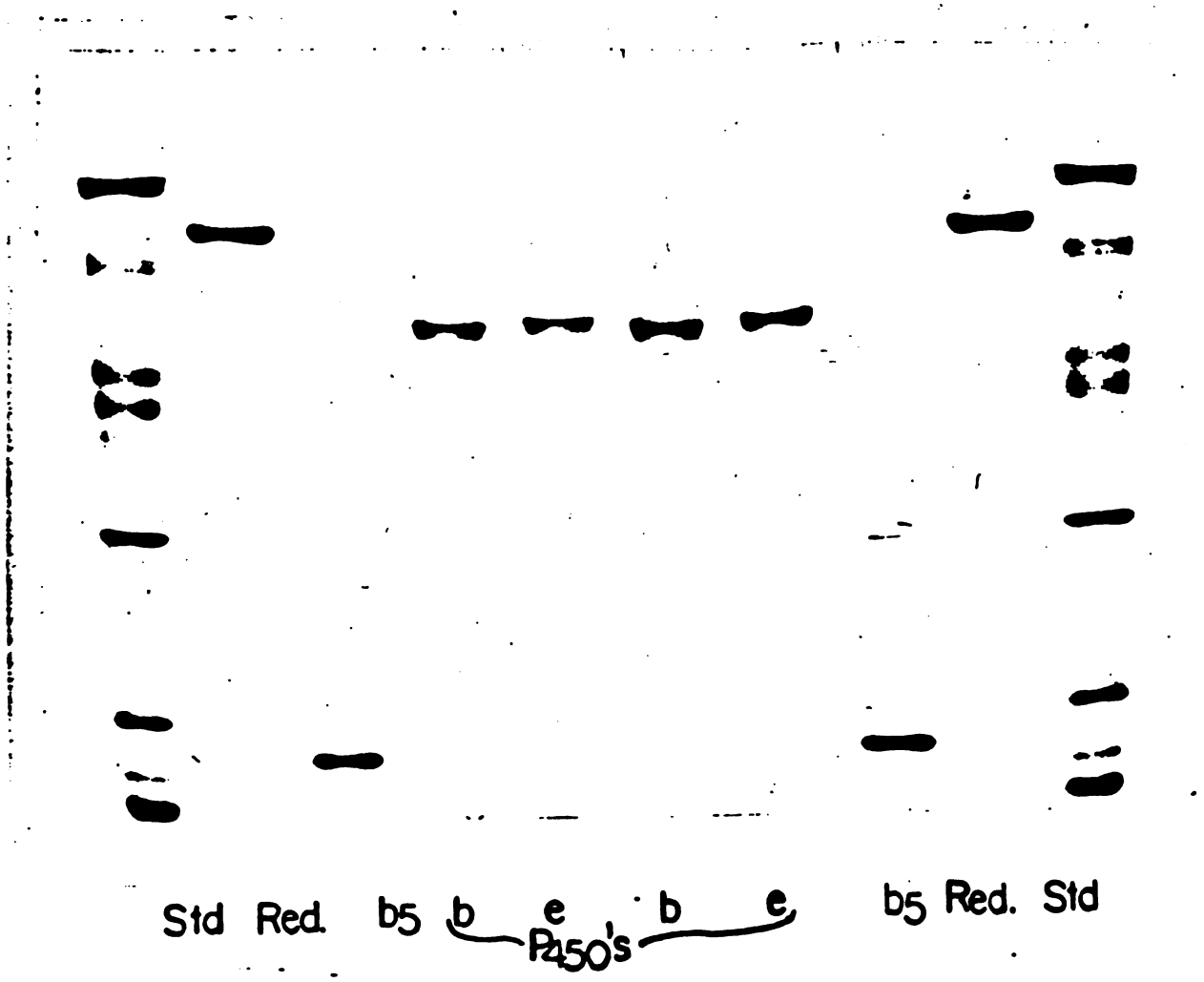

Purified P-450, Reductase and b_5 were analysed by SDS Gel Electrophoresis. The lanes are labelled. Molecular weight standards (94, 67, 43, 30, 20, 14 kD) are in lanes 1 and 10.

P-450 reductase was eluted, and the cholate was removed by extensive dialysis as described for P-450. The purity of the reductase was assessed by SDS PAGE (Figure 2.3) and by activity assays. (Appendix II). The activity was always greater than 40 umol cytochrome c reduced / min/mg protein.

3. Reconstitution

The purified P-450 was reconstituted with its reductase by mixing 1 nmol of P-450 with 2 nmol of reductase and adding 20 ul of a 2 mg/ml solution of dilauroylphosphatidylcholine (Serdary Research Labs, Port Huron Michigan)in water containing 1 mM DETAPAC. This mixture was incubated for 10 minutes at room temperature, and then diluted to 1 ml with buffer C (Appendix II). Substrate can then be added and assays performed. This reconstitution scheme was optimized for the amount of lipid and the amount of reductase, always keeping the concentration of P-450 at 1 nmol/ml. The data shown in Figure 2.4 demonstrate that 40 ug/ml dilauroylphosphatidylcholine and 2 nmol/ml reductase are optimal. Experiments also demonstrated that reaction rates are faster at 37^{o}C than at room temperature, so all incubations were at 37 ^{o}C.

4. Cytochrome b_5 Experiments

Purified cytochrome b_5 was occasionally added to the reconstitution system. Waxman and Walsh (1982) reported a potentiation of 7-EC deethylase activity when b_5 was added to the reconstitution system at the same time as the reductase and P-450, but this effect was not observed in our hands. We found instead that 2 nmol/ml reductase in the absence of b_5 gives

Figure 2.4

Optimization of P-450 Reconstitution with P-450 Reductase and Dilauroylphosphatidylcholine

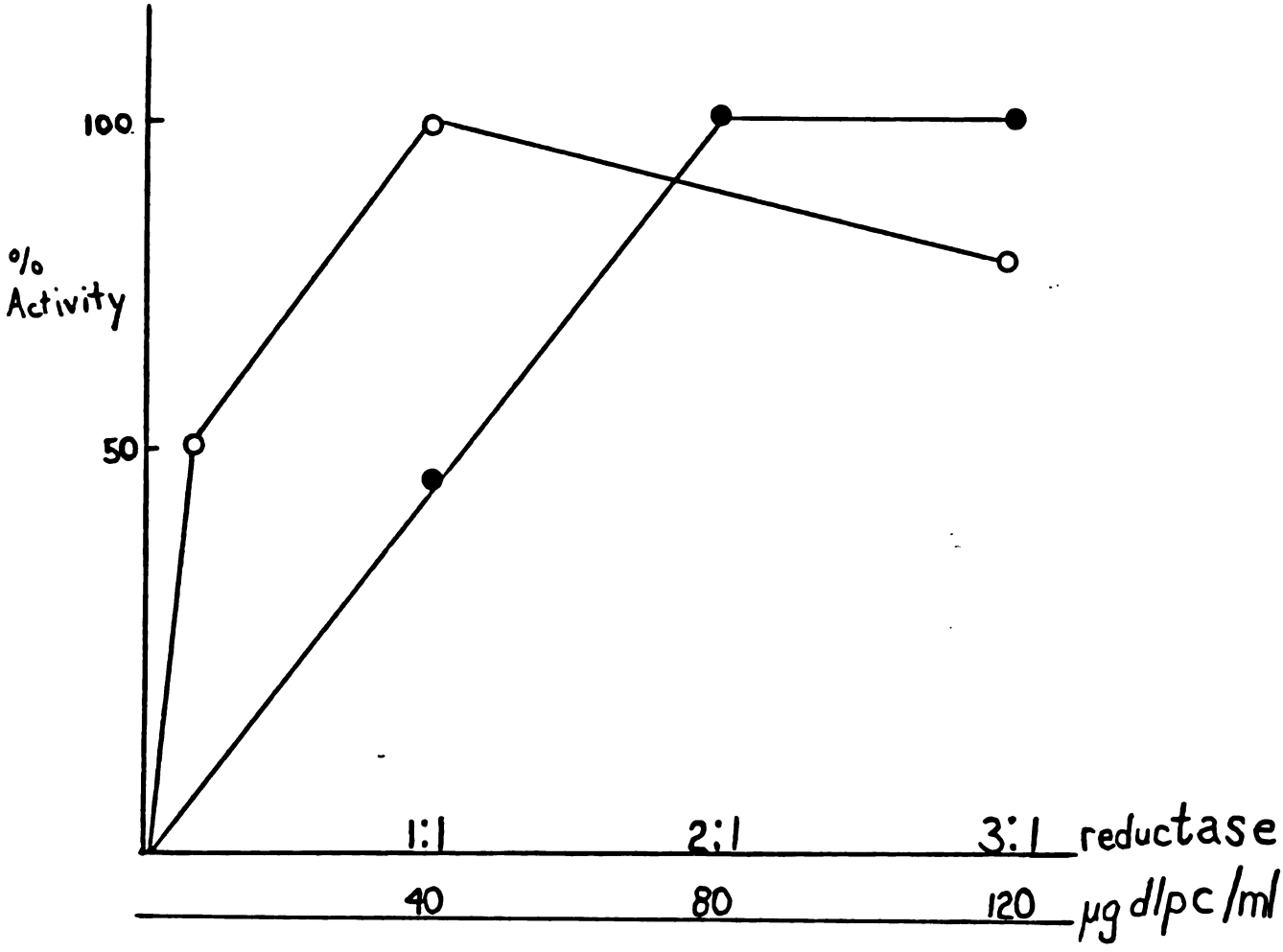

Cytochrome P-450 (1 nmol) was reconstituted with varying amounts of reductase (1, 2, or 3 nmol) (●) and with varying amounts of a sonicated solution of dilauroylphosphatidylcholine (○).

maximal activity and that b_5, under all conditions, inhibits 7-EC activity by at least 50%. This is in agreement with observations reported by Coon's group, who described the method of addition of b_5 to the reconstitution system that we now use (Gorsky and Coon, 1986). They demonstrated that no inhibition is observed if b_5 is added after reconstitution and dilution of the protein mixture.

Addition of b_5 to the purified, reconstituted P-450b with phenylacetylene dramatically affects the partition ratio (Chapter 4). In an attempt to determine whether these effects were due to the ability of b_5 to transfer electrons to P-450 (see Chapter 1 for discussion) or merely to a protein effect, a cytochrome b_5 derivative incapable of transferring electrons was required. The preparation of b_5 in which the heme iron was replaced by manganese has been described (Cinti and Ozols, 1975). PPIXMn(II) was introduced into apo b_5 as described by these authors, but the apo b_5 was prepared by extraction with 2-butanone followed by dialysis against buffer D (Appendix II). The overall yield was 65%. The absorbance spectrum of the native b_5 and the manganese substituted b_5 are shown in Figure 2.5. The specific content of the protein was 55 nmol/mg protein and the protein was pure as assessed by SDSPAGE.

E. Model Reactions

1. Meta-Chloroperbenzoic Acid Oxidations

The meta-chloroperbenzoic acid (MCPBA) oxidation of some acetylenic substrates was studied to model the cytochrome P-450 oxidation reaction as well as to determine if an isotope effect

Figure 2.5

Electronic Absorption Spectra of Cytochrome b_5 and Manganese-Substituted Cytochrome b_5

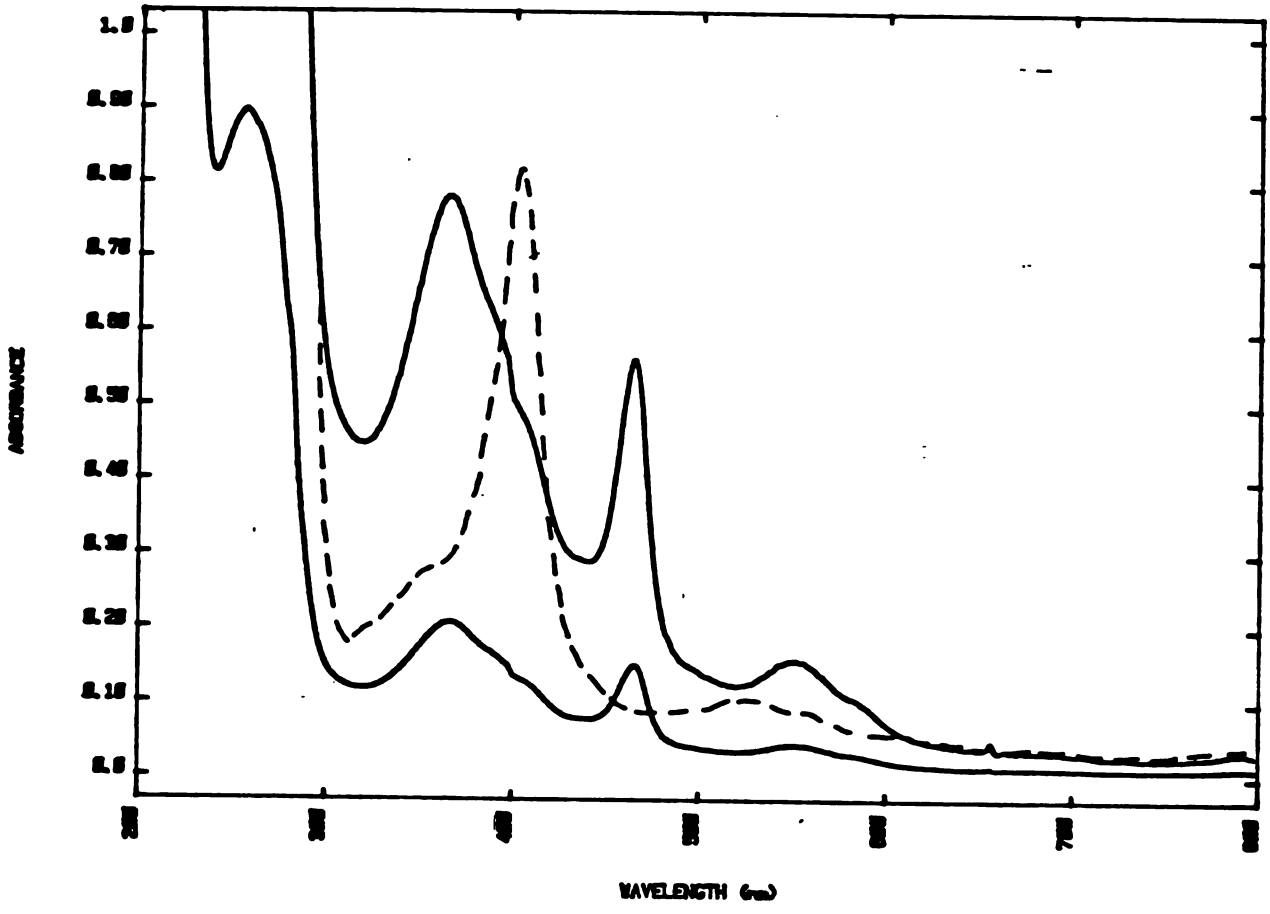

Electronic Absorption Spectra of Cytochrome b_5 (- - - - -) and Manganese- Substituted Cytochrome b_5 (————). The Manganese-b_5 shows the split Soret band typical of Manganese PPIX.

occurred in the chemical oxidation reaction. Initial work followed that of Ortiz de Montellano and Kunze (1980), but later, the reaction conditions were altered in an attempt to increase the oxidation rate. It should be noted that the turnover of acetylenes by MCPBA is extremely slow under even the best conditions. The MCPBA utilized in these studies was dissolved in ether, washed thrice with a 100 mM potassium phosphate buffer, dried over sodium sulphate, and crystallized prior to use to remove m-chlorobenzoic acid.

The oxidation of biphenylacetylene was monitored by an electronic absorption method. A three-fold molar excess of MCPBA dissolved in 1 ml of dichloromethane was added to a solution of 19 mg (0.1 mmol) of either biphenylacetylene or [1-^{2}H]biphenylacetylene in 10 ml of dichloromethane containing 1% (v/v) methanol. Small aliquots (10 ul) were withdrawn at various times from the stirred mixture and added to 10 ml of dichloromethane. The absorption of these solutions at 273 nm(the λ max of biphenyalcetylene) and 254 nm (the λ max of biphenylacetic acid) were recorded. The details of the assay are presented in Section C.5. The reaction kinetics were calculated for both substrate disappearance and product formation. More MCPBA was added at 12 hour intervals. The kinetics were linear throughout the reaction time. The presence of MCPBA did not interfere with the assay because its extinction coefficient is much less than that of the biphenyl compounds.

The oxidation of phenylacetylene was studied by the gas chromatography assay described in the "Assays" section. A 0.25 M

solution of MCPBA in dry benzene was prepared and split into two 20 ml aliquots. Phenylacetylene or [1-^{2}H]phenylacetylene was added neat to the aliquots so that the final concentration of the acetylene was 0.25M. Small aliquots of 0.2 ml were withdrawn from the reaction mixtures at various times and were added to a biphasic mixture of 0.8 ml of benzene and 1 ml of a 0.1% bicarbonate solution containing the internal standard. The mixture was extracted and the organic layer containing the unreacted substrate was removed. The aqueous layer was acidified with 2 ml of 2N HCl and the phenylacetic acid product was back extracted into ether. The ether solution was methylated with diazomethane and analyzed by the gas chromatography assay.

2. Fenton's Reagent Oxidations

Phenylacetylene was oxidized by Fenton's Reagent to determine if the oxidation by P-450 could be modeled by hydroxyl radical oxidants. Phenylacetylene or [1-^{2}H]phenylacetylene (final concentration 0.25M) was added to a rapidly stirred, freshly prepared mixture of $FeCl_2$ (0.25M) and hydrogen peroxide (0.25M) in 10 ml of distilled, deionized water at 25^{o}C. The mixture was stirred for 24 hours, but gas chromatographic analysis indicated that the reaction was complete almost immediately. The organic products were extracted with ether, methylated with diazomethane, and analysed by GC/MS.

3. Porphyrin Models

Tetraphenylporphyrins (TPP) are often used to model cytochrome P-450 catalysis. "Carbene" complexes analogous to those thought to occur in P-450 have been generated by reducing

the Fe(III) TPP with activated iron powder under anaerobic conditions, a process that mimics reductive turnover by P-450. The reduced porphyrin, which is unstable to oxygen, was typically generated in situ under anaerobic reducing conditions. All solvents were placed over molecular sieves to remove water and degassed immediately before use by pumping to 0.1 torr and then purging with argon at least 7 times, or until the solvents "crack". Schlenk tubes and a vacuum manifold were used for these procedures. Iron powder (500mg) was placed in a Schlenk tube with a stir bar and was activated by washing twice with glacial acetic acid, then twice with methanol and finally with the reaction solvent which is 9:1 dichloromethane:methanol. A solution of TPPFe(III)Cl plus the reactant, usually diazoacetophenone, in a 1:1 ratio was degassed and added to the activated iron powder via a cannula. The solution was allowed to stir for 30 minutes to 1 hour. The product was isolated by pumping away the solvent. This procedure was adapted from Bruice et al (1981). Often the products of these reactions were stable adducts of the reactant with the porphyrin, that could be isolated by filtration of the dichloromethane solution and recrystallization from dichloromethane-pentane mixtures.

CHAPTER 3

KINETIC ISOTOPE EFFECTS ON THE OXIDATION OF ACETYLENES

A. Biphenylacetylene Oxidation

Previous work in this laboratory (Ortiz de Montellano and Kunze, 1980 and 1981) demonstrated that if the acetylenic hydrogen in biphenylacetylene was replaced by deuterium, the product of the chemical or cytochrome P-450 mediated oxidation was biphenylacetic acid in which the deuterium had shifted quantitatively to the vicinal carbon. Furthermore, labeling of the benzylic carbon of the acetylene with ^{13}C showed that the shift involved the hydrogen and not the biphenyl group (Ortiz de Montellano and Kunze, 1981). A mechanism was initially proposed that invoked an intermediate oxirene that could rearrange to yield the biphenylacetic acid metabolite, as well as undergo attack by the porphyrin ring nitrogen to form a heme adduct (Ortiz de Montellano and Kunze, 1980b). The proposed mechanism was presented in Scheme 1.5. As a test of this mechanism, and as a possible probe of the catalytic mechanism, a search was made for a kinetic isotope effect on the observed 1,2 shift. Initial studies were also designed to confirm the identity of the metabolite and the probable mechanism of its formation.

McMahon et al (1981) observed a kinetic isotope effect on the oxidation of biphenylacetylene when the acetylenic hydrogen

was replaced with deuterium. To explain this result, they proposed that the oxygen was inserted into the carbon-hydrogen bond. The quantitative shift of the acetylenic hydrogen to the benzylic carbon observed in our laboratory (Ortiz de Montellano and Kunze, 1980; 1981) argued against this hypothesis, but confirmation that the oxygen was actually provided by the enzyme was necessary. A ketene intermediate is expected if the hydrogen shifts during oxygen transfer, so that only one atom of $^{18}O_2$ should be incorporated into the biphenylacetic acid (Scheme 3.1).

1. $^{18}O_2$ Incorporation

The incubation of $^{18}O_2$ with hepatic microsomes and biphenylacetylene was performed (Chapter 2), the metabolic extract methylated with diazomethane, and the reaction mixture analysed by GC/MS. A control mixture from an incubation under an unlabeled oxygen atmosphere was analysed in the same way, and the results were compared. The GC/MS scans for the appropriate chromatographic peak were summed and a mass spectrum was recorded. The percent incorporation was calculated from the peak height at 228 (molecular ion of the ^{18}O-labelled compound) versus the sum of the peak heights at 226 (molecular ion of the unlabelled compound) plus that at 228. The amount of ^{18}O incorporated (79.6%) was calculated from the mass spectra which are shown in Figure 3.1. There were no ions at m/e = 230 indicating that only one atom of ^{18}O was incorporated into each biphenylacetic acid molecule. This result is consistent with π-bond oxidation similar to that caused by MCPBA (Lewars, 1983) in which the intermediate ketene is formed (Scheme 3.1). The ketene

Figure 3.1

^{18}O Incorporation During the Oxidation of Biphenylacetylene by Microsomal P-450

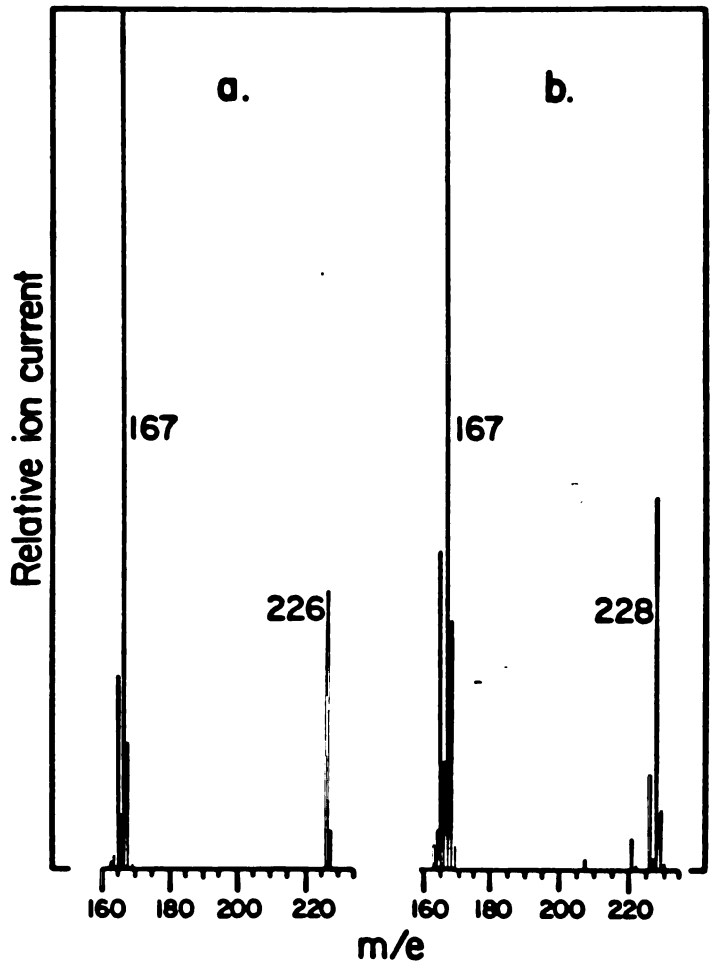

Mass spectra of methyl biphenylacetate obtained from incubations of biphenylacetylene with microsomes from phenobarbital-induced rats under (a) a normal atmosphere and (b) and atmosphere of $^{18}O_2$. The lower mass regions are not shown.

Scheme 3.1

The Mechanism of ^{18}O Incorporation into Biphenylacetylene During Its Oxidation by P-450

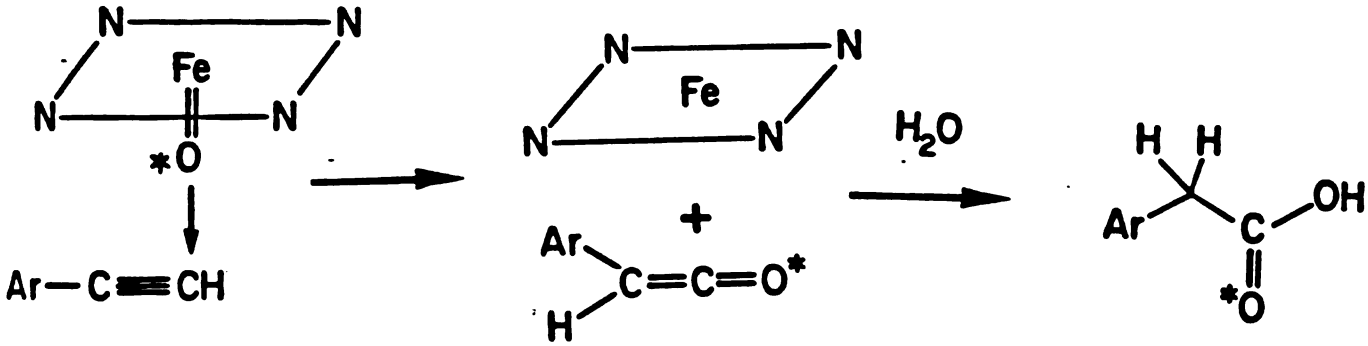

thus forms via the 1,2 shift of the acetylenic hydrogen as has been proposed in this laboratory.

2. Kinetic Isotope Effect on Biphenylacetylene Oxidation by Peracids

The kinetic isotope effect observed by McMahon et al (1981) appeared to be occurring by a mechanism similar to that known to occur when arylaceylenes are oxidized by MCPBA. The possibility that the oxidation of biphenylacetylene by MCPBA may also manifest a kinetic isotope effect was investigated using the same reaction conditions and spectrometric assay described for the metabolic studies. In this experiment, the corrected absorbance was plotted directly and the amount of biphenylacetic acid methyl ester was calculated from the slope. The change in absorbance at 273 nm as well as the change in absorbance at 254 nm were linear over 24 hours as long as more MCPBA was added at 12 hours. A plot of the lines is shown in Figure 3.2. The kinetic isotope effects were calculated from the slopes and are listed in Table 3.1.

Figure 3.2

Oxidation of Biphenylacetylene and [1-^{2}H]Biphenylacetylene by Metachloroperbenzoic Acid

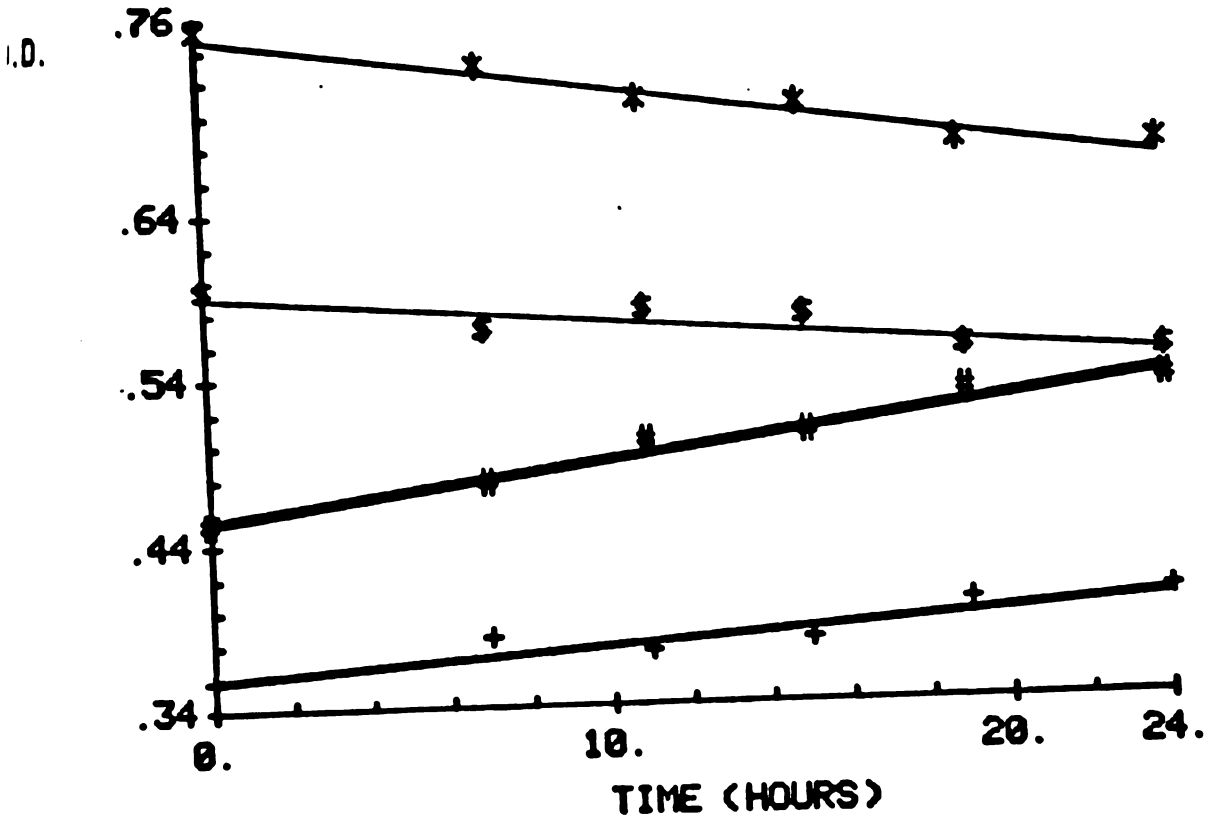

Analysis by electronic absorption spectroscopy of reactions of biphenylacetylene (*, #) or [1^{2}H]biphenylacetylene ($, +) with metachloroperbenzoic acid in benzene solution containing 1% methanol (room temperature). The absorbance at 273 nm was monitored to determine loss of biphenylacetylene, and the absorbance at 255 nm was monitored to determine the production of methyl biphenylacetate.

TABLE 3.1

Kinetic Isotope Effects on Acetylene Oxidations

Substrate (Oxidant)	Kinetic Isotope Effect
biphenylacetylene	
MCPBA	[a]1.73 (methylbiphenylacetate production)
	[a]1.90 (loss of biphenylacetylene)
	avg. = 1.8 ± 0.1
microsomal P-450	[b]1.4 ± 0.2
phenylacetylene	
MCPBA	[a]1.7 ± 0.3
microsomal P-450	[a]1.8 ± 0.2 (gas chromatography assay)
	[a]1.6 ± 0.2 (GC/MS assay)
microsomal P-450 (low substrate)	[b]1.2 ± 0.2 (gas chromatography assay)
purified P-450b	[a]1.8 ± 0.2 (GC/MS assay)
purified P-450b (25°C)	[a]1.1 ± 0.2 (GC/MS assay)

note: The errors are [a]the standard deviations of the slopes determined by linear regression, or [b] the standard deviations of averaged values obtained at a single time.

Although the reaction of MCPBA with biphenylacetylene is

extremely slow, the kinetics were clean enough to measure the kinetic isotope effect. The rate of the 1,2 shift of the acetylenic hydrogen is thus clearly sensitive to isotopic substitution. An isotope effect should therefore be observed in the enzymatic reaction if the rate limiting step is the isotopically sensitive step.

3. Kinetic Isotope Effect on Biphenylacetylene Oxidation by P-450

The absorbance assay (Chapter 2) was used to compare the rates of microsomal oxidation of biphenylacetylene and [1-^{2}H]biphenylacetylene. Microsomes (10 ml at 3 nmol P-450/ml) were incubated at 37^{o}C with biphenylacetylene or [1-^{2}H]biphenylacetylene and NADPH regenerating system. At 10, 20 and 30 minutes after addition of the NADPH, 1 ml aliquots were removed and added to vials containing 9 ml of 5% H_2SO_4 in methanol. The vials were allowed to stand overnight at 4^{o}C to precipitate the protein. A portion (5ml) of each solution was then transferred to a vial containing 5 ml of water and 5 ml of dichloromethane. The mixture was extracted, and the absorbance of the dichloromethane layer was measured. A standard curve was prepared to determine the linearity of the assay. The amount of biphenylacetic acid was calculated using the equation presented in Chapter 2. The results showed that all the metabolism occurred within the first 10 minutes, so that precision of the kinetic isotope effect could be improved by averaging the amount of metabolite obtained at 10, 20 and 30 minutes. A primary kinetic isotope effect of 1.4 (Table 3.1) is observed on the

oxidation of biphenylacetylene by microsomal cytochrome P-450.

4. Inactivation of Cytochrome P-450 by Biphenylacetylene

Biphenylacetylene was shown to inactivate microsomal cytochrome P-450 while simultaneously being oxidized to biphenylacetic acid. The partitioning of the two pathways could be probed by studying the effects of isotopic substitution on the rate of inactivation. During the experiment in which the kinetic isotope effect was measured, aliquots of enzyme were also removed and analysed for P-450 destruction by the Soret assay (Chapter 2). These data are presented in Table 3.2. It is obvious from the data that the extent of enzyme inactivation is so small as to be barely significant. Furthermore, although there is no detectable difference in destruction between the protio and deutero biphenylacetylene, it is unlikely that a difference would be detected because the total amount of destruction is so small. Attempts were therefore made to determine the reason for the low enzyme inactivation and to try to increase it.

TABLE 3.2

Inactivation of Microsomal P-450 by Arylacetylenes

Substrate	Induction	Loss of P-450 (%)[a]	
		10 min	20 min
Biphenylacetylene	Phenobarbital	4.5	6.4
	Arochlor 1254	3.2	3.5
	Clofibrate	ND[b]	ND
[1-^{2}H]-Biphenylacetylene	Phenobarbital	4.2	7.9

[a]The values reflect a 4% correction for loss of chromophore in the absence of substrate. The standard deviations for the individual values do not exceed 1%.

[b]ND indicates no detectable chromophore loss.

Biphenylacetylene was sparingly soluble in the buffer so attempts were made to increase the amount of substrate in the microsomal suspension by prolonging the preincubation period, but the same amount of enzyme inactivation was observed in all cases. The absorbance of the microsomes was measured at 273 nm (the λ max of biphenylacetylene) after preincubation for up to 30 minutes with biphenylacetylene. These measurements showed that the concentration of biphenylacetylene was increased so that the small amount of enzyme inactivation is not due to limited substrate availability.

Attempts were made to increase the biphenylacetylene oxidase activity by preparing hepatic microsomes from rats pretreated with agents that induce other P-450 isozymes. Rats pretreated with an inducer of the fatty acid hydroxylase class of P-450's (clofibrate) were obtained from N. Reich. Rats were also pretreated with Arochlor 1254, an inducer of the arylhydrocarbon hydroxylase isozymes by injecting the rats once with 500 mg/kg in corn oil 5 days prior to the experiment. Microsomes were prepared as usual from these rats. After incubation of the microsomes with biphenylacetylene, Soret loss was measured. Data presented in Table 3.2 show none of the inducers increased biphenylacetylene oxidase activity. The unavoidable conclusion is that the isozyme responsible for the metabolism of biphenylacetylene is a minor form that is rapidly inactivated.

B. Phenylacetylene Oxidation

1. Kinetic Isotope Effect on the Oxidation of Phenylacetylene by Peracids

The kinetic isotope effect on biphenylacetylene oxidation was not suitable as a probe of the catalytic mechanism, in part because of its rather small magnitude, but mainly because enzyme inactivation was barely detectable. This prevented comparison of the isotope effects on the rates of metabolite formation and enzyme inactivation. Phenylacetylene, however, has been shown to cause approximately 25% inactivation of microsomal P-450 (Ortiz de Montellano and Kunze, 1980b), so the potential utility of this compound was investigated.

The chemical oxidation of phenylacetylene by MCPBA was first investigated with a gas chromatography assay (Chapter 2). The reaction conditions were patterned after those of Ogata et al (1973), who studied the MCPBA oxidation of para-substituted phenylacetylenes. MCPBA (1.93 g) was dissolved in 40 ml of dry benzene, the benzene solution was divided into two aliquots, and 0.2 ml of phenylacetylene and [1-^{2}H]phenylacetylene were added respectively to the two solutions. Every hour, an aliquot (0.2 ml) was removed and added to a vial containing 0.8 ml of benzene, 4ul of internal standard solution, and 0.1 ml of 0.1N NaOH. The acids were extracted into the basic aqueous phase, which was then separated, and neutralized with 2 ml of 2N HCl. This mixture was then back extracted into ether, methylated with diazomethane, and analyzed by gas chromatography. The only significant (>5%) product obtained in these experiments was phenylacetic acid. A typical gas chromatogram is shown in Figure 3.3. GC/MS analysis of the product from [1-^{2}H]phenylacetylene showed that as in the case of biphenylacetylene, the acetylenic hydrogen shifted

Figure 3.3

Gas Chromatographic Analysis of Phenylacetylene Oxidation Products

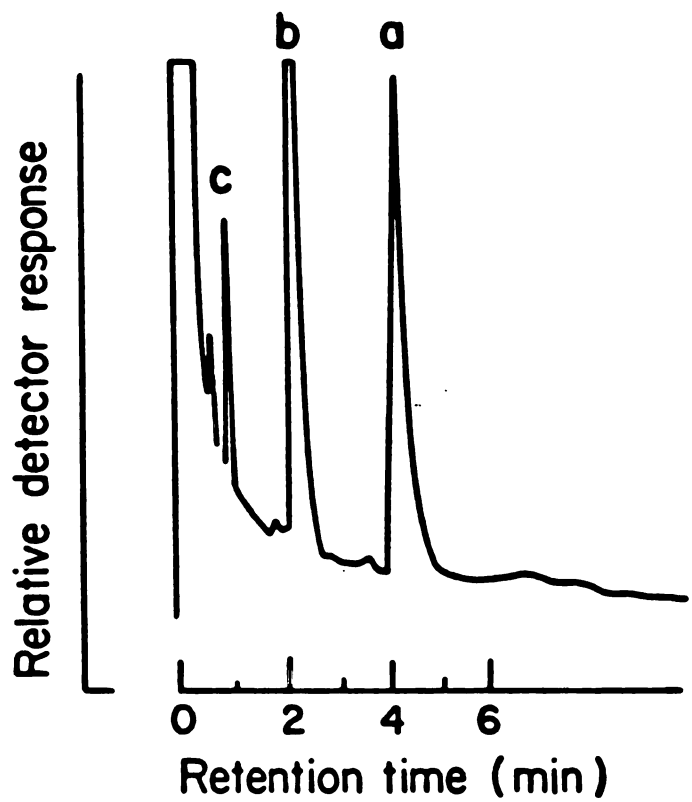

Gas-liquid chromatographic analysis of the extract from an incubation of phenylacetylene with microsomes from phenobarbital-induced rats. Methyl phenylacetate (a), methyl benzoate (the internal standard) (b), and phenylacetylene (c) are identified by the corresponding letter in the chromatogram.

quantitatively to the benzylic carbon. The mass spectra from a typical experiment are shown in Figure 3.4. The kinetic isotope effect on the oxidation reaction was determined from the gas chromatographic data. The areas of the phenylacetic acid and internal standard (benzoic acid) peaks were compared and the ratio of the areas used to calculate the yield of phenylacetic acid. The data obtained from the best experiment is presented in Figure 3.5. The slopes of the lines obtained by plotting peak area ratios (phenylacetic acid area/internal standard area) vs time were calculated using a least squares fit. The resulting kinetic isotope effect is 1.7 (Table 3.1). Although the standard deviation in this experiment was somewhat large, the data demonstrate the existence of a kinetic isotope effect of the same magnitude as that observed on biphenylacetylene oxidation.

2. Oxidation of Phenylacetylene by Fenton's Reagent

Fenton's reagent is thought to oxidize substrates by forming highly reactive hydroxyl radicals. Phenylacetylene was oxidized by Fenton's reagent in order to determine if this reagent was a good model for the enzymatic oxidation of phenylacetylene. The oxidation, carried out as described in Chapter 2, was analyzed by GC/MS. The resulting chromatogram is shown in Figure 3.6. The identities of some of the many products obtained by this oxidation have been determined from the mass spectra obtained for each peak, and the identified products are listed in the legend. Attempts to measure the kinetic isotope effect in the Fenton's oxidation were fruitless because phenylacetic acid, the product of the 1,2 hydrogen shift, represented less than 5% of the total

Figure 3.4

Mass Spectra of Oxidation Products of Phenylacetylene and [1-^{2}H]Phenylacetylene

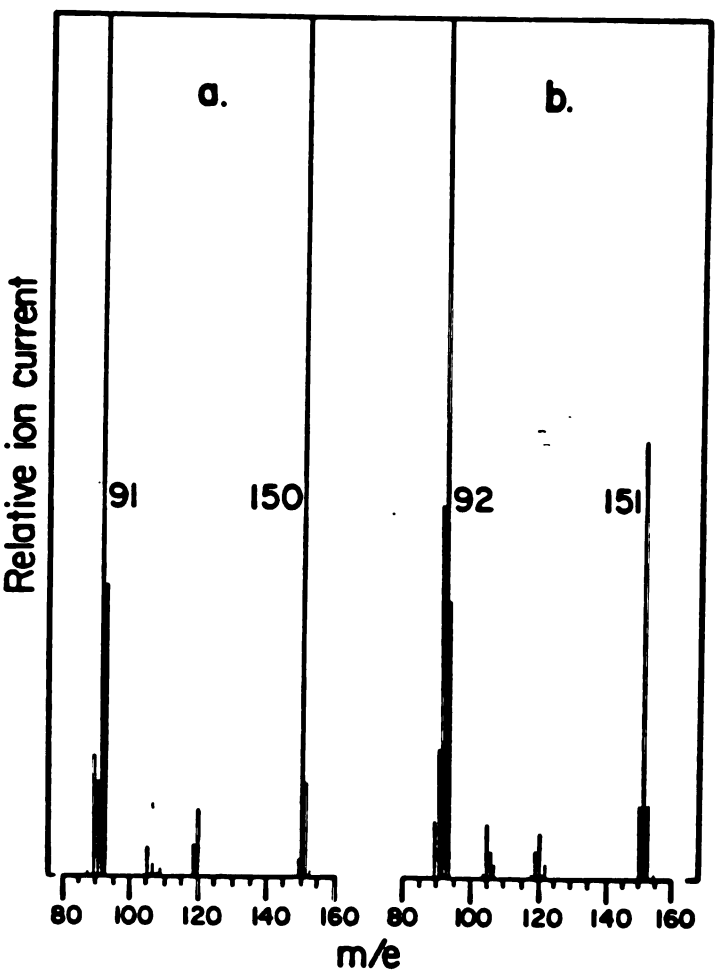

Mass spectra of methylphenylacetate obtained from microsomal incubations of (a) phenylacetylene and (b) [1-^{2}H]phenylacetylene. The lower mass regions are not shown.

Figure 3.5

Kinetic Isotope Effect on the Oxidation of Phenylacetylene by Metachloroperbenzoic Acid

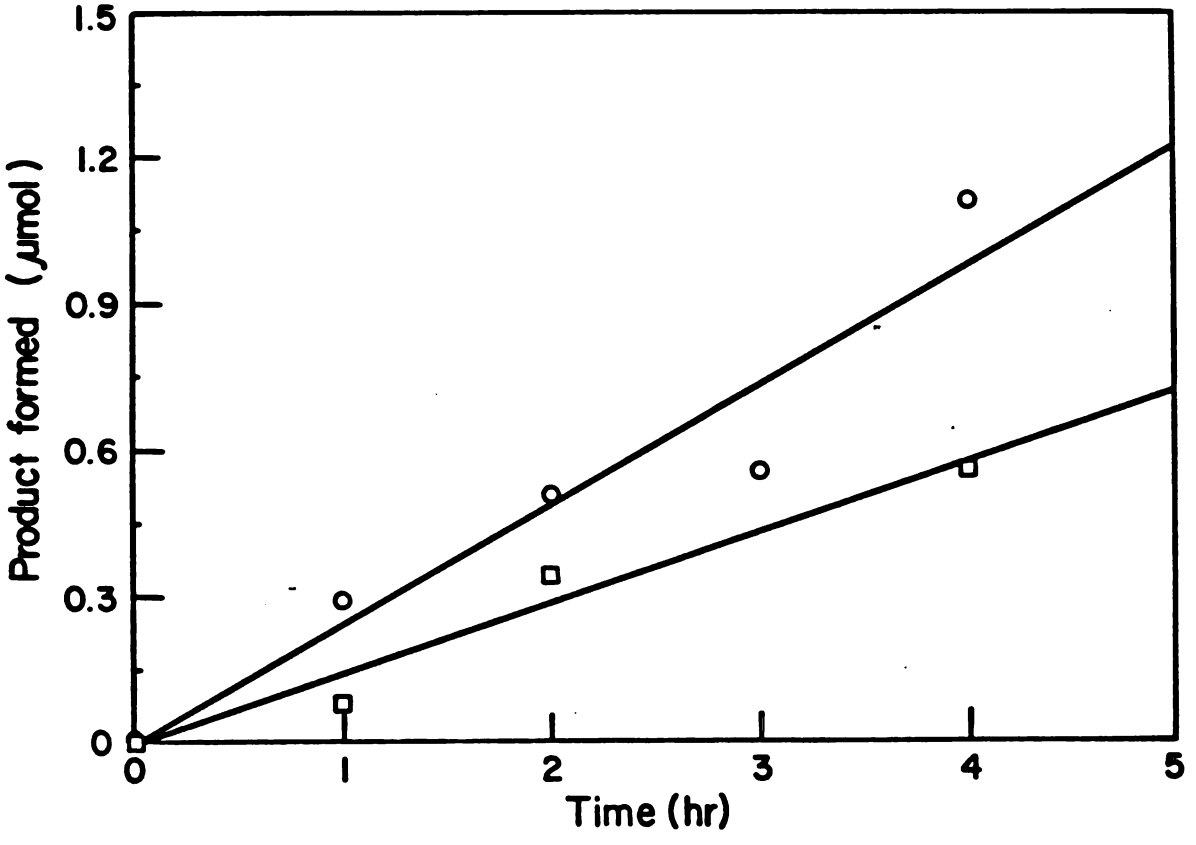

The oxidation of (a) phenylacetylene to phenylacetate (○) and (b) [1-^{2}H]phenylacetylene to [2-^{2}H]phenylacetate (□) by m-chloroperbenzoic acid in anhydrous benzene.

Figure 3.6

Gas Chromatographic/ Mass Spectrometric Analysis of the Reaction of Phenylacetylene with Fenton's Reagent

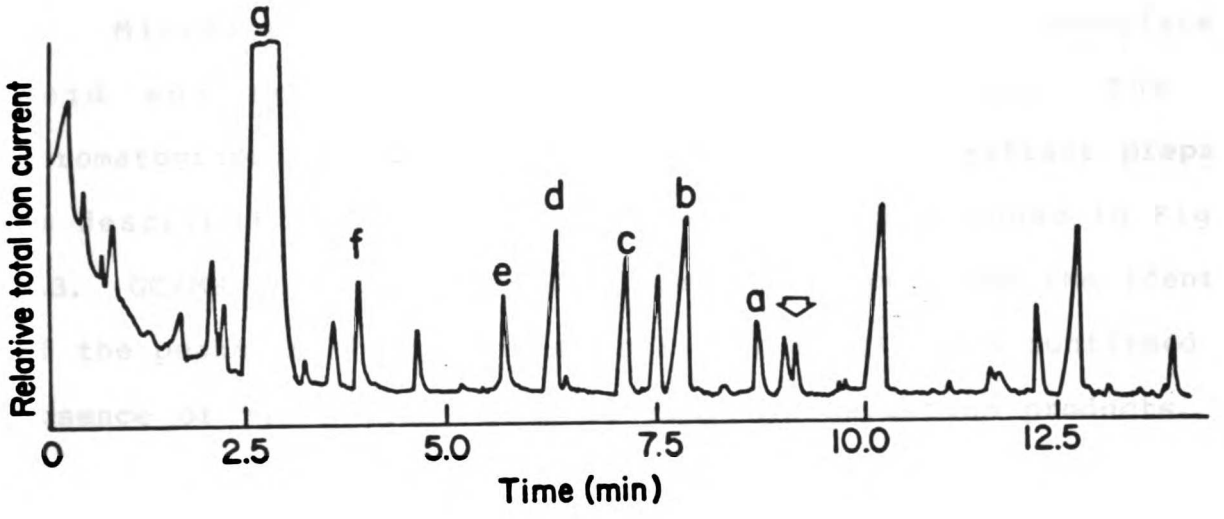

Analysis by GC/MS of the methylated organic fraction from the Fenton oxidation of phenylacetylene. The total mass spectrometric ion current is plotted. Methyl phenylacetate is indicated by the arrow. Other tentatively identified (retention time, mass spectrum) peaks are (a) 1-phenyl-1,2-ethanediol, (b) phenylacetone, (c) methyl benzoate, (d) acetophenone, (e) phenylacetaldehyde, (f) benzaldehyde, and (g) phenylacetylene.

products and was barely measurable. Clearly, Fenton's reagent is a very different oxidant from MCPBA, which only produced one detectable product. These models provide a good theoretical basis on which to interpret the results from the enzymatic studies.

3. Kinetic Isotope Effect on the Oxidation of Phenylacetylene by Microsomal P-450

Microsomal P-450 oxidized phenylacetylene to phenylacetic acid and to no other detectable products. The gas chromatographic tracing of a typical metabolic extract prepared as described in Chapter 2 was similar to that shown in Figure 3.3. GC/MS analysis of these incubations confirmed the identity of the peaks in the gas chromatographic tracing and confirmed the absence of metabolites such as ring hydroxylation products. The absence of acetophenone indicates that the oxygen is always transferred to the terminal carbon in the metabolites. A specific search was made for the ring hydroxylated products which could have formed from [1-^{2}H]phenylacetylene due to metabolic switching (Harada et al, 1982), but these were not detected. As with biphenylacetylene, the oxidation of [1-^{2}H]phenylacetylene produced phenylacetic acid in which the deuterium had shifted quantitatively to the benzylic carbon. Mass spectra of the methylphenylacetates resulting from the GC/MS analyses were identical to those shown in Figure 3.4.

The rate of microsomal oxidation of phenylacetylene was compared to that of [1-^{2}H]phenylacetylene using a gas chromatography assay (Chapter 2). The results are shown in Figure

3.7. The amounts of products produced were determined standard curves. The rates of formation of the protio and deutero phenylacetic acids, obtained from the slopes of the lines, are 0.30 nmol/min/nmol P-450 for phenylacetylene and 0.17 nmol/min/nmol P-450 for [1-^{2}H]phenylacetylene. The correlation coefficients for the lines are 0.98. The kinetic isotope effect is therefore 1.8 +/-0.2 (Table 3.1). Clearly, phenylacetylene oxidation by microsomal P-450 also manifests a significant primary kinetic isotope effect on the overall reaction rate.

The kinetic isotope effect on the rate of oxidation of phenylacetylene by microsomal P-450 was also determined by GC/MS analysis of incubations which contained equal amounts of protio and deuterophenylacetylene. In this experiment, the two substrates compete directly for the active site of the enzyme. The kinetic isotope effect obtained by these experiments is 1.6 (Table 3.1), in good agreement with that obtained by the non-competitive experiment.

These results confirm the generality of the 1,2 shift during the oxidation of arylacetylenes and define the slowest step in their oxidation by P-450 as the oxygen transfer step. The results also suggest that the best model for the oxidation of phenylacetylene by P-450 is the chemical oxidation by MCPBA which manifests an identical product distribution and kinetic isotope effect.

4.Enzyme Inactivation by Phenylacetylene and the Partition Ratio

The inactivation of microsomal P-450 by phenylacetylene and

Figure 3.7

Kinetic Isotope Effect on the Oxidation of Phenylacetylene by Microsomal P-450

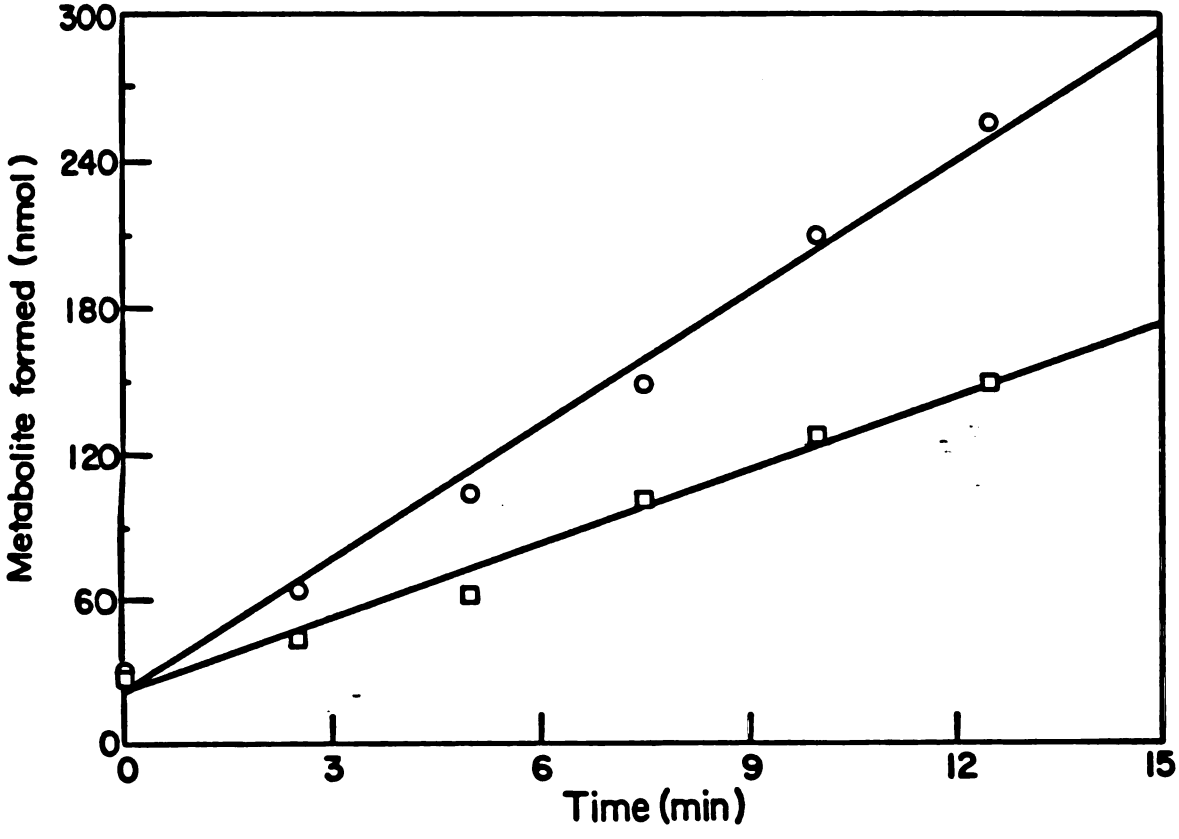

The metabolism of (a) phenylacetylene to phenylacetic acid (O) and (b) [1-^{2}H]phenylacetylene to [2-^{2}H]phenylacetic acid (□) by hepatic microsomes from phenobarbital induced rats.

[1-^{2}H]phenylacetylene was assessed by the Soret loss assay (Chapter 2). Phenylacetylene or [1-^{2}H]phenylacetylene was added neat to the incubations such that the nominal concentration was 9 mM. The fraction of the total P-450 Soret absorbance lost in 30 minutes (32%) was assumed to represent 100% of the inactivatable P-450 in the microsomal mixture. If this assumption is made, the log of the amount of P-450 (nmol) remaining plotted vs. time gives a log linear result indicative of first order kinetics of enzyme inactivation (Figure 3.8). The unexpected and striking result from these studies is that there is no difference between the inactivation by phenylacetylene and [1-^{2}H]phenylacetylene. In this case, the total amount of enzyme destruction is easily measured, so that any difference in inactivation rates due to isotopic substitution should be observable. A difference of 1.8 (the observed kinetic isotope effect on metabolite formation) would cause a factor of 1.8 difference in the rates of inactivation based on the kinetics of partitioning discussed in Chapter 1.

The partition ratio between metabolite production and enzyme inactivation changes upon isotopic substitution because the rate of metabolite formation changes but the rate of enzyme inactivation remains constant. The partition ratios (in nmol metabolite produced vs nmol enzyme inactivated) were calculated at each time point and averaged because they were constant over time. The resulting partition ratios are 26 for phenylacetylene and 15 for [1-^{2}H]phenylacetylene. These results suggest that metabolite formation and enzyme inactivation diverge at an early

Figure 3.8

Inactivation of Microsomal P-450 by Phenylacetylene and [1-^{2}H]Phenylacetylene

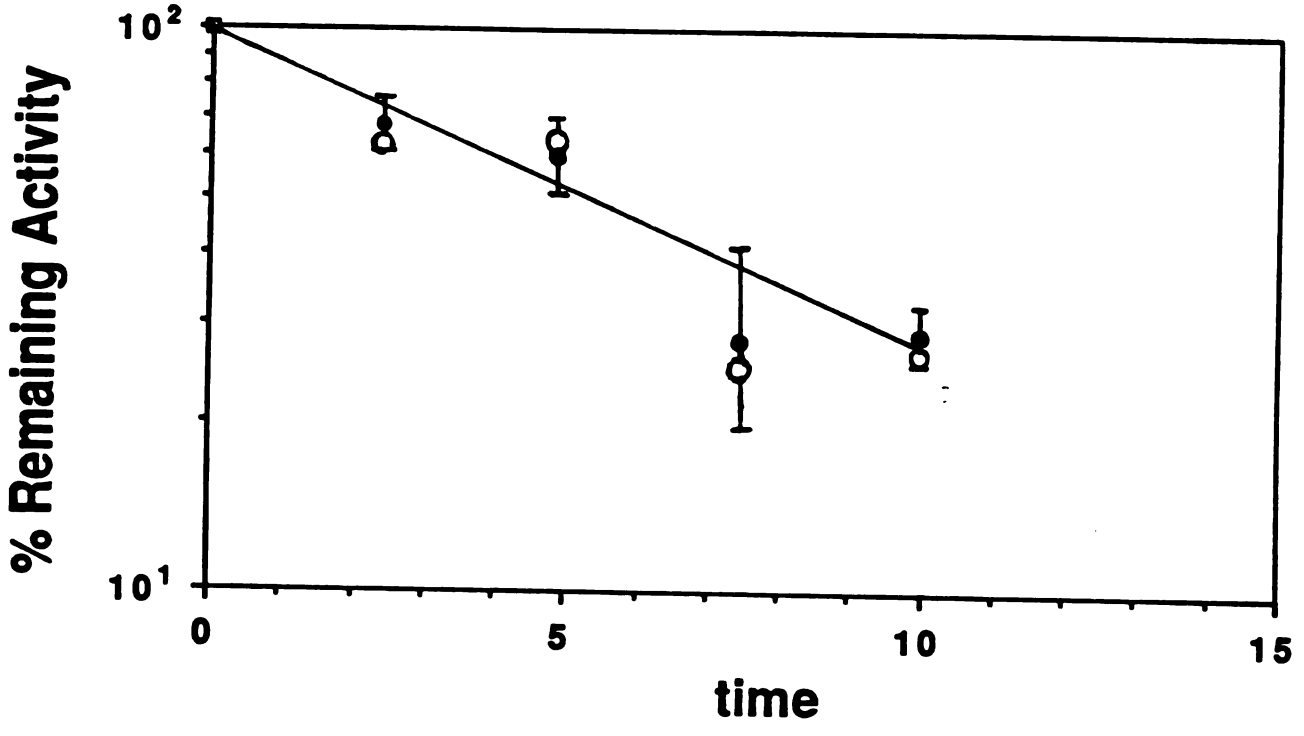

The loss of cytochrome P-450 caused by phenylacetylene (●) and [1-^{2}H]phenylacetylene (○) as a semilog function of time, assuming that the 30% maximum loss of cytochrome P-450 observed in long-term incubations is equal to 100% of the vulnerable enzyme.

step in the catalytic pathway.

The concentration dependence of the partition ratio was studied by decreasing the concentration of phenylacetylene until the amount of enzyme inactivation was decreased 50%. Under these conditions, the rate of metabolite formation was similarly decreased, and the kinetic isotope effect was no longer observed (Table 3.1). This result is that expected for a simple kinetic scheme in which the isotopically sensitive step is rate limiting, and shows that both metabolite formation and enzyme inactivation depend similarly on substrate binding.

5. Kinetic Isotope Effect on the Oxidation of Phenylacetylene by Purified Cytochrome P-450b

One explanation for the observation that metabolite formation appeared unrelated to enzyme inactivation was that two different isozymes were responsible for the two pathways. Although this was unlikely based on the fact that the partition ratio did not change with time, confirmation was required. In order to demonstrate that the two pathways were occurring in the same enzyme, a single highly purified cytochrome P-450 was employed. The choice to purify the major phenobarbital inducible isozyme was based on the observation that in microsomes, 30% of the total P-450 (approximately the content of P-450b in microsomes from phenobarbital pretreated rats) was inactivated by phenylacetylene. The procedure for purification of P-450b, which was described by Waxman and Walsh (1982), has been discussed in Chapter 2, and Appendix II.

The reconstituted enzyme (Chapter 2) was incubated with 9 mM

phenylacetylene or [1-^{2}H]phenylacetylene. The apparent spectroscopic binding constant for phenylacetylene was found to be 0.8 mM (Chapter 2) so that a 9 mM substrate concentration is well over that which saturates the enzyme. The incubations were similar to the microsomal assays, but the reactions occurred more rapidly so that analyses were performed at shorter time intervals. Again GC/MS analysis confirmed that phenylacetic acid was the only detectable oxidation product. The results were essentially the same as those shown in Figure 3.4 except that 30 to 40% of the deuterium label was routinely lost through an unidentified exchange reaction. No deuterium loss was observed when GC/MS analysis was performed on [1-^{2}H]phenylacetylene that was reisolated from the incubation mixture. It was thus necessary to study the kinetic isotope effect in the pure enzyme system by GC/MS analysis of the metabolites from a 1:1 mixture of phenylacetylene and [1-^{2}H]phenylacetylene. The "non-competitive" experiment using the gas chromatographic assay, due to the exchange reaction, gave small isotope effect values. In any event, the data could be corrected for this exchange, and the kinetic isotope effect could be determined. The amount of phenylacetic acids formed with time from phenylacetylene and [1-^{2}H]phenylacetylene were determined by comparing the total ions in the methyl phenylacetate peak to those in the internal standard (methyl 4-phenyl-1-butyrate) peak with the help of a standard curve. The results are plotted in Figure 3.9. The turnover was 1nmol/min/nmol P450 for phenylacetylene, and 0.6 nmol/min/nmol P-450 for [1-^{2}H]phenylacetylene, and the kinetic isotope effect was

Figure 3.9

Kinetic Isotope Effect on the Oxidation of Phenylacetylene by Purified, Reconstituted P-450

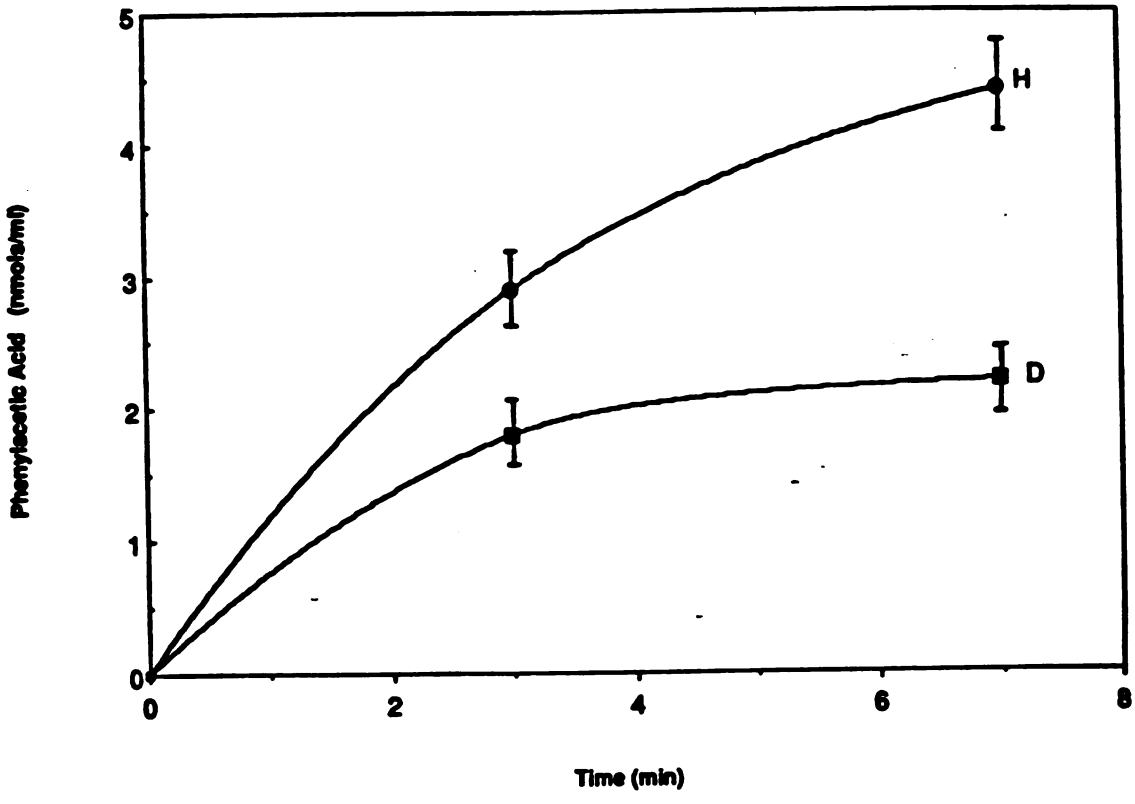

Formation of deuterated (D) and undeuterated (H)phenylacetic acids in incubations of reconstituted cytochrome P-450b as monitored by GC/MS of methylated organic extracts.

1.8 +/-0.2 (Table 3.1).

The temperature dependence of the kinetic isotope effect was determined by repeating the experiment at 25°C. Under these conditions, no kinetic isotope effect was observed suggesting that at this temperature, another step becomes rate limiting (Table 3.1).

6. Inactivation of Purified P-450b by Phenylacetylene

The inactivation of purified, reconstituted P-450b was measured using both the Soret loss and 7- ethoxycoumarin deethylase (7-EC) activity assays (Chapter 2). The incubations were identical to those used to measure metabolite formation. The Soret and 7-EC activity losses were calculated relative to the 0 time point measured just prior to adding NADPH to start the reaction. The percent remaining Soret absorbance and activity are plotted in Figure 3.10. All the activity was lost by 20 minutes but 27% of the Soret remained at 30 minutes. Both activity loss and Soret loss were log linear as expected from the presence of only one isozyme. Absolutely no difference was observed in the inactivation rate by phenylacetylene or [1-^{2}H]phenylacetylene. The results obtained with the pure enzyme system were thus exactly the same as those previously obtained in microsomes.

The partition ratios for phenylacetylene and [1-^{2}H]phenylacetylene were calculated for the pure enzyme system. Since GC/MS was used to analyze the kinetic isotope effect, inactivation could not be measured simultaneously. To calculate the partition ratios, the phenylacetic acid production (in

Figure 3.10

Inactivation of Purified, Reconstituted P-450b by Phenylacetylene and [1-^{2}H]Phenylacetylene Measured by Soret Loss and Activity Loss

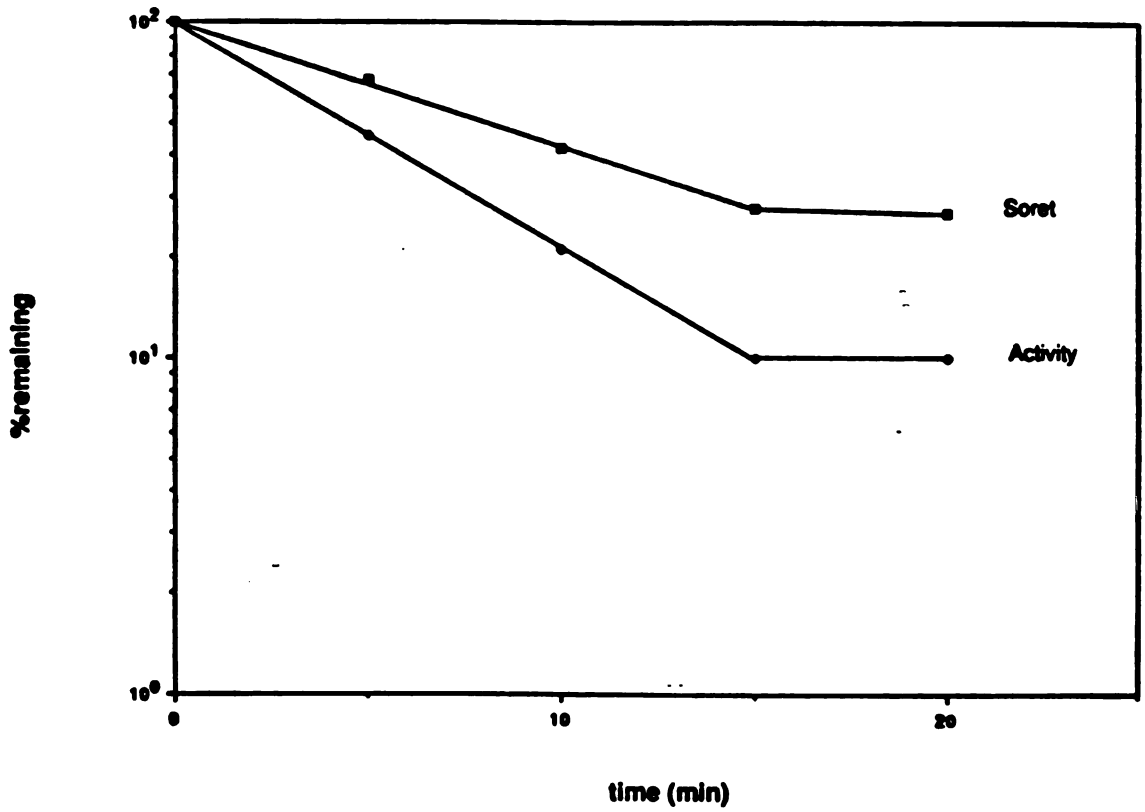

Loss of Chromophore and 7-ethoxycoumarin O-deethylase activity in incubations of reconstituted P-450b with phenylacetylene (9mM). The points obtained if [1-^{2}H]phenylacetylene is used are superimposable on those shown for the unlabelled substrate.

nmol/minute/nmol P-450) determined by GC/MS was compared to activity loss (in the same units) determined separately by the 7-EC deethylase activity assay. Since the metabolite formation was determined in a competitive incubation from a 1:1 mixture of phenylacetylene to [1-^{2}H]phenylacetylene, the metabolite formation was multiplied by 2 to obtain the value expected from a non-competitive experiment. The calculated partition ratios were 20 for phenylacetylene and 12 for [1-^{2}H]phenylacetylene. These values are quite close to those observed in microsomes, suggesting that the active isozyme in the microsom was P-450b. The data also suggest that purifying and reconstituting the enzyme does not alter its catalytic properties sith respect to phenylacetylene.

The discrepancy between Soret loss and activity loss was investigated further to determine if another form of inactivation was occurring which did not cause loss of the Soret band. Inactivation of P-450b by 1-aminobenzotriazole (ABT) was measured by both methods as a control. This compound is known to inactivate a broad spectrum of P-450 isozymes by forming benzyne which alkylates the prosthetic heme group (Ortiz de Montellano and Mathews, 1981). In this case, the discrepancy between Soret loss and activity loss was only 10% as can be seen in Figure 3.11 This result suggests that, at least with certain substrates, Soret loss and activity loss can be closely correlated.

A specific search was made for inactivation products that may absorb at 450 nm and thus artifactually contribute to the absorbance measured in the Soret loss assay. Concentrated,

Figure 3.11

Inactivation of Purified, Reconstituted P-450b by 1-Aminobenzotriazole Measured by Soret Loss and Activity Loss

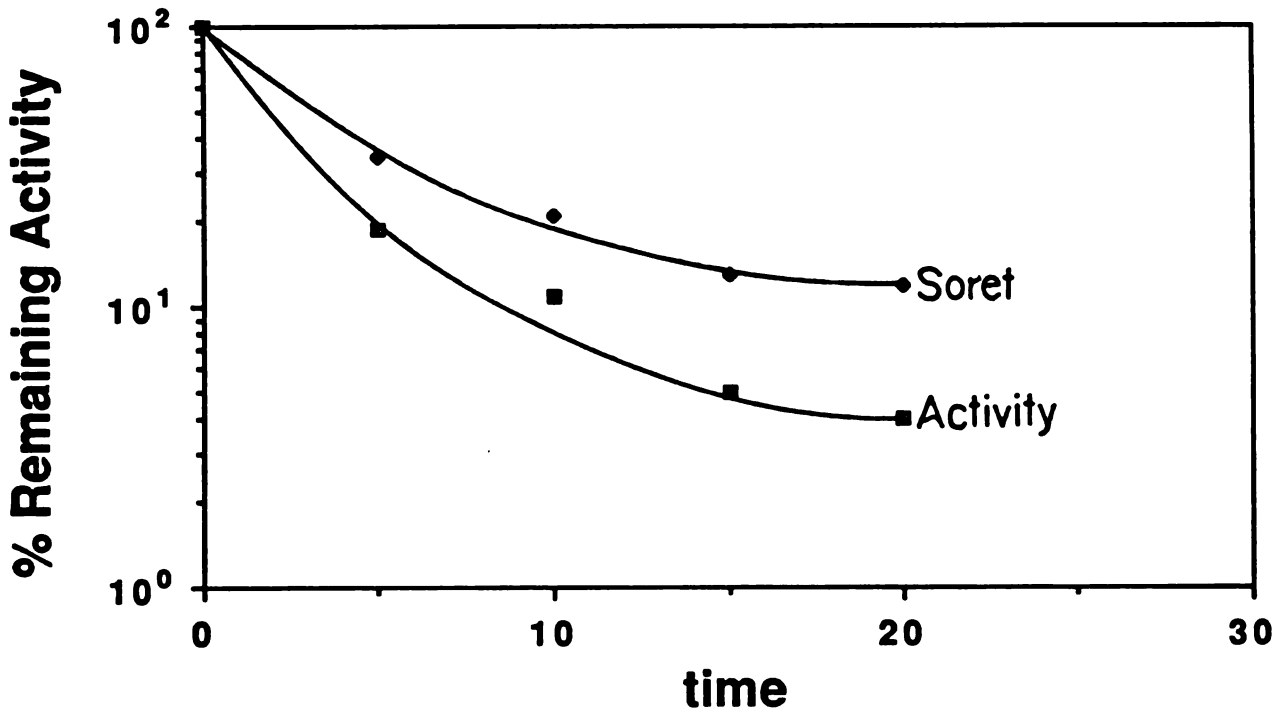

The Loss of Chromophore and 7-ethoxycoumarin O-dethylase activity in incubations of reconstituted P-450b with 1-aminobenzotriazole (5mM).

reconstituted P-450b was prepared by mixing 5 nmol of P-450 with 10 nmol of reductase in a total volume of 1 ml with 20 ul of dilauroylphosphatidylcholine solution. The mixture was incubated for 10 minutes at room temperature, 9mM phenylacetylene or 5 mM ABT was added, and the solution was warmed to 37°C. After 5 minutes, NADPH was added, and the absorption spectrum was recorded at various times until 10 minutes. The spectra are shown in Figure 3.12. Indeed, a new absorbance occurs upon turnover of the substrates that contributes to the Soret measurement. A calculation of the contribution of the absorbance to the absorbance measured in the assay for phenylacetylene induced Soret loss was performed. The absorbance difference ($O.D._{450} - O.D._{490}$) was normalized for the concentration of P-450 used in the Soret loss experiments, and then the contribution of this amount of residual absorbance to the Soret measurement was determined. The result was that the new absorbance would contribute 27% of the total Soret measurement. This is exactly the amount of residual Soret which is observed. The new absorbance in the ABT-inactivated P-450 occurs at 480 nm instead of 445 nm, so it would be expected to contribute less to the 450 nm Soret measurement.

7. Heme Adduct Formation During Turnover of Phenylacetylene

Formation of an N-alkylated PPIX derivative from phenyalcetylene turnover in rats was reported previously (Ortiz de Montellano and Kunze, 1980b), but the yield was quite low and the adduct appeared to be unstable to purification by HPLC. Two further attempts were thus made to isolate the N-alkylated

Figure 3.12

Electronic Absorption Spectra of Purified, Reconstituted P-450 After Inactivation by Phenylacetylene or 1-Aminobenzotriazole

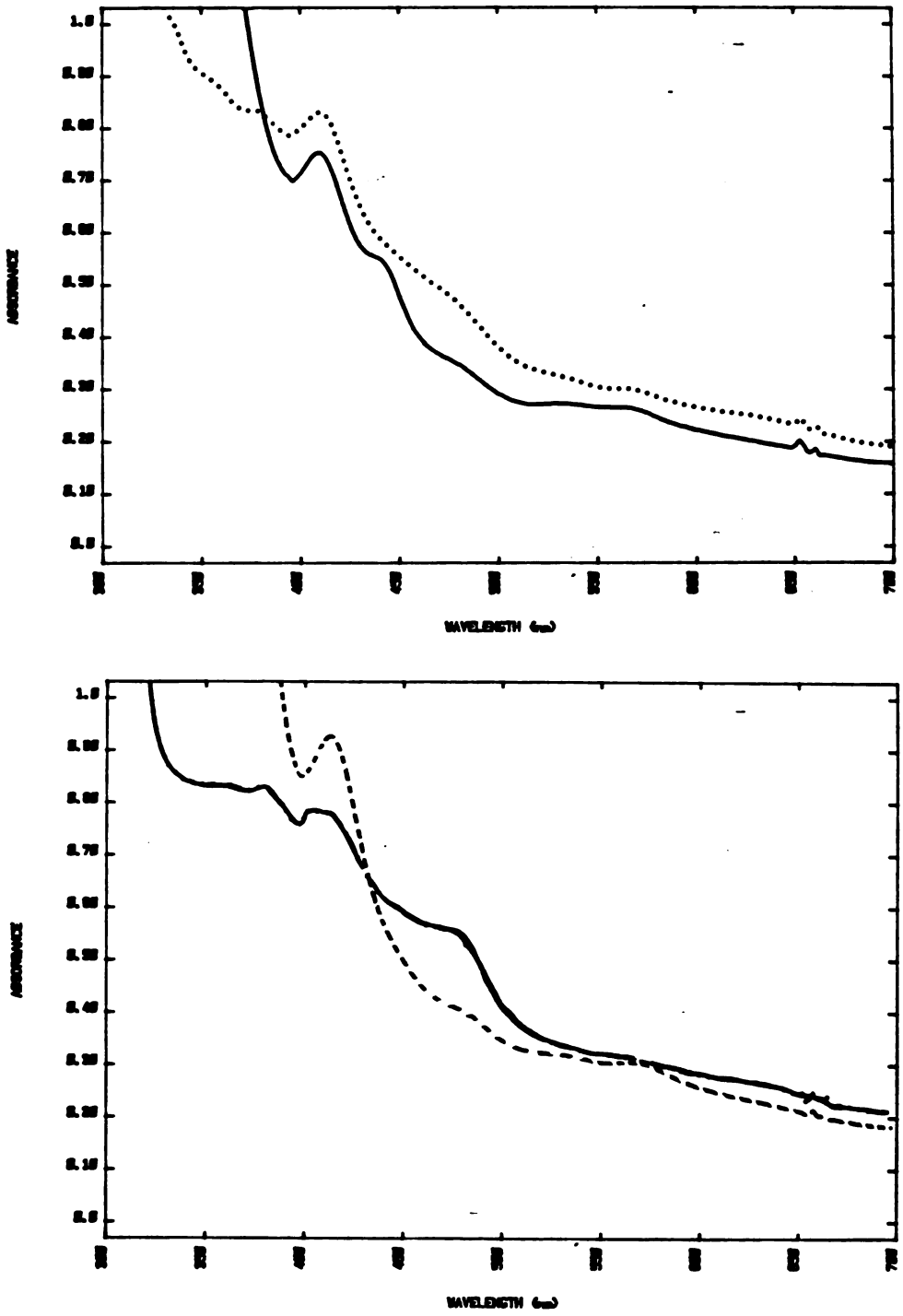

Concentrated (10 nmol/ml), reconstituted P-450b was incubated with either (a) phenylacetylene or (b) 1-aminobenzotriazole. The absolute electronic absorption spectrum was recorded before the addition of NADPH (----) and after 10 minutes of incubation (————).

porphyrin resulting from metabolism of phenylacetylene in rats. Injection of the phenylacetylene as a neat liquid gave a better yield of the N-alkylated porphyrin than injection of the phenylacetylene in dimethylsulfoxide. The yield was still quite low, however; approximately 20 ug of N-alkylated PPIX was isolated from the livers of 10 phenobarbital induced rats which were injected i.p. with 400 mg/kg of neat phenylacetylene. Although this was not enough for NMR characterization of the adduct, it was possible to identify the structure by comparison with an authentic sample. The expected N-alkylated porphyrin was generated via another route involving reaction of diazoacetophenone with microsomal P-450. This reaction and the resulting products are discussed in Chapter 5. The structure of the diazophenone - porphyrin adduct was thus shown unequivocally to be that in the inset in Figure 3.13. The HPLC retention times of the diazoacetophenone adduct, both as the free base and as the zinc complex, were identical to those for the adduct isolated from rats treated with phenylacetylene. The structure of the adduct is consistent with those formed in the reaction of other terminal acetylenes with P-450 (Ortiz de Montellano and Kunze, 1980b; 1981). It should be noted that all the heme adducts resulting from oxidation of acetylenes have structures in which the oxygen has been transferred to the internal carbon of the terminal acetylene and the terminal carbon is bound to the porphyrin nitrogen.

Phenylacetylene oxidation by P-450 causes loss of 7-EC deethylase activity, a concomitant loss of the Soret band, and

Comparison of HPLC Retention Times of the Zinc Complex and Free Base Diazoacetophenone-PPIX Adduct and the Phenylacetylene-PPIX Adduct

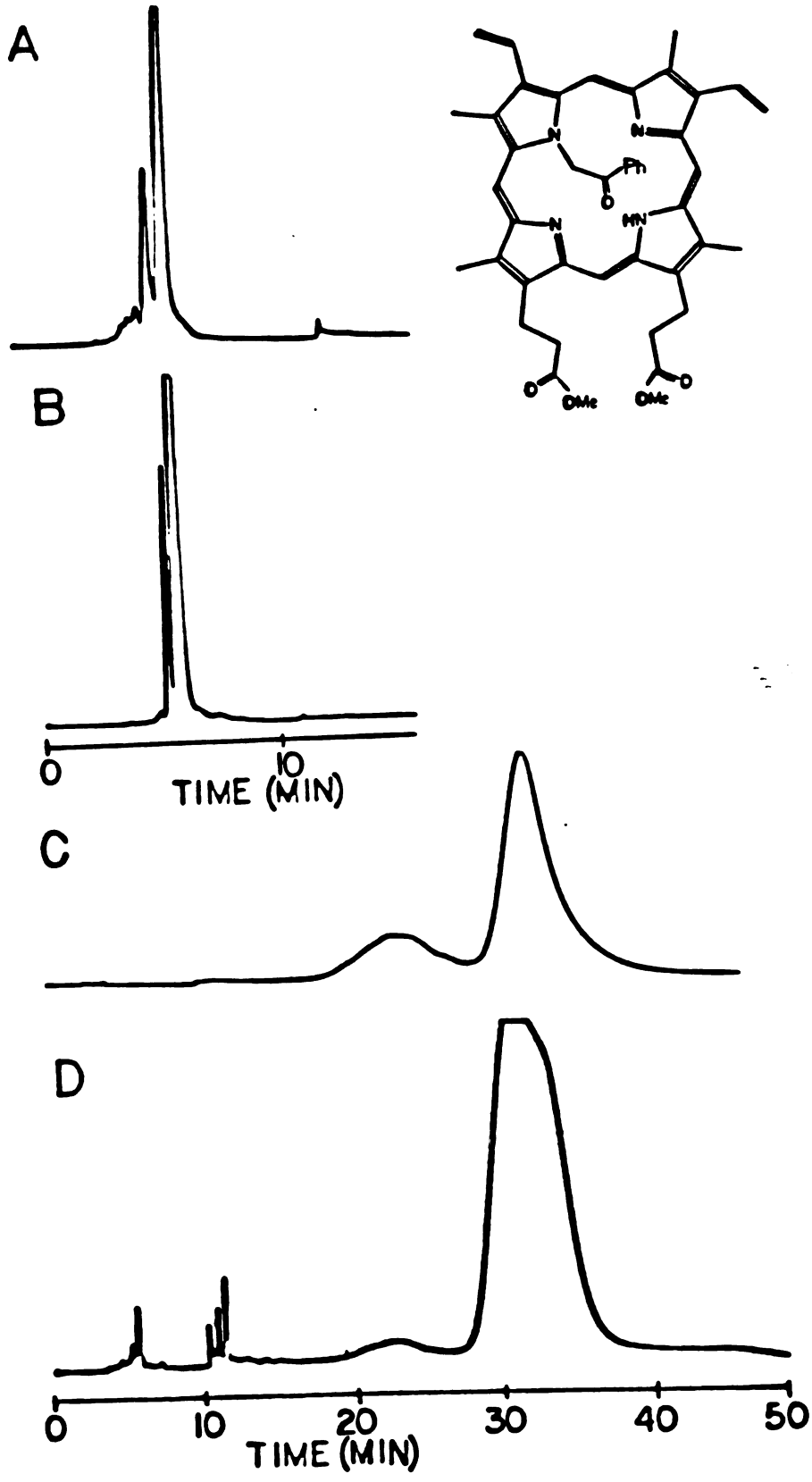

Comparison by high pressure liquid chromatography of the dimethyl esterified N-alkylporphyrin isolated from phenylacetylene-treated rats and the dimethyl ester of authentic N-(2-phenyl-2-oxoethyl)-protoporphyrin IX: (A) free base of the phenylacetylene pogment, (B) free base of the authentic porphyrin, (C) zinc complex of the phenylacetylene pigment and (D) zinc complex of the authentic porphyrin. The chromatographic conditions are given in Chapter 2. The structure of the porphyrin is shown in the inset.

formation of a 445 nm absorbing species that is most likely the heme adduct. The structure of the heme adduct, by analogy, is that in which the terminal carbon of the acetylene is bound to the porphyrin nitrogen, and the oxygen atom is bound to the internal carbon. Soret loss and activity loss measurements give identical results, suggesting that they reflect the same enzymatic pathway. Whether heme adduct formation is quantitatively responsible for inactivation or not, the insensitivity of inactivation to isotopic substitution suggests that it diverges from the pathway leading to metabolite formation early in the catalytic process. The pathway leading to enzyme inactivation cannot involve initial transfer of the oxygen to the terminal carbon of the acetylenic bond because this would result in hydrogen migration and isotopic sensitivity. It must involve either transfer of the oxygen to the internal carbon or abstraction of an electron from the π-system. In either case, the pathways probably do not undergo any common chemical steps (Scheme 3.2).

Scheme 3.2

Alternate Explanations for the Early Divergence of Metabolite Formation and Heme Alkylation During the Turnover of Arylacetylenes by P-450

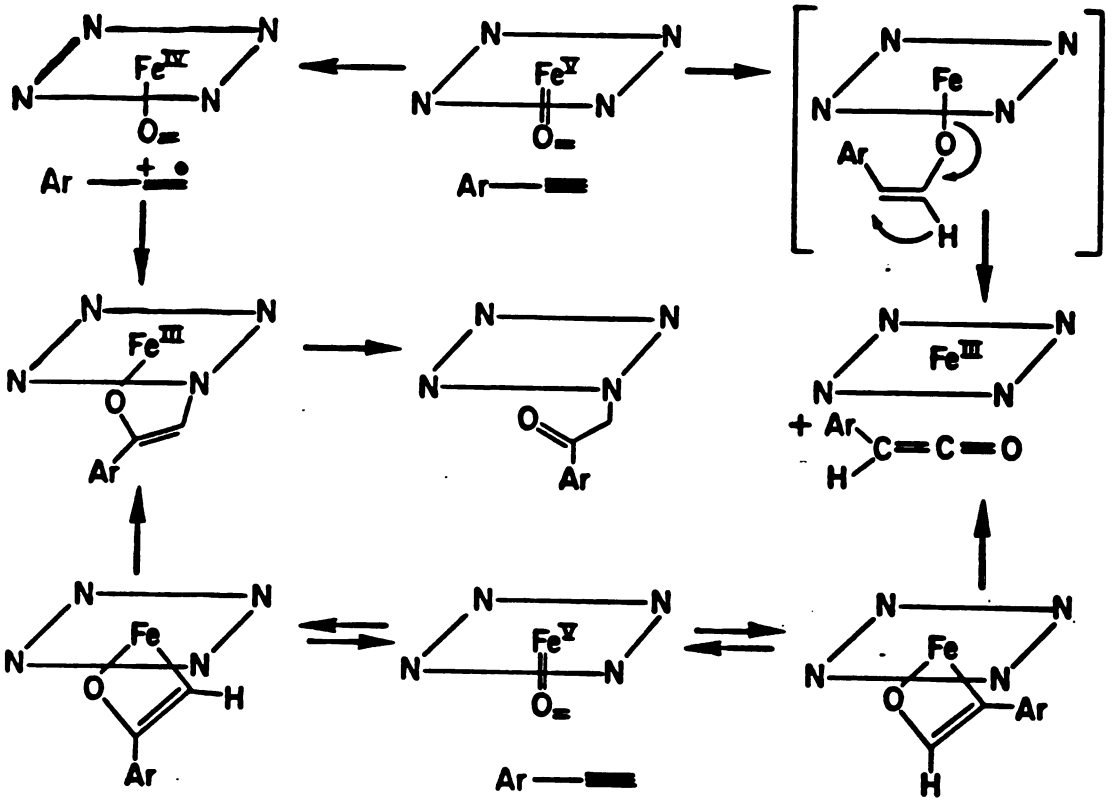

CHAPTER 4

ELECTRONIC AND STERIC EFFECTS ON ACETYLENE OXIDATION

A. Electronic Effects on Phenylacetylene Oxidation

The finding that the rate of oxidation of phenylacetylene to phenylacetic acid is sensitive to replacement of the acetylenic hydrogen by deuterium, but that enzyme inactivation is not, suggests that the two catalytic pathways diverge at an early point in the reaction. To explain this difference, it was postulated that metabolite formation might involve oxygen insertion while enzyme inactivation might involve radical abstraction as shown in Scheme 3.2. One way to test this hypothesis is to electronically perturb the reaction and examine the effects of the perturbation on both pathways as well as on the overall partition ratio. A well established linear free energy correlation exists between the electron donating ability of a para substituent on a benzene ring and the ease of reactions at the benzylic carbon. The para substituent effects have been measured for the ionization of benzoic acid and relative values assigned to the measured substituent effects (Hammett, 1937). The sigma constants thus obtained correlate with inductive effects, and the sigma$^+$ constants with resonance as well as inductive effects. The slope of the line obtained from plotting the log of the reaction rate against the appropriate substituent constants indicates the sensitivity of the reaction to electronic effects. If the reaction is an electrophilic substitution, the slope of

the line will be negative because electron donating substituents will increase the reaction rate. A correlation of this type has been obtained for the MCPBA oxidation of *para* substituted phenylacetylenes (Ogata et al, 1973).

1. Metabolites From Substituted Phenylacetylenes

Several para-substituted phenylacetylenes [*p*-methyl (p-Me), *p*-chloro (p-Cl), *p*-nitro (p-NO_2) and phenylacetylene] have been used to probe the electronic effects on metabolite formation and enzyme inactivation. Preliminary GC/MS experiments indicated that the only significant (>10%) metabolite in all cases was the corresponding phenylacetic acid. GC/MS analysis of the oxidation of the p-Me derivative showed formation of a small amount of the methyl hydroxylation product (Figure 4.1). Analytical conditions for the individual methyl phenylacetates were determined using standard phenylacetic acids (Chapter 2). In each case, the metabolite was identified by gas chromatographic coelution and by GC/MS. Standard curves were prepared using 4-phenyl-1-butyric acid as the internal standard, and inclusion of this internal standard in each extraction mixture allowed the rates of production of the substituted phenylacetic acids to be determined (in nmol/min/nmol P-450). The incubations were conducted and analyzed as described in Chapter 2, and the results are shown in Figure 4.2. The metabolite formation is not linear with time because the enzyme is simultaneously inactivated.

The log of the phenylacetic acid formed at each time point was plotted against the sigma or $sigma^+$ coefficients for the substituents. The lines were fit by linear regression analysis

Figure 4.1

Gas Chromatographic/Mass Spectrometric Analysis of the Products from the Oxidation of (p-methylphenyl)Acetylene by Purified, Reconstituted P-450b

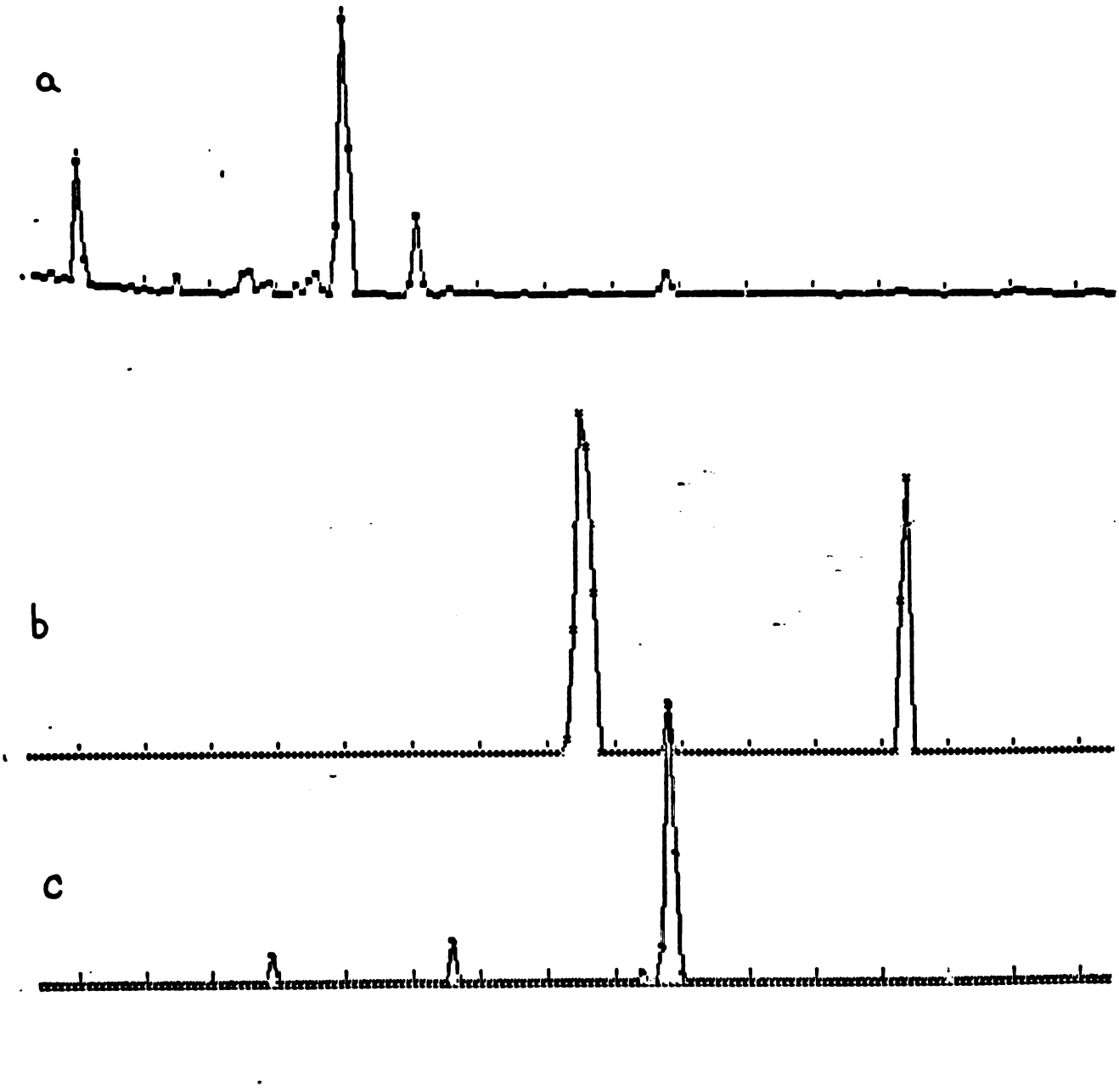

Gas chromatographic/mass spectrometric analysis of the methylated organic extract from an incubtation of (p-methylphenyl)acetylene with purified, reconstituted P-450b. A portion of the chromatogram is plotted showing (a) the total ions detected, (b) the total ions detected at m/e = 132 (the hydroxy methyl product) multiplied by 1024 and (c) the total ions detected at m/e = 164 (methyl p-methylphenylacetate) multiplied by 128.

Figure 4.2

Oxidation of para-Substituted Phenylacetylenes by Purified, Reconstituted P-450b to the Corresponding <u>para</u>-Substituted Phenylacetic Acids

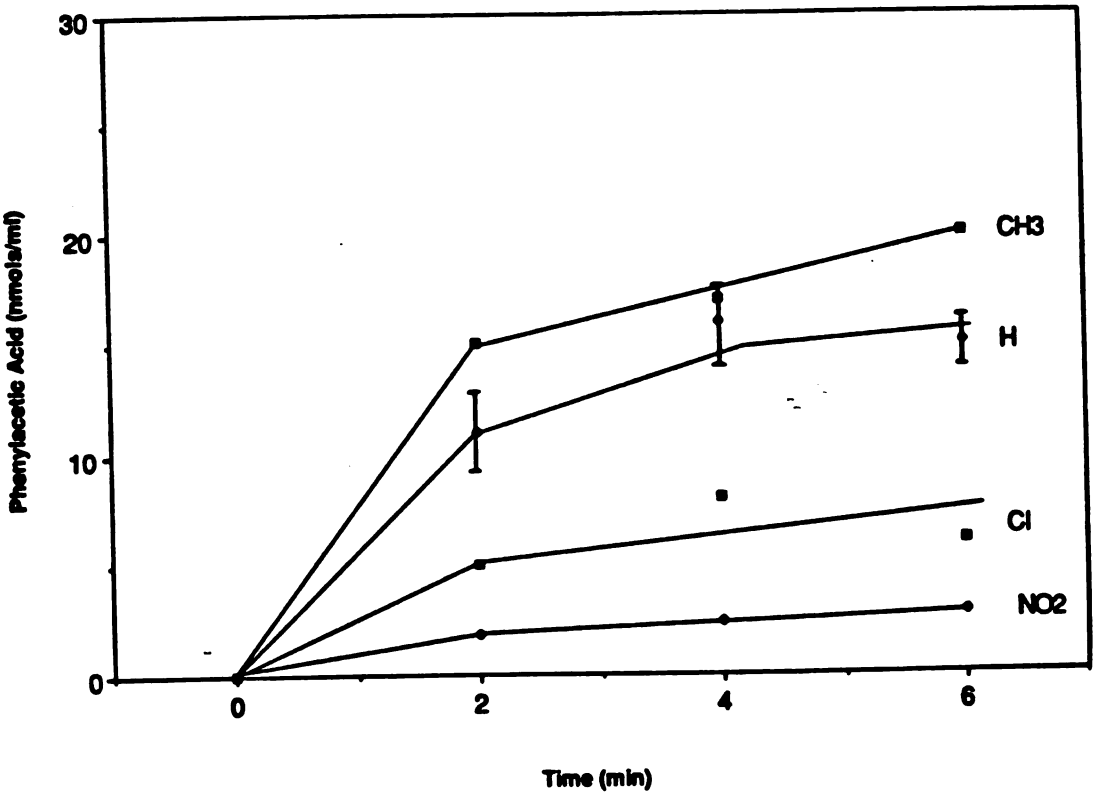

Concentrations of the substituted phenylacetic acid metabolites as a function of time of incubation of substituted phenylacetylenes with reconstituted cytochrome P-450b. The substituent on the phenylacetic acid is indicated. The experimental conditions are given in Chapter 2. The standard deviations for phenylacetic acid production are indicated by bars. The standard deviations for the other measurements are similar but are not shown for the sake of clarity.

and the resulting correlation coefficients were >0.95. The 2 minute points, which gave the best correlation, are plotted in Figure 4.3. The slope of the line obtained from the plot is -2.2 which clearly indicates that electron density is being siphoned from the benzylic carbon in the transition state. Both the sigma constants and the sigma$^+$ constants correlate well with the reaction rates, but a better correlation is obtained with the sigma constants (0.99 vs 0.96). In order to distinguish between the sigma and sigma$^+$ correlation, the oxidation of p-methoxyphenylacetylene would have to be examined because methoxy is one of the few substituents that contributes significant electron density by resonance. This compound was not studied because O-demethylation would be expected to compete with acetylene oxidation.

2. Enzyme Inactivation

All the para-substituted phenylacetylenes were found to inactivate purified, reconstituted P-450b. The inactivation rate was determined by the 7-EC deethylase assay (Chapter 2). This assay was also used to estimate the relative "binding constants" in terms of the amount of competitive inhibition of 7-EC deethylase activity. All the substrates were incubated at a nominal concentration of 9 mM with purified, reconstituted P-450b, but the actual concentration is unknown since they are all marginally soluble. The 7-EC deethylase activity was measured at 0, 2, 4, and 6 minutes after addition of NADPH and the activity was calculated relative to the activity at 0 minutes. The 100% activity was determined by assaying an aliquot removed just prior

Figure 4.3

Linear Free Energy Correlation of the Rates of Production of <u>para</u>-Substituted Phenylacetic Acids with the Sigma and Sigma$^+$ Substituent Constants

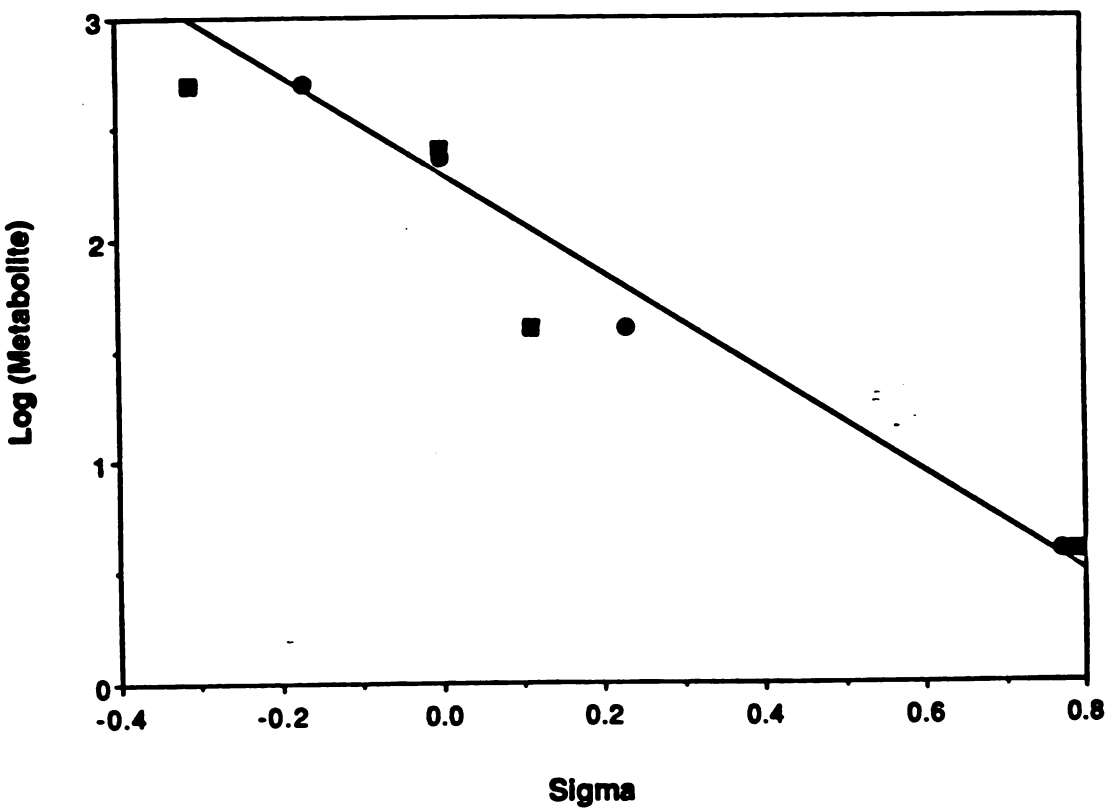

Plot of the logs of the initial rates of formation of substituted phenylacetic acids versus the sigma (●) and sigma$^+$ (■) substituent constants. The values of the sigma and sigma$^+$ constants are from Lowry and Richardson. The correlation coefficient for the sigma correlation (line shown) is r^2= 0.989 and that for the sigma$^+$ correlation (line not shown) is r^2=0.961.

to adding NADPH to initiate the reaction. Figure 4.4 shows the data from a typical inactivation experiment. Although there was some variability in the data, no significant difference in enzyme inactivation by the para-substituted phenylacetylenes was observed. Because the rate of metabolite formation correlates with the sigma constants, and enzyme inactivation remains unchanged, the calculated partition ratios also correlate with sigma. The rho value is -2.3, and the correlation coefficient is 0.999 (Figure 4.5).

The inactivation rates do not correlate with substrate binding as assessed by competitive inhibition of 7-EC activity. Competitive inhibition was measured by adding a 30 ul aliquot of the reconstituted enzyme after preincubation with 9 mM substrate to the standard 7-EC activity assay mix. The concentration of the acetylenes in the 7-EC assay was thus 150 uM, while that of 7-EC was 500 uM. The inhibition of activity can be determined as a percent of the activity in the absence of any acetylenic substrate. The resulting values for the substituted acetylenes are listed in Table 4.1. It should be noted that although the amount of competitive inhibition varies widely, and p-nitrophenylacetylene does not appear to compete at all, the substrates must be binding because the extent of enzyme inactivation is the same for all the substrates.

Figure 4.4

Inactivation of Purified, Reconstituted P-450b by para-Substituted Phenylacetylenes

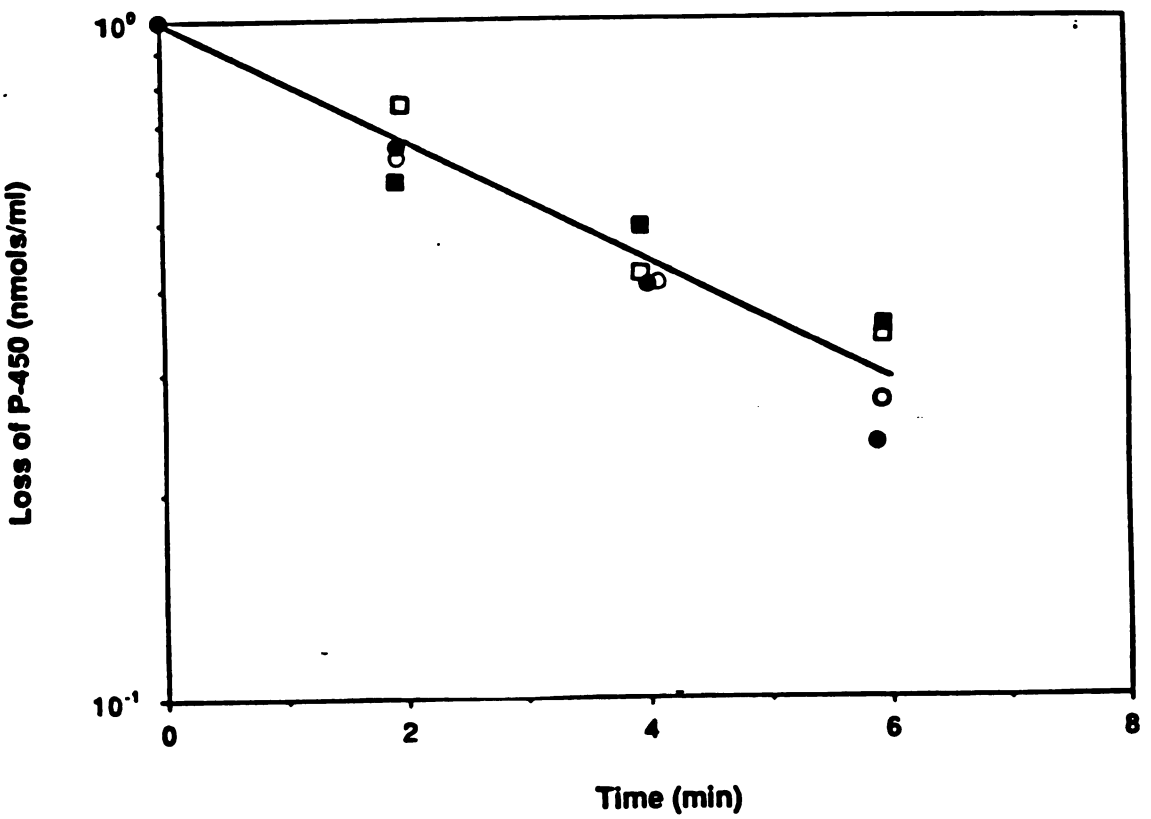

Inactivation of reconstituted cytochrome P-450 by substituted phenylacetylenes. The symbols correspond to the methyl (○), chloro (□), nitro (●), and unsubstituted (■) phenylacetylenes.

Figure 4.5

Linear Free Energy Correlation of the Partition Ratios for the Oxidation of <u>para</u>-Substituted Phenylacetylenes with the Sigma Substituent Constants

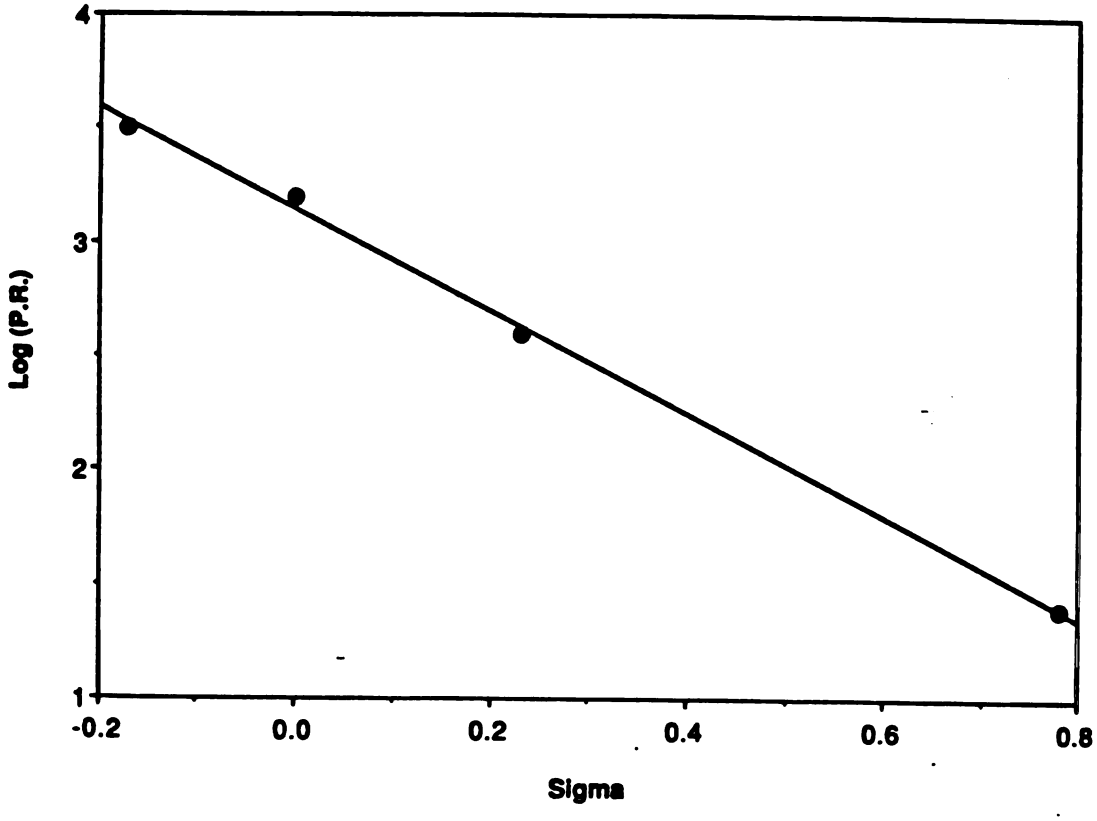

Correlation of the partition ratios (metabolite formation/ enzyme inactivation) with substituent constants for the series of substituted phenylacetylenes.

TABLE 4.1

Competitve Inhibition, Metabolite Formation, and NADPH Consumption by Substituted Phenylacetylenes

Substrate	Competitive Inhibition (%)	Metabolite Formation	NADPH Consumption
		(nmol/min/nmol P-450)	
none	--	--	24
p-Me	84%	7.5	25
p-H	35%	5.5	43
p-Cl	80%	2.5	14
p-NO_2	0%	0.9	52
o-Me	66%	--	--

The data clearly indicate that the rate of enzyme inactivation is insensitive to substituent effects. Several explanations for this observation are possible. If the slowest step in the catalytic pathway is not the substrate oxidation step, the rate would not be expected to vary with substitution. Even if the substrate oxidation step is rate limiting, the transition state of the inactivation reaction may not involve substantial charge build-up on the benzylic carbon. In either case, these data rule out the postulated radical cation intermediate because its formation involves generation of positive charge at the benzylic carbon which would be sensitive to substituents. These results are best reconciled with either a direct oxygen transfer mechanism in which oxygen transfer to the benzylic carbon results directly in formation of the heme adduct whereas transfer to the terminal carbon results in ketene formation or with a metallooxetene mechanism (Scheme 4.1).

B. Steric Effects on Phenylacetylene Oxidation

1. Ortho- vs para-methylphenylacetylene

The most likely mechanisms for enzyme inactivation by phenylacetylene require delivery of the oxygen to the benzylic carbon. This should result in development of positive charge on the terminal carbon of the acetylenic bond and a hybridization change from sp to sp^2 at both the benzylic and terminal carbons. Model building suggests that such a pathway could be sensitive to steric effects if the ortho positions of the benzene ring are occupied. The pathway leading to phenylacetic acid production would also be expected to be sensitive to steric effects since it

Scheme 4.1

The Most Likely Mechanism of Phenylacetylene Oxidation by P-450

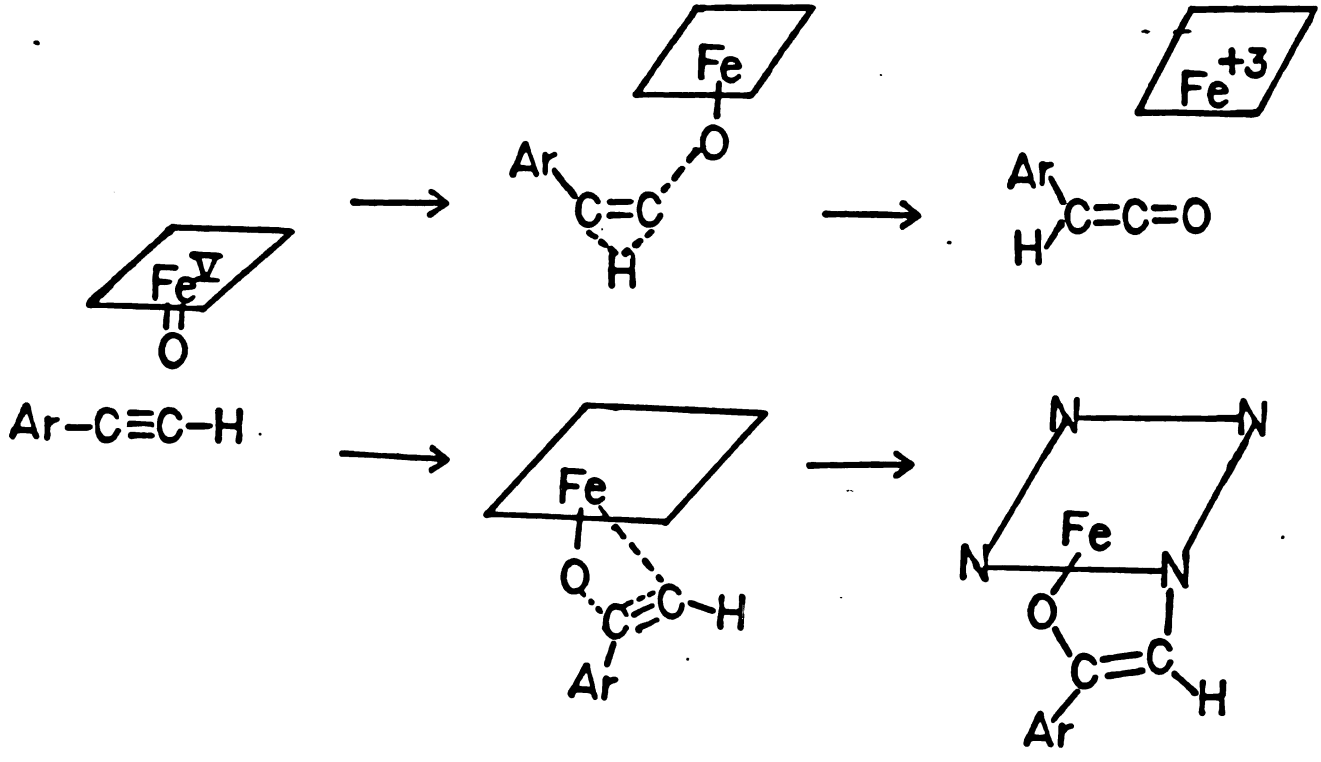

undergoes a similar hybridization change and must involve phenyl group movement towards the porphyrin ring. Also, if the ortho substituents are methyl groups, it may be possible to observe metabolic switching from π-bond oxidation to benzylic carbon oxidation. A direct comparison was made of the rates of oxidation of ortho-methylphenylacetylene and para-methylphenylacetylene. The inductive effect of the methyl group in either position should be approximately the same, so observed differences should reflect steric effects.

GC/MS experiments were initially performed to determine the relative amounts of methyl hydroxylation. Relative amounts of the products were calculated from the total ions in each peak. Standards were only available for the phenylacetic acids, so the hydroxymethyl compounds were identified on the basis of their mass spectra. The relative amount of p-hydroxymethylphenylacetylene was 5 - 10% and that of o-hydroxymethylphenylacetylene 3 - 6%. The production of ortho- and para-methylphenylacetic acids, the major metabolites, was measured (Chapter 2). The capillary gas chromatograph was capable of separating the two phenylacetic acids, so the rates of metabolite formation were determined competitively by incubating a 1: 1 mixture of ortho- and para-methylphenylacetylene with purified, reconstituted P-450b. The result (Figure 4.6) shows no significant steric effect on metabolite formation: in fact, the ortho methyl group increases phenylacetic acid production by a factor of 2. This increase is not due to better binding of the ortho derivative in the active site (Table 4.1) and suggests

Figure 4.6

Oxidation of (ortho-Methylphenyl)Acetylene and (para-Methylphenyl)Acetylene by Purified, Reconstituted P-450b

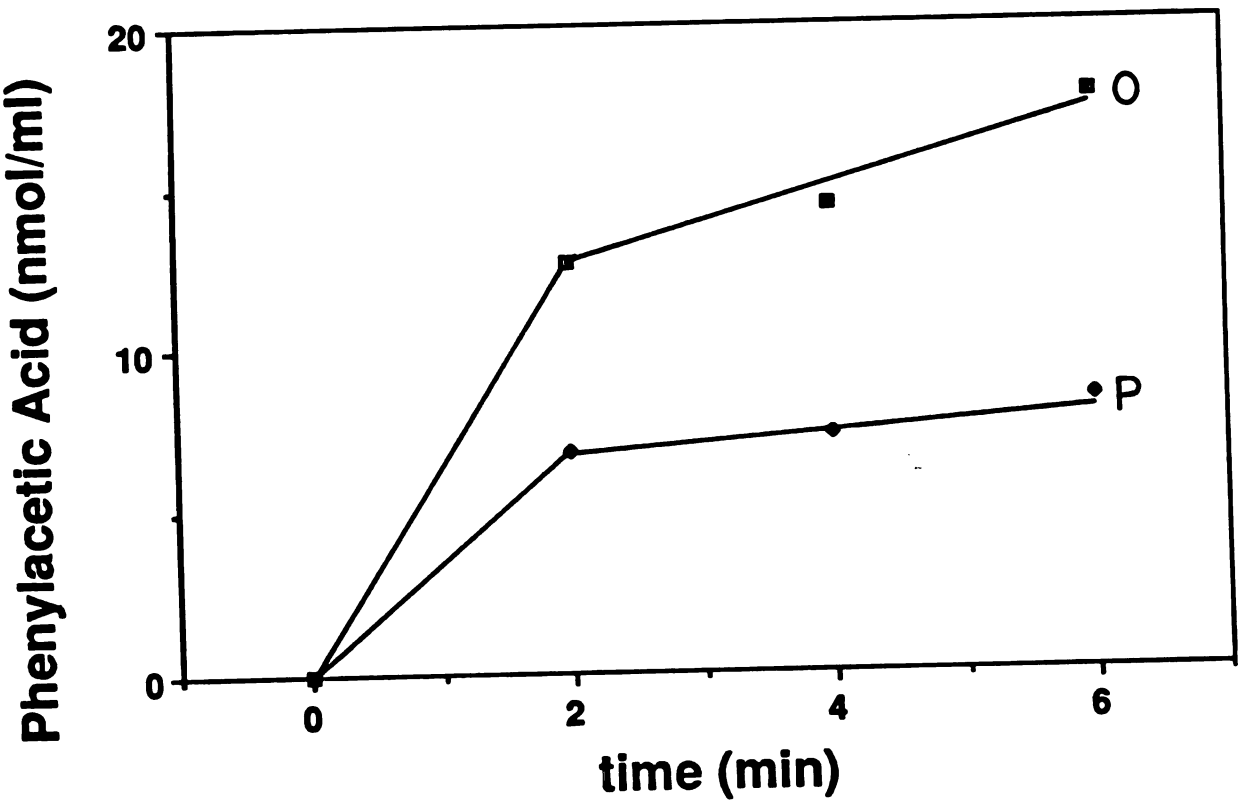

Concentration of o-methylphenylacetic acid (O) and p-methylphenylacetic acid (P) as a function of the time of incubation of the corresponding acetylenes with reconstituted P-450b.

Figure 4.7

Inactivation of Purified, Reconstituted P-450b by ortho-Substituted Phenylacetylenes

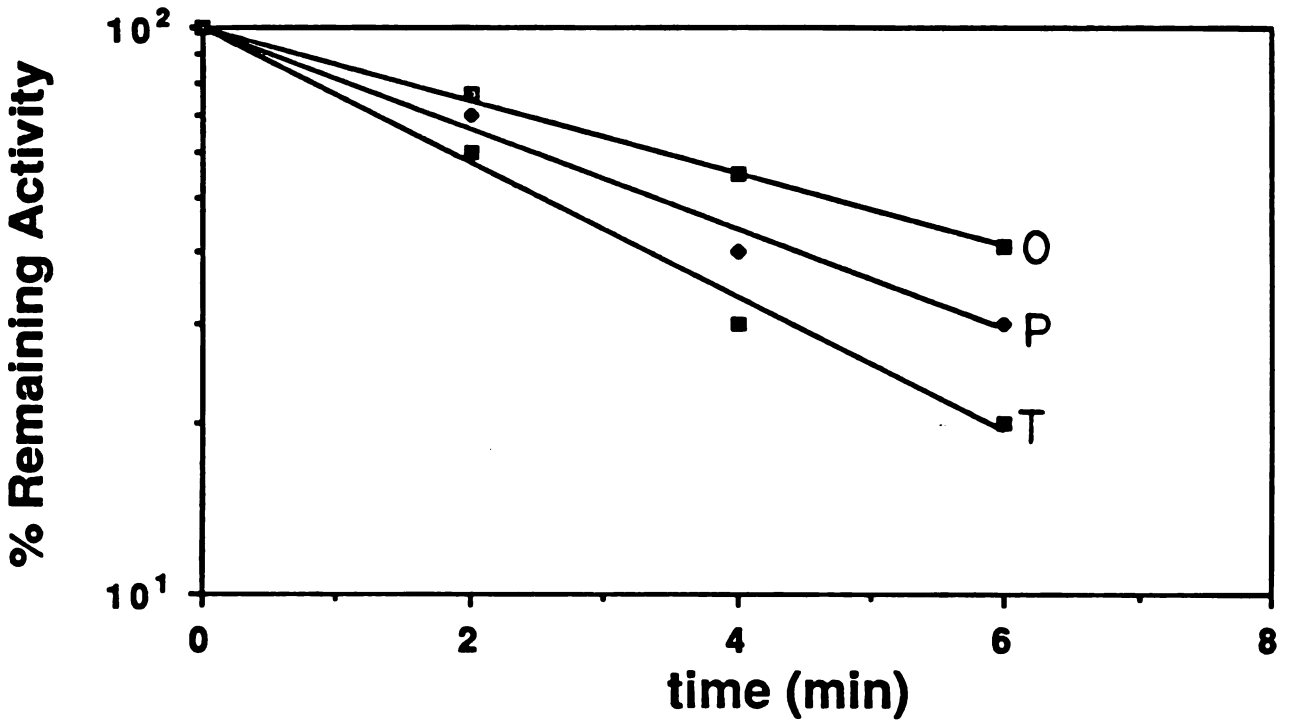

Inactivation of reconstituted P-450b caused by p-methyl (P), o-methyl (O), and 2,4,6-trimethyl (T) phenylacetylenes.

Scheme 4.2

The Proposed Orientation of Phenylacetylene in the Active Site Based on Steric Effects

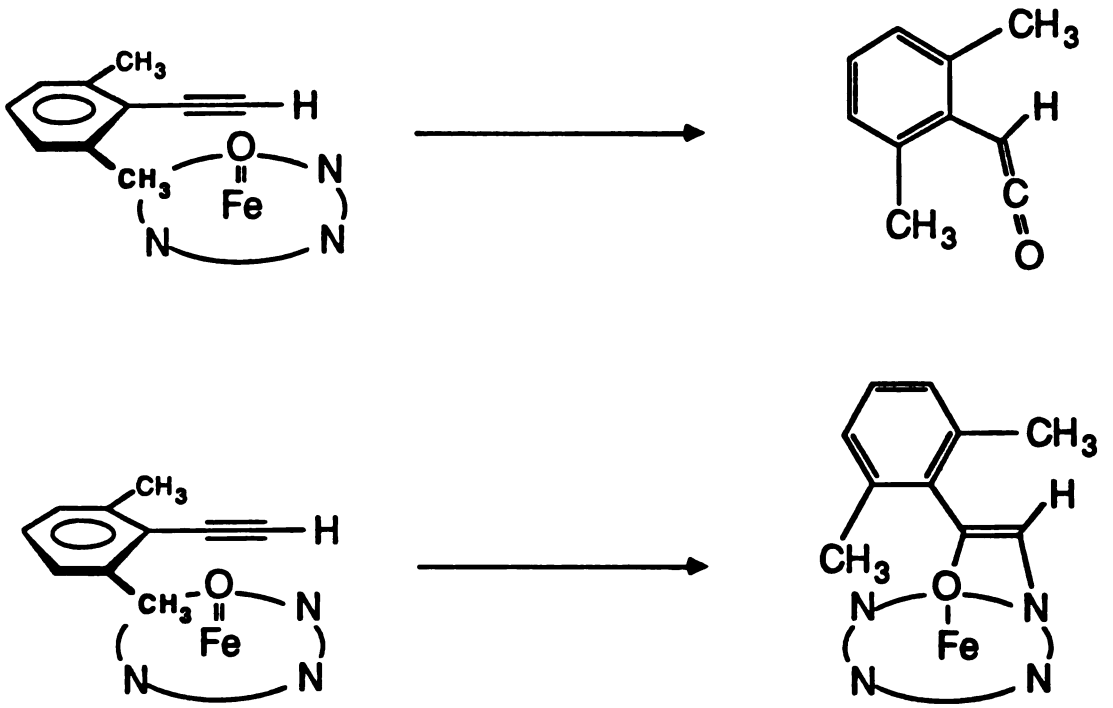

that the sigma coefficients for the ortho and para derivatives are not equal (Fujito and Nishioka, 1976).

2. Inactivation of P-450 by Ortho-substituted Phenylacetylenes.

Steric Effects on enzyme inactivation were initially measured by comparing the rates of inactivation by ortho- and para-methylphenylacetylene using the 7-EC deethylase activity assay (Chapter 2). Although the para-derivative was marginally more effective as an inactivator, the difference was small. Since the ortho- derivative had only one ortho substituent, it was possible that it was bound with the methyl group away from the porphyrin ring. A compound with two ortho methyl substituents, o,o,p-trimethylphenylacetylene was therefore prepared and incubated with purified, reconstituted P-450b. Parallel reactions with the ortho- and para-methylphenylacetylenes were performed and the results were compared (Figure 4.7). The results show no significant steric effect on enzyme inactivation even with the trimethylphenylacetylene which has methyl groups at both ortho positions. This result suggests that the phenylacetylenes are binding above and parallel to the heme ring, and that oxygen insertion into the π-bond occurs from directly under the benzylic carbon without substantial movement of the phenyl ring in the transition state (Scheme 4.2).

C. Styrene vs Phenylacetylene

The kinetic isotope effect on the overall rate of phenylacetylene oxidation by P-450 indicates that the oxygen

transfer step is the slowest step in the catalytic pathway for this substrate. In general, the second electron transfer step has been postulated to be the slowest step (White and Coon, 1980 and references therein) and substrate oxidation proceeds rapidly after generation of the iron oxo species. These results, taken together, suggest that phenylacetylene is particularly difficult to oxidize, but a direct comparison of the rate of oxidation of phenylacetylene with that of another substrate has never been done. Styrene was chosen as the substrate for this comparison because it is oxidized by P-450b and differs from phenylacetylene only in that the olefinic bond is oxidized instead of the acetylenic bond.

A 1:1 mixture of phenylacetylene and styrene was incubated with purified, reconstituted P-450b. After 1 or 2 minutes, an aliquot (1 ml) was removed and extracted with 1 ml of ether to obtain styrene oxide. A separate aliquot (1 ml) was removed and added to a vial containing 5 ml ether, 1 ml 2 N HCl and internal standard and the resulting mixture was extracted to obtain phenylacetic acid. The latter extract was methylated with diazomethane and the two extracts were combined and analyzed by gas chromatography. A typical chromatogram is shown in Figure 4.8. Standard curves were generated by treating mixtures of styrene oxide and phenylacetic acid in the same manner as the metabolic mixtures and analyzing them by gas chromatography. The turnover numbers are 6.3 umol/min/nmol P-450 for styrene and 4.1 nmol/min/nmol P-450. The results show that the rate of styrene oxide production is approximately 1500 times faster than the rate

Figure 4.8

Gas Chromatographic Analysis of the Products from Oxidation of a 1:1 Mixture of Styrene and Phenylacetylene

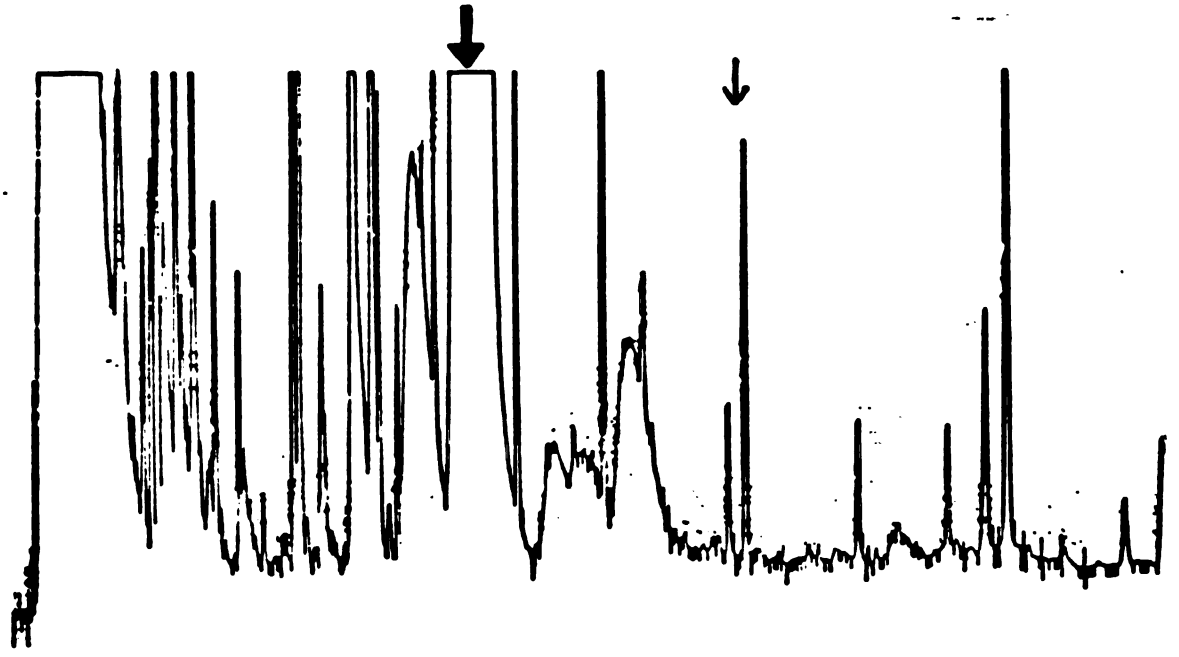

A 1:1 mixture of styrene and phenylacetylene was incubated with reconstituted P-450b to determine the relative rates of oxidation. The mixture was extracted as described in the text and the extracts were recombined and analysed. Styrene oxide is identified by the heavy arrow, and methyl phenylacetate by the light arrow.

of phenylacetic acid production. It is reasonable then, that the slowest step in the oxidation of phenylacetylene by P-450b is indeed the oxygen transfer step.

D. NADPH Consumption

One explanation for the observation that perturbations of the pathway leading to metabolite formation do not effect the rate of enzyme inactivation is that a third pathway partitions from the same intermediate, and that the intermediate is partitioning preferentially into this pathway (see discussion of partitioning in Chapter 1). The presence of a third pathway is also suggested by the fact that total turnover of the substituted phenylacetylenes decreases with increasing electron-withdrawing ability of the substituents. The further reduction of the iro oxo species to water is one candidate for this third pathway. Measurement of increased water production is impossible, of course, but since the reduction requires 2 additional electrons, measurements of the consumption NADPH could uncover such a pathway.

NADPH consumption was measured in incubations of the para substituted phenylacetylenes with purified, reconstituted P-450b by continuously monitoring the NADPH absorbance at 340 nm (Chapter 2). The data were analyzed by linear regression, and the resulting slopes were divided by the extinction coefficient of NADPH to obtain the NADPH consumption (nmol/min/nmol P-450). These data are presented in Table 4.1. Although the trend in the data is in the right direction, it is clear that NADPH consumption does not correlate well with the substituent effects.

In the case of p-chlorophenylacetylene, the NADPH consumption is even slower than that in the absense of a substrate. This suggests that even this pathway is not independent of the rate of oxidation of the substrate, and that the rate of turnover of the enzyme depends of the oxidizability of the substrate. Control experiments indicate that NADPH consumption in the absence of P-450 is negligible (0.7 nmol/min/nmol P-450 or 0.3% of the total) and that p-chlorophenylacetylene does not alter reductase activity.

E. Partition Ratio Perturbation by Cytochrome b_5

Enzyme inactivation by phenylacetylenes appears to be insensitive to both isotope and substituent effects. Phenylacetylenes nevertheless have different partition ratios than other substrates, so their structure in some way determines the rate of inactivation, but neither the rate determining step nor the inactivating species has been defined. Addition of cytochrome b_5 to incubations of phenylacetylene with purified, reconstituted P-450b was shown to inhibit the rate of enzyme inactivation but the mechanism of the inhibition was unknown. The partition ratio of phenylacetylene oxidation by purified, reconstituted P-450b was measured in the presence and absence of b_5 in an attempt to discern the nature of the inhibition. The results from this experiment are shown in Table 4.2.

TABLE 4.2

Effects of Cytochrome b_5 On Phenylacetylene Oxidation by P-450

Time (min)	b_5	Inactivation (nmol)	Metabolite Formation (nmol)	Partition Ratio
2	--	0.23	0.54	
4	--	0.46	0.97	21
2	$+b_5$	0	0.9	
4	$+b_5$	0.15	1.2	72
2	$+b_5$(Mn)	0.20	N.D.	
4	$+b_5$(Mn)	0.40	N.D.	N.D.

note: N.D. indicates the values were not determined. The abbreviation: b_5(Mn) refers to the Manganese substituted cytochrome b_5.

Addition of b_5 to the reconstitution system causes approximately a three fold increase in the partition ratio. This effect is due entirely to the ability of b_5 to protect the enzyme from phenylacetylene-mediated destruction. To distinguish whether the b_5 effect is electronic or allosteric, apo b_5 was reconstituted with manganese PPIX (Chapter 2). This prothetic group substitution yields a b_5 molecule that has approximately the same protein structure but is incapable of transferring electrons (Cinti and Ozols, 1975). As the data in Table 4.2 show, the Mn-b_5 has no effect on the enzyme inactivation caused by phenylacetylene. This result clearly shows that protection of P-450 from phenylacetylene-mediated destruction is electronically mediated by b_5.

CHAPTER 5

PUTATIVE INTERMEDIATES : α-KETOCARBENES

The oxidation of acetylenes by peracids has been suggested to generate an oxirene either as an unstable intermediate or as a transition state (Scheme 1.8). The oxirene either may rearrange to of 2 isomeric α-ketocarbenes or these may form directly. The α-ketocarbenes can also be obtained from the Wolff rearrangement of α-diazoketones (Wolff, 1902, 1912). Thermal or photochemical Wolff rearrangements proceed with isomerization of the α-ketocarbenes presumably via an oxirene (Sus, 1944 and Fenwick et al, 1973), but isomerization is not observed during rearrangements catalyzed by Ag+ or Cu+ (Casanova et al, 1950; Yates and Crawford, 1966; Yates and Fugger, 1957; and Matlin and Sammes, 1972). Acetylene oxidation by P-450 forms the same product as is formed by peracid oxidation suggesting that possible intermediates in the reaction may be members of the "oxirene manifold". An alternate route to these intermediates is via the α-diazoketones which should decompose in the presence of reduced P-450 to the corresponding α-ketocarbenes. The reaction of reduced P-450 with ethyldiazoacetate (EDA), a commercially available α-diazoketone, was first studied to determine the metabolic fate of such compounds. The two isomeric α-diazoketones which would yield the isomeric α-ketocarbenes expected from oxidation of phenyalcetylene are diazoacetophenone (DAP) and 2-diazophenylacetaldehyde. The metabolism of

diazoacetophenone has been studied in detail; 2-diazophenylacetaldehyde is synthetically inaccessible (Appendix I). Its methyl analog, 1-diazo-1-phenyl-2-propanone (Me-DAP) was therefore investigated.

A. Diazoketone Metabolism

1. Complex Formation

Difference absorbance spectra were obtained for the reactions of EDA, DAP and Me-DAP by comparing the absorbance spectra of incubations of microsomes with each compound plus or minus NADPH (Figure 5.1). In each case, the formation of a complex with a λ max of 445 nm was indicated by the spectrum. This absorbance is similar to that of complexes observed in the reductive turnover of such compounds as halocarbons and methylene dioxyphenyl derivatives (Mansuy et al, 1974; Wolf et al, 1977 and Franklin, 1971) The extinction coefficient of the complex appeared to be similar to that of the reduced CO complex. The complex derived from EDA could be generated in the absence of NADPH and was rapidly formed, but the other two complexes only formed in the presence of NADPH. Exclusion of oxygen from the incubation by bubbling with argon increased the yield of the complex. The maximum yield of complex was obtained when $Na_2S_2O_4$ was substituted for NADPH.

Reaction of purified, unreconstituted P-450b with diazoketones and $Na_2S_2O_4$ results in the development of an analogous absorbance (λ max 440 nm) at the expense of the native P-450 Soret band (Figure 5.2). In the case of DAP, the magnitude of the absorbance is equal to that of the original

Figure 5.1

Electronic Absorption Spectra of the Complexes of -Diazoketones with Microsomal P-450

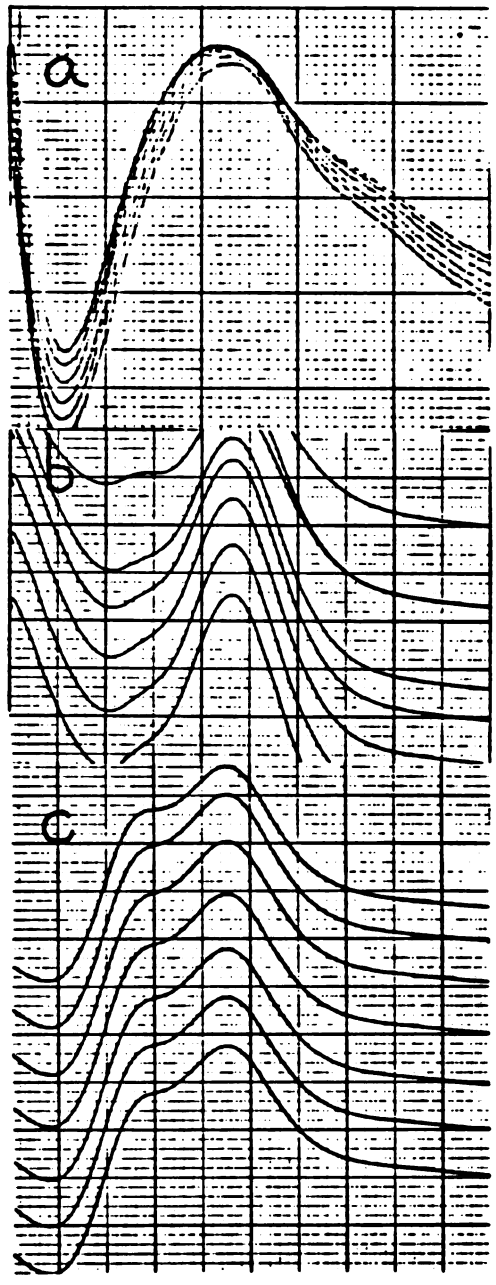

The Electronic Absorption Spectra of incubations of microsomal P-450, NADPH and (a) Ethyldiazoacetate, (b) Diazoacetophenone, and (c) 1-diazo-1-phenyl-2-propanone. The series of spectra are repeated scans during a 10 minute period.

Figure 5.2

Electronic Absorption Spectrum of the Complex of Diazoacetophenone with Purified P-450b

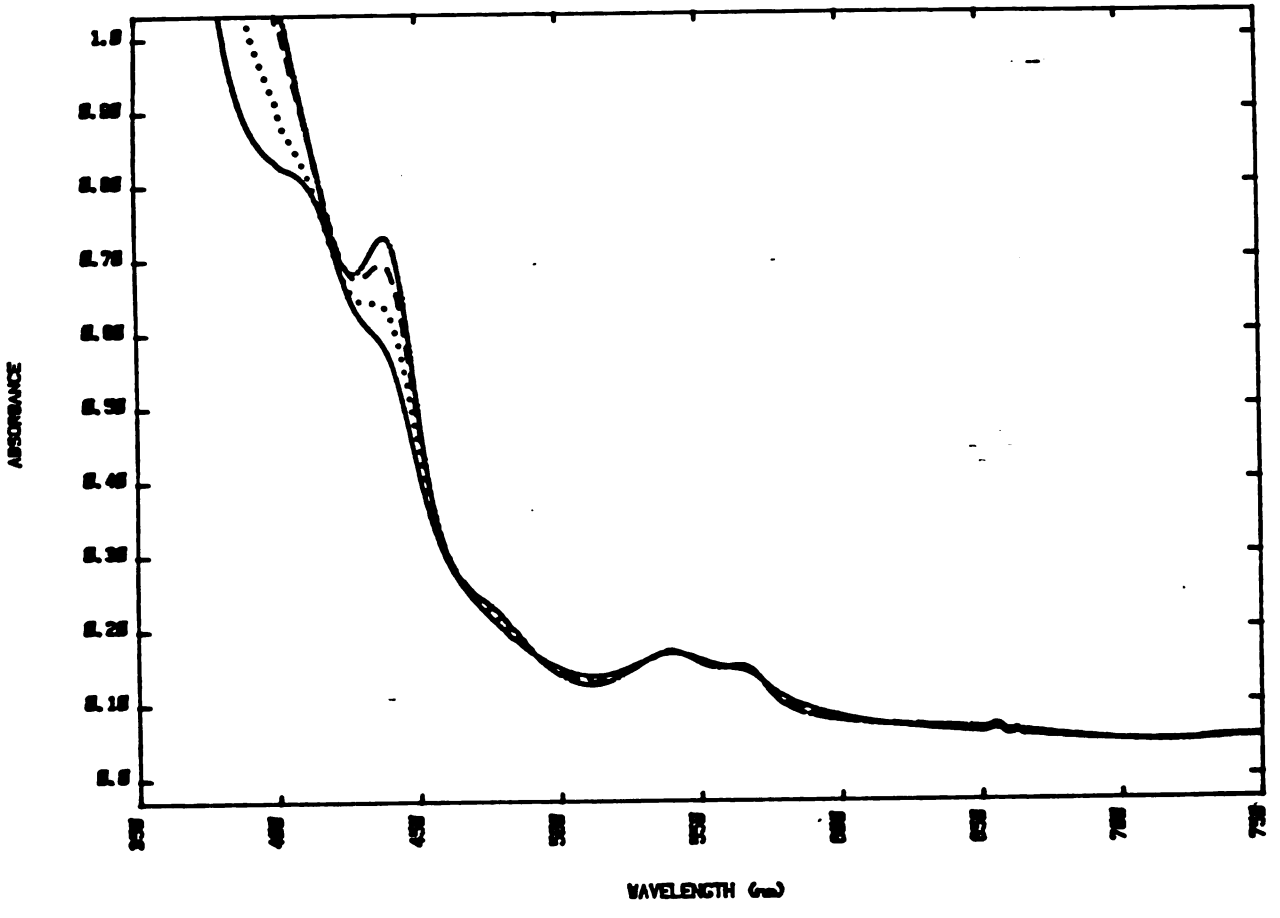

Purified P-450b was incubated with diazoacetophenone and then reduced with $Na_2S_2O_4$ to form the 445 nm complex.
The spectrum immediately after addition of $Na_2S_2O_4$ (——) shows the native P-450 Soret band at 418 nm that disappears with time to form the 445 nm complex. The complex is completely formed after 2 to 3 minutes (·—·—·).

Soret. This suggests quantitative conversion of the protein to the new complex, although the extinction coefficient of the complex is unknown. The other diazoketones also formed complexes with pure P-450b but the extent of conversion was variable. Figure 5.3 shows the complexes formed from Me-DAP and EDA. Purified P-450cam, a soluble P-450 obtained from Pseudomonas putida, also quantitatively forms a complex with DAP and EDA (Figure 5.4). Formation of the EDA complex in pure enzyme, unlike the reaction in microsomes, required reduction by $Na_2S_2O_4$.

2. Metabolite Formation

The fact that the λ max of each complex was at 445 nm, a position very similar to the carbene complexes obtained with such diverse compounds as halocarbons and methylene dioxyphenyl derivatives suggested that the diazoketones may indeed be forming carbene complexes. A search was therefore made for metabolites indicative of carbene intermediates. Microsomes were treated with DAP in the presence or absence of NADPH for 1 hour. The metabolites were then isolated by acidification and ether extraction. The ether extracts were methylated with diazomethane and analysed by GC/MS. Two products were obtained. Phenylacetic acid was isolated from both of the incubations, so that its formation is independent of NADPH. This is the product expected from thermal or photochemical decomposition of DAP and presumably results from formation of the oxirene because the oxygen migrates to the terminal carbon. Benzoic acid, the only observable NADPH dependent product, probably forms oxidatively by a mechanism along the lines of that shown in Scheme 5.1.

Scheme 5.1

The Mechanism of Oxidative Formation of Benzoic Acid from Diazoacetophenone

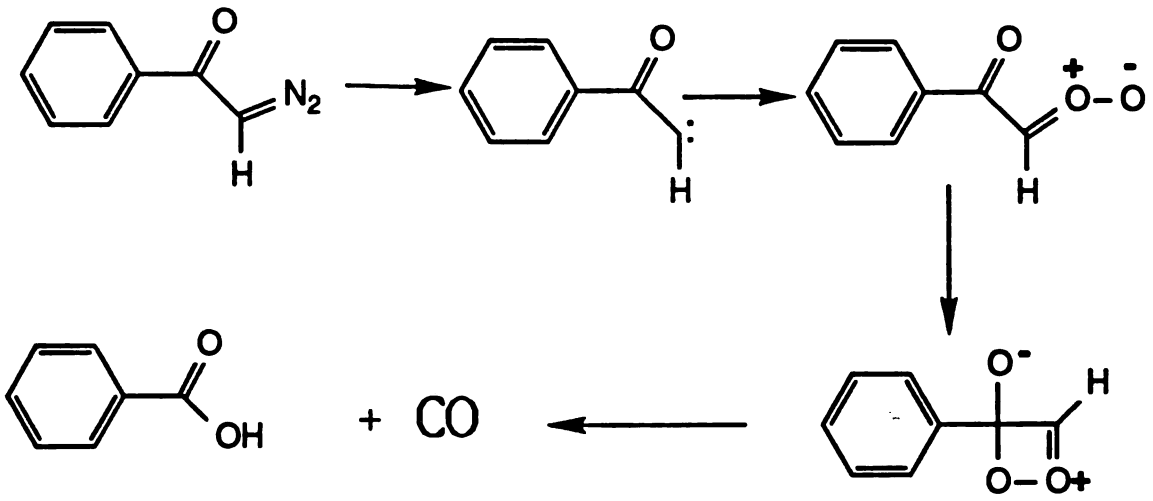

Figure 5.3

Electronic Absorption Spectra of the Complexes of Ethyldiazoacetate and Me-DAP with Purified P-450b

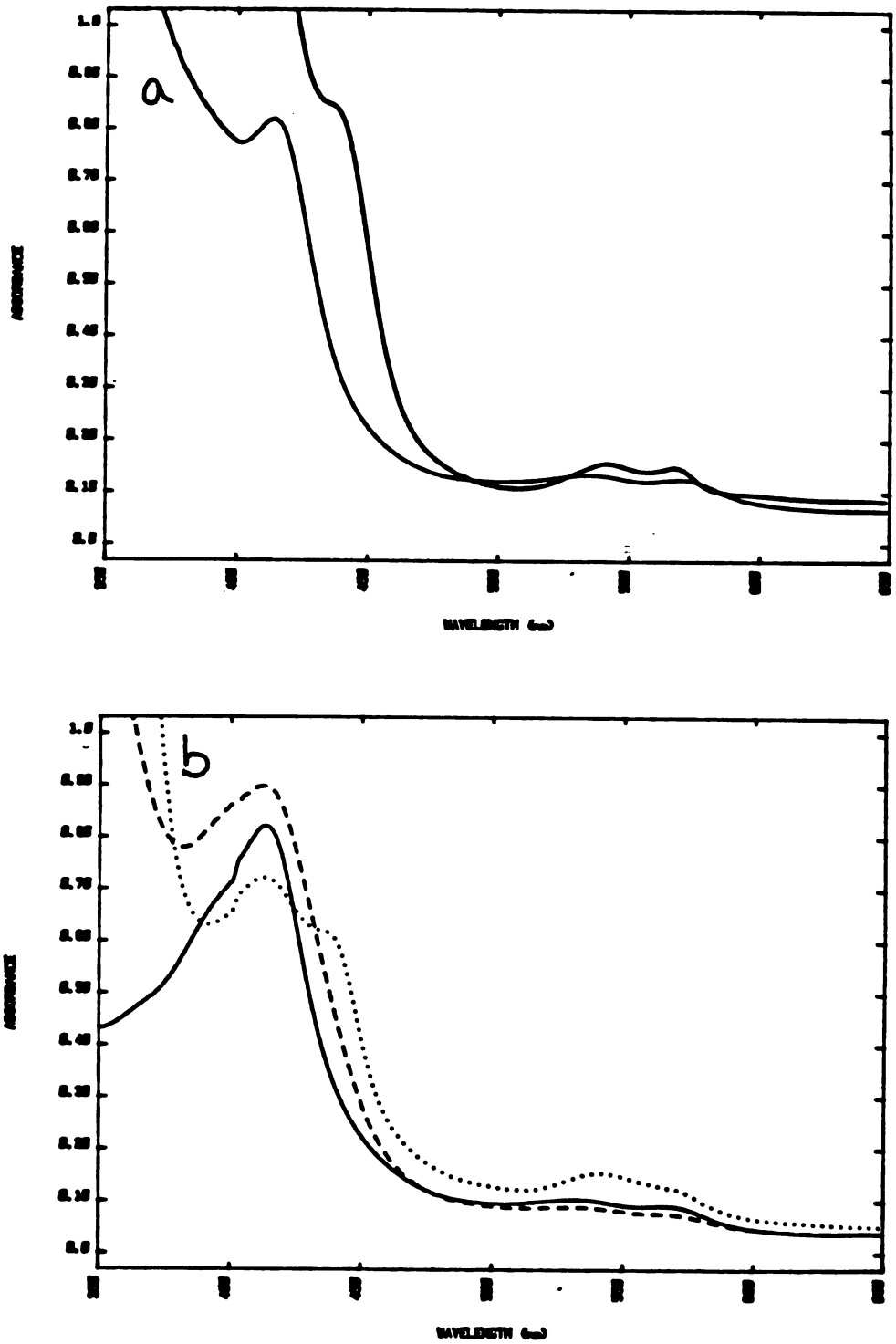

Purified P-450b was incubated with (a) ethyldiazoacetate, or (b) 1-diazo-1-phenyl-2-propanone and then reduced with $Na_2S_2O_4$ to form the 445 nm complexes. The spectra in (b) show the native P-450 Soret band (——), the Soret of reduced P-450 (- - - -), and the 445 nm complex (.....).

Figure 5.4

Electronic Absorption Spectra of Complexes of Ethyldiazoacetate and Diazoacetophenone with P-450cam

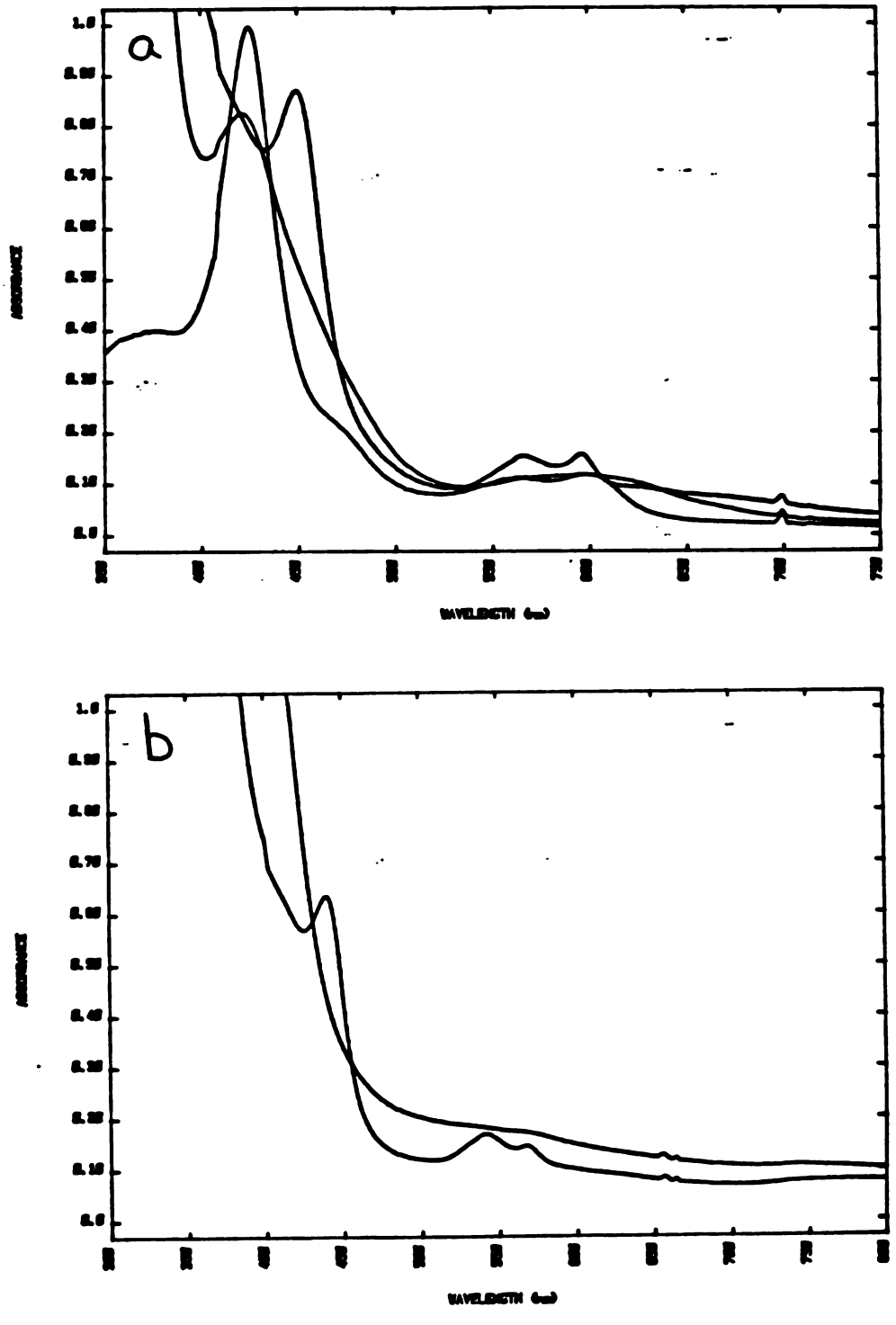

Purified P-450cam was incubated with (a) diazoacetophenone or (b) ethyldiazoacetate and then reduced with $Na_2S_2O_4$ to form the 445 nm complexes. The spectra in (a) show the native P-450 Soret band at 418 nm, the reduced P-450, and the fully formed complex at 445 nm.

3. Enzyme Inactivation

All three diazoketones caused time dependent destruction of microsomal P-450 as measured by the Soret loss assay (Chapter 2). The data from these experiments are plotted in Figure 5.5. Soret loss was observed in all cases, but the EDA induced loss was not NADPH dependent. Soret loss does not appear to correlate well with complex formation because DAP, which gave a higher yield of complex than Me-DAP, caused a smaller decrease in the Soret. Since the complex formed in the reaction of DAP with P-450 absorbs at 445 nm, it was thought possible that an increase in the absorbance at 450 nm due to the complex contributed to the artifactually small decrease in the Soret absorbance. Attempts were made to decompose the complex with $K_3Fe(CN)_6$ prior to measurement of the soret, but no further Soret loss was observed.

4. Heme Adduct Formation

The observation of Soret loss suggested that perhaps the diazoketones were forming N-alkylated porphyrins directly or from the decomposition of carbene complexes. Isolation of the diazoketone heme adducts was performed using the in vitro procedure (Chapter 2) because the diazoketones were not expected to survive in vivo injection and metabolism.

Microsomes from 10 rats (4000 nmol) were incubated for 1 hour with EDA and were worked-up as usual. The structure of the heme adduct that was obtained from this incubation was unequivocally shown to be that in Figure 5.6. Mass spectral analysis (FDMS) gave the molecular ion at m/e 676 with a small component at m/e 662 due presumably to the transesterified

Figure 5.5

Inactivation of Microsomal P-450 by α-Diazoketones

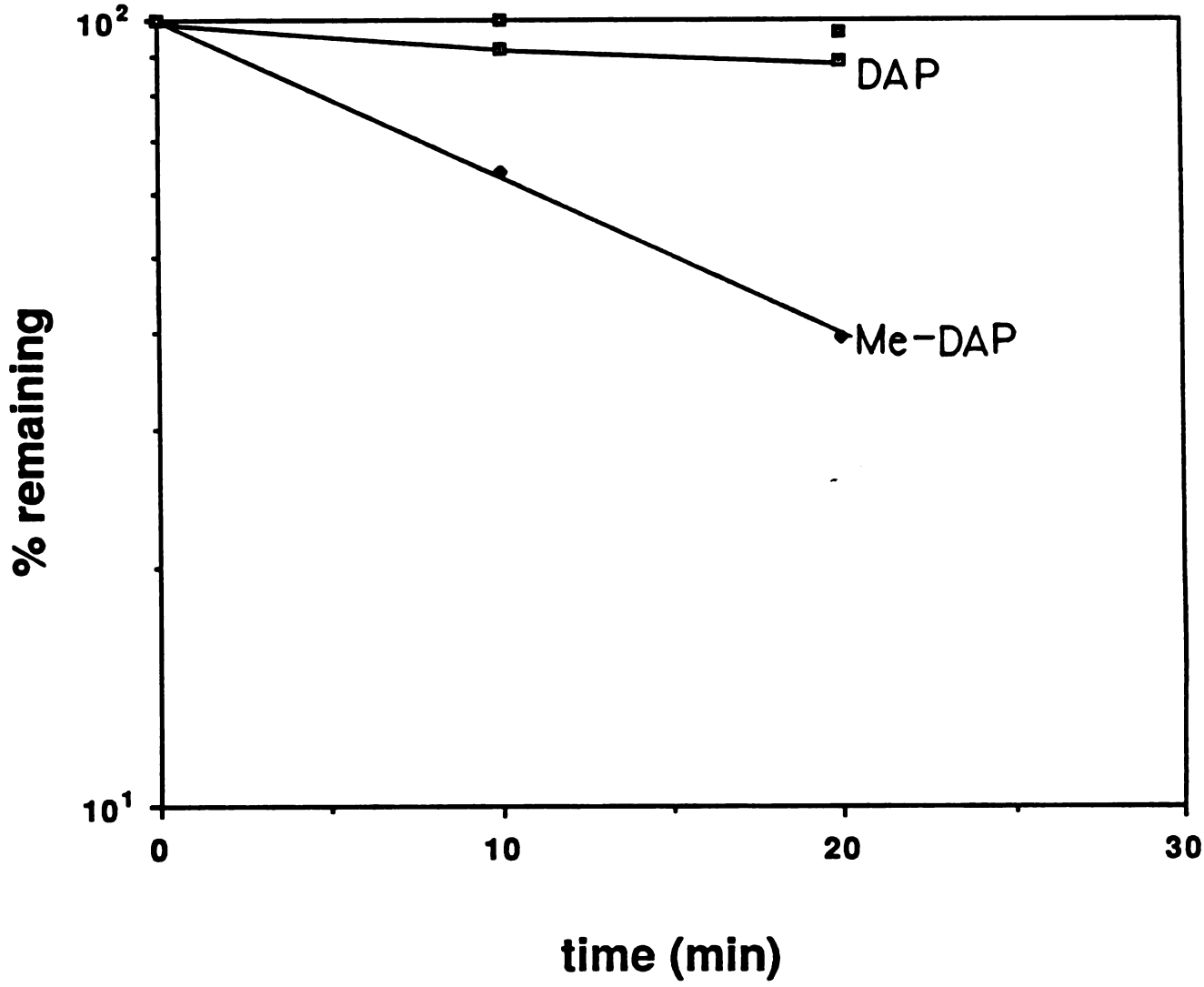

Loss of the P-450 chromophore caused by (a) diazoacetophenone and (b) 1-diazo-1-phenyl-2-propanone in incubations of the diazoketones with microsomal P-450 from phenobarbital-induced rats. The substrate independent loss is also shown. The loss of chromophore caused by ethyldiazoacetate was not dependent on NADPH.

Figure 5.6

500 MHz ^{1}H-NMR Spectrum of the Zinc Complex of the Ethyldiazoacetate-PPIX Adduct

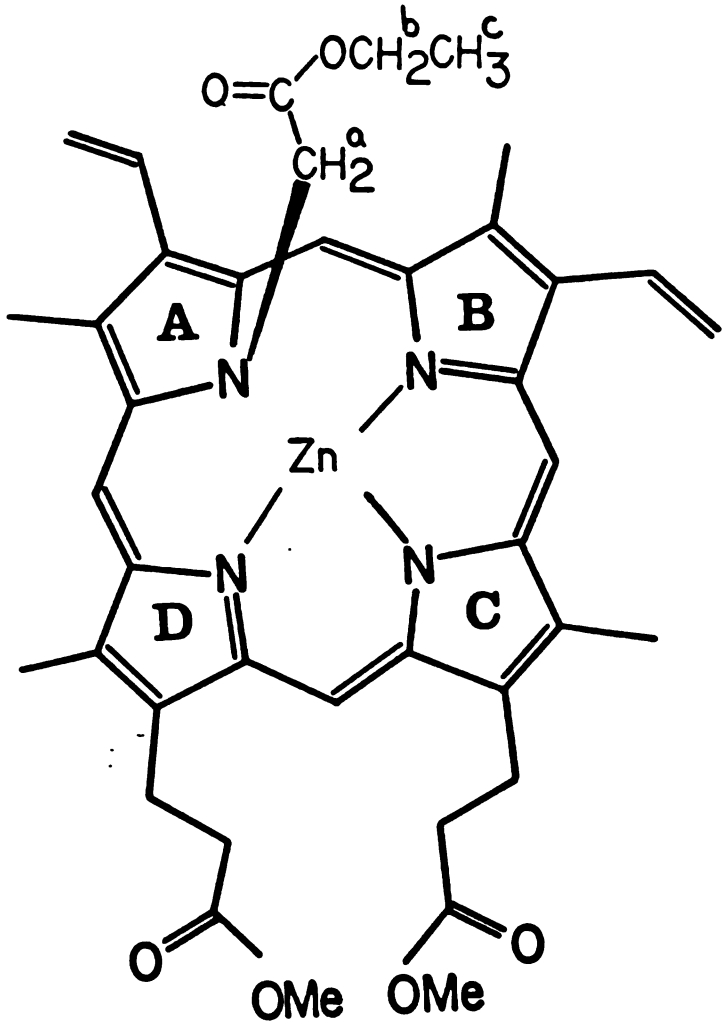

The NMR spectrum from -5 to 12 ppm is shown for a single isomer of the EDA-PPIX adduct. The meso protons are shown in the inset. Protons of interest are labelled on the structure and the corresponding peaks are labelled with the same letter on the spectrum. The peak listing can be found in Table 5.1.

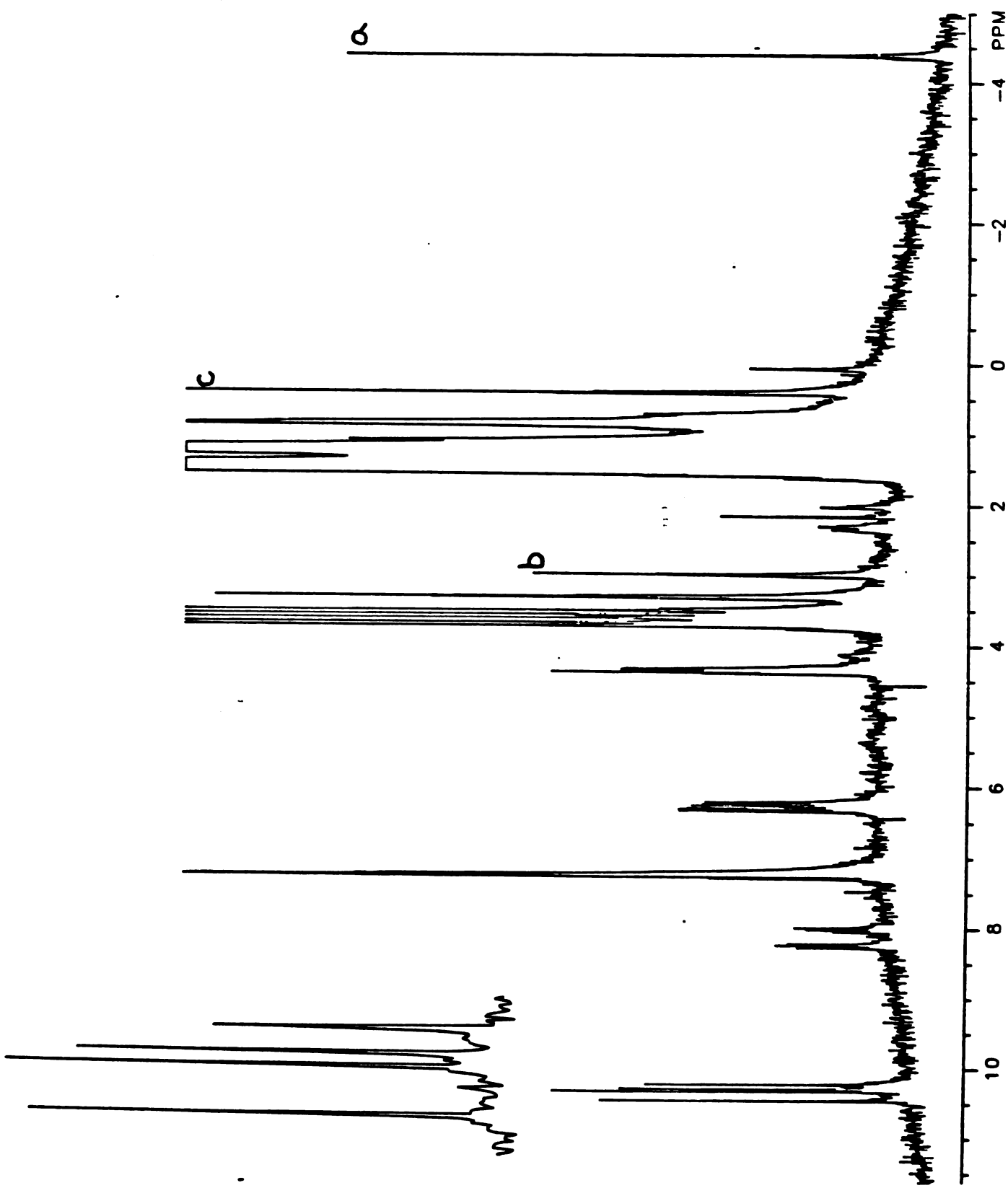
a
c
b
10
8
6
4
2
0
-2
-4
PPM

compound in which the ethoxy group is replaced by a methoxy during work up. NMR analysis was performed on a single isomer (either A or B ring alkylated) which was separated by HPLC (2:1 hexane : tetrahydrofuran) from the other isomers. The expansion of the meso protons in the inset in Figure 5.6 shows that there is only one isomer. The 500 MHz ^{1}H-NMR spectrum (Figure 5.6) shows splitting of the internal vinyl protons, which indicates that alkylation has occurred on pyrrole rings A or B. The shoulder on the soret band in the absorbance spectrum is consistent with this interpretation (Figure 5.7) (Kunze and Ortiz de Montellano, 1981). The chemical shifts and integrations of all the resonances in the NMR spectrum are tabulated in Table 5.1. NMR decoupling experiments enabled unambiguous assignment of all the ethoxy group protons (Figure 5.8).

Heme adduct formation was also observed in incubations of microsomes with DAP. The heme adduct was purified and characterized by absorbance and NMR spectroscopy and mass spectrometry. The molecular weight from both LSIMS and FD mass spectrometry is m/e 709. The absorbance spectrum (Figure 5.9) shows no shoulder on the Soret band, consistent with C or D ring alkylation. This is supported by splitting of the propionic acid internal methylene protons in the NMR spectrum (Figure 5.10). The NMR spectrum shows a small amount of a minor isomer that could not be removed by HPLC without unacceptable decomposition of the adduct. The NMR chemical shifts and integrals are tabulated in Table 5.1.

Figure 5.7

Electronic Absorption Spectrum of the Zinc Complex of the Ethyldiazoacetate-PPIX Adduct

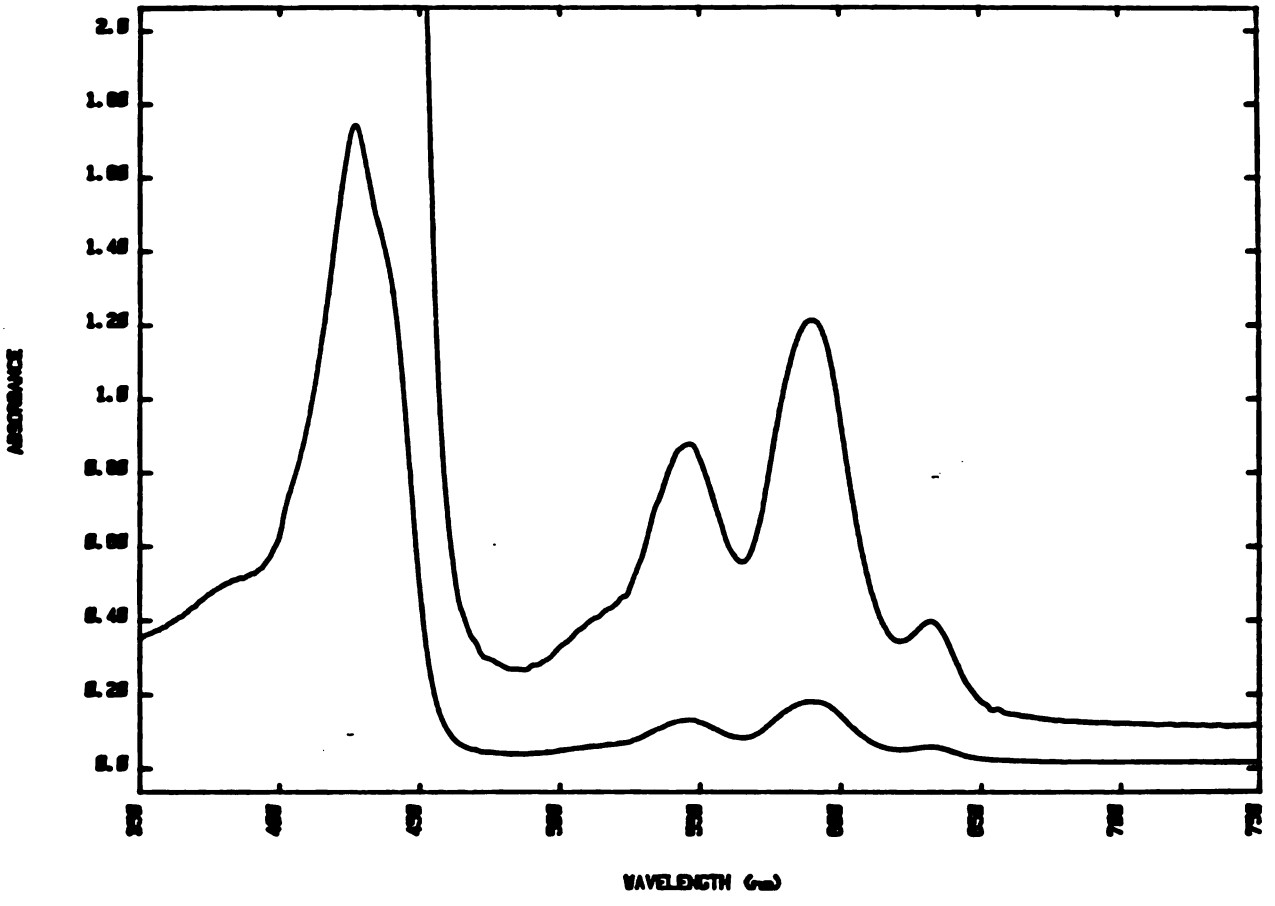

The electronic absorption spectrum of the EDA-PPIX adduct shows a soret band at 430 nm with the long wavelength shoulder indicative of A or B ring alkylation.

Figure 5.8

500 MHz ^{1}H-NMR Decoupling of the Ethoxy Group Protons in the Zinc Complex of the Ethyldiazoacetate-PPIX Adduct

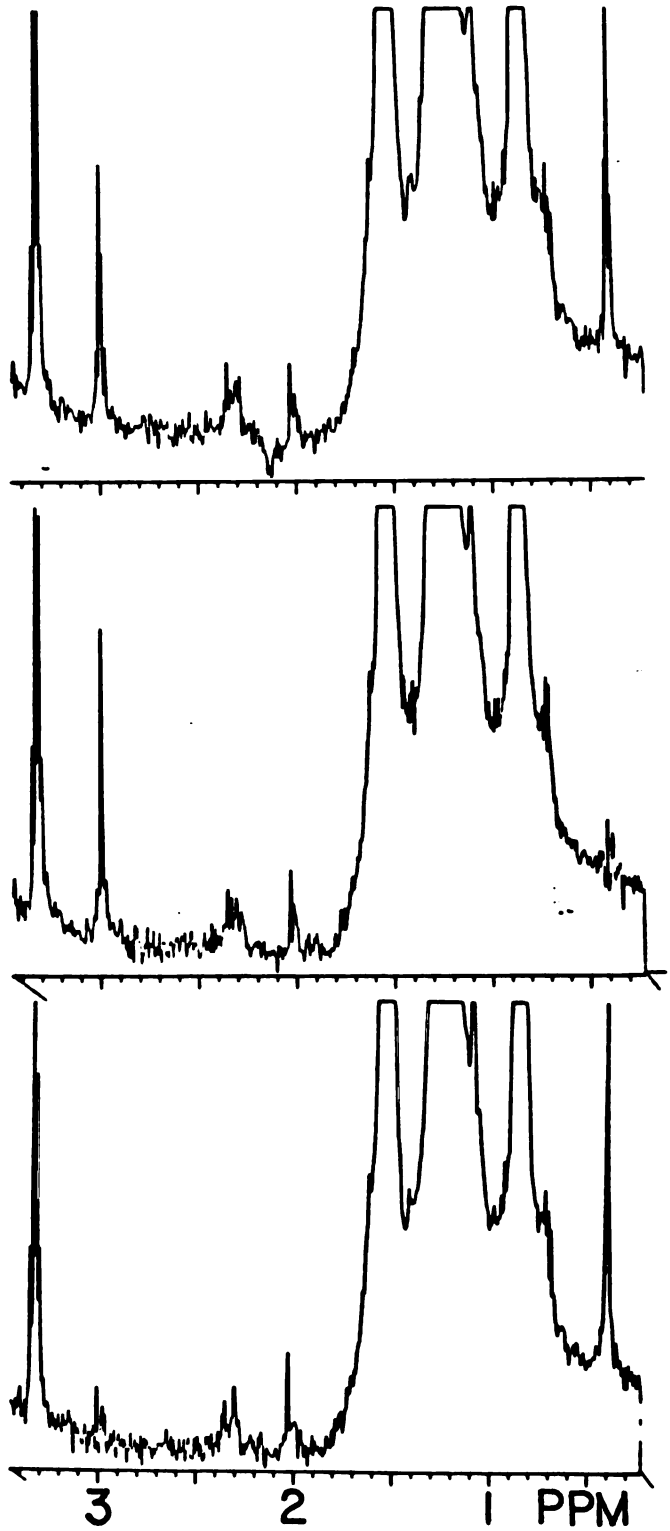

The ethoxy group protons in the EDA-PPIX adduct were identified by decoupling. (a) The undecoupled spectrum shows the methyl protons at 0.4 ppm coupled to the methylene at 3.0 ppm. (b) Irradiation of the methyl protons (indicated by the arrow) causes the methylene protons to become a singlet. (c) Irradiation of the methylene protons (indicated by the arrow) causes the methyl group to become a singlet.

Figure 5.9

Electronic Absorption Spectrum of the Zinc Complex of the Diazoacetophenone-PPIX Adduct

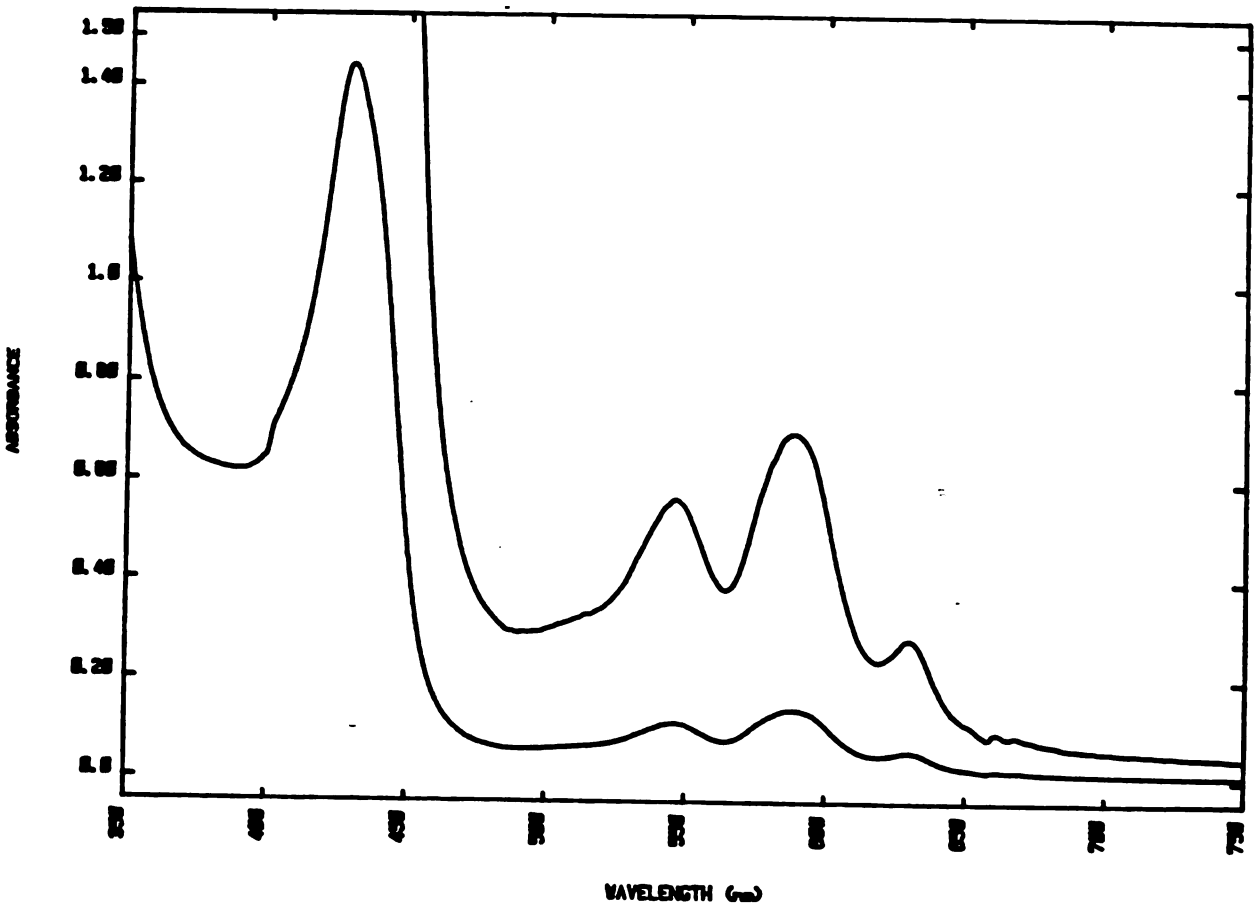

The electronic absorption spectrum of the DAP-PPIX adduct shows no shoulder on the soret band (430 nm). This is consistent with C or D ring alkylation.

Figure 5.10

500 MHz ^{1}H-NMR Spectrum of the Zinc Complex of the Diazoacetophenone-PPIX Adduct

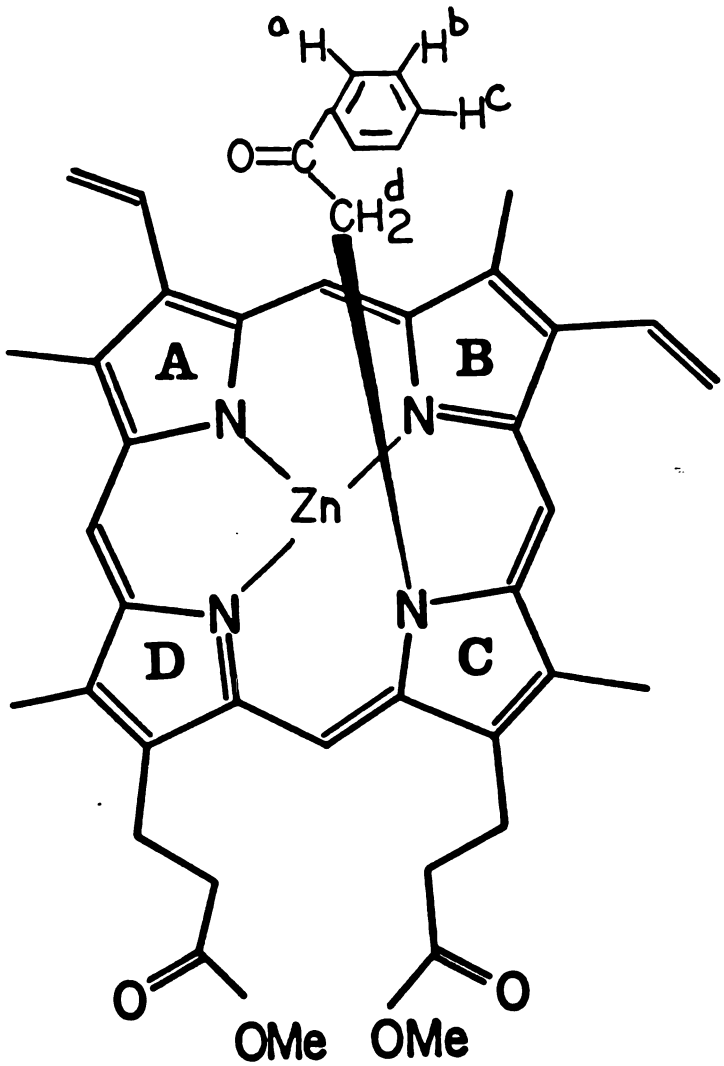

The NMR spectrum from -5 to 12 ppm is shown for a mixture of DAP-PPIX adduct isomers. The mixture consists largely of C/D porphyrin ring alkylated products based on the internal vinyl protons at 8.2 ppm. Protons of interest are labelled on the structure below and the corresponding peaks are labelled with the same letter on the NMR spectrum. The peak listing is presented in Table 5.1.

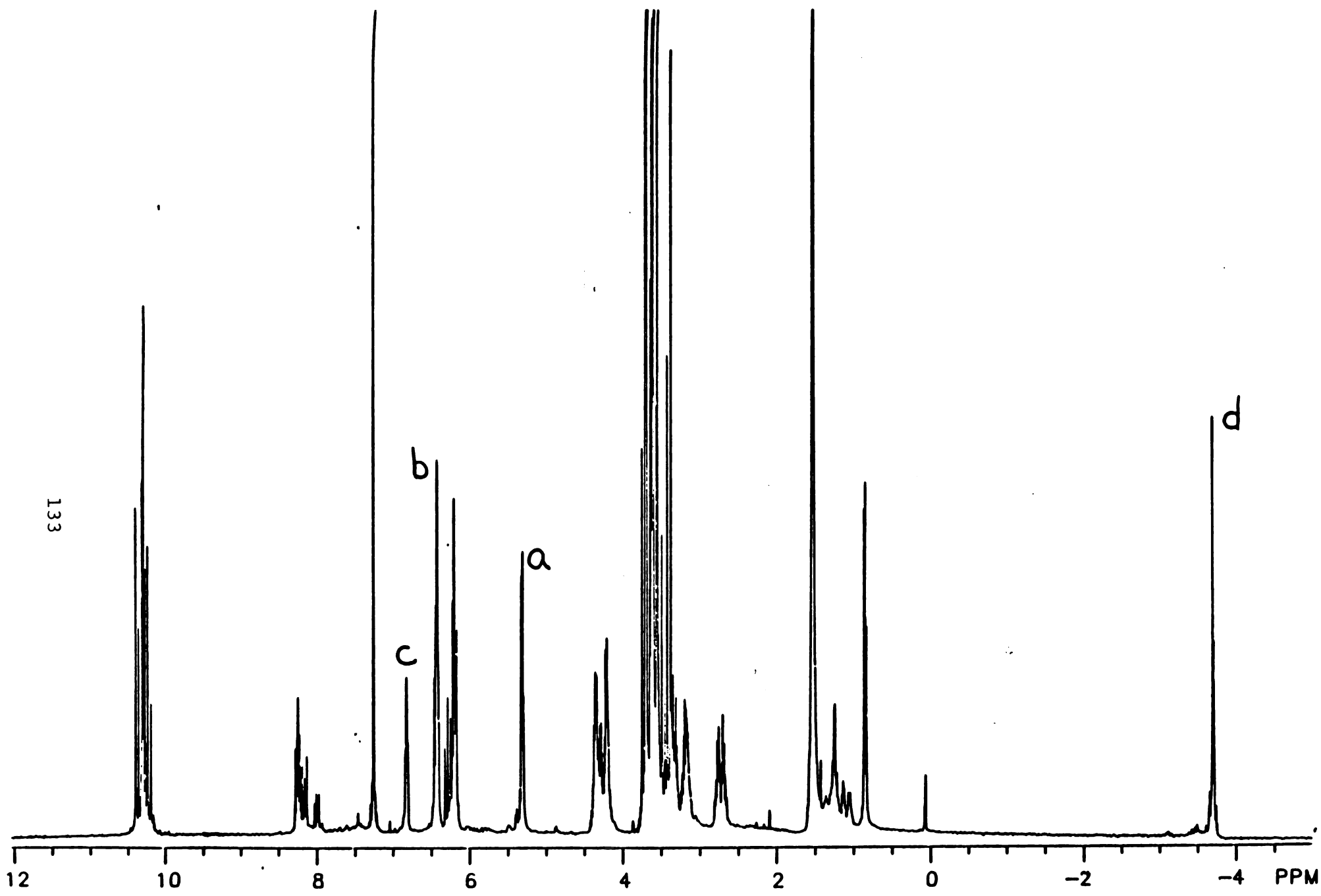
a
b
c
d
12
10
8
6
4
2
0
−2
−4
PPM

TABLE 5.1

Chemical Shifts and Integration of the Proton Signals in the Spectra of N-Alkyl PPIX Adducts

	EDA Adduct		DAP Adduct	
Assignment	Chem. Shift	Integration	Chem. Shift	Integration
porphyrin ring				
meso	10.6 - 10.1	4 (4s)	10.4 - 10.2	4 (m)
internal vinyl	8.4 - 7.8	2 (2m)	8.4 - 7.9	2 (m)
external vinyl	6.4 - 6.02	4 (m)	6.52 - 6.12	6 (m)
internal methylenes	4.46 - 4.15	4 (q)	4.46 - 4.12	4 (2m)
methyls and external methylenes	3.80 - 3.45	18 (m)	3.83 - 2.98	22 (m)
N-Alkyl group				
N-methylene	-4.34 - -4.45	2 (s)	-3.35 - -3.77	2 (s)
ethoxy methylene	3.04 - 2.92	2 (q)		
ethoxy methyl	0.44 - 0.31	3 (t)		
para phenyl			6.88 - 6.75	1 (t)
meta phenyl			under external vinyls	
ortho phenyl			5.44 - 5.22	2 (dd)

The abbreviations used are m, multiplet; q, quartet; s, singlet; t, triplet; d, doublet; dd, doublet of doublets

Decoupling experiments were analyzed by subtraction because the meta protons of the phenyl ring were hidden under the external vinyl protons of the porphyrin ring. The subtraction spectra are shown in Figure 5.11. These data permit unequivocal determination of the structure of the adduct (Figure 5.9) which, in analogy with that formed from EDA, has the diazo carbon bound to the pyrrole nitrogen. The diazo group itself is lost, presumably as N_2.

Purified, unreconstituted P-450b was reacted with DAP and $Na_2S_2O_4$ to form the 440 nm complex as already described. The reaction mixture was then added to cold 5% H_2SO_4/methanol to isolate the N-alkylated porphyrin. Indeed, a small amount of N-alkylated porphyrin (approximately 14 ug, 10% yield) was isolated. The porphyrin coeluted with authentic DAP pigment by thin layer chromatography and the absorbance spectrum (Figure 5.12) was identical.

Attempts were made to isolate an N-alkylated porphyrin from Me-DAP, but none was observed. This is consistent with unpublished observations that secondary adducts are both less stable and more difficult to isolate.

B. Model Reactions

Diazoketones, as shown above, form complexes with P-450 to yield N-alkylated porphyrins. These results suggest that carbene complexes analogous to those described by others are intermediates in the reaction but do not actually prove their existence as discrete species. Tetraphenylporphyrin (TPP) models have been used to generate stable carbene complexes from several

Figure 5.11

500 MHz ^{1}H-NMR Decoupling of the Phenyl Group Protons in the Zinc Complex of the Diazoacetophenone-PPIX Adduct

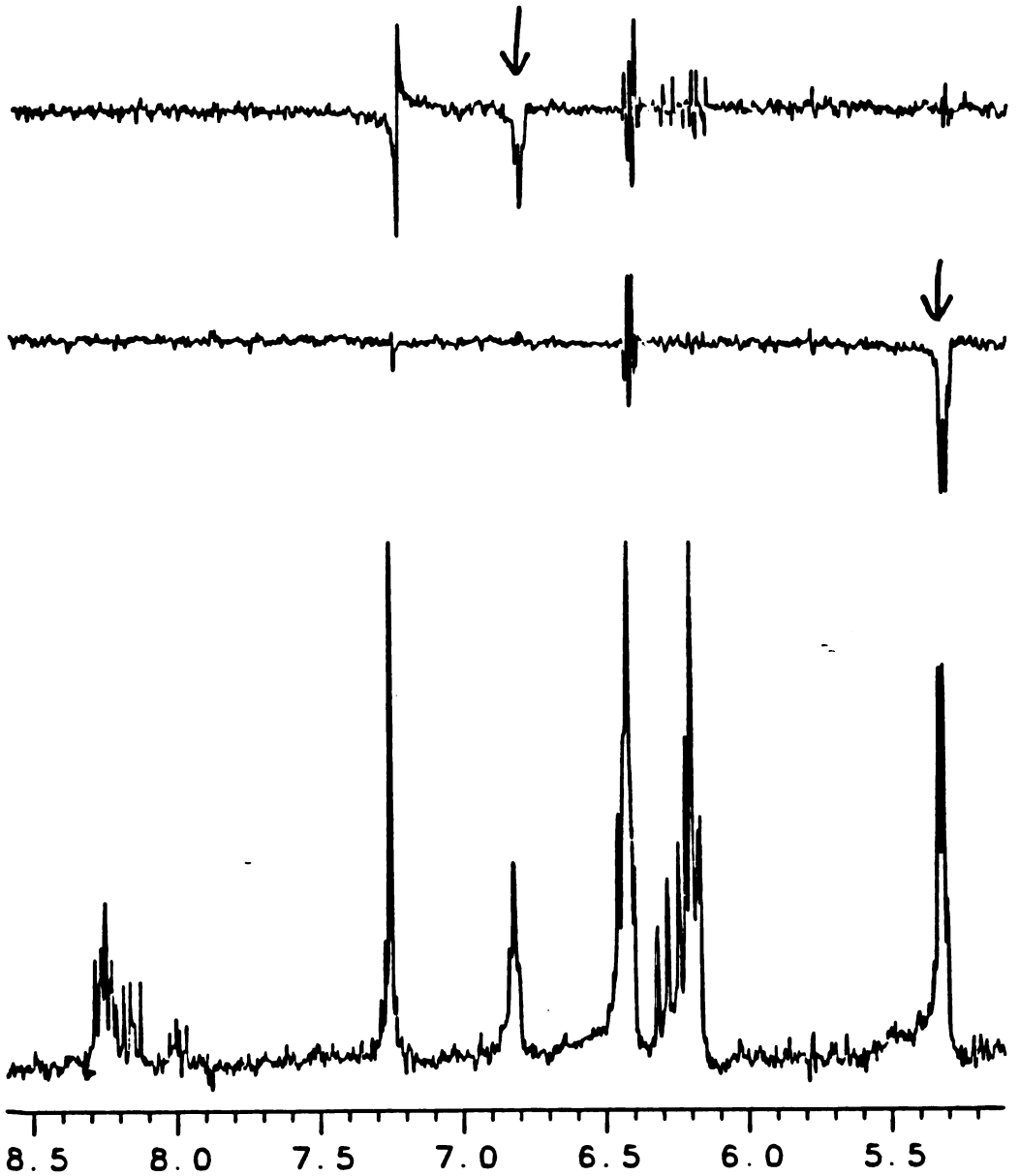

The phenyl group protons in the DAP-PPIX adduct were identified by subtraction decoupling because the meta protons are hidden under the external vinyl protons. (a) The para proton was irradiated (indicated by the arrow) and the resulting spectrum was subtracted from a spectrum collected during irradiation at 5.8 ppm. The meta protons are identified as a disturbance in the baseline at 6.5 ppm. (b) Irradiation of the ortho protons causes the same disturbance after subtraction (c) The undecoupled spectrum which was subtracted from the two decoupled spectra is shown.

Figure 5.12

Electronic Absorption Spectrum of the Zinc Complex of the Diazoacetophenone-PPIX Adduct Isolated from Purified P-450b

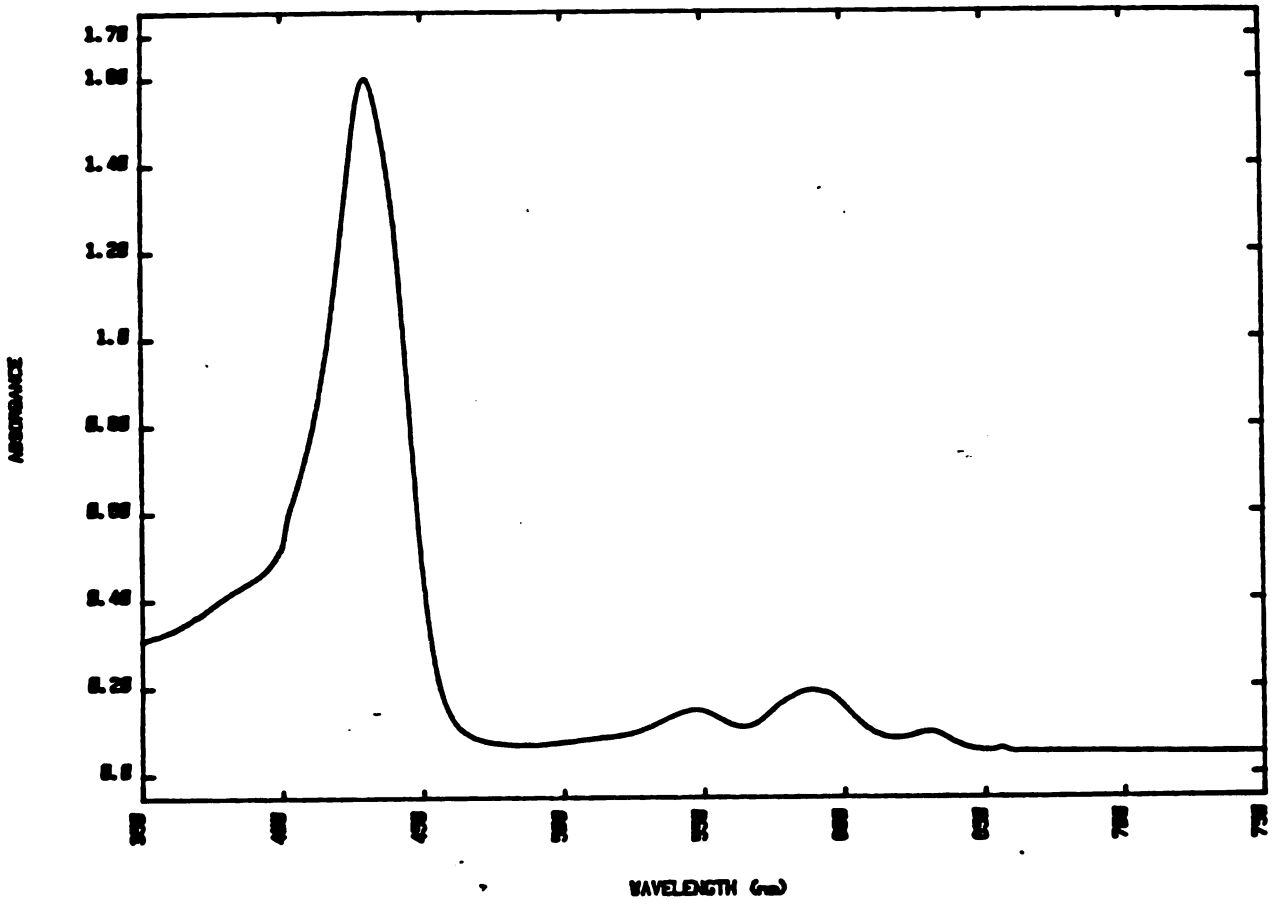

Purified P-450b was incubated with diazoacetophenone and then reduced with excess $Na_2S_2O_4$ to form the 445 nm complex. The mixture was mixed with 5% H_2SO_4/methanol and analysed for N-alkyl porphyrin formation. The electronic absorption spectrum of the DAP-PPIX adduct thus isolated is identical to that shown in figure 5.9.

halocarbons and the structures of these complexes have been unambiguously established (Mansuy et al, 1978; Olmstead et al, 1982). EDA has been shown to react with metalloporphyrins, but the crystal structure of the product shows the carbon bridging the metal and a nitrogen of the porphyrin ring. The intermediacy of a carbene complex in the reductive metabolism of diazoketones thus remains a matter of conjecture because no such complex has been directly observed (Johnson et al, 1975; Johnson and Ward, 1977). In an attempt to identify the structure of the 445 nm complex obtained from reaction of P-450 with DAP, model studies were performed to isolate a model complex to which the enzymatic product could be compared.

The reaction of TPP with DAP under anaerobic, reducing conditions (Chapter 2) quantitatively yields an emerald green complex (TPP-DAP complex) which crystallizes from dichloromethane/pentane and a variety of other solvents. The key to the structure of this product lies in its absorbance spectrum (Figure 5.13) which is similar to that obtained by Mansuy et al (1984; 1986) for the adduct shown in Figure 5.14. The long wavelength Soret band is more consistent with oxygen ligation to the iron than with a carbene or iron - nitrogen bridged structure (λ max = 408 nm and 428 nm respectively) (Mansuy et al, 1977 and Mansuy et al, 1979). The LSIMS mass spectrum (Figure 5.15) shows a molecular ion for the DAP adduct (m/e = 787) analogous to those for the adduct formed with P-450. The other peaks in the mass spectrum correspond to the chloride salt of this adduct (m/e = 822), TPP itself(m/e = 668, and the chloride salt of TPP (m/e =

Figure 5.13

Electronic Absorption Spectrum of the Diazoacetophenone-Tetraphenylporphyrin Complex

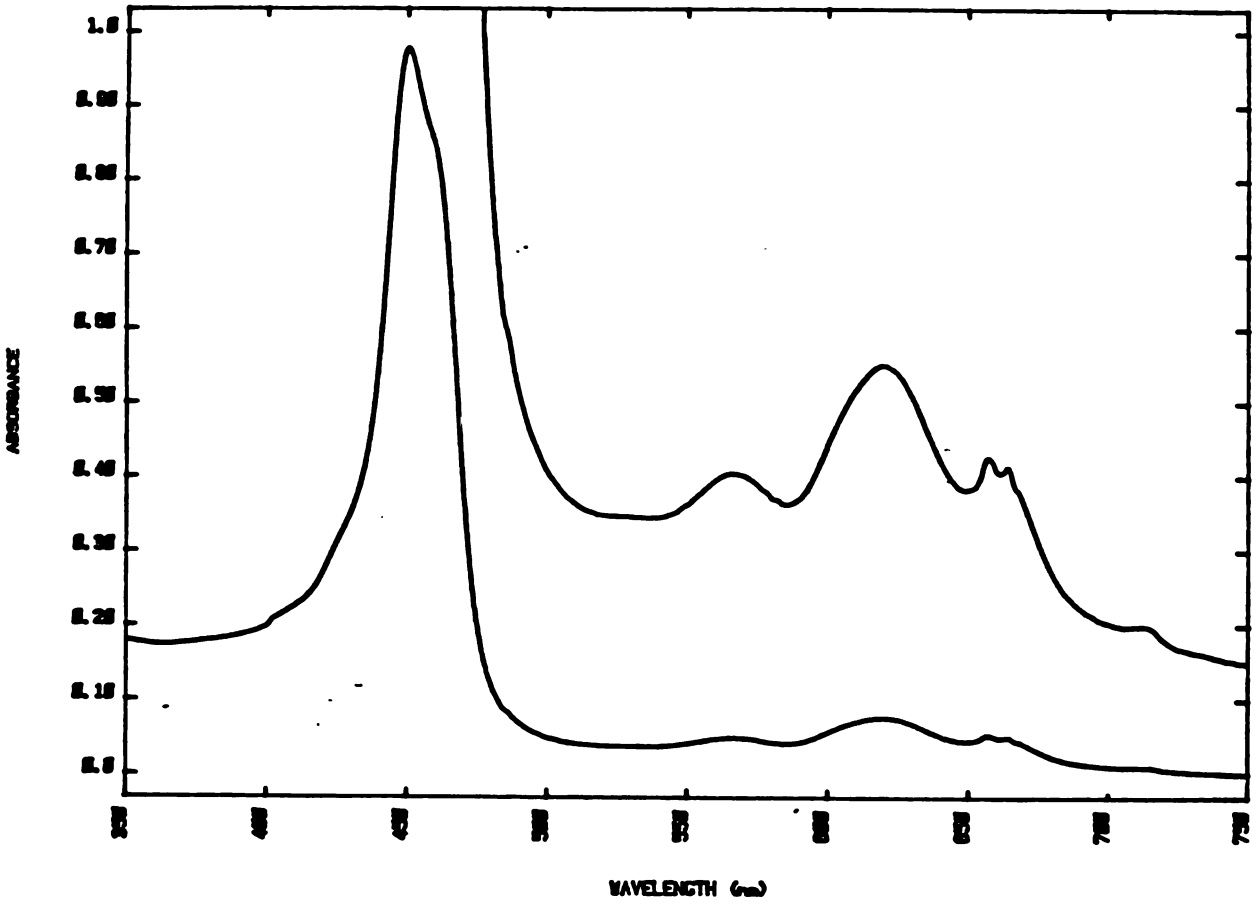

Diazoacetophenone was reacted with TPPFe(II) under anaerobic, reducing conditions. A stable product with a Soret band at 455 nm was immediately formed.

Figure 5.14

Structure of the Bis-N-Alkyl Complex Reported by Mansuy et al, (1985)

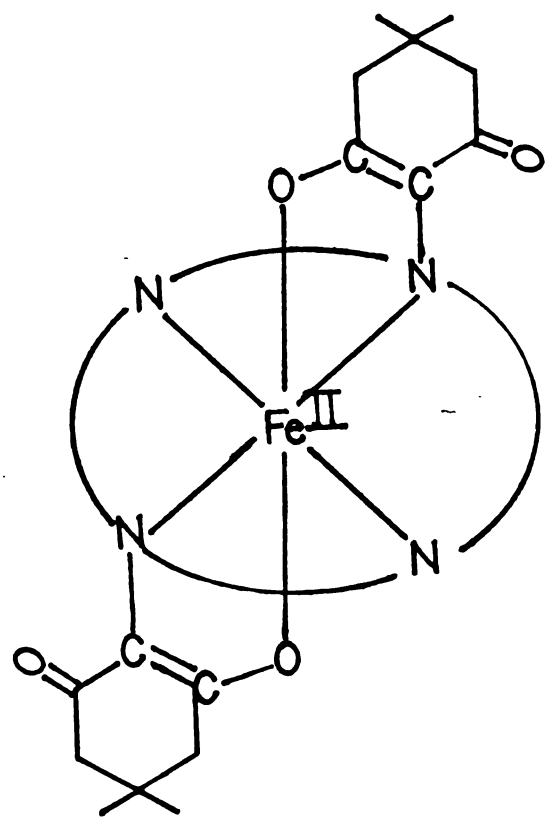

The Soret maximum of this bis complex is at 462 nm.

Figure 5.15

LSIMS Mass Spectrum of the Diazoacetophenone-Tetraphenylporphyrin Complex

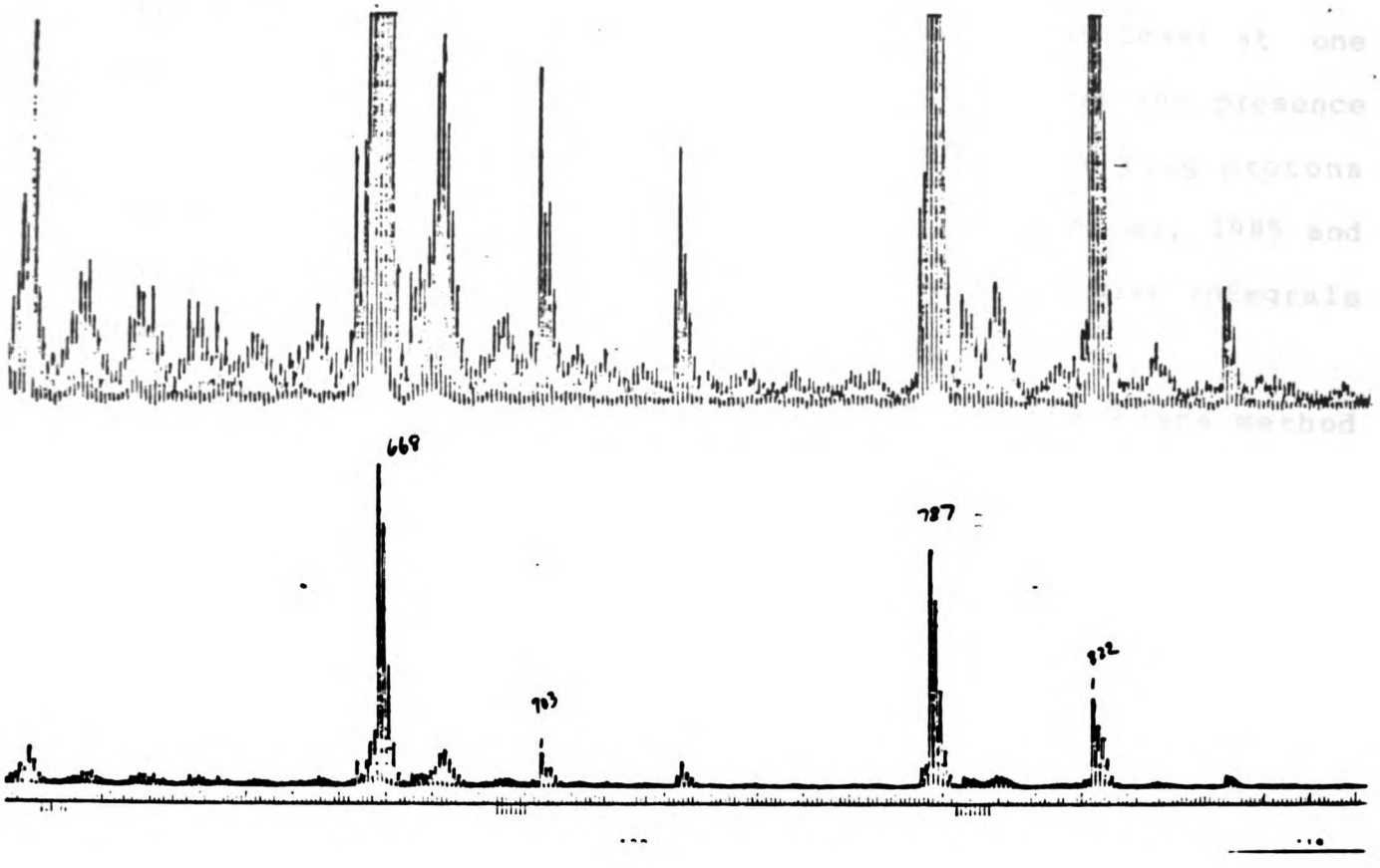

The LSIMS mass spectrum of the TPP-DAP complex in sulfolane shows the molecular ion at m/e 787 expected for the structure shown in Figure 5.16 as well as that for a chloride addition product at m/e 822 and fragments corresponding to TPP chloride (m/e 703) and TPP itself (m/e 668).

703. The TPP and TPP chloride were probably fragments since they occurred in the spectra of the crystallized adduct. The fact that chloride ions complex well with the porphyrin suggest that it is not a neutral carbene complex but rather an N-alkylated species that can undergo reversible protonation at least at one site. The 500 MHz NMR spectrum (Figure 5.16) shows the presence of an iron and the pattern of phenyl and pyrrole ring protons expected of an N-alkylated Fe^{II} porphyrin (Balch et al, 1985 and Balch and Renner, 1986). The chemical shifts and peak integrals for the NMR signals are given in Table 5.2.

Magnetic susceptibility measurements by the Evans method (Chapter 2) gave a frequency difference in the NMR signals of the tetramethylsilane protons in the presence and absence of the TPP-DAP complex of 47.05 Hz. The magnetic susceptibility calculated from this value, using the equations presented in Chapter 2 is 5.6 +/- 0.2. The expected μ_{eff} can be calculated from the quantum mechanical equation $\mu_{eff} = [4S(S+1) + L(L+1)]^{1/2}$ (Cotton and Wilkinson, 1980). The relevent values are 5.48 for high spin Fe(II), and 5.92 for high spin Fe(III). The observed magnetic succeptibility for the TPP-DAP complex is thus most consistent with a high spin ferrous product.

Figure 5.16

500 MHz ^{1}H-NMR Spectrum of the Diazoacetophenone-Tetraphenylporphyrin Complex

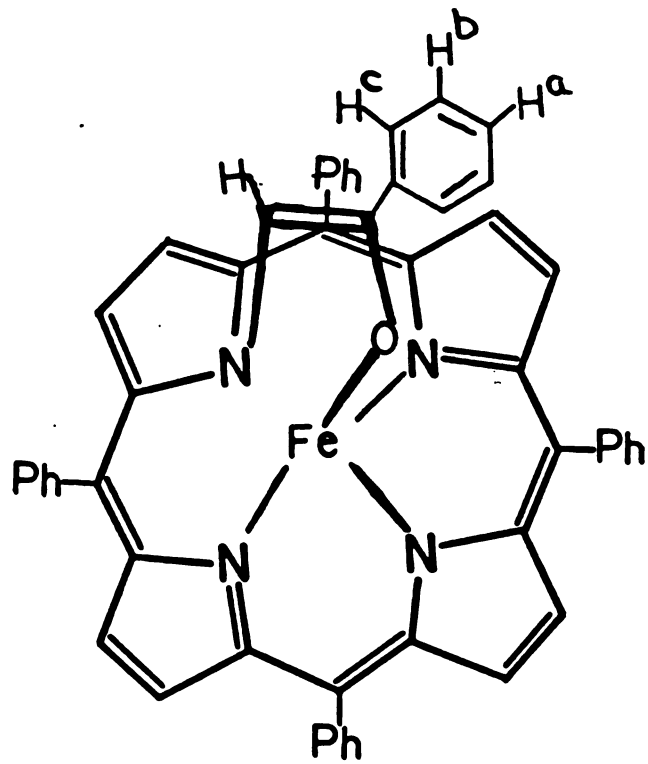

The NMR spectrum of the TPP-DAP complex was recorded from -40 to +150 ppm at both room temperature and -25^{o}C to be sure all the peak widths were as narrow as possible. The spectrum shown includes all the observable peaks. The spectrum is nearly identical to those reported by Balch et al, 1985, and the peak assignments are based on their assignments (Table 5.2).

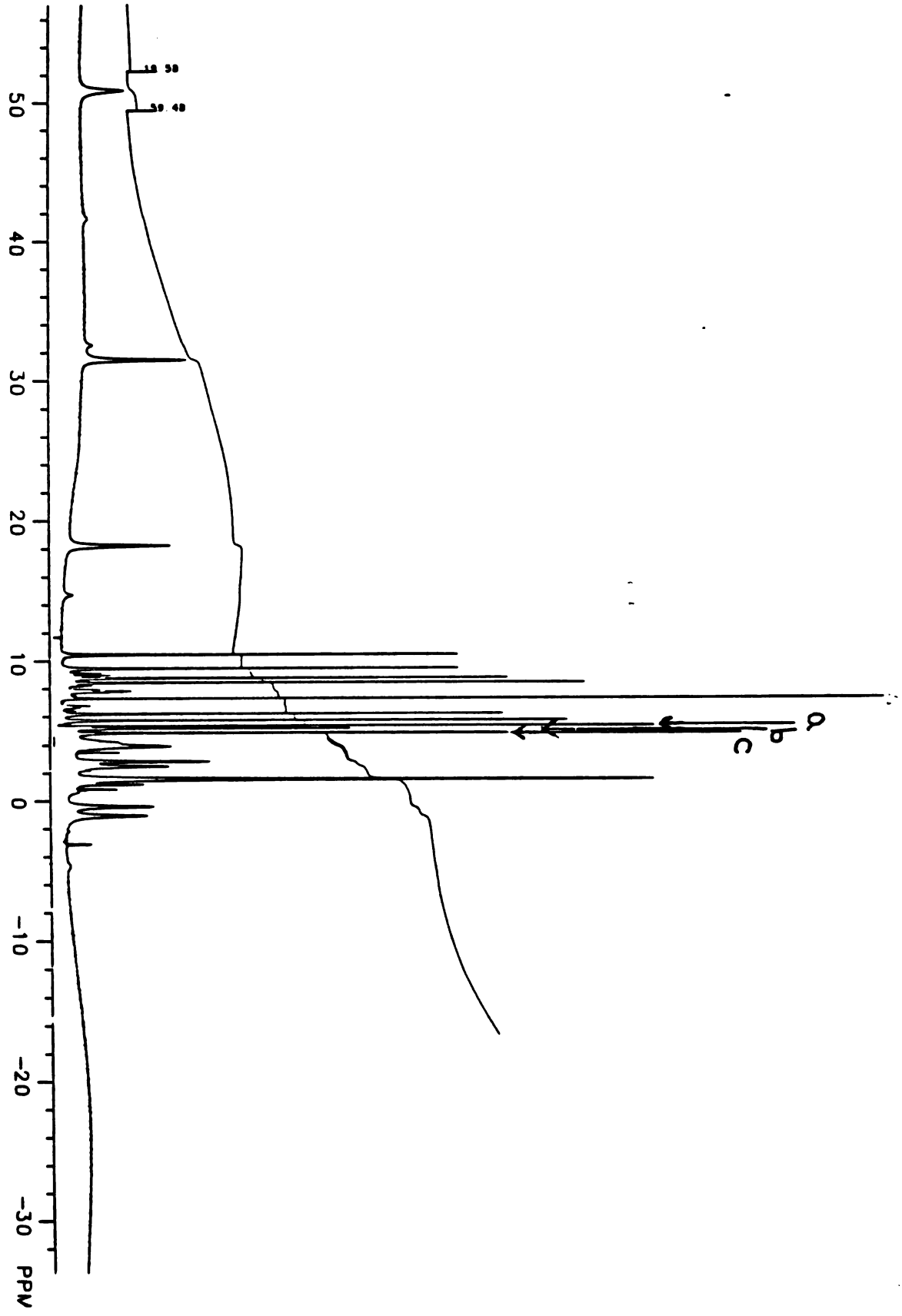
50
40
30
20
10
0
-10
-20
-30
PPM
a
b
c

TABLE 5.2

Chemical Shifts and Peak Integrals for the Protons in the TPP-DAP Complex

Assignment	Chemical Shift	Integration
pyrroles	51.01	2
	31.41	2
	-.40	2
	-1.1	2
o-phenyls	18.18	2
	3.91	2
	2.87	2
	2.40	2
m-phenyls	10.40	2
	9.40	2
	8.91	2
	6.16	2
p-phenyls	8.73	2
	5.70	2
N-alkyl group		
p-phenyl	5.31	1
m-phenyl	5.11	2
o-phenyl	4.81	2

note: The porphyrin proton assignments are based on literature values (references given in the text). The N-alkyl group protons were identified as the only remaining peaks in the spectrum. All peaks were broadened and no coupling was observed.

Transformation of the TPP-DAP complex into the free base N-alkyl TPP adduct was extremely facile. The conversion occurred under such mildly acidic conditions as treatment with silica gel. The LSIMS mass spectrum shows a molecular ion at m/e 732 consistent with removal of the iron and addition of 2 protons (Figure 5.17). The NMR spectrum of the resulting N-alkyl TPP adduct, shown in Figure 5.18, is tabulated in Table 5.3. The absorbance spectrum (Figure 5.19) also fully supports the structure shown in the inset of Figure 5.18. The protons of the DAP phenyl group are found with the appropriate chemical shifts and coupling constants in the NMR spectrum.

The free base porphyrin was transformed into the zinc (II) complex. The LSIMS mass spectrum of this complex shows a molecular ion at m/e 795 as required for insertion of zinc into the porphyrin. The isotope pattern is also indicative of the presence of zinc (Figure 5.20). Its NMR and absorbance spectra are completely consistent with the assigned structure (Figures 5.21 and 5.22). The NMR data is tabulated in Table 5.3. The IR spectra were also obtained, but metal ligated enols and ketones are found in the same region (1650 - 1700), so the data are not particularly useful.

Figure 5.17

LSIMS Mass Spectrum of the Free Base of the N-Alkyl Porphyrin Obtained from the Diazoacetophenone-Tetraphenylporphyrin Complex.

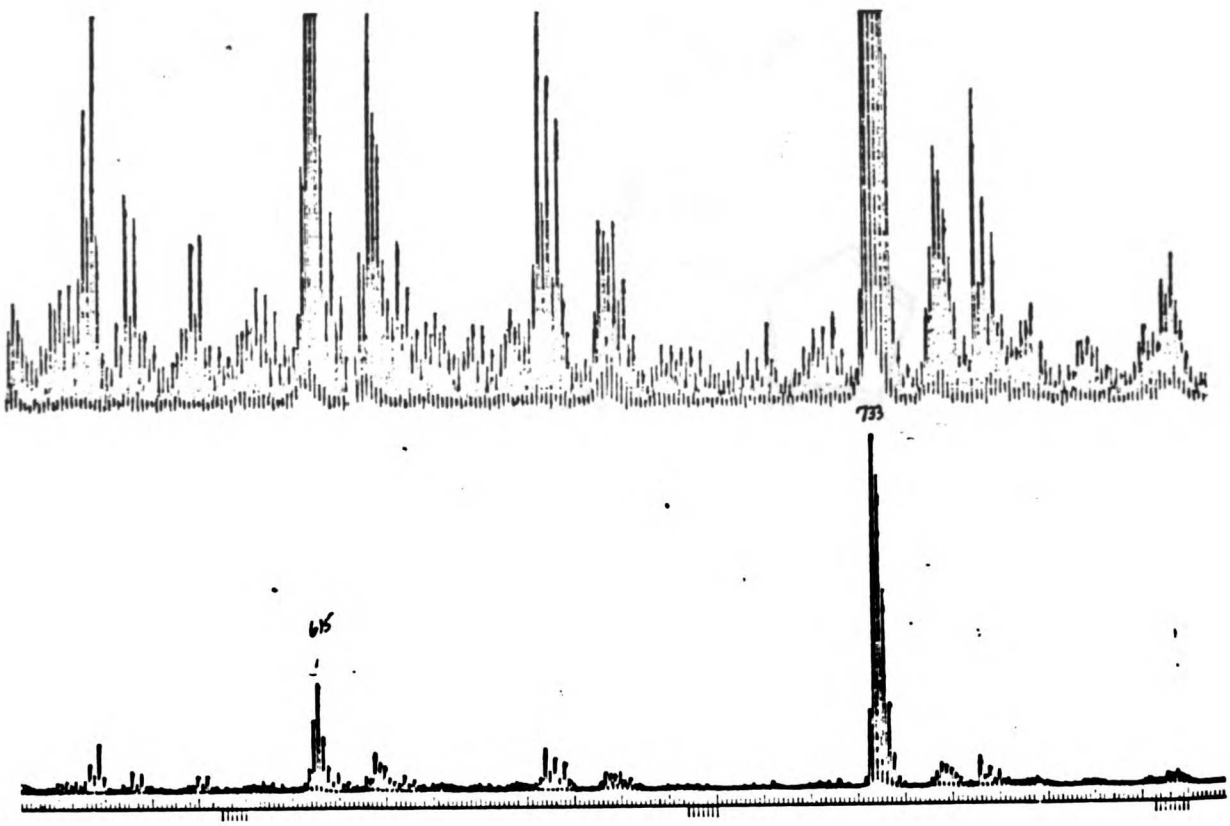

The TPP-DAP complex was demetallated over night with 5% H_2SO_4/methanol and analysed by LSIMS mass spectrometry in sulfolane. The spectrum shows the expected adduct at m/e 733 and also a small porphyrin fragment molecular ion at m/e 615.

Figure 5.18

500 MHz ^{1}H-NMR Spectrum of the Free Base of the N-Alkyl Porphyrin Obtained from the Diazoacetophenone-Tetraphenylporphyrin Complex

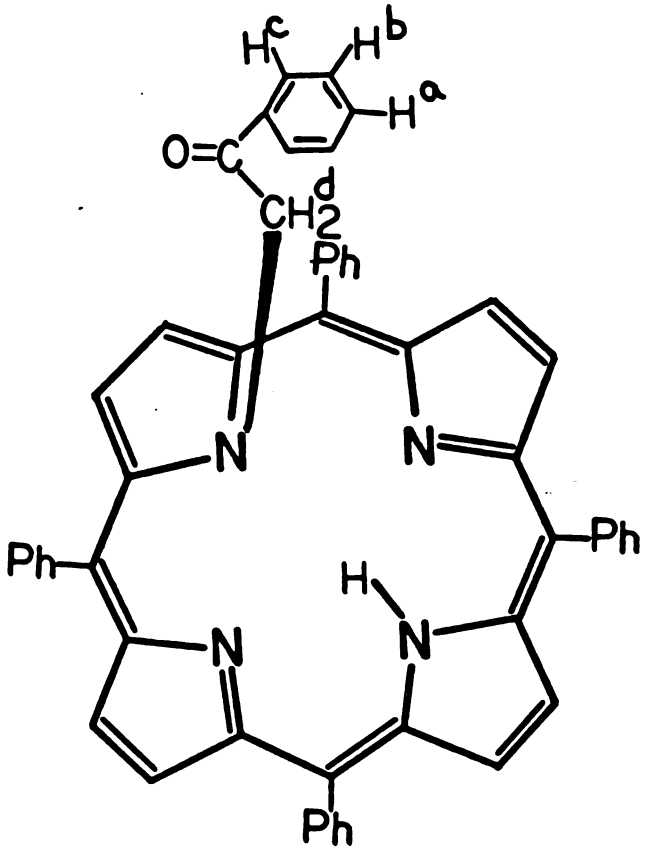

Thepeaks in the NMR spectrum showm below are tabulated in Table 5.3. The N-alkyl group protons are labelled with the same letters as the corresponding peaks in the NMR spectrum.

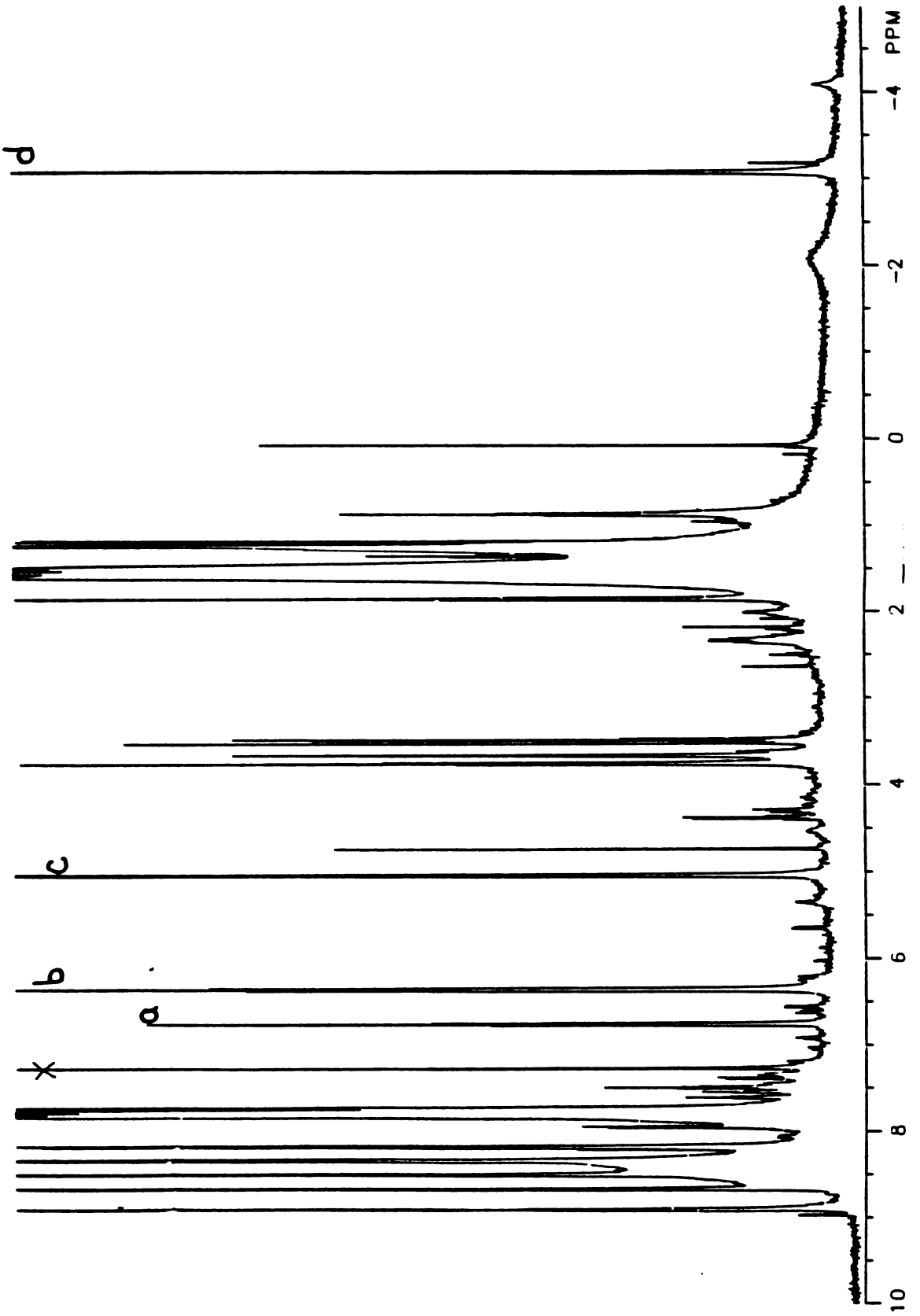
d
c
b
a
×
10
8
6
4
2
0
-2
-4
PPM

Figure 5.19

Electronic Absorption Spectrum of the Free Base N-Alkyl Porphyrin Obtained from the Diazoacetophenone-Tetraphenylporphyrin Complex

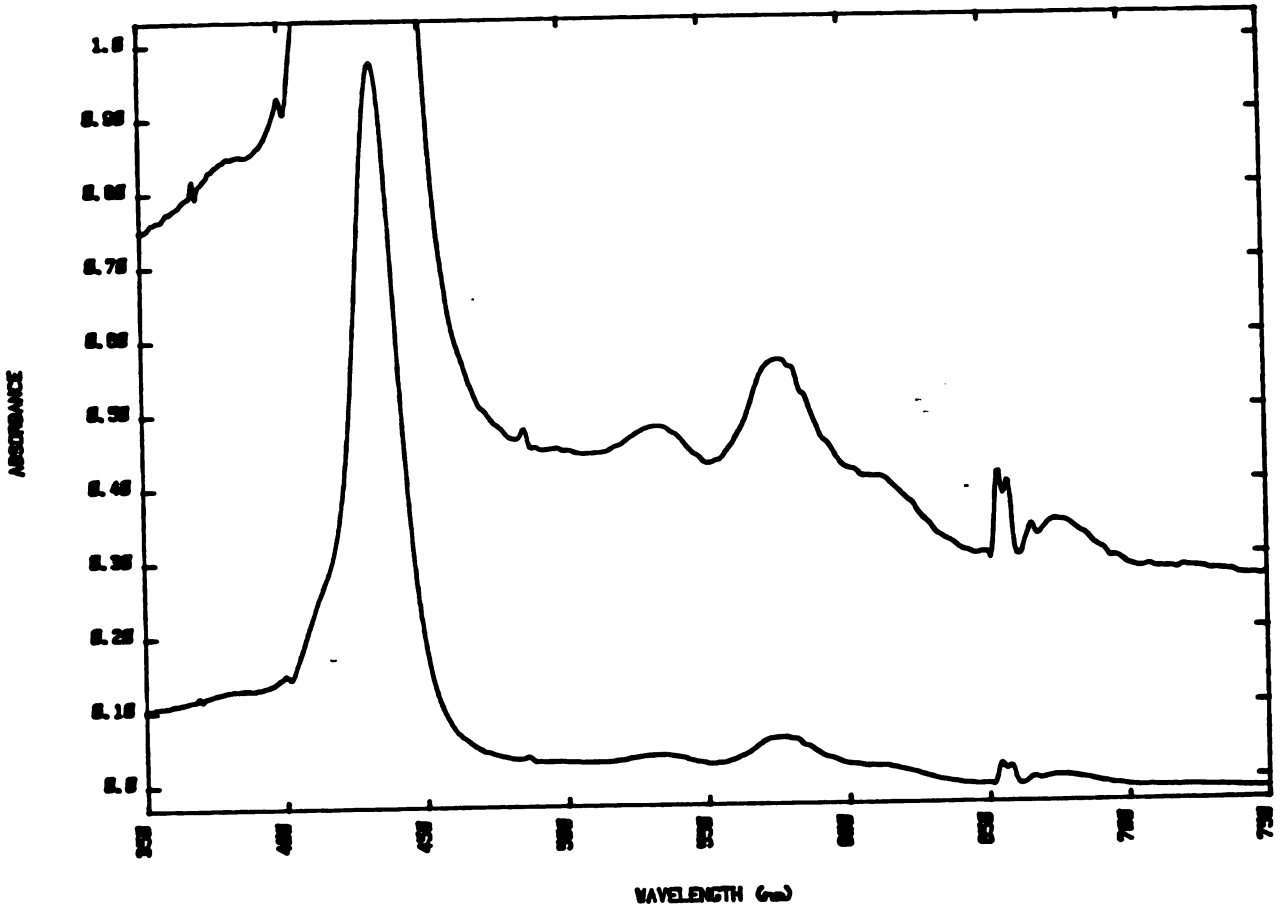

The TPP-DAP complex was demetallated over night with 5% H_2SO_4/methanol. The electronic absorption spectrum has the expected soret maximum at 420 nm.

Figure 5.20

LSIMS Mass Spectrum of the Zinc Complex Obtained from the Free Base Diazoacetophenone-Tetraphenylporphyrin Adduct

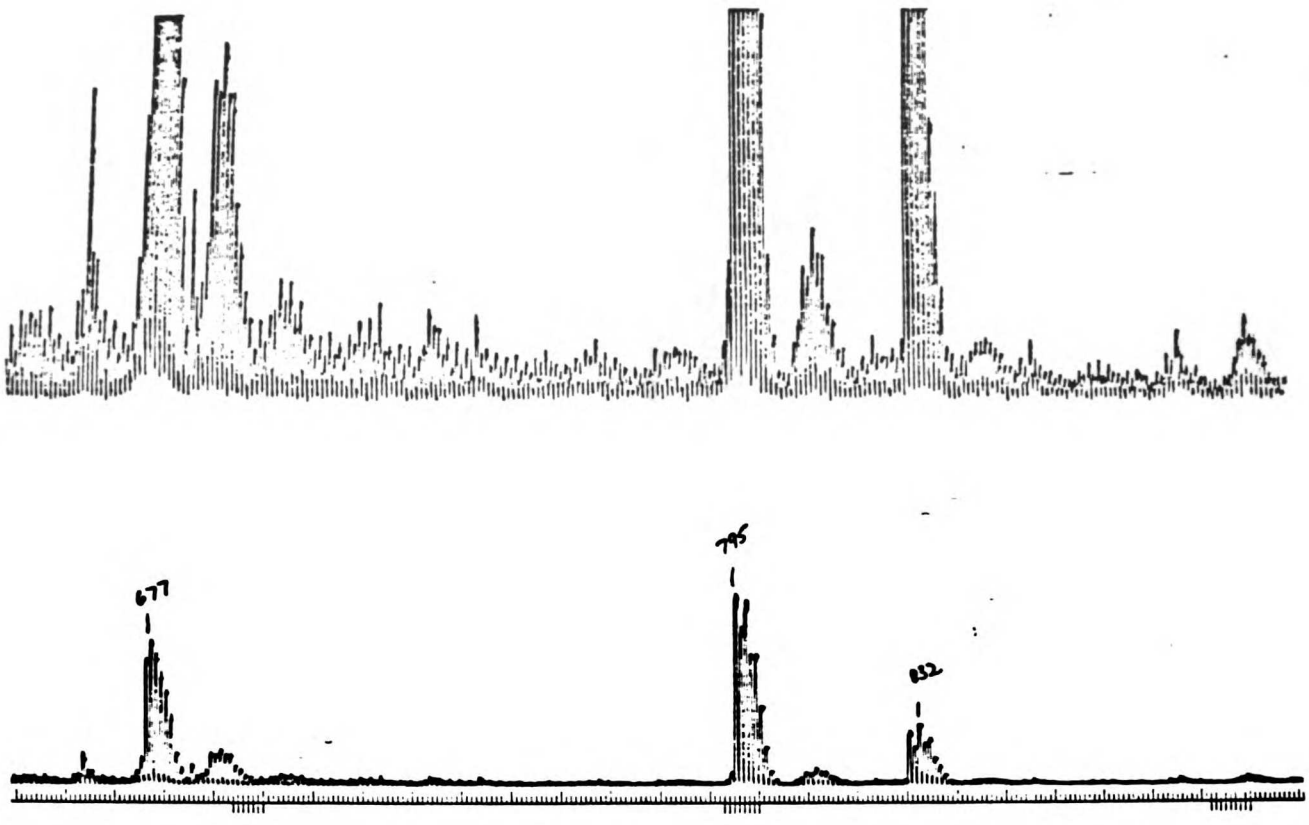

The zinc complex of the DAP-TPP adduct was prepared by treatment of the free base adduct with $Zn(OAc)_2$ in methanol. The acetate counterion was exchanged for chloride, and the mass spectrum was recorded in tetraglyme. The molecular ion expected for the structure shown in Figure 5.21 is m/e 795, and the isotope pattern is that expected for a zinc complex.

Figure 5.21

500 MHz ^{1}H-NMR of the Zinc Complex of the Diazoacetophenone -Tetraphenylporphyrin Adduct

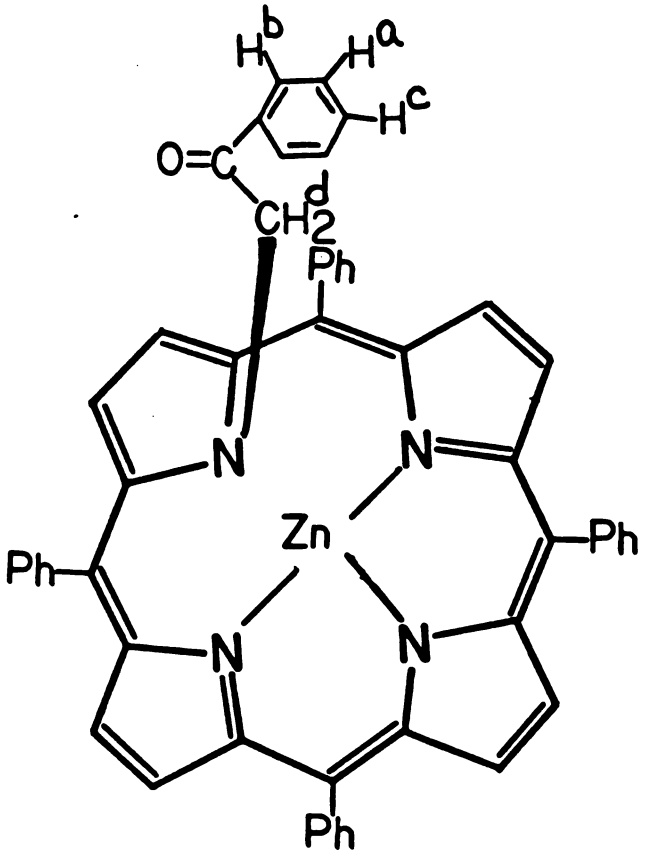

The peaks in the NMR spectrum of the zinc complex of the TPP-DAP adduct were assigned by reference to Balch et al, 1985. The protons in the N-alkyl group are labelled with the same letters in the structure and on the NMR spectrum.

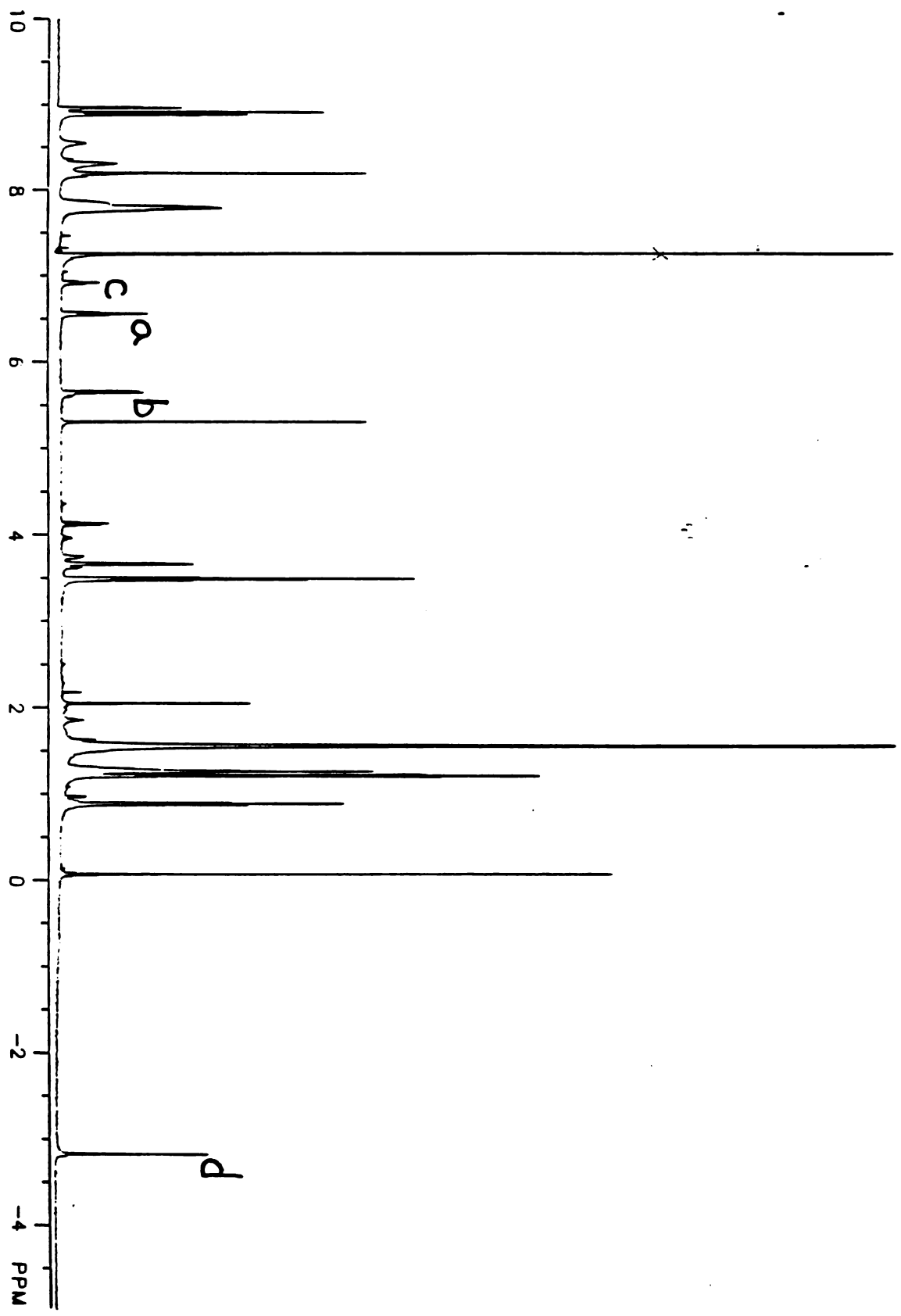
10
8
6
4
2
0
-2
-4
PPM
c
a
b
d

Figure 5.22

Electronic Absorption Spectrum of the Zinc Complex of the Diazoacetophenone-Tetraphenylporphyrin Adduct

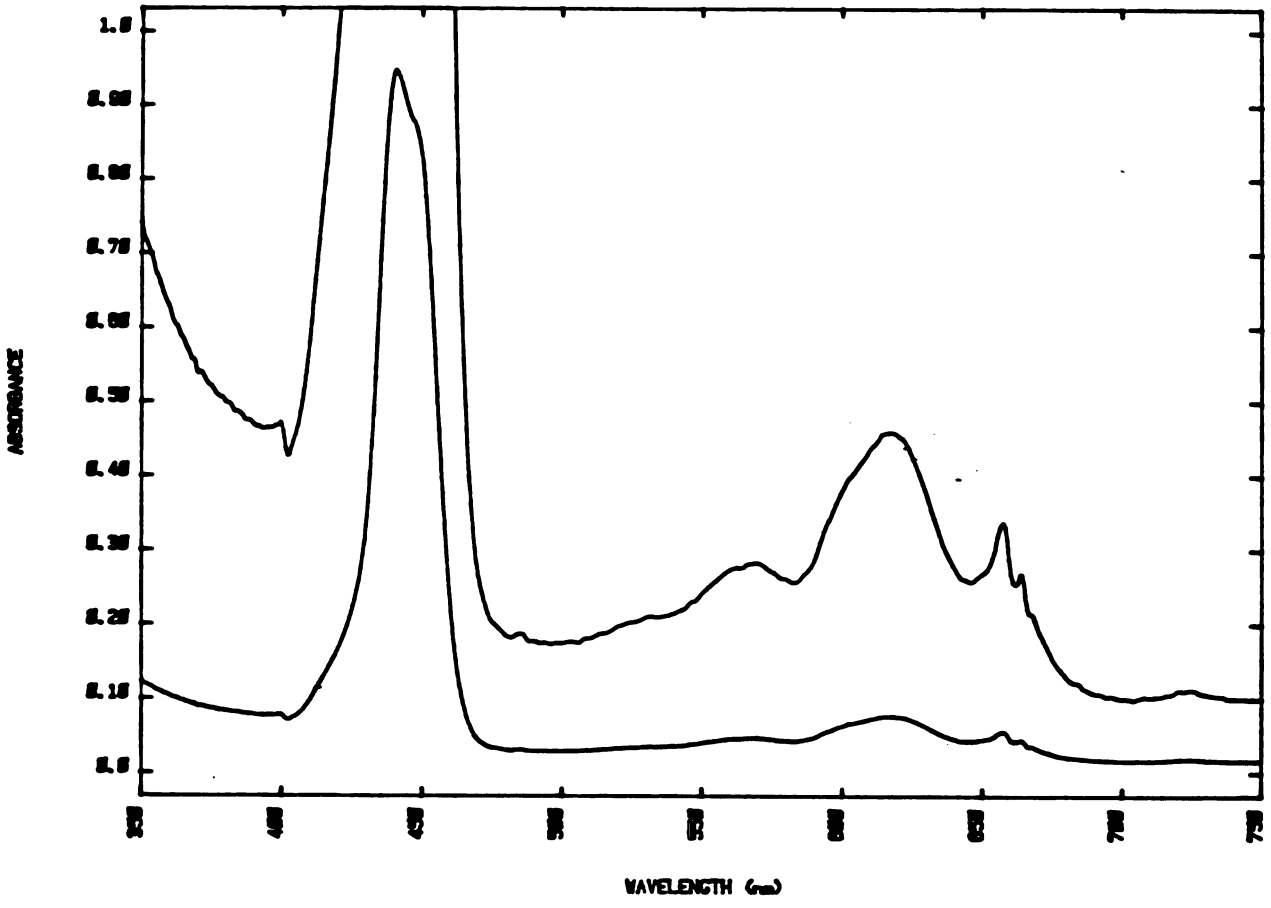

The zinc complex of the TPP-DAP adduct was prepared by adding $Zn(OAc)_2$ to a solution of the porphyrin. The resulting blue-green complex has a soret maximum at 435 nm.

TABLE 5.3

Chemical Shifts and Integrations of Protons in the N-Alkyl-TPP Adducts

	TPP-DAP free base		TPP-DAPZn (II)	
Assignment	Chemical Shift	Integration	Chemical Shift	Integration
pyrroles	8.99 - 8.80	2 (s)	8.99 - 8.77	6 (m)
and phenyls	8.70 - 8.57	2 (s)	8.62 - 8.42	2 (s)
	8.59 - 8.07	10 (m)	8.39 - 8.05	8 (m)
	7.97 - 7.60	14 (m)	7.89 - 7.66	12 (m)
N-alkyl group				
N-methylene	-2.99 - -3.21	2 (s)	-3.11 - -3.24	2 (s)
p-phenyl	6.81 - 6.55	1 (t)	6.95 - 6.83	1 (t)
m-phenyl	6.44 - 6.15	2 (dd)	5.66 - 5.52	2(dd)
o-phenyl	5.17 - 4.92	2 (d)	5.36 - 5.21	2 (d)

note: Abbreviations are the same as in Table 5.1.

A parallel reaction of TPP with Me-DAP under anaerobic reducing conditions failed to yield any complex. The TPP reactions thus mimic the enzymatic situation in that the secondary adduct also does not form.

C. ^{13}C-NMR Experiments

1. Model Reactions

Complexes of carbon monoxide with the heme groups of proteins and with model porphyrins have been studied by ^{13}C-NMR spectroscopy (Behere et al, 1985; Matwyioff et al, 1973; Moon and Richards, 1974; Mansuy et al, 1978). The data show that carbons directly attached to the iron of the porphyrin ring have chemical shift values of approximately 200 ppm (referenced to $CDCl_3$ at 77.5 ppm). The presence of axial ligands alters the chemical shift values by only 5 - 10 ppm. Strong evidence for the structures of the DAP complex, both in the enzyme and model porphyrin, would be provided by their ^{13}C-NMR chemical shift values because the shifts for metal ligated carbenes are unique. Diazoacetophenone was prepared with ^{13}C-enrichment at the appropriate carbon (Appendix I) and allowed to react with TPP. The ^{13}C-NMR and the ^{1}H-NMR spectra of [1-^{13}C]DAP is shown in Figure 5.23. The coupling constant of the diazomethine hydrogen to the carbon is 198 Hz. The structure, as expected, has only one hydrogen attached to the diazo carbon. The ^{13}C-NMR spectrum of the TPP-DAP complex prepared from labelled DAP is shown in Figure 5.24. The ^{13}C signal is again split into a doublet, this time with a coupling constant of approximately 122 Hz. The chemical shift value of 92 ppm as well as the splitting of the

Figure 5.23

^{13}C-NMR and ^{1}H-NMR spectra of Diazoacetophenone

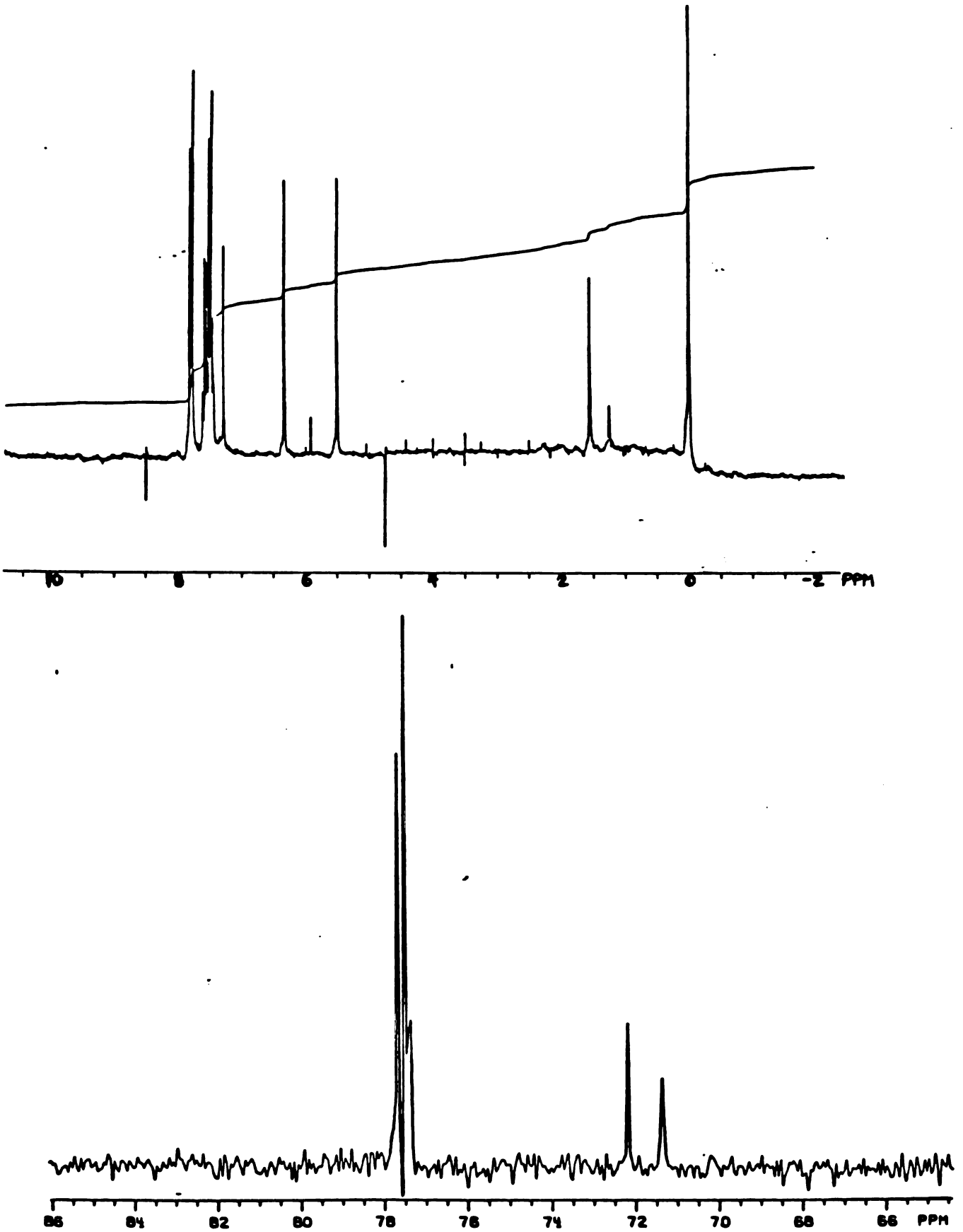

The ^{13}C-NMR spectrum of DAP shows the carbon split by 204Hz. The ^{1}H-NMR spectrum more accurately gave 198 Hz. The solvent is deuterochloroform which resonates at 77.5 in the ^{13}C-NMR spectrum and 7.25 ppm in the ^{1}H-NMR spectrum.

Figure 5.24

^{13}C-NMR Spectrum of the ^{13}C-Diazoacetophenone-Tetraphenylporphyrin Complex

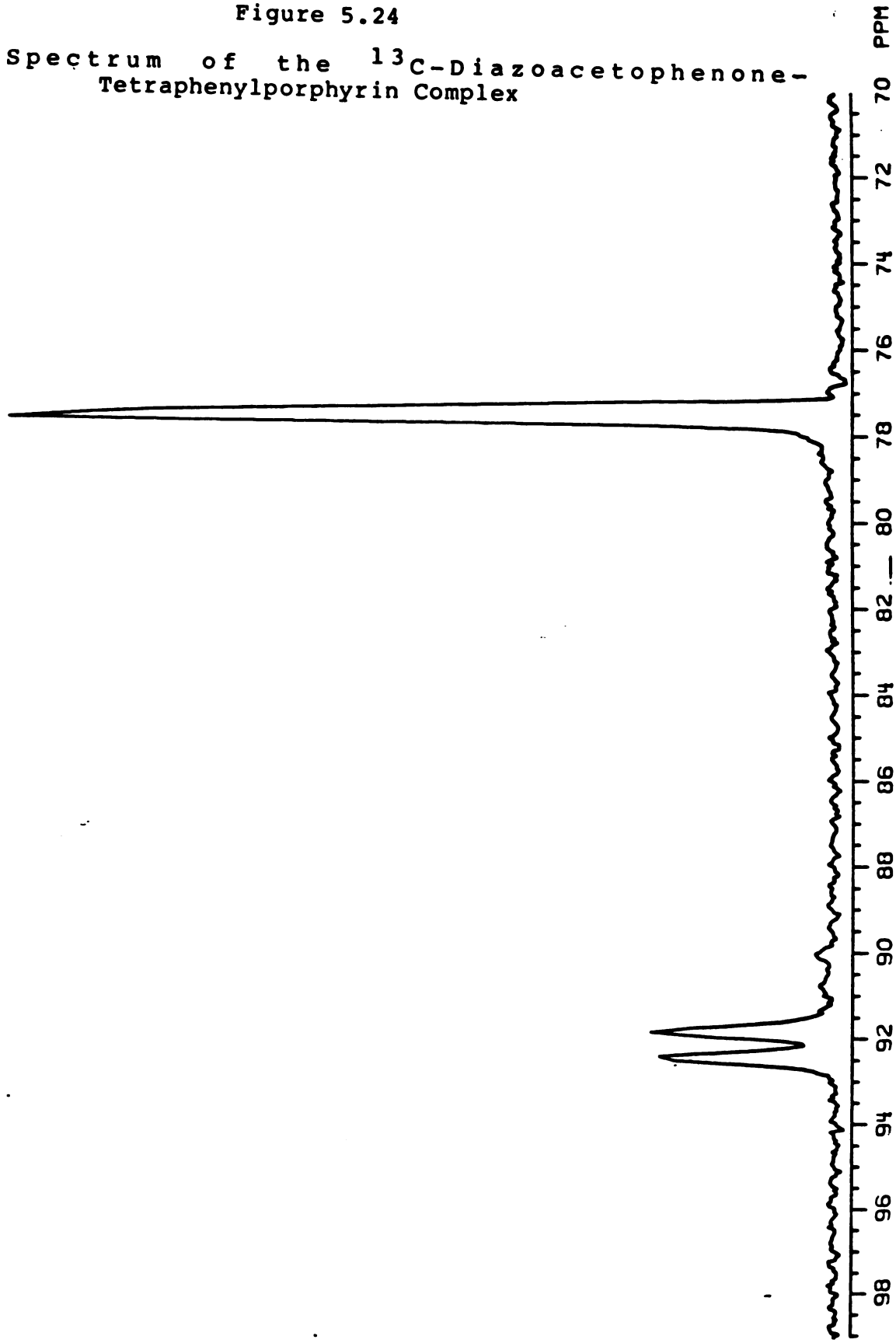

^{13}C-DAP was reacted with TPPFe(II) to generate the TPP-DAP complex. The undecoupled ^{13}C-NMR spectrum indicates the diazo carbon is enolic. The peaks are broadened due to paramagnetic effects. The deuterochloroform solvent peak is also broadened.

line indicates that the carbon is enolic (Pretsch-Clerc et al, 1983). The ^{13}C-NMR spectrum of the free base porphyrin after removal of the iron by treatment with 5% H_2SO_4/methanol is shown in Figure 5.25. The chemical shift of the carbon is now 126.6 ppm. The lines are considerably sharper since the molecule is no longer paramagnetic.

2. Enzymatic Reactions

The P-450cam DAP complex was prepared under anaerobic conditions using the ^{13}C-labeled DAP. The ^{13}C-NMR spectra of the [^{13}-C]DAP complex of P-450 cam is shown in Figure 5.26. The reference line in this case was taken to be the unreacted DAP, which was assigned the same chemical shift as that observed in $CDCl_3$ solution. Two species appear to be present, one with a chemical shift similar to the TPP-DAP complex (88.8 ppm), and one similar to the free base porphyrin (128.6 ppm). The chemical shift differences between the model system and the protein are surprisingly small considering the differences in the structures of the porphyrins. Clearly, similar reactions are occurring in the protein and in the model system, and neither one involves a stable iron-carbene complex. Apparently the presence of the oxygen precludes formation of a carbene intermediate, and allows direct attack on the porphyrin ring forming a highly stable enol intermediate in which the oxygen is bound to the iron and the carbon is bound to the pyrrole ring nitrogen. It is also likely that a stable carbene intermediate does not form in the metabolism of acetylenes because the carbene would be identical to that obtained from DAP. The observance of a 445 nm band upon

Figure 5.25

^{13}C-NMR Spectrum of the N-Alkyl Porphyrin Obtained from the ^{13}C-Diazoacetophenone-Tetraphenylporphyrin Complex

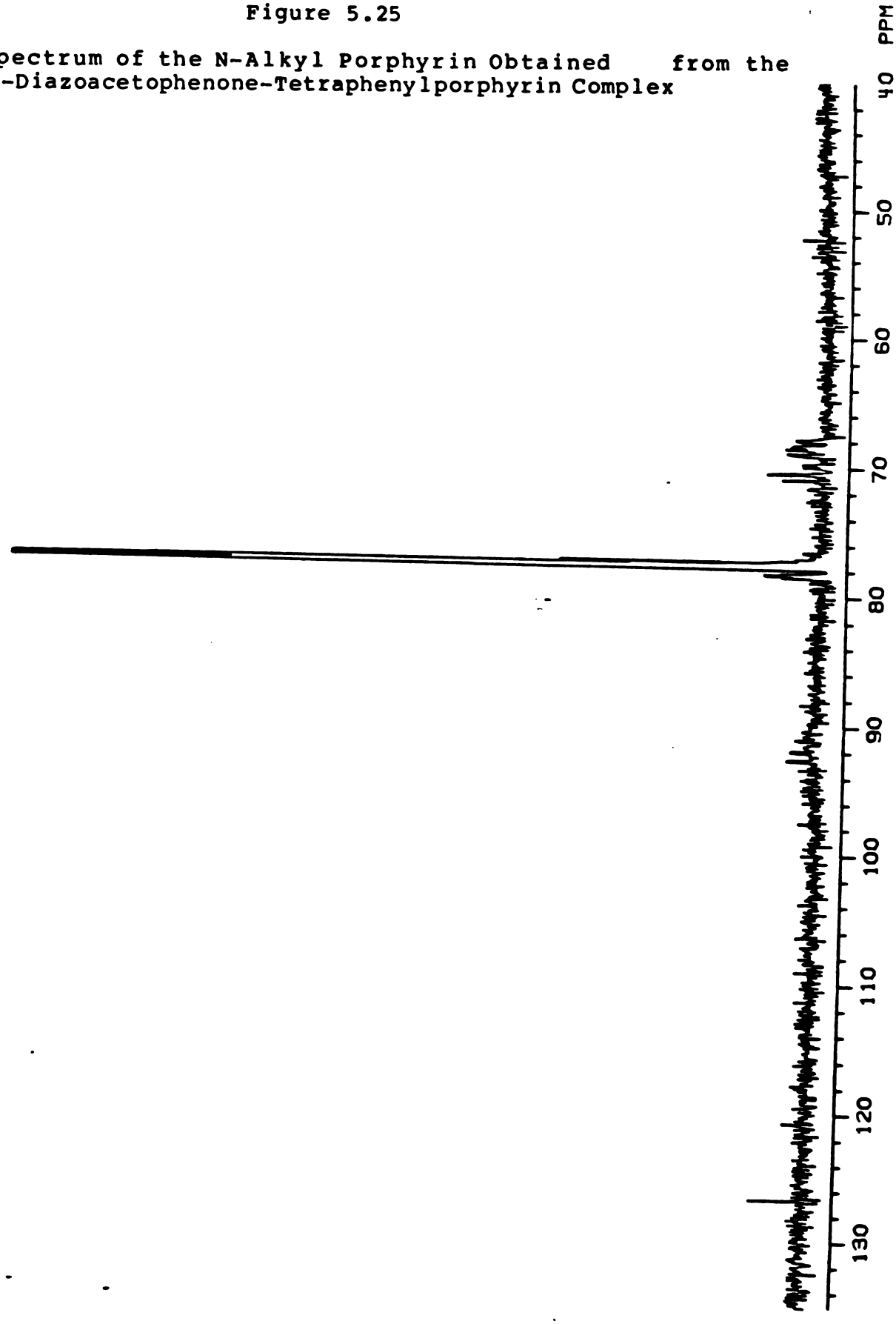

The ^{13}C-NMR spectrum of the free base ^{13}C-TPP-DAP complex shows a narrow peak at 128 ppm assigned to the N-methylene carbon. The solvent is deuterochloroform at 77.5 ppm.

Figure 5.26

^{13}C-NMR Spectrum of the ^{13}C-Diazoacetophenone Complex with P-450cam

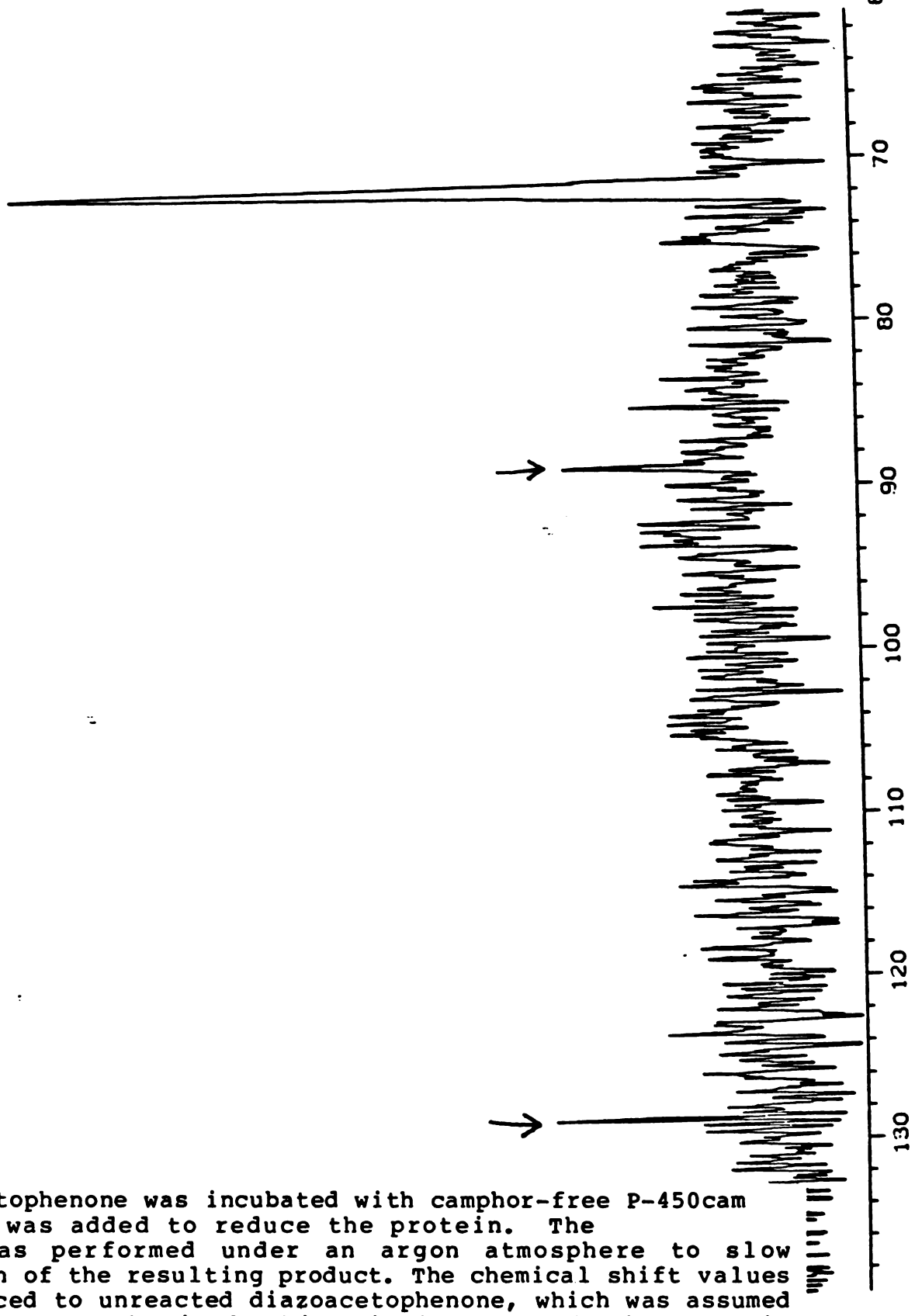

^{13}C-Diazoacetophenone was incubated with camphor-free P-450cam and $Na_2S_2O_4$ was added to reduce the protein. The procedure was performed under an argon atmosphere to slow decomposition of the resulting product. The chemical shift values were referenced to unreacted diazoacetophenone, which was assumed to have the same chemical shift in buffer solution and in chloroform. Two peaks (indicated by arrows) are visible, one at 88 ppm, and one at 128 ppm.

reaction of P-450 with phenylacetylene suggests that the same sort of N-alkyl adduct is formed during the suicide inactivation of P-450 by this compound (see Figure 3.12).

CHAPTER 6

DISCUSSION AND CONCLUSIONS

Oxidation of arylacetylenes to arylacetic acids by cytochrome P-450 or metachloroperbenzoic acid (MCPBA) proceeds with a 1,2 shift of the acetylenic hydrogen (Ortiz de Montellano and Kunze 1980; 1981). This shift, shown previously to occur during biphenylacetylene oxidation, appears to be the major metabolic pathway for arylacetylenes since the arylacetic acids are the major metabolites from all the arylacetylenes studied. In fact, the oxidation of methyl-substituted phenylacetylenes results in less than 10 percent benzylic hydroxylation products, indicating that acetylenic bond oxidation competes favorably with this metabolic pathway (Figure 4.1). Aliphatic acetylenes also undergo acetylenic bond oxidations, but in this case the pathway is usually a minor metabolic route (C. Wheeler, E.A. Komives, unpublished results).

A comparison of the chemical oxidation of phenylacetylene either by MCPBA or Fenton's reagent to the enzymatic oxidation by P-450 reveals a striking similarity between the MCPBA and P-450 oxidations. The only product in both cases is phenylacetic acid in which the acetylenic hydrogen has migrated quantitatively to the vicinal carbon (Figures 3.3 and 3.4). Fenton's reagent, on the other hand, yields a myriad of products of which less than 5 percent is phenylacetic acid (Figure 3.6).

The biphenylacetic acid produced from biphenylacetylene by

P-450 under an atmosphere of $^{18}O_2$ contains one ^{18}O-atom. This labeling pattern is that expected if the acetylenic bond is oxidized to a ketene intermediate that is trapped by water to yield biphenylacetic acid (Figure 3.1). Peracid oxidations of acetylenes are also believed to proceed through such a ketene intermediate (Lewars, 1983).

The 1,2 shift of the acetylenic hydrogen during the oxidation of biphenylacetylene and phenylacetylene by MCPBA occurs with a kinetic isotope effect of 1.8 (Table 3.1). The magnitude of the kinetic isotope effect is precisely that expected for a 1,2 hydrogen shift in which a bending rather than stretching vibration is being affected. Theoretical studies indicate that while the linear scission of a C-H bond (180^{o}) occurs with a maximum kinetic isotope effect of 7.9, the maximum kinetic isotope effects for bent transition states are 3.0 (120^{o}), 1.7 (90^{o}) and 0.9 (60^{o}) (More O'Ferrall, 1970). The theoretical predictions are supported by measurements of bending kinetic isotope effects in several chemical transformations. The magnitudes of these isotope effects are the same as those observed during phenylacetylene oxidation (Table 6.1). This first demonstration of a kinetic isotope effect on the rate of oxidation of acetylenes by MCPBA requires that the hydrogen shifts in concert with oxygen transfer to the π-bond and rules out the formation of an oxirene intermediate in this transformation (Scheme 6.1a). The possibility that an oxirene intermediate forms and then decomposes in an isotopically sensitive step is incompatible with the renowned instability of

Scheme 6.1

The Mechanism of Oxidation of Acetylenes by Peracids and P-450

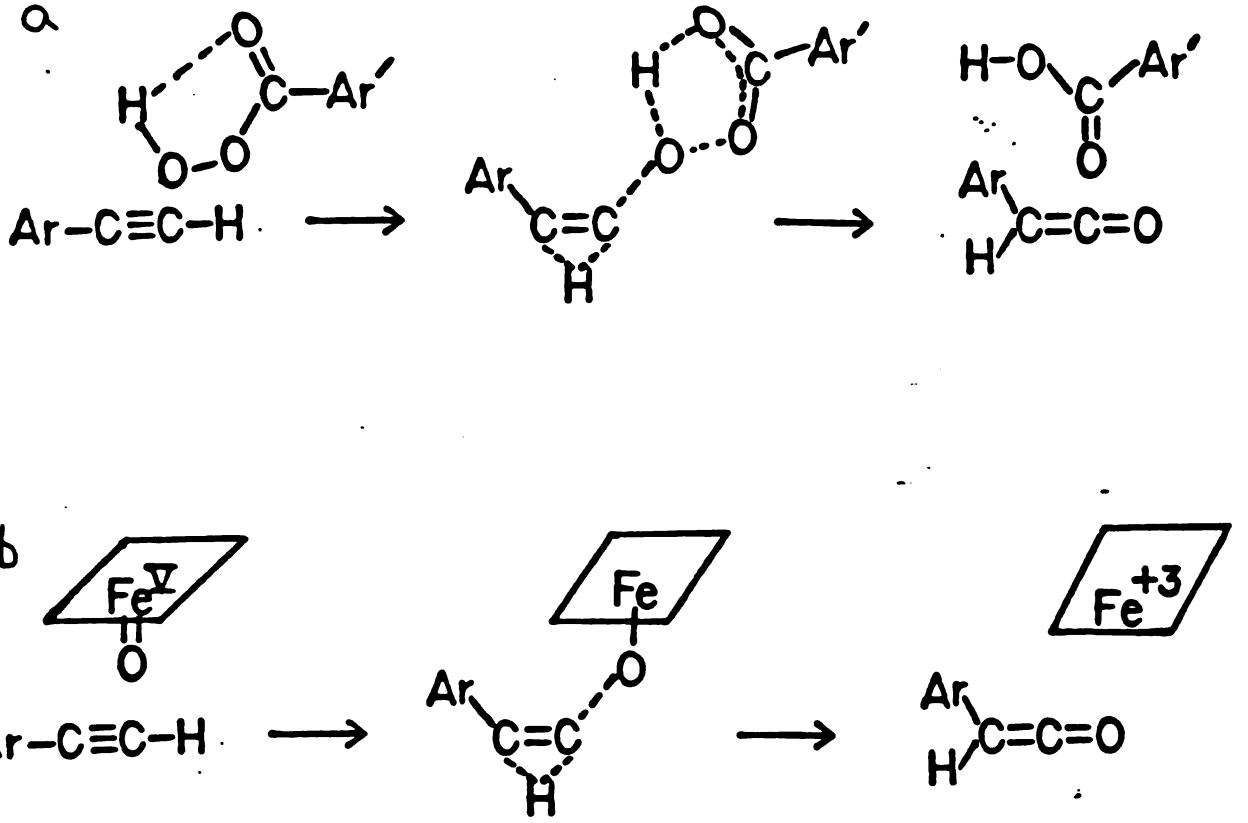

the oxirene (Lewars, 1983; Torres et al, 1983; Laganis et al, 1983).

TABLE 6.1

Bending Kinetic Isotope Effects

Reaction	Kinetic Isotope Effect	Reference
Pinacol rearrangement	2.7 - 3.3	Collins et al, 1959.
Amine oxide pyrolysis	2.7 - 3.2	Chiao & Saunders, 1978.
Carbene insertions into C-H bonds	0.9 - 2.5	Simons and Rabonovitch, 1963.
1,2 Shift of H to vicinal carbene	1.7	Kyba & Hudson, 1978.
Epoxide ring cleavage concerted with 1,2 H shift	1.59	Gillilan et al,1982.

Cytochrome P-450 oxidation of phenylacetylene occurs with a kinetic isotope effect identical to that obtained during MCPBA oxidation (Table 3.1). The full manifestation of a kinetic isotope effect on the overall rate of P-450 oxidation is almost unprecedented (see Chapter 1). This observation implies either that the step in which hydrogen migration occurs is a slow step in the enzymatic reaction or that metabolic switching is unmasking the kinetic isotope effect (Jones et al, 1986).

The fact that hydrogen migration occurs simultaneously with oxygen transfer in the oxidation of acetylenes by MCPBA suggests that the oxygen adds asymmetrically to the π-bond. This hypothesis, which has theoretical basis (Koller and Plesnicar, 1982), predicts the generation of positive charge on the benzylic carbon during the reaction. A Hammett sigma$^+$ correlation has been demonstrated for the oxidation of para-substituted phenylacetylenes by perbenzoic acid (Ogata et al, 1973). The large negative rho value (-1.4) indicates substantial positive charge build-up is occurring on the benzylic carbon in the transition state of the reaction.

Rates of oxidation of para-substituted phenylacetylenes by P-450 also correlate well with theHammett sigma and sigma$^+$ coefficients of the substituents. In the enzymatic reaction, the rho value is even larger (-2.2) indicating that even more positive charge accumulates on the benzylic carbon in the transition state than in the peracid reaction (Figure 4.3). In this case, both sigma (inductive effects) and sigma$^+$ (resonance effects) constants correlate well. The substituents employed in

the enzymatic study do not allow differentiation of the two effects because none of them contributes significantly to resonance stabilization. p-Methoxyphenylacetylene would be expected to give a much higher rate due to resonance stabilization, but would also be expected to undergo O-demethylation.

The similarities between the P-450 catalyzed reaction and the peracid oxidations of phenylacetylene strongly suggest the mechanisms of the two reactions are analogous. Virtually the only products in both cases are the phenylacetic acids in which the acetylenic hydrogen has undergone a 1,2 shift. The hydrogen shift is accompanied by a kinetic isotope effect of 1.8 in both reactions. The hydrogen shift must occur in concert with oxygen delivery to the π-bond in the case of peracid oxidation and probably in the case of P-450 as well. Support for an asymmetric oxygen transfer in both reactions is provided by the observation of large negative rho values, which indicates substantial charge accretion at the benzylic carbon in the transition state. In both cases the mechanism appears to be two electron oxygen transfer to the π-bond concerted with 1,2 hydrogen migration to directly generate the ketene (Scheme 6.1b).

The rate of enzyme inactivation is unaltered by deuterium substitution (Figure 3.10). This result indicates that a product of oxygen transfer to the terminal carbon, such as the ketene, is not the alkylating species. The structure of the isolated heme adduct (Figure 5.10), which has the oxygen bound to the benzylic carbon, as well as the structures of other heme adducts that

result from acetylene oxidation (Ortiz de Montellano and Kunze, 1981; Ortiz de Montellano et al, 1982; Kunze et al, 1982) are consistent with this interpretation. The unstable oxirene can not be the alkylating species: its intermediacy has already been ruled out. The insensitivity of enzyme inactivation to isotopic substitution furthermore indicates that a common intermediate is not undergoing metabolic switching. The rate of enzyme inactivation would be expected to increase by a factor of 1.8 if switching were occurring and this increase could easily be measured. It should be noted that since the partition ratios for phenylacetylene (26) and [1-^{2}H]phenylacetylene (14) are both greater than 1, alterations in the rate of metabolite formation, the faster pathway, will always be reflected in the rate of the slower pathway if the two pathways diverge from a common intermediate. The only situation in which switching would not be observed would be if a third, more rapid, pathway diverges from the same intermediate. It appears, then, that enzyme inactivation diverges from metabolite formation at an early point along the catalytic pathway, probably before oxygen transfer. One can envision several mechanisms to account for early partitioning between metabolite formation and enzyme inactivation (Scheme 3.2). Two likely possibilities are the radical cation mechanism and the metallooxetene mechanism (see Chapter 1 for a discussion of these mechanisms in porphyrin model systems). The radical cation mechanism leads to the postulate that metabolite formation occurs by oxygen transfer, but enzyme inactivation occurs when the enzyme abberantly abstracts an electron from the

π-system instead of inserting the oxygen. The resulting π-radical cation could inactivate the enzyme by binding to the porphyrin ring and would be less selective as to which carbon recombined with the oxygen. The metallooxetene mechanism proposes that the oxygen normally adds to the terminal carbon to generate metabolite, but occasionally adds to the benzylic carbon causing enzyme inactivation.

These two mechanisms can be distinguished by analyzing the electronic effects on the inactivation pathway. If formation of a radical cation is the first step leading to inactivation, the rate of enzyme inactivation by substituted acetylenes in which the substituent is electron withdrawing should decrease. Radical cation formation is energetically difficult and would be expected to be the slow step in the inactivation pathway. The metallooxetene inactivation mechanism, in contrast, would probably not be sensitive to the substituents because oxygen transfer to the benzylic carbon results in accretion of positive charge on the terminal carbon that is insulated from the phenyl ring. The finding that P-450 inactivation by para-substituted phenylacetylenes does not change with substituents ranging from methyl to nitro argues strongly against the radical cation mechanism. The most likely mechanisms for enzyme inactivation therefore involve direct oxygen transfer to the benzylic carbon without prior radical cation formation (Scheme 4.1).

The exact nature of the mechanism of inactivation of P-450 by acetylenes is still unknown. Some information may be gained from the study of heme alkylation by the α-diazoketones,

particularly diazoacetophenone, the diazoketone that generates the same heme adduct as is generated by phenylacetylene. The structure of the adduct has been unambiguously determined to be that shown in Figure 5.10. The terminal carbon of the acetylenic π-bond is attached to the porphyrin ring nitrogen and the activated oxygen atom to the benzylic carbon. Both diazoacetophenone and phenylacetylene give 445 nm complexes with purified, concentrated P-450 that are readily observable (Figures 3.12 and 5.2). ^{13}C-NMR (Chapter 5) studies suggest that the 445 nm complex has the same basic structure as the model TPP-DAP complex shown in Figure 5.16. Alkylation by both the diazoketones and phenylacetylene appears not to involve a carbene intermediate, but rather appears to involve direct formation of the N-alkylated porphyrin in which the oxygen of the adduct is enolized and bound to the iron. This complex appears to be highly stable in non-polar solvents but demetallates readily in protic solvents such as water. It seems reasonable, then, to propose that the N-alkylated structure forms almost immediately, and that intermediates, if formed, are transient. This hypothesis is consistent with direct addition of the activated oxygen to the benzylic carbon either to form the metallooxetene as a transient intermediate or to form the enolic porphyrin adduct directly (Scheme 4.1).

The point at which partition toward either metabolite formation or enzyme inactivation occurs remains to be defined. Deuterium substitution of the acetylenic hydrogen and para substitution of the phenyl ring only alter the rate of

metabolite formation and not enzyme inactivation. The partition ratios change with these substrate perturbations (Figure 4.5), which clearly indicates that partitioning occurs either at or before addition of the oxygen to the acetylenic π-bond since the pathways behave as parallel, independent processes. In order to explain the observation that metabolite formation and enzyme inactivation appear to be independent pathways occurring at the same active site, one must invoke either a difference in binding or an event in which the activated oxygen switches between the two carbons of the π-bond.

It is unlikely that an enzyme renowned for its lack of substrate specificity would bind a molecule such as phenylacetylene so tightly in a particular orientation that the oxygen would be targeted to a particular carbon of the π-bond. The most likely explanation, then, is that substrate binding is not specific, but that switching is not observed because a third, more rapid, pathway exists for decomposition of the intermediate. The third pathway most probably would be further reduction of the iron oxo intermediate to water. This phenomenon has been suggested by stoichiometry experiments in which the consumption of NADPH could not be accounted for by the production of H_2O_2 and metabolites. This led to the proposal that an unmeasureable product such as water is produced (Gorsky et al, 1984; Zhukov and Archakov, 1982; Staudt et al, 1974). Table 6.2 shows the results of an analysis in which NADPH consumption was assumed to partition into the three pathways described above, and the amount of NADPH which is unaccounted for by metabolite formation and

enzyme inactivation is assumed to be that which is responsible for the further reduction of the iron oxo. The calculations are based on the assumption that the total amount of NADPH consumed was coupled to formation of the iron oxo species and that this corresponds to the "steady state" concentration of this intermediate.

TABLE 6.2

Stoichiometry of NADPH Consumption, Metabolite Formation and Enzyme Inactivation

Substrate	Total NADPH	Metabolite	Inactivation	Reduction
			(in nmol/min/nmol P-450)	
p-CH_3	25±3	7.5±1	0.19± 0.4	17.3
p-H	43±5	5.0±1	0.19±0.4	37.8
p-Cl	14±2	2.5±0.5	0.19±0.4	11.5
p-NO_2	52±5	0.9±0.2	0.19±0.4	51.7
p-CH_3 altered	25	3.75	0.22	21.1
p-CH_3 altered	25	1.0	0.23	23.8

Table 6.2 clearly shows that further reduction to water could indeed account for the lack of observation of metabolic switching between enzyme inactivation and metabolite formation. In the worst possible case, that of p-methylphenylacetylene, the NADPH consumption used in further reduction is 70% of the total. The two columns labeled "p-CH_3 altered" show the calculated amount of enzyme inactivated if metabolite formation decreases. The calculations show that even if the metabolite formation was decreased by a factor of 8, it would not measurably affect the rate of enzyme inactivation. Clearly, these data raise many unanswered questions. First, one might expect a correlation between NADPH consumption and the ease of oxidation of the acetylene based on the theory that more reduction to water would occur if the substrate were harder to oxidize. The data can be imagined to fit such a trend, but the correlation is not at all significant. One explanation for the lack of correlation is that the substrates are affecting NADPH consumption in some other way that does not correlate with their oxidizability. The ability of some substrates to affect NADPH consumption and uncoupling of the P-450 cycle (Chapter 1) has been documented previously (Miller et al, 1983; Benford and Bridges, 1983; Huang et al, 1983; Dalet et al, 1983) and may be occurring here. The marked decrease in NADPH consumption when P-450b is incubated with p-chlorophenylacetylene suggests that, indeed, some substrates can effect the overall NADPH consumption in some way. The NADPH consumption in the absence of substrate is routinely almost 2 fold as great as in the presence of p-chlorophenylacetylene

(Table 4.1). Control experiments indicate this compound has no effect on the activity of the P-450 reductase, so it must in some way be decreasing the turnover rate of P-450 even with respect to the rate of autooxidation in the absence of substrate. A further indication that the substrates can directly influence the overall turnover rate of P-450 is the fact that styrene is oxidized 1500 times faster than phenylacetylene, at a turnover rate of 6.3 umol/min/nmol P-450. This rate of NADPH consumption required to achieve this turnover rate is at least 100 times greater than that measured during phenylacetylene turnover. Clearly, substrates have a profound effect both on the turnover rate of P-450 and on the consumption of NADPH.

The observation that all the phenylacetylenes destroy P-450 at exactly the same rate prompted an investigation into partition ratio perturbations by P-450 effectors that might alter the rate of inactivation by these substrates. Steric effects on metabolite formation and enzyme inactivation were investigated by placing methyl groups ortho to the acetylenic bond in phenylacetylene. In no case did these methyl groups hinder inactivation and, in one case, actually activated metabolite formation. This surprising result is only consistent with the binding of phenylacetylenes above and parallel to the porphyrin ring. It is still puzzling why the ortho groups do not get hydroxylated in this orientation, but one explanation is that the acetylenic bond complexes with the iron oxo species predisposing it toward π-bond oxidation.

Cytochrome b_5, which has been shown to be involved in

several steps of the P-450 catalytic cycle (see Chapter 1), causes a profound protection from inactivation by phenylacetylenes and thus increases the partition ratio by a factor of three (Table 4.2). Manganese substituted b_5, however, had no effect on inactivation. The protective effect thus appeared to be mediated electronically and not merely allosterically by a protein-protein interaction. The nature of this protection, and its relation to the mechanism of P-450 inactivation by phenylacetylenes, remains to be studied. One possibility is that it influences the "third pathway" of reduction of the iron oxo species to water and alters the velocity of enzyme inactivation by changing the concentration of the active oxygen species. The fact that metabolite formation remains constant in the presence and absence of b_5, however, suggests that the effect of b_5 may be more complicated.

One intriguing explanation is that b_5 alters the distribution of electrons in the active oxygen species so that two distinct iron oxo species are present, one of which has a propensity for enzyme inactivation and the other of which has a propensity for metabolite formation. This possibility is suggested by the observation that compounds I of catalase and horseradish peroxidase are isoelectronic (and isoelectronic with the activated oxygen in P-450), but are spectrally distinguishable. Theoretical studies indicate that the unpaired electron on the porphyrin ring resides preferentially in the a_{1u} orbital in catalase, and in the a_{2u} orbital in horseradish peroxidase. The unpaired electron density is distributed very

differently in these two orbitals, 100 times as much density is found on each of the ring nitrogens in the a_{2u} orbital as compared with the a_{1u} orbital (Hanson et al, 1981). It is easy to imagine how cytochrome b_5 might alter the formation of these two intermediates, or change their equilibrium, and thus change the partition ratio. The high concentration of unpaired electron density on the porphyrin ring nitrogens could predispose this activated oxygen species to heme alkylation, which may involve simultaneous oxygen transfer and N-alkylation. In this case, the pathways of enzyme inactivation and metabolite formation are totally separate, and a "third pathway" would not be necessary to account for the lack of metabolic switching. Detailed stoichiometry studies as well as a more thorough characterization of the b_5 effect are neccessary to resolve this question.

Mechanistic parallels can be drawn between the π-bond oxidation of acetylenes and olefins. P-450 oxidizes both classes of compounds to a metabolite and to a heme adduct. The resulting heme adducts have analogous structures (Ortiz de Montellano, 1985). The mechanism of olefin oxidation by porphyrin model systems is controversial, but the two most likely mechanisms are a radical cation mechanism and a metallooxetane mechanism (see Chapter 1). Olefin oxidation by P-450 also may proceed by either one of these mechanisms. Acetylenes have proven, and will continue to prove, useful as probes of the catalytic mechanism of π-bond oxidation by P-450. From studies of acetylene oxidation, one can conclude that the π-radical cation is an unlikely intermediate in either the pathway leading to metabolite

formation or that leading to enzyme inactivation. The fact that the energy required to remove an electron from phenylacetylene (279 kcal/mol) and styrene (232 kcal/mol) are very similar suggests that radical cation formation from styrene would also be unlikely (CRC Handbook, 1972). It certainly could not explain the 1500 fold increase in the rate of metabolite formation. Metallooxetane formation is a likely possibility based on the results of the acetylene studies as well as several observations in the enzyme. The metallooxetane intermediate would be expected to undergo cis-hydrogen migration, albeit slowly, to form a trace of the aldehyde (see Chapter 1 for references). This mechanism could also explain the exchange of the terminal hydrogens of propene (Groves 1986). The increased stability of the metallooxetane compared to the metallooxetene, as well as the stability of the epoxide product that would result from oxygen bond migration in the metallooxetanes, could explain the increased partition ratios (typically 300) of olefins as compared to acetylenes (typically 4 to 40) (Schemes 6.2 and 6.3). If the metallooxetene ever forms during the oxidation of acetylenes, it must lead to heme adduct formation because the hydrogen shifts and the ketene is directly formed when the oxygen adds to the terminal carbon (Scheme 4.1). Although extension of the results from acetylene oxidation reactions to predict the mechanism of olefin oxidation reactions must be done with caution, the information that is gained can be used to design experiments to further dissect the mechanism of olefin oxidation by P-450.

Scheme 6.2

The Metallooxetane Mechanism for Olefin Oxidation by P-450

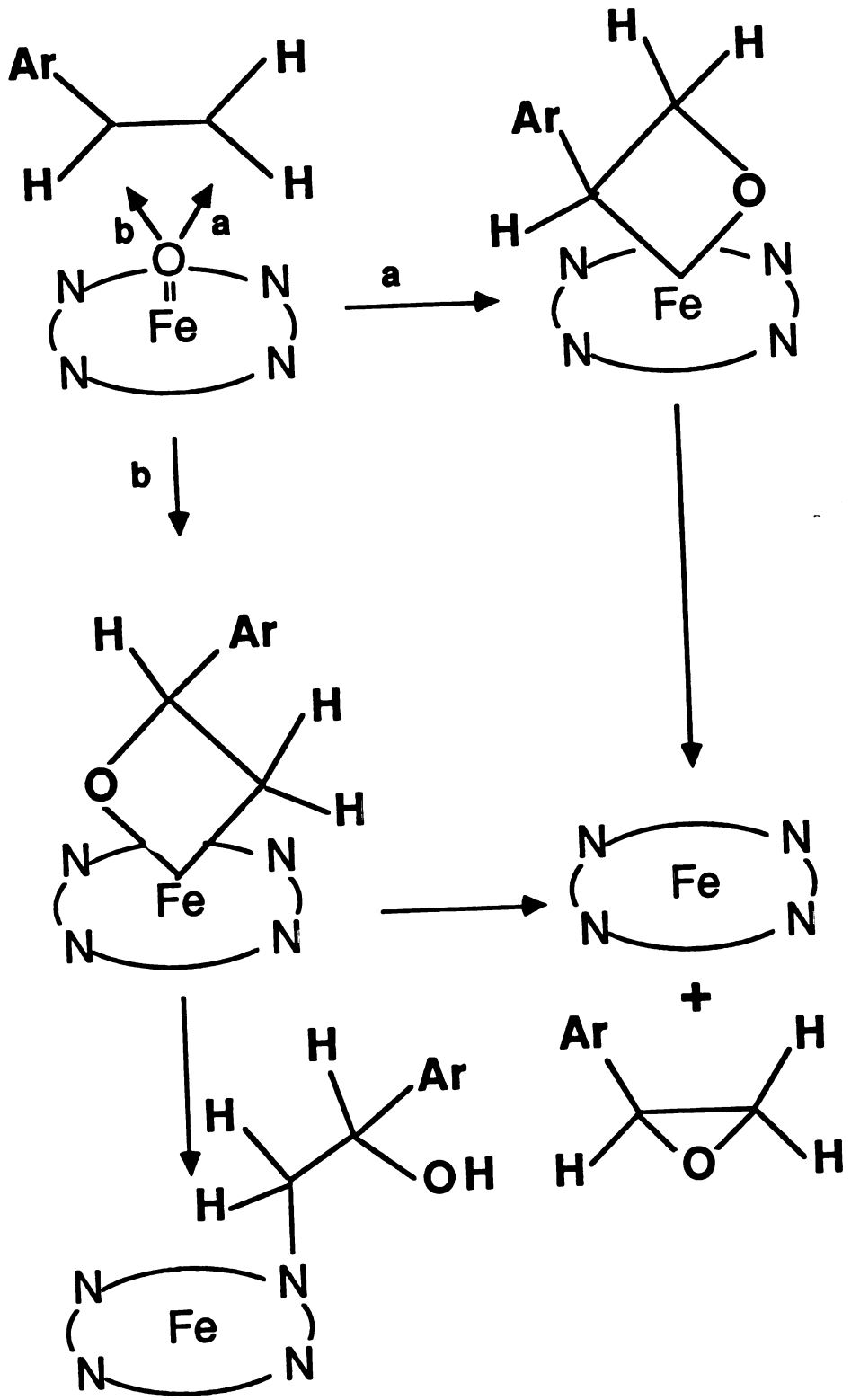

Scheme 6.3

The Metallooxetene Mechanism for Acetylene Oxidation by P-450

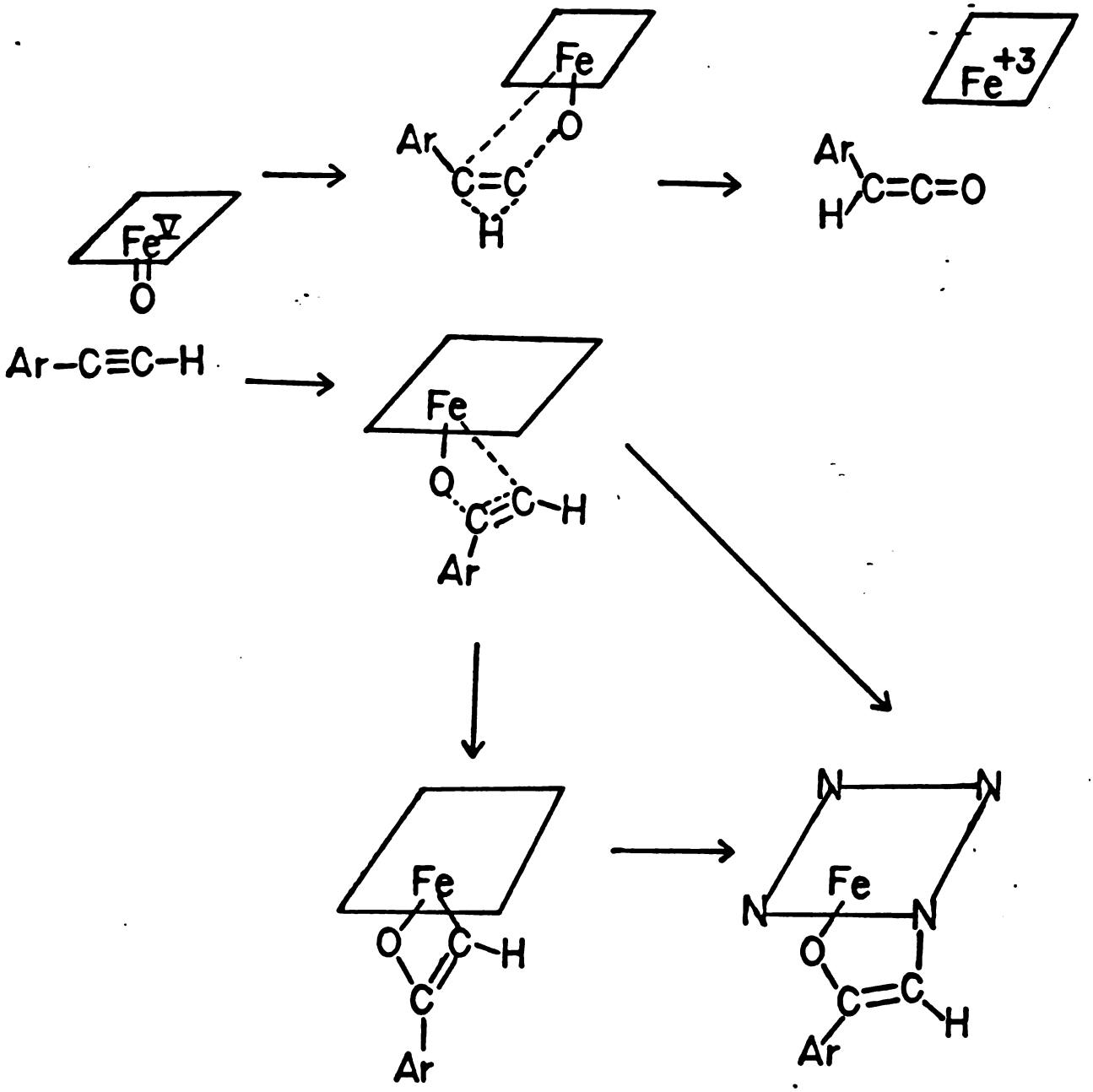

REFERENCES

Aldrichimica Acta (1983) 16: 3.

Allen, A.D. and Cook, C.D. (1963) Can. J. Chem. 41: 1084 - 1087.

Auclair, C., DeProst, D. and Hakim, J. (1978) Biochem. Pharmacol. 203: 551 - 558.

Balch, A.L. and Renner, M.W. (1986) J. Am. Chem. Soc. 108: 2603 - 2608.

Balch, A.L., Chan, Y-W., La Mar, G.N., Latos-Grazynski, L. and Renner, M.W. (1985) Inorg. Chem. 24: 1437 - 1443.

Battioni, J-P., Artaud, I., Dupre, D., Leduc, P., Akhrem, I., Mansuy, D., Fischer, J., Weiss, R. and Morgenstearn-Badarau, I. (1986) J. Am. Chem. Soc. 108: 5598 - 5607.

Behere, D.V., Gonzalez-Vegara, E. and Goff, H.M. (1985) Biochem. Biophys. Res. Commun. 131: 607 - 613.

Benford, D.J. and Bridges, J.W. (1983) Biochem. Pharmacol. 32: 2225 - 2230.

Bjorkhem, I. (1977) Pharmac. Ther. A. 1: 327 - 348.

Bjorkhem, I. and Hamberg, M. (1972) Biochem. Biophys. Res. Commun. 17: 333 - 340.

Bonfils, C., Balny, C and Maurel, P. (1981) J. Biol. Chem. 256: 9457 - 9465.

Bradford, M. (1976) Anal. Biochem. 72: 248.

Bruice, T.C., Furter, P.G. and Ball, S.S. (1981) Am. Chem. Soc. J. 103: 4578 - 4580.

Callot, H.J. and Schaffer, E. (1980) Tet. Lett. 21: 1375.

Callot, H.J., Chevriei, B. and Weiss, R. (1978) J. Am. Chem. Soc. 100: 4733.

Casanova, R., Reichstein, T. (1950) Helv. Chim. Acta 33: 417.

Chang, C.K. and Kuo, M.S. (1979) J. Am. Chem. Soc. 101: 3413 - 3415.

Chiao, W-B. and Saunders, W.H. (1978) J. Am. Chem. Soc. 100: 2802 - 2805.

Ciabattoni, J., Campbell, R.A., Renner, C.A. and Concannon, P.W. (1970) J. Am. Chem. Soc. 92: 3826 - 3828.

Cinti, D.L. and Ozols, J. (1975) Biochim. Biophys. Acta 410: 32 - 44.

Cleland, W.W. (1963) Biochim. Biophys. Acta 67: 104 - 137.

Collins, C.J., Rainey, W.T., Smith, W.B. and Kaye, I.A. (1959) J. Am. Chem. Soc. 81: 460 - 466.

Concannon, P.W. and Ciabattoni, J. (1973) J. Am. Chem. Soc. 95: 3284 - 3289.

Cotton, F.A. and Wilkinson, G. (1980) "Advanced Inorganic Chemistry" (Fourth Edition) Wiley and Sons, New York. 627.

CRC Handbook of Chemistry and Physics (1972) R.C. Weast, ed. Chemical Rubber Company, Cleveland, pp. E-62.

Cristol, S.J., Beggon, A., Norris, W.P. and Ramsey, R.S. (1954) J. Am. Chem. Soc. 76: 4558 - 4561.

Dalet, C., Anderson, K.K., Dalet-Beluche, I., Bonfils, C. and Maurel, P. (1983) Biochem. Pharmacol. 32: 593 - 601.

Debey, P. and Balny, C. (1973) Biochimie 55: 329 - 332.

ElMasri, A.M., Smith, J.N. and Williams, R.T. (1958) Biochem. J. 68: 199 - 204.

Evans, D.F.(1959) J. Chem. Soc. 2003 - 2005.

Fenwick, J., Frater, G., Ogi, K. and Strausz, O.P. (1973) J. Am. Chem. Soc. 95: 124.

Franklin, M.R. (1971) Xenobiotica 1: 581 - 591.

Fujito, T. and Nishioka, T. (1976) Prog. Phys. Org. Chem. 12: 49 - 89.

Gillilan, R.E., Pohl, T.M. and Whalen, D.L. (1982) J. Am. Chem. Soc. 104: 4482 - 4484.

Goldstein, M.J. and Dolbier, W.R. (1965) J. Am. Chem. Soc. 87: 2293 - 2295.

Gorsky, L.D. and Coon, M.J. (1986) Drug Met. and Disp. 14: 89 - 96.

Gorsky, L.D., Koop, D.R. and Coon, M.J. (1984) J. Biol. Chem. 259: 6812 - 6817.

Greenlee, W.F. and Poland, A. (1978) J. Pharm. Exp. Ther. 205: 596.

Groves, J.T., Avaria, Neisser, G.E., Fish, K.M., Imachi, M. and Kuczkowski, R.L. (1986) J. Am. Chem. Soc. 108: 3837 - 3838.

Groves, J.T., Kruper, W.J. and Haushalter, R.C. (1980) J. Am. Chem. Soc. 102: 6375 - 6377.

Groves, J.T., Nemo, T.E. and Meyers, R.S. (1979) J. Am. Chem. Soc. 101: 1032 - 1033.

Groves, J.T. and Watanabe, Y. (1986) J. Am. Chem. Soc. 108: 507 - 508.

Groves, J.T., Watanabe, Y. and McMurry, T.J. (1983) J. Am. Chem. Soc. 105: 4489 - 4490.

Groves, J.T., McClusky, G.A., White, R.E. and Coon, M.J. (1978) Biochem. Biophys. Res. Commun. 81: 154 - 160.

Groves, J.T. and McMurry, T.J. (1986) in "Cytochrome P-450: Structure, Mechanism and Biochemistry" P.Ortiz de Montellano, ed., Plenum Press, New York. 1 - 28.

Guengerich, F.P. (1978) J. Biol. Chem. 253: 7931 - 7939.

Hammett, L.P. (1937) J. Am. Chem. Soc. 59: 96.

Hanson, L.K., Chang, C.K., Davis, M.S., Fajer, J. (1981) J. Am. Chem. Soc. 103: 663 - 670.

Hanzlik, R.P. and Shearer, G.O. (1975) J. Am. Chem. Soc. 97: 5231.

Hanzlik, R.P. and Shearer, G.O. (1978) Biochem. Pharmacol. 27: 1441 - 1444.

Hanzlik, R.P., Shearer, G.O., Hamburg, A. and Gillessee, T. (1978) Biochem. Pharmacol. 27: 1435.

Harada, N., Miwa, G.T., Walsh, J.S. and Lu, A.Y.H. (1984) J. Biol. Chem. 259: 3005 - 3010.

Harada, N., Miwa, G.T. and Lu. A.Y.H. (1982) Fed. Proc. 41: 1405.

Hjelmeland, L.M., Aronow, L. and Trudell, J.R. (1977) Biochem. Biophys. Res. Commun. 76: 541 - 549.

Huang, M-T., Chang, R.L., Fortner, J.G. and Conney, A.H. (1981) J. Biol. Chem. 256: 6829 - 6836.

Iyanagi, T., Anan, F., Imai, Y. and Mason, H.S. (1978) Biochem. 17: 2224 - 2230.

Johnson, A.W. and Ward. D. (1976) J. Chem. Soc. Perkin Trans. I: 720.

Johnson, A.W., Ward, D., Batten, P., Hamilton, A.L., Skelton, G. and Elson, C.M. (1975) J. Chem. Soc. Perkin Trans. I: 2076.

Jones, J.P., Korzekwa, K.R., Rettie, A.E. and Trager, W.F. (1986) J. Am. Chem. Soc. 108: 7074 - 7078.

Koller, J. and Plesnicar, B. (1982) J. Chem. Soc. Perkin II : 1361 - 1365.

Kunze, K.L., Mangold, B.L.K., Wheeler, C., Beilan, H.S. and Ortiz de Montellano, P.R. (1983) Biochem. 21: 1331 - 1339.

Kunze, K.L. and Ortiz de Montellano, P.R. (1981) J. Am. Chem. Soc. 103: 4225 - 4230.

Kuthan, H., Tsuji, H., Graf, H., Ullrich, V., Werringloer, J. and Estabrook, R.W. (1978) FEBS Lett. 91: 343 - 345.

Kyba, E.P. and Hudson, C.W. (1977) J. Org. Chem. 42: 1935 - 1939.

Laemmli, U.K. (1970) Nature 227: 680 - 685.

Laganis, E.D., Janik, D.S., Curphey, T.J. and Lemal, D.M. (1983) J. Am. Chem. Soc. 105: 7457 - 7459.

Lange, M. and Mansuy, D. (1981) Tet. Lett. 22: 2561 - 2564.

Latos-Grayzynski, Cheng, R., LaMar, G.N. and Balch, A.L. (1981) J. Am. Chem. Soc. 103: 4270 - 4272.

Lewars, E.G.(1983) Chem. Rev. 83: 519-534.

Liebler, D.C. and Guengerich, F.P. (1983) Biochem. 22: 5482 - 5489.

Lindsay-Smith, J.R. and Sleath, P.R. (1982) J. Chem. Soc. Perk. Trans. II: 1009 - 1015.

Lu, A.Y.H. and Miwa, G.T. (1982) in "Cytochrome P-450, Biochemistry, Biophysics, and Environmental Implications", E. Hietanen, M. Latinen, and O. Hanninen, eds. Elsevier Biomedical Press, B.V.

Mansuy, D., Battioni, J-P., Akhrem, I., Dupre, D., Fischer, J., Weiss, R. and Morgenstern-Badarau, I. (1984) J. Am. Chem. Soc. 106: 6112 - 6114.

Mansuy, D., Lange, M., Chottard, J.C. and Guerein, P. (1977) J. Chem. Soc. Chem. Commun. 648 - 649.

Mansuy, D., Lange, M. and Chottard, J.C. (1978) J. Am. Chem. Soc. 100: 3214 - 3215.

Mansuy, D., Nastainczyk, W. and Ullrich, V. (1974) Arch. Pharmakol. 285: 315.

Mansuy, D., Lange, M., and Chottard, J.C. (1979) J. Am. Chem. Soc. 101: 6437.

Mansuy, D., Lange, M., Chottard, J.C., Bartoli, J.F., Chevrier, B. and Weiss, R. (1978) Angew. Chem. Int. Ed. Engl. 17: 781 - 782.

Mansuy, D., LeClaire, J., Fontcave, M. and Momenteau, M. (1984) Biochem. Biophys. Res. Commun. 119: 319 - 325.

Mansuy, D., Levocelle, L., Artaud, I. and Battioni, J-P. (1985) Nouv. J. Chim. 9: 711 - 716.

Mashiko, T., Dolphin, D., Nakano, T. and Traylor, T.G. (1986) J. Am. Chem. Soc. 107: 3735 - 3736.

Matlin, S.A. and Sammes, P.G. (1972) J. Chem. Soc. Perkin I: 2623.

Matwiyoff, N.A., Vergamini, P.J., Needham, T.E., Gregg, C.T., Volpe, J.A. and Caughey, W.S. (1973) J. Am. Chem. Soc. 95: 4429 - 4431.

Maynert, E.W., Foreman, R.L. and Watabe, T. (1970) J. Biol. Chem. 245: 5234 - 5238.

McDonald, R.N. and Schwab, P.A. (1964) J. Am. Chem. Soc. 86: 4866 - 4871.

McMahon, R.E., Turner, J.C., Whitaker, G.S. and Sullivan, H.R. (1981) Biochem. Biophys. Res. Commun. 99: 662 - 667.

Miller, R.E. and Guengerich, F.P. (1982) Biochem. 21: 1090 - 1097.

Miller, M.S., Huang, M-T., Jeffrey, A.M. and Conney, A.H. (1983) Mol. Pharmacol. 24: 137 - 145.

Miwa, G.T., Harada, N. and Lu, A.Y.H. (1985) Arch. Biochem. Biophys. 239: 155 - 162.

Miwa, G.T., Walsh, J.S. and Lu. A.Y.H. (1982) in "Advances in Pharmacology and Therapeutics II", E. Yoshida, ed.

Miwa, G.T., Walsh. J.S. and Lu, A.Y.H. (1984) J. Biol. Chem. 259: 3000 - 3004.

Moon, R.B. and Richards, J.H. (1974) Biochem. 13: 3437.

More O'Ferrall, R.A. (1970) J. Chem. Soc. B: 785 - 790.

Musselman, B.D., Watson, J.T. and Chang, C.K. (1986) Org. Mass. Spec. (in Press).

Northrup, D. (1975) Biochem. 14: 2644 - 2651.

Noshiro, M., Ullrich, V. and Omura, T. (1981) Eur. J. Biochem. 116: 521 - 526.

Ogata, Y., Sawaki, Y. and Ohno, T. (1982) J. Am. Chem. Soc. 104: 216 - 219.

Olmstead, M.M., Cheng, R-J. and Balch, A.L. (1982) Inorg. Chem. 21: 4143 - 4148.

Omura,T. and Sato, R. (1964)J. Biol. Chem. 239: 2370, 2379.

Ortiz de Montellano, P.R., ed. (1986) "Cytochrome P-450 Structure, Mechanism, and Biochemistry", Plenum Press, New York.

Ortiz de Montellano, P.R. (1985) in "Bioactivation of Foreign Compounds" Academic Press, New York. 121 - 155.

Ortiz de Montellano, P.R. and Kunze, K.L. (1980) J. Am. Chem. Soc. 102: 7373 - 7375.

Ortiz de Montellano, P.R. and Kunze, K.L. (1980b) J. Biol. Chem. 255: 5578 - 5585.

Ortiz de Montellano, P.R. and Kunze, K.L. (1981) Arch. Biochem. Biophys. 209: 710 - 712.

Ortiz de Montellano, P.R. and Mathews, J.M. (1981) Biochem. J. 195: 761 - 764.

Ortiz de Montellano, P.R. and Mico, B.A. (1980) Mol. Pharmacol. 18: 128 - 135.

Ortiz de Montellano, P.R. and Reich, N.O. (1986) in "Cytochrome P-450 Structure, Mechanism, and Biochemistry", P.R. Ortiz de Montellano, ed. Plenum Press, New York, 273 - 314.

Ortiz de Montellano, P.R., Mangold, B.L.K., Wheeler, C., Kunze, K.L. and Reich, N.O. (1983) J. Biol. Chem. 258: 4208 - 4213.

Ortiz de Montellano, P.R., Beilan, H.S., Kunze, K.L. and Mico, B.A. (1981) J. Biol. Chem. 256: 4395 - 4399.

Ortiz de Montellano, P.R., Kunze, K.L., Beilan, H.S., and Wheeler, C. (1982) Biochem. 21: 1331 - 1339.

Ortiz de Montellano, P.R., Stearns, R.S. and Langry, K.C. (1984) Mol. Pharmacol. 25: 310 - 317.

Ortiz de Montellano, P.R. (1985) in "Bioactivation of Foreign Compounds", M.W. Anders, ed. Academic Press, New York, 121 - 155.

Ozols, J. and Strittmatter, P. (1964) J. Biol. Chem. 239: 1018 - 1023.

Pompon, D. and Coon, M.J. (1984) J. Biol. Chem. 259: 15377 - 15385.

Poulos, T.L., Finzel, B.C. and Howard, A.J. (1986) Biochem. 25: 5314 - 5322.

Poulos, T.L., Finzel, B.C., Gunsalus, I.C., Wagner, G.C. and Kraut, J. (1985) J. Biol. Chem. 260: 16122 - 16130.

Pretsch-Clerc, Seibl and Simon (1983) Tables of Spectral Data for Structure Determination of Organic Compounds, Springer-Verlag, New York.

Regitz, M., Menz, F. and Ruter, J. (1967) Tet. Lett. 8: 739 - 742.

Schenkman, J.B., Remmer, H. and Estabrook, R.W. (1967) Mol. Pharmacol. 3: 113 - 123.

Schroder, M. and Constable, E.C. (1982) Chem. Commun. 734 - 736.

Sharpless, K.B., Teranishi, A.Y. and Backvall, J-E. (1977) J. Am. Chem. Soc. 99: 3120 - 3128.

Shephard, E.A., Pike, S.F., Rabin, B.R. and Phillips, I.R. (1983) Anal. Biochem. 129: 430 - 433.

Shirazi, A. and Goff, H.M. (1982) J. Am. Chem. Soc. 104: 6318 - 6322.

Simons, J.W. and Rabinovitch, B.S. (1963) J. Am. Chem. Soc. 85: 1023 - 1024.

Staudt, H., Lichtenberger, F. and Ullrich, V. (1974) Eur. J. Biochem. 46: 99 - 106.

Stille, J.K. and Whitehurst, D.D. (1964) J. Am. Chem. Soc. 86: 4871 - 4876.

Strausz, D.P., Gosavi, R.K., Denes, A.S. and Czizmadia, I.G. (1976) J. Am. Chem. Soc. 98: 4784 - 4786.

Sullivan, H.R., Roffey, P. and McMahon, R.E. (1979) Drug Met. Disp. 7: 76 - 80.

Sus, O. (1944) Ann. Chem. 556: 65.

Tabushi, I. and Yazaki, A. (1981) J. Am. Chem. Soc. 103: 7371 - 7373.

Tanaka, K. and Yoshimine, M. (1980) J. Am. Chem. Soc. 102: 7655 - 7662.

Thompson, J.A., and Holtzman, J.T. (1974) Drug Met. Disp. 2: 577 - 582.

Torres, M., Bourdelande, J.L., Clement, A. and Strausz, O.P. (1983) J. Am. Chem. Soc. 105: 1698 - 1700.

Wade, A., Symons, A.M., Martin, L. and Parke, D.V. (1979) Biochem. J. 184: 509 - 517.

Watabe, T. and Akamatsu, K. (1974) Biochem. Pharmacol. 23: 1845 - 1851.

Watabe, T., Ueno, Y. and Imazumi, J. (1971) Biochem. Pharmacol. 20: 912 - 913.

Waxman, D.J. and Walsh, C. (1982) J. Biol. Chem. 257: 10446 - 10457.

Werringloer, J. and Kawano, S. (1980) in "Biochemistry, Biophysics and Regulation of Cytochrome P-450. J.A. Gustafsson, D. Carlstedt-Duke, A. Mode, and J. Rafter, eds. Elsevier/North Holland, Amsterdam. pp. 359 - 362.

White, R.E. and Coon, M.J. (1980) Ann. Rev. Biochem. 49: 315 - 356.

Williams,C.H. and Kamin, H. (1962) J. Biol. Chem. 237: 587 - 595.

Wolf, C.R., Mansuy, D., Nastainczyk, W., Deutschmann, G. and Ullrich, V. (1977) Mol. Pharmacol. 13: 698.

Wolff, L. (1902) Ann. Chem. 325: 129.

Wolff, L. (1912) Ann. Chem. 394: 23.

Yates, P. and Crawford, R.J. (1966) J. Am. Chem. Soc. 88: 1562.

Yates, P. and Fugger, J. (1957) J. Chem. Ind. (London) 1511.

Yukawa, Y. and Ibata, T. (1969) Bull. J. Chem Soc. Japan 42: 802 - 805.

Zukov, A.A. and Archakov, A.L. (1982) Biochem. Biophys. Res. Commun. 109: 813 - 818.

APPENDIX I

SYNTHESES

1. Biphenylacetylene

Biphenylacetylene was prepared by the method of Wade et al (1979) as modified by Ortiz de Montellano and Kunze (1981). 4-Acetylbiphenyl (2 g) and PCl_5 (16 g) were placed in a 200 ml round flask containing 120 ml of anhydrous pyridine. The flask was equipped with an air condenser and drying tube, and was heated to 50 °C in an oil bath for 12 - 16 hours. The reaction mixture was then poured slowly into 400 ml of 2 N HCl and extracted three times with dichloromethane. The solution was washed once with water, dried over Na_2SO_4 and concentrated by rotary evaporation. The product, purified by column chromatography on a 1 x 60 cm column of 50 - 70 mesh silica gel eluted with hexane, was recrystallized from hexane. The yield after recrystallization was typically 30%: NMR 7.49 - 7.25 (m,10,aryl H), 3.12 ppm (s,1,acetylenic H).

2. [1-^{2}H]Biphenylacetylene

Deuterium exchange of the acetylenic hydrogen of biphenylacetylene was accomplished as described by Ortiz de Montellano and Kunze (1980). A 2 ml aliquot of a commercial solution of n-butyl lithium in hexane (3 mmol) was added dropwise under nitrogen at -78 °C to a stirred solution of biphenylacetylene (122 mg, 0.7 mmol) in 20 ml of dry

tetrahydrofuran. The resulting solution was allowed to warm to 0°C and was stirred for 1 hr before 2 ml of deuterated water (99.97% deuterium, Aldrich gold label) was carefully added and the mixture allowed to stir for 1 hour at room temperature. The mixture was then extracted with diethyl ether, the organic layers combined and dried over Na_2SO_4, and the residue purified by chromatography and recrystallized as for biphenylacetylene. NMR and mass spectrometric analyses of the purified product (65 -70% yield) indicated greater than 95% incorporation of deuterium.

3. [1-^{2}H]Phenylacetylene

A solution of 10 ml phenylacetylene (9.1 mmol) in 30 ml of anhydrous tetrahydrofuran was treated with a solution of n-butyl lithium in hexane (100 ml, 150 mmol) as described above for biphenylacetylene. After quenching the reaction with 15 ml of deuterated water, the product was extracted with ether. The ether solution was dried over Na_2SO_4 and the ether was removed by distillation (atmospheric pressure, 45 - 50°C). The product was purified by vacuum distillation (1 torr, 30 °C). NMR and mass spectrometric data indicated the product was 97 % deuterated.

4. Substituted Acetylenes

p-Methyl-, p-chloro-, o-methyl- and o,o,p-trimethylphenylacetylene were obtained by the method of Allen and Cook (1963). p-Nitrophenylacetylene was obtained by the method of Cristol et al, (1954). All were purified by distillation under reduced pressure. NMR and mass spectrometric data confirmed the assigned structures.

The synthesis of o-methylphenylacetylene is given below in

detail as an example of the general method.

PCl_5 (8.9 g) was dissolved in o-methylacetophenone (5 g) in a 50 ml round bottom flask equipped with a reflux condenser. The solution was refluxed at 100 - 120 °C for 1 hour, and then vacuum distilled at 1 torr. The major product distilled at 34 - 36 °C. NMR data confirmed the structure of the expected chloroolefin: 7.24 - 7.19 (m,4,aryl H), 5.64, 5.62, 5.34, 5.32 (dd,2,vinyl H), and 2.41 ppm (s,3,methyl H). The 3.5 ml of chloroolefin obtained after distillation was refluxed overnight at 60 - 80 °C with a solution of 5 g KOH in 15 ml absolute ethanol in a 100 ml round bottom flask equipped with a reflux condenser. The mixture was then vacuum distilled at 1 torr. The major component distilled at 25 - 27 °C, and NMR confirmed it to be the acetylene: 7.24 - 7.13 (m,4,aryl H), 3.26 (s,1,acetylenic H), and 2.45 ppm (s,3,methyl H).

5. Protoporphyrin IX Manganese complex

The preparation of the manganese complex of PPIX was performed as described by Ozols and Strittmatter (1964). Briefly, a 1 % solution (0.25 g/2.5 ml) of PPIX in a 1:1 mixture of chloroform : pyridine was prepared. A 3% solution (0.75 g /2.5 ml) of $Mn(OAc)_2$ in glacial acetic acid was added to the porphyrin solution. The mixture was refluxed and stirred at 90 °C for 20 minutes, and the solvent was removed by rotary evaporation. The residue was taken up in water and adjusted to pH 4 with NaOH. Upon cooling, a precipitate formed which was isolated by filtration and purified by a second cycle of precipitation. The absorbance spectrum was identical to that

reported previously.

6. Diazoacetophenone

Diazoacetophenone (DAP) was synthesized by the method of Yukawa and Ibata (1969). All glassware which might come in contact with diazomethane had clear glass joints and was from the Diazald Kit (Aldrich). Freshly distilled benzoyl chloride (3 ml, 0.03 mol) was dissolved in 30 ml of anhydrous diethyl ether and added dropwise over 30 minutes to 75 ml of a stirred ethereal solution of diazomethane (approx. 0.07 mol) held at 0°C with an ice bath. The mixture was allowed to stir for an additional hour, and the ether was removed under a stream of nitrogen. Hexane was added until the residue dissolved and the product was recrystallized by concentrating the hexane solution under a stream of nitrogen. The yield was typically 30 - 40%: NMR 7.82 - 7.26 (m,5,aryl H),and 5.89 ppm (s,1,diazomethine H); FTIR 2100(s), 1600, 1630 (s), 1430, 1380 cm^{-1} (s).

7. [1-^{13}C]Diazoacetophenone

The synthesis of [1-^{13}C]diazoacetophenone (^{13}C-DAP) was similar to that for diazoacetophenone. [^{13}C]diazald (MSD Isotopes) was converted to [1^{13}C]diazomethane by the Aldrich method (Aldrichimica Acta, 1983).

Potassium hydroxide (0.23 g) was dissolved in 0.4 ml of water and added to 1.2 ml of 95% ethanol in a 50 ml clear seal round bottom flask fitted with a clear seal distillation adapter, small condenser, vacuum adapter and receiving flask (Diazald Kit). Because the volumes were so small, a rubber septum was used instead of a dropping funnel. The [^{13}C]diazald (1 g) in 40 ml

of anhydrous diethylether was added rapidly, and the rubber septum was replaced. The distillation flask was heated in a water bath to 50 ^{o}C and the diazomethane was collected in the receiving flask. The condenser and receiving flask were covered with dry ice to improve the yield. Approximately 20 ml of [1-^{13}C]diazomethane was obtained.

The entire yield of diazomethane was placed in the 100 ml flask and 0.6 ml of freshly distilled benzoyl chloride in 15 ml of anhydrous diethylether was added via a dropping funnel over 20 minutes. The reaction, carried out as described for diazoacetophenone, yielded 0.2 g. The ^{13}C content was presumed to be that of the starting diazald (92%). ^{13}C-NMR in $CDCl_3$ gave a doublet (72.168, 71.305 ppm relative to the $CDCl_3$ at 77.5 ppm) with a coupling constant of approximately 207.6 Hz. ^{1}H-NMR ($CDCl_3$): 7.8 - 7.4 (m,5,aryl H), 6.32 and 5.50 ppm (d,1,diazomethine H). In this case the ^{13}C -^{1}H coupling constant was more accurately determined to be 197.9 Hz.

8. 1-Diazo-1-phenyl-2-propanone

The synthesis of 1-diazo-1-phenyl-2-propanone (Me-DAP) was patterned after that described by Regitz, et al (1967). Basically, the reaction involves coupling of the azido group from tosylazide with phenylacetone under basic conditions.

Tosylazide was prepared by dissolving 21.5 g tosylchloride in 125 ml of 95% ethanol and adding it to a solution of 8.75 g sodium azide in 25 ml water. The mixture was stirred for 1 hr, but the tosylchloride never completely dissolved. The solution was decanted into 500 ml of distilled, deionized water on ice.

The tosylazide oiled out. After washing with 3 small portions of water, the yield was 17 g of tosylazide.

Phenylacetone was prepared from 2-phenylethanol by chromate oxidation. 2-Phenylethanol (10 ml) in 44 ml of acetone was cooled to 0°C on ice. A mixture of chromium trioxide (10.3 g), 15 ml of water and 9 ml of conc. H_2SO_4 was prepared and diluted with 30 ml of water. This oxidizing agent was added dropwise with stirring via a pressure equalizing funnel to the 2-phenylethanol with care that the temperature did not rise above 10 °C. The mixture was stirred for 1 hour and warmed to room temperature. A small amount of sodium bisulfite was then added until the top layer turned green. The two layers were extracted separately with petroleum ether. The extracts were combined, and were washed twice with saturated NaCl, twice with saturated sodium carbonate, and once more with saturated NaCl. The solution was dried with $MgSO_4$, and the solvent was removed by rotary evaporation. The product was purified twice by vacuum distillation: NMR 7.29 - 7.24 (m,5,aryl H), 3.67 (s,2,methylene H), and 2.13 ppm (s,3,methyl H). The yield was 5.5 ml (55%).

Phenylacetone (3.3 g) was combined with 4.88 g of tosylazide and 13.2 ml of ethanol in a 100 ml three neck round bottom flask equipped with a dropping funnel. The flask was cooled to -10°C with an ice/salt bath. A solution of 2.6 g potassium ethoxide in 30 ml of ethanol was added dropwise with stirring. The solution turned deep brown indicating an anion was forming, so additional tosylazide was added until the color

disappeared. The reaction was warmed to room temperature and stirred for an additional 15 minutes before it was poured into 200 ml of water and extracted 3 times with ether. The ether layer was dark red, but after rotary evaporation, drying with Na_2SO_4, redissolution in ether, and drying a second time, a yellow-orange glass resulted. The glass crystallized from ether with scratching. The melting point was 56°C (Lit. 59-60°C): NMR: 7.47 - 7.25 (m,5, aryl H), and 2.35 ppm (s,3, methyl H).

9. 2-Diazophenylacetaldehyde

The synthesis of 2-diazophenylacetaldehyde was attempted because it would yield the carbene of structure isomeric to that expected from diazoacetophenone. The synthesis was patterned after that for Me-DAP. Tosylazide was prepared as described. Tosylazide (0.4 g) was dissolved in 20 ml of ethanol at -10°C in a salt/ice bath and 5 g of phenylacetaldehyde was added. Potassium ethoxide (3.2 g) in 38 ml of 95% ethanol was added dropwise very slowly and in the dark with stirring. The reaction turned dark red immediately. After warming the solution to room temperature, and pouring it into water, the mixture was extracted with ether. This time it was not possible to dry the ethereal solution and solvent removal by rotary evaporation appeared to cause decomposition of the compound. A red glass was isolated, but it could not be recrystallized and its NMR and IR were variable. This compound, which has never been reported before, appeared to be unstable and could not be isolated by standard procedures. The NMR and IR data suggest that hydration of the aldehyde may be occuring.

APPENDIX II

PROTEIN PURIFICATION

The purpose of this appendix is to describe in detail the purification of P-450b, the major phenobarbital inducible isozyme, P-450 reductase, and cytochrome b_5.

The following reagents were used in the protein purification:

Glycerol - (Aldrich Gold Label)
DE 52 - Whatman
Emulgen 911 - Kao Atlas Corp. (gift)
Sodium Cholate - Sigma
Gold Label Sodium Cholate - Calbiochem
Biogel HTP (Hydroxylapatite) - Biorad
Phosphates - Fisher
SDS PAGE reagents - Biorad
2'5'-ADP Sepharose - Pharmacia
DETAPAC - Sigma
Dilauroylphosphatidylcholine - Serdary Research Labs
Protein Assay Solution - Biorad
Chelex resin - Biorad
Sephadex G-75 Superfine - Sigma
all water was deionized and glass distilled

The following stock solutions were required for all of the enzyme preparations:

100 mM EDTA = 37.2 g EDTA / 1 l

0.5 mM K_2HPO_4 = 28.5 g / 500 ml

0.5 mM KH_2PO_4 = 34 g / 500 ml

A. P-450 Reductase Purification

The procedure for purification of P-450 reductase which is described in detail here is essentially that of Shephard et al, 1983. The following buffers were required for the purification:

Solubilization Buffer (1 l)
0.1 M KPi = 2.72 g KH_2PO_4 + 18.26 g K_2HPO_4
20 % glycerol = 200 ml
1 mM dithiothreitol (dtt) = 0.155 g
1 mM EDTA = 10 ml stock sln.
2 uM FMN = 1 mg
2 mM PMSF = 10 ml of a 200 mM solution in ethanol

adjust to pH = 7.25

Equilibration Buffer (2 l)
10 mM KPi = 4.56 g K_2HPO_4
20% glycerol = 400 ml
0.1 % Emulgen 913 = 2 g /20 ml and add
0.02 mM EDTA = 0.4 ml stock sln
0.2 mM dtt = 0.062 g
adjust pH to 7.25

Wash Buffer I (1 l)
300 mM KPi = 68.4 g K_2HPO_4
20 % glycerol = 200 ml
0.1% Emulgen 913 = 1 g /10 ml and add
0.1 mM EDTA = 1 ml stock sln.
adjust to pH = 7.7

Wash Buffer II (1 l)
30 mM KPi = 6.84 g K_2HPO_4
20 % glycerol = 200 ml
0.1 mM EDTA = 1 ml stock sln
0.15 % deoxycholate = 1.5 g
adjust pH to 7.7

Elution Buffer (250 ml)
30 mM KPi = 1.71 g K_2HPO_4
20 % glycerol = 50 ml
0.1 mM EDTA = 0.25 ml stock sln.
0.15 % deoxycholate = 0.375 g
1 mM NADP = 0.191 g
adjust to pH = 7.7

Dialysis Buffer was Buffer C from the P-450 prep.

The purification procedure began with preparation of microsomes from 30 rats. They can be frozen in the solubilization buffer at -70, and later thawed on ice. The microsomes were adjusted to a protein concentration of 10 mg / ml using the Biorad assay (see below). The microsomal proteins were solubilized using a 20% sodium cholate (w/v) solution to a final concentration of 0.7%. To the resulting mixture, 3.5 ml / 200 ml of a 1.5% (w/v) solution of protamine sulfate was added and the mixture was centrifuged for 1 hr at 100,000g. The only column which was used in the purification was a 2',5' ADP Sepharose 4B affinity column.

The resin was obtained freeze-dried from Pharmacia in 5 g lots. One 5 g lot was required per preparation, but the resin can be regenerated as per the manufacturer's instructions, and reused. The resin was swollen in the equilibration buffer for at least 4 hrs, and the column was packed in the cold. The solubilized protein was loaded on the column at 10 mg protein / ml and a flow rate of 0.3 - 0.5 ml / min. After loading, the protein on the column was washed with 350 ml of each of the wash buffers, and finally eluted in a tight band with the elution buffer. It was then dialysed against the buffer C for at least 3 days with 3 changes of buffer, and was stored in this buffer in aliquots at -70.

P-450 reductase activity is assayed using the cytochrome c reduction assay developed by Williams and Kamin (1962) with slight modifications. According to D. Waxman, the flavin spectrum gives unreliable results, and this activity assay is preferable.

The following solutions are required:

Buffer (1 l)
300mM KPi = 8.16 g KH_2PO_4 + 54.8 g K_2HPO_4 pH = 7.7
0.1 mM EDTA = 1 ml stock sln.

Cytochrome C (Sigma type III)
40 uM = 14.2 mg / 10 ml buffer (keep dark)

NADPH
0.1 mM = 10.4 mg / 2.5 ml buffer (keep cold)

Each assay was carried out at 30°C using the constant temperature equilibrator attached to the Aminco spectrophotometer. The cytochrome c solution (1.4 ml) is combined with 0.7 ml of buffer, and an appropriate amount of the protein

(for P-450 reductase at 4 nmol / ml, 1 ul is appropriate). This solution is split and equal amounts are added to the two cuvettes in the Aminco and their temperature is allowed to equilibrate for 5 minutes. 20 ul of the NADPH solution is added to the sample cuvette, and the increase in absorbance at 550 nm is monitored with time. The Aminco parameters are: band pass = 3.0; time base = 2 sec / in.; O.D. = 0.5. The amount of cyt. C reduced per unit time is quantitated using e = 21 $cm^{-1}mM^{-1}$, and the activity is reported as micromoles cyt.C reduced per min. per mg. protein. For P-450 reductase, this value should be > 40.

Reductase which was prepared as described here typically had an activity of 50 umol cyt. c reduced/min/mg protein, and yields were 300 - 500 nmol as calculated from total protein (assuming 100% purity).

B. P-450 and Cytochrome b_5 Purification

P-450 and cytochrome b_5 were prepared simultaneously from the same batch of microsomal protein. The procedure, which is adapted from that of Waxman and Walsh (1982), involves several DE 52 (Whatman DEAE Cellulose) columns followed by chromatography on Bio-rad HTP (hydroxylapatite) and finally detergent removal.

The solutions and buffers required for the procedure are listed below:

The same stock solutions that were used in the reductase purification were required, as well as:

0.5 M Ammonium Sulfate = 264 g / 4 l d H_2O

50 % (w/v) PEG 8000 = 250 g PEG 8000 / 500 ml ddH_2O

Solubilization Buffer (1 l)
100 mM KPi = 2.72 g KH_2PO_4
18.26 g K_2HPO_4

30 % glycerol = 300 ml
1 mM EDTA = 10 ml stock sln.
adjust to pH = 7.4

Buffer A (4 liters for DE 52 equilibration, 4 liters for columns)
10 mM KPi = 1.36 g KH_2PO_4
6.85 g K_2HPO_4
20 % glycerol = 800 ml
0.1 mM EDTA = 4 ml stock sln.
0.5 % Na Cholate = 20 g
0.2 % Emulgen 911 = 8 g / 80 ml and add
adjust pH = 7.4

Buffer A + 20 mM KCl (4 l)
The same as Buffer A + 5.96 g KCl

Buffer A + 110 mM KCl (1 l)
from Buffer A + 20 mM KCl, add 6.71 g KCl

Buffer B (4 l)
20% glycerol = 800 ml
20 uM EDTA = 1.6 ml stock sln.
0.2% Emulgen 911 = 8 g /80 ml, and add.

Buffer B + 10 mM KPi (4 l)
same as Buffer B + 1.36 g KH_2PO_4
6.85 g K_2HPO_4
adjust to pH = 7.4

Buffer B + 15 mM KPi (4 l)
same as Buffer B + 2.04 g KH_2PO_4
10.271 g K_2HPO_4
adjust to pH = 7.4

Buffer B + 35 mM KPi (1 l)
use 1 liter of Buffer B + 0.95 g KH_2PO_4
6.39 g K_2HPO_4
adjust to pH = 7.4

Buffer B + 45 mM KPi (1 l)
use 1 liter of Buffer B + 1.224 g KH_2PO_4
8.22 g K_2HPO_4
adjust to pH = 7.4

Buffer B + 90 mM KPi (2 l)
use 2 liters of Buffer B + 4.9 g KH_2PO_4
32.86 g K_2HPO_4
adjust to pH = 7.4

Buffers for detergent exchange on HTP:

Equilibration Buffer (1 l)
10 mM KPi = 0.34 g KH_2PO_4
1.712 g K_2HPO_4

20 % glycerol = 200 ml
adjust to pH = 7.4

Wash Buffer I (1 l -> 2 x 500 mls)
10 mM KPi = 0.34 g KH_2PO_4
1.712 g K_2HPO_4
20 % glycerol = 200 ml
adjust to pH = 7.4
This buffer was split into 2 x 500 ml and 0.25 g Emulgen 911 was added to one of the 500 ml for Wash buffer I, the rest was used for Wash Buffer II.

Wash Buffer II (500 ml)
Buffer above + 2.5g of gold label Na Cholate for 0.5 %.

Wash Buffer III (500 ml)
50 mM KPi = 0.85 g KH_2PO_4
4.28 g H_2HPO_4
20 % glycerol = 100 ml
0.5 % Na Cholate = 2.5 g gold label
adjust to pH = 7.4

Elution Buffer (1 l)
150 mM KPi = 4.08 g KH_2PO_4
27.39 g K_2HPO_4
20 % glycerol = 200 ml
1.5% Na Cholate = 15 g gold label
adjust to pH = 7.4

Buffer C (4 l)
100 mM KPi = 10.88 g KH_2PO_4
73.04 g K_2HPO_4
20 % glycerol = 800 ml
20 uM EDTA = 1.6 ml stock sln.
adjust to pH = 7.4

The following buffers were used in the simultaneous purification of cytochrome b_5:

Buffer D (2 x 4 l)
20 mM Tris acetate = 5.8 g Tris acetate
5.8 g Tris
0.1 mM EDTA = 4 ml stock sln.
0.4 % deoxycholate = 16 g
ajust pH = 8.1

Buffer D + 0.2 M Na SCN (750 ml)
750 ml Buffer D + 12.15 g NaSCN

Buffer E (2 l)
10 mM Tris Acetate = 1.45 g Tris acetate
1.45 g Tris
50 mM KCl = 7.45 g KCl
0.1 mM EDTA = 2 ml EDTA stock sln.

adjust to pH + 8.1

Buffer E + 120 mM KPi + 0.4% deoxycholate (1 l)
same as Buffer E, with 20 g K_2HPO_4 and 4 g deoxycholate
adjust pH = 8.1 with KH_2PO_4 stock solution

The DE 52 column packing and columns themselves require excessive equilibration, and were prepared the day before. The amount of DE 52 required for each 2.4 x 50 cm column is the amount that fits loosely in a 400 ml beaker. The resin for the three columns was combined and soaked over night in water. The following day it was equilibrated in a large buchner funnel with the following washes :

5 x with water
3 x with 0.5M ammonium sulfate
exhaustively with water

The resin was then slurried in buffer A, and the pH was adjusted to 7.4. Finally, it was washed with buffer A in the funnel until the supernatant liquid had the same pH and conductivity as buffer A itself. The partially dried resin was slurried with the appropriate buffer and the columns were poured and equilibrated. The first DE 52 column was slurried in buffer A and equilibrated over night the night before the first day of the prep. The second DE 52 column was slurried with buffer A + 20 and equilibrated the night before the second day of the prep. The third DE 52 column was slurried with buffer D and required extensive equilibration, so was usually prepared with the second one and equilibrated the night before the second day of the prep, and the equilibration continued into the second day.

The microsomes from approx. 30 phenobarbital induced male S.D. rats weighing 250 - 300 grams were prepared as usual. They were occasionally frozen in the solubilization buffer until the

first day of the prep at which time they were thawed on ice, and rehomogenized. The protein concentration of the microsomes was determined using the Biorad assay. The protein concentration was adjusted to 10 - 12 mg / ml, and the amount of sodium cholate required for solubilization was calculated as 2.3 x (w/w) the amount of protein. The cholate was dissolved in a small amount of solubilization buffer and added dropwise to the stirring microsomal suspension. The mixture was stirred for 30 minutes and a 50 % PEG solution was added to a final concentration of 10 %. This mixture was stirred for 10 minutes, and centrifuged for 45 minutes at 35,000g. The supernatants were combined, adjusted to a final PEG concentration of 16 %, stirred for 10 minutes, and centrifuged at 100,000g for 90 minutes. The pellets were combined and homogenized in about 30 ml of buffer A to an O.D. upon 1 : 10 dilution of 0.6 - 0.8 at 417 nm.

The homogenate was loaded on the first DE 52 column and equilibrated with 1/2 column volume of buffer A. It was then eluted over night at 0.6 ml / min with buffer A + 20. At this stage, the cytochrome b_5 remained at the top of the column, and the major phenobarbital inducible P-450 isozymes formed a band about half way down the column. Other P-450 isozymes pass through the column during the elution with buffer A and buffer A + 20. The resin was extruded, and the resin containing the cyt. b_5 was placed in an empty column and washed with buffer D. The resin containing the P-450 was placed at the top of the second DE 52 column, and a linear gradient of buffer A + 20 to buffer A + 110 (900 ml total) was established at a flow rate of about 1.2 ml /

min. Fractions were collected (10 ml), and assayed for absorbance at 295, 417, and 650 nm for protein, heme, and background respectively.

The resin containing cytochrome b_5 was placed at the top of the third DE 52 column, and a linear gradient of buffer D to buffer D + 0.2 M NaSCN (1.5 l total) was established. The b_5 didn't come off till the end of this gradient, so the two columns could be run simultaneously, and the fraction collector switched from one to the other after the P-450 column was finished.

The separation of P-450b and P-450e was partially accomplished on the second DE 52 column. The extent of separation was best monitored by SDS PAGE before fractions were pooled. The fractions containing mostly P-450b or mostly P-450e were pooled. The remaining P-450e in the P-450b and vice versa was removed on Biorad HTP. The pooled fractions were dialysed against buffer B + 10 for P-450b or buffer B + 15 for P-450e. HTP columns were prepared in these same buffers using the formula of 8 ml HTP / 120 nmol P-450.

P-450b was loaded on the HTP column equilibrated with buffer B + 10, and washed with buffer B + 35 to remove any residual P-450e. Usually, the P-450e was not visible, and the P-450b began to spread on the column, so it was not advisable to run more than 400 mls of B + 35 through the column. The P-450b was eluted with B + 90, and dialysed against B + 10.

P-450e was loaded on the HTP column equilibrated with buffer B + 15, and eluted with buffer B + 45 in a fairly sharp band. After the P-450e appeared to have stopped coming off, the remaining P-450b which was still on the column could be eluted

using buffer B + 90. The P-450e was dialysed again against buffer B + 15. The P-450b obtained from the P-450e prep could be combined with the rest of the P-450b if SDS PAGE indicated it was free of P-450e.

The final step in the P-450 purification is the removal of the Emulgen by substitution with Na cholate. This detergent exchange is accomplished on HTP. Both P-450b and P-450e could be loaded on HTP columns equilibrated with detergent exchange equilibration buffer. The amount of HTP was determined using the previously defined formula. The proteins were slowly brought into cholate by decreasing the concentration of emulgen, and increasing the concentration of cholate in each buffer. The column was washed with at least 200 mls of each of the wash buffers listed above, and the protein was eluted in a fairly tight band with the elution buffer. The cholate was removed by extensive dialysis against buffer C.

The cyt. b_5 collected from the third DE 52 column was passed through a 2 ml 2',5' ADP Sepharose column equilibrated with the reductase equilibration buffer to remove any residual reductase. It was then loaded on a HTP column prepared in buffer E using the formula of 20 ml HTP / 300 nmol b_5. The b_5 was washed extensively with buffer E to remove residual emulgen, then eluted with buffer E +120 + deoxycholate. Residual contaminants in the cyt. b_5 preparation were removed by concentrating the protein to 0.5 ml and loading it on to a 1.5 x 115 cm column of Sephadex G-75 superfine equilibrated in buffer D.

All proteins were dialysed against 4 liters of buffer C which was

treated batchwise with Chelex resin to remove trace metals. The dialysis was for 3 days at 4°C with daily changes of buffer. After dialysis, the proteins were aliquoted into 1 ml portions and frozen at -70 °C in eppendorf tubes.

The protein purifications were continuously monitored by the following assays:

Protein Assay: The Bio-Rad assay (Bradford, 1976) has been found to be preferable since it is not interfered with by glycerol or emulgen, and is simpler and faster than the Lowry assay. It was performed exactly as described in the literature obtained with the assay solution, and duplicate BSA standards were used at 8, 24, 56, and 80 ugms.

P-450 spectral assay: The nmolar concentration of P-450 in any buffer was easily determined by the difference spectrum of the reduced P-450 - CO complex vs CO - complexed P-450. O.D. at 450 nm was measured using an extinction coefficient of 91,000 M^{-1} cm^{-1}.

Cyt. b_5 spectral assay: The nmolar concentration of cyt. b_5 in any buffer can be determined by the difference spectrum of reduced vs oxidized cyt. b_5. O.D. at 426 - 406 was measured using an extinction coefficient of 185,000 M^{-1} cm^{-1}.

Emulgen Content: The amount of emulgen present at the end of the purification should give an A_{407} to A_{280} ratio of 0.7 - 0.9. This corresponds to 50 - 70 nmol emulgen / nmol P-450 if one uses the extinction coefficients; Eml_{280} = 1300 M^{-1}, $Heme_{407}$ = 90,000 M^{-1}, $P\text{-}450_{280}$ = 30,000 M^{-1}.

Polyacrylamide Gel Electrophoresis: SDS PAGE was used to monitor the isozyme population during chromatography as well as the

purity of the proteins, and was done by the method of Laemmli (1970) as described in the Bio-rad catalog.

C. P-450 Reconstitution

P-450 and P-450 reductase were thawed on ice and mixed at room temperature for a final concentration of 1 nmol/ml for P-450 and 2 nmol /ml of reductase. A solution of 2 mg/ ml dilauroylphosphatidylcholine (dlpc) in water with 1 mM DETAPAC was preparedand sonicated for 10 minutes at power = 6 with a Branson Sonicator equipped with a microprobe sonicating tip. 20 ul/ml (40 ug /ml) of the dlpc solution was added to the proteins immediately after sonicating, and the concentrated mixture of proteins and dlpc was allowed to stand for 10 minutes at room temperature. Buffer C was added to bring the final volume to 1 ml, and this solution was then used immediately for enzyme assays. This reconstitution scheme has been optimized (based on 7-ethoxycoumarin deethylase activity) for all protein concentrations and dlpc concentration (data shown in Chapter 2).

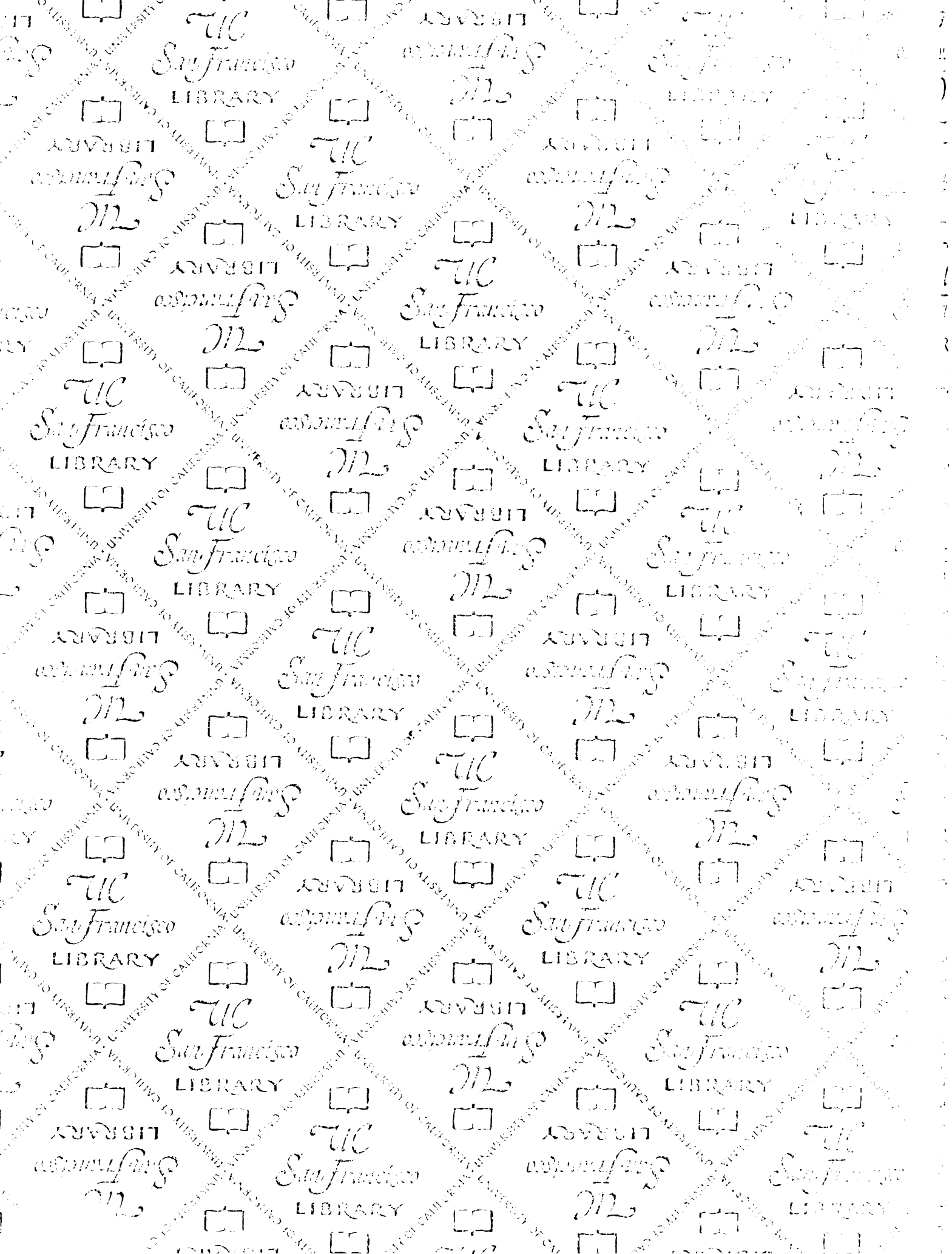
UC
San Francisco
LIBRARY

The San Francisco Public Library

FOR REFERENCE

NOT TO BE TAKEN FROM THE ROOM

BRODART CAT. NO. 23 012 PRINTED IN U.S.A.